The Retina In Cystic Fibrosis

A thesis submitted to Cardiff University for the degree of Doctor of Philosophy

Rachel Hiscox

School of Optometry and Vision Sciences
Cardiff University

October 2013

Supervisors:
Dr Katharine Evans, Professor Christine Purslow,
Professor Rachel North

Summary

Cystic fibrosis (CF), an autosomal recessive inherited disease, is caused by defective function of CF Transmembrane Conductance Regulator (CFTR), an epithelial ion channel that facilitates chloride secretion. Previous research has identified a number of ocular complications in CF, including impaired dark adaptation (DA) which has been attributed to concomitant vitamin A deficiency (VAD) and CF-related diabetes (CFRD). However, CFTR has been localised to the retinal pigment epithelium (RPE) and it is proposed that abnormal DA could be a primary manifestation of CF. DA is similarly impaired in individuals with type 1 and 2 diabetes and is thought to be caused by retinal hypoxia as oxygen inhalation ameliorates abnormal thresholds. It is unknown if CFRD similarly affects the retina. The aim of this thesis was to investigate DA during oxygen inhalation in CF subjects with and without CFRD to gain further insight about the aetiology of this abnormal DA. The work also aimed to examine retinal structure using optical coherence tomography (OCT) to determine the consequences of CFTR dysfunction at the RPE, with the hypothesis that the retina would be thickened in CF due to CFTR dysfunction.

Final DA thresholds were not significantly elevated in CF subjects as a whole compared to controls during the inhalation of air. However, when grouped according to diabetic status, CFRD subjects showed a significantly elevated final rod threshold which was ameliorated following oxygen inhalation. This suggests that the retina is hypoxic in CFRD subjects and that impaired DA in CF is secondary to CFRD rather than a primary manifestation of CFTR malfunction at the RPE. Contrary to the proposed hypothesis, retinal and RPE/Photoreceptor layer thickness was significantly thinner in CF subjects compared to healthy controls. However, this was not observed in CFRD subjects. These results suggest that impaired CFTR function at the RPE does not directly affect retinal structure. It is subsequently hypothesised that retinal thinning in CF may be secondary to accelerated aging, early onset AMD or impaired formation of photoreceptor outer segments due to fatty acid deficiency.

In conclusion, this is the first study to determine that retinal structural and functional abnormalities are not caused directly by CFTR dysfunction but are a secondary manifestation of the disease. Further research is necessary to understand the impact of these findings. Following these findings, individuals with CF, particularly those with CFRD, and eye care practitioners should be educated about the ocular associations of the disease.

Acknowledgements

I can't quite believe three years is over and I am at the end of this incredible journey. There are many people who have helped me along this road to whom I owe thanks, so here goes…

First and foremost, thank you to my supervisors, Dr Katharine Evans, Professor Christine Purslow and Professor Rachel North. Without your continued support, guidance, knowledge and friendship I am sure that I would not have made it this far. Thank you to Professor John Dodge for your kind advice and invaluable knowledge and to Tony Redmond, statistics guru. Thank you also to Sue, Leanne, Greg and Robin – without you the building would surely fall apart. Thank you to everyone who took the time to help with data collection, especially those who gave up their time on a sunny day to sit in the dark with me!

Thank you to Dr Ketchell and all the CF team at the All Wales Adult Cystic Fibrosis Centre for your kind support with recruitment and your invaluable knowledge on all things CF. Of course, massive thanks must be paid to all the CF patients who gave their precious time to help with this research. I can only hope that I would be so generous with my time if I was in the same position. Your endurance and strength is admirable.

To everyone who has passed through room 2.10 – Tamsin, Allannah, Claire, Matt, Diti and Hanim – thank you for putting up with me! Thank you also to the other friends I have made along the way – Claire, Steph and Sian. The last three years would not have been the same without each of you. A special thank you to Ally who has shared in the ups and downs from the very start as an office-mate, flat-mate, gym-buddy, travel-companion and all round true friend. Thanks for all the laughs, even if they were mostly at my expense! I'm not quite sure what I will do without my side-kick. Thank you to my undergrad uni girls – Susie, Jo, Helen, Rachael, Amy, Hetal, Gopi and Meesh – for keeping me sane throughout this process!

Thank you to Huw, for being by my side over the last two years, keeping me smiling and just being you! You're the best! Finally, I would like to express the biggest thanks of all to my mum and dad. Without your constant love, support and unwavering belief in me, I would not be where I am today.

Phew – that was emotional!

Contents

List of Figures

List of Tables

Abbreviations

3D-OCT	Three dimensional optical coherence tomography
ACBT	Active cycle of breathing technique
AD	Autogenic drainage
AL	Axial length
AMD	Age-related macular degeneration
AMP	Adenosine monophosphate
ANOVA	Analysis of variance
AQP	Aquaporin
AO	Adaptive optics
ASL	Airway surface layer
ATP	Adenosine triphosphate
BMD	Bone mineral density
C-domain	Carbon terminus
cAMP	Cyclic adenosine monophosphate
Ca^{2+}	Calcium ion
CaCC	Calcium-activated chloride channel
CF	Cystic fibrosis
CFRD	Cystic fibrosis related diabetes
CFRD FH-	Cystic fibrosis related diabetes without fasting hyperglycaemia
CFRD FH+	Cystic fibrosis related diabetes with fasting hyperglycaemia
CFTR	Cystic fibrosis transmembrane conductance regulator
Cl^-	Chloride ion
Cl^-:HCO_3^-	Chloride: bicarbonate exchanger
ClC	Voltage gated chloride channel
CLCA	Calcium activated chloride channel
CLCA1	Calcium activated chloride channel 1
CLCA 2	Calcium activated chloride channel 2
COR	Coefficient of repeatability
CoV	Coefficient of variation
CPD	Cycles per degree
CS	Contrast sensitivity
CS	Central area of ETDRS
CSF	Contrast sensitivity function
CV	Colour vision
D	Dioptres

DA	Dark adaptation
DNA	Deoxyribonucleic acid
DR	Diabetic retinopathy
DR:LT	Dark rise: Light trough
ENaC	Epithelial sodium channel
EOG	Electro-oculogram
ER	Endoplasmic reticulum
ERG	Electroretinogram
ETDRS	Early treatment diabetic retinopathy study
FD-OCT	Frequency/Fourier domain optical coherence tomography
FO	Fast oscillations
H_2O	Water
HbA1c	Glycosylated haemoglobin
HCO_3^-	Bicarbonate ion
HFCC	High frequency chest compression
ICC	Intraclass correlation coefficient
IGT	Impaired glucose tolerance
II	Inferior inner area of ETDRS
IO	Inferior outer area of ETDRS
IPM	Inter-photoreceptor matrix
IS	Immunofluorescence Staining
K^+	Potassium ion
KCS	Keratoconjunctivitis sicca
mRNA	Messenger Ribonucleic Acid
MSD	Membrane spanning domain
Na^+	Sodium ion
NaCl	Sodium chloride
$Na^+:K^+$	Sodium: potassium pump
$Na^+:2HCO_3^-$	Sodium: bicarbonate co-transporter
$Na^+:K^+:2Cl^-$	Sodium: potassium: chloride co-transporter
NBD	Nucleotide binding domain
NGT	Normal glucose tolerance
NI	Nasal inner area of ETDRS
NO	Nasal outer area of ETDRS
OCT	Optical coherence tomography
OGTT	Oral glucose tolerance test
ORCC	Outwardly rectifying chloride channels

P and PD	Percussion and Postural Drainage
PD	Potential difference
PTC	Premature termination codon
PEP	Positive expiratory pressure
PI	Pancreatic insufficiency
PKA	Protein kinase A
PS	Pancreatic sufficiency
R-domain	Regulatory domain
RPE	Retinal pigment epithelium
RT	Retinal thickness
RT-PCR	Reverse transcription polymerase chain reaction
SaO_2	Arterial oxygen saturation
SD	Standard deviation
SER	Spherical equivalent refraction
SF	Spatial frequency
SI	Superior inner area of ETDRS
SLD	Superluminescent diode
SO	Superior outer area of ETDRS
SRS	Subretinal space
TBUT	Tear break up time
TD-OCT	Time domain optical coherence tomography
TI	Temporal inner area of ETDRS
TO	Temporal outer area of ETDRS
UHR	Ultrahigh resolution
VA	Visual acuity
VAD	Vitamin A deficiency
VEP	Visual evoked potential

Chapter 1 Introduction

1.1 Outline

This thesis describes a series of studies which investigate the structure and function of the retina in cystic fibrosis (CF). Cystic fibrosis (CF) is the most common lethal hereditary autosomal recessive disorder in Caucasian populations (Hurt and Bilton, 2012). Currently, it affects over 9,000 people in the UK alone, with an incidence of 1 in 2500 live births (Cystic Fibrosis Trust, 2013).

Cystic fibrosis (CF) is caused by defective function of CF Transmembrane Conductance Regulator (CFTR), an epithelial ion channel that facilitates chloride secretion. Previous studies into the effect of CF on the eye have identified a number of ocular characteristics of the disease including dry eye, conjunctival xerosis, reduced crystalline lens transparency, reduced macular pigment density, impaired dark adaptation, reduced contrast sensitivity and abnormal electrophysiological results. Whilst there is a relatively large body of research on the anterior ocular effects of CF, there is little published research on the retina in CF. Additionally, it is unclear whether ocular abnormalities seen in CF are caused by primary dysfunction of CFTR or due to secondary complications of the disease, including vitamin A deficiency (VAD) and CF-related diabetes (CFRD). Therefore, the aim of this thesis is to explore the structure and function of the retina in cystic fibrosis, through use of optical coherence tomography (OCT) and dark adaptation (DA), respectively.

This thesis begins by providing background information on CF and the ocular complications previously described in the literature. It then introduces OCT and DA, the two techniques which will be used to investigate the retinal structure and function in this thesis. The following chapters present the development of OCT and DA protocols for this study, along with the overall results and conclusions.

1.2 Cystic Fibrosis

1.2.1 *Pathogenesis*

The genetic defect in CF is a chromosomal mutation in the middle of the long arm of chromosome 7 (Riordan et al., 1989), which results in the defective function of the membrane protein, Cystic Fibrosis Transmembrane Conductance Regulator (CFTR). Located at the apical

membrane of epithelial cells throughout the body, the principle function of CFTR is to act as a phosphorylation-dependent chloride ion (Cl^-) channel (Li et al., 2007). CFTR is also a key channel in chloride mediated fluid transport, and plays a vital role in the homeostasis of fluid throughout the body.

Mutations in CFTR result in a variable loss of chloride transport in epithelial cells, causing imbalance of fluid and electrolyte levels, resulting in dehydrated viscous secretions. CFTR expression has been found in the pancreas, salivary gland, lung, gastrointestinal tract, kidney, uterus and testes (Trezise and Buchwald, 1991), and the eyes (Wills et al., 2001; Cao et al., 2010), amongst other places. Disruption in CFTR expression leads to multi-organ dysfunction, with the respiratory, gastrointestinal, hepatobiliary and reproductive systems being most affected (Lewis et al., 2003). The pathological finding in these organs is accumulation of thick viscous secretions associated with progressive scarring and destruction.

1.2.2 *CFTR*

The CFTR protein belongs to the superfamily of adenosine triphosphate (ATP)-binding cassette (ABC) transporters. These are integral membrane proteins that use the energy generated from ATP to translocate a variety of molecules across cellular membranes (Biemans-Oldehinkel, Doeven and Poolman, 2006). CFTR is unique among ABC proteins in that its transmembrane domains comprise an ion channel that permits bidirectional permeation of anions.

1.2.2.1 CFTR Function

The principle function of CFTR is to act as a phosphorylation-dependent chloride ion (Cl^-) channel located at the apical membrane of epithelial cells (Anderson et al., 1991; Cheng et al., 1991; Bear et al., 1992; Li et al., 2007). In addition to conducting Cl^- across epithelial cell membranes, CFTR also down-regulates transepithelial sodium ion (Na^+) transport via the epithelial sodium channel (ENaC) (Knowles, Gatzy and Boucher, 1983; Anderson et al., 1991; Stutts et al., 1995; Kunzelmann et al., 2000), and regulates calcium-activated chloride channels (CaCC) and potassium ion (K^+) channels. It is hypothesised that CFTR may also act as a regulator of other ion channels such as the outwardly rectifying chloride channels (ORCC). CFTR is known to be directly or indirectly involved in bicarbonate ion (HCO_3^-) transport in a number of tissues, including the airways, intestine and pancreas (Poulsen et al., 1994).

However, permeability to HCO_3^- is much lower than that of Cl^-, and under most conditions CFTR principally conducts Cl^- transport. Due to the influence of CFTR on other ion channels, the overall effect of defective CFTR function not only results in reduced epithelial Cl^- permeability, but also enhanced Na^+ permeability of the cell membrane (Ashcroft, 2000).

CFTR directly or indirectly mediates glutathione efflux (Linsdell and Hanrahan, 1998; Gao et al., 1999; Velsor, van Heeckeren and Day, 2001; Ballatori et al., 2009). Glutathione is an antioxidant protein which is required for the immune response and many critical cell processes including cell differentiation, proliferation and apoptosis (Ballatori et al., 2009; Galli et al., 2012). It is also a major component of cellular defense against oxidative stress and injury (Gao et al., 1999). In healthy individuals, glutathione is present in the airway surface fluid which lines the lung epithelium, and is responsible for breaking disulfide bonds to reduce viscosity of mucous, and regulating inflammation and the immune response (Cantin et al., 2007). Whilst glutathione is present within the lung itself in CF patients, none is present in the airway surface layer of lung epithelia and blood plasma (Roum et al., 1993; Ballatori et al., 2009). Neutrophil glutathione may also be decreased in CF patients (Tirouvanziam et al., 2006), indicating that glutathione deficiency is systemic (Roum et al., 1993).

1.2.2.2 CFTR Structure

According to the general domain architecture of ABC transporters, CFTR has two membrane spanning domains (MSD), two nucleotide binding domains (NBD) and a central, highly charged regulatory (R) domain (Riordan et al., 1989), as shown in Figure 1.1. Each MSD contains six membrane-spanning alpha helices, portions of which form a chloride-conductance pore to transport Cl^- and other compounds across the membrane (Rowe, Miller and Sorsscher, 2005). Channel activity is governed by the two NBDs; the ion pore is believed to be opened by ATP-binding to the NBDs, and closed by hydrolysis of ATP (Gadsby, 2009). The R domain which lies between the first NBD and the second MSD, links the two homologous transporter halves and contains multiple phosphorylation sites. Phosphorylation by protein kinase A (PKA) at these sites stimulates the ATPase activity and channel gating, hence increasing the channel activity (Riordan et al., 1989; Cheng et al., 1991; Ostedgaard, Baldursson and Welsh, 2001). The final component of CFTR is made up of three amino acids (threonine, arginine, and leucine) which are responsible for connecting the C- domain of CFTR to the PDZ-type receptors (a common structural domain), which anchors CFTR to the cytoskeleton (Short et al., 1998).

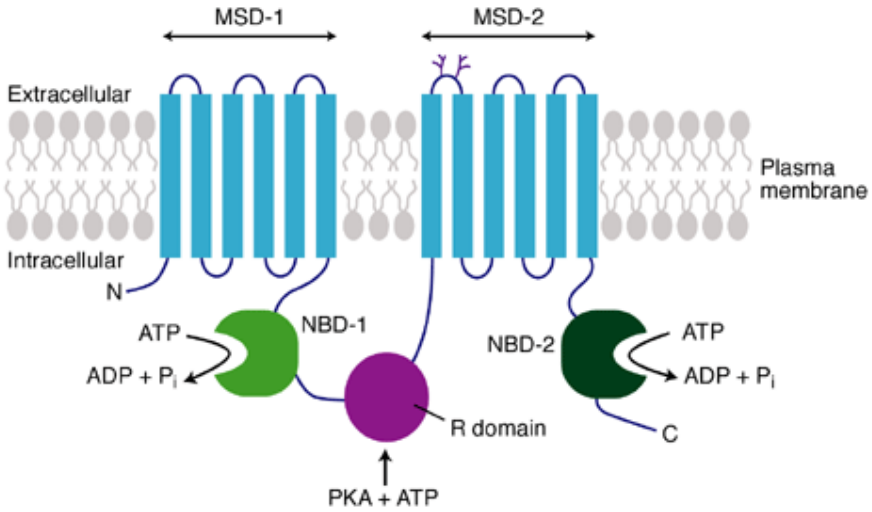

Figure 1.1 Schematic diagram of CFTR structure. Image from: Davidson and Dorin (2001) Key: MSD, membrane spanning domain; N, nitrogen terminal; ATP, adenosine triphosphate; ADP, adenosine diphosphate; P, phosphate; NBD, nucleotide binding domain; PKA, protein kinase A; R, regulatory; C, carbon terminal.

1.2.2.3 Mutations in CFTR

To date, more than 1800 naturally occurring CFTR mutations have been identified (The Cystic Fibrosis Genetic Analysis Consortium, 2011) with the effect on CFTR ranging from reduced Cl^- secretion to complete absence from epithelial membranes (Rowntree and Harris, 2003). The different mutations can be classified into groups according to their known or predicted molecular mechanism of dysfunction, and the varying consequences on CFTR biogenesis, metabolism and function (Zielenski, 2000; Proesman, Vermeulen and De Boeck, 2008). This classification system was first proposed by Tsui, 1992, and has subsequently been refined into the five main groups as outlined in Table 1.1 (Tsui, 1992; Zielenski, 2000; Proesman et al., 2008). Population genetics have shown that a single mutation, an in-frame deletion of three bases encoding phenylalanine 508, known as ΔF508, accounts for approximately 70% of the mutant CFTR alleles present in the CF population (Bobadilla et al., 2002).

Table 1.1 Classification of CFTR defects in CF

Defect Class	Type of Mutation	Effect of Mutation	Phenotype	Incidence (%)
Class 1	Nonsense mutations e.g. G542X	*No CFTR Synthesis* Premature termination of CFTR translation resulting in no CFTR at the apical membrane	Severe	< 7
Class 2	Missense; Amino Acid Deletion e.g. ΔF508	*Abnormal CFTR processing and trafficking* Defective CFTR on the endoplasmic reticulum that cannot be trafficked to the apical membrane	Severe	85
Class 3	Missense; Amino Acid Change e.g. G551D	*Abnormal CFTR regulation* Defective CFTR spans the apical membrane, but has defective regulation	Mild	< 3
Class 4	Missense; Amino Acid Change e.g. R117H	*Altered CFTR conductance* Defective CFTR protein spans the apical membrane but has decreased chloride conductance	Mild	5
Class 5	Missense; Amino Acid Change e.g. A455E	*Reduced CFTR synthesis* Fully processed functional CFTR but with a reduced numbers of transcripts	Mild	

1.2.2.3.1 Genotype-phenotype correlations

The variation in CF genotypes provides a clear rationale for the phenotypic effects of specific mutations. However, genotype-phenotype studies have demonstrated that the process of phenotype realisation is complex and variable. Inheritance of the same mutation can result in remarkably variable manifestations of the disease (Kerem et al., 1990; McKone et al., 2003), suggesting environmental factors and modifying genes play an important role in influencing CF disease severity (Zielenski, 2000). The extent to which CF phenotype is determined by specific genotypes varies considerably from organ to organ. The degree of correlation between CFTR genotype and CF phenotype is highest for pancreatic involvement and lowest for pulmonary function (Zielenski, 2000).

1.2.3 *Characteristics of CF*

As CFTR is expressed in multiple organs throughout the body, the manifestations of CF are widespread, allowing classification of CF as a multi-system disorder. Common CF characteristics consist of bronchiectasis (Ratjen and Doring, 2003), malnutrition secondary to pancreatic insufficiency and increased metabolic rate (Kerem and Kerem, 1996; Durie, 2000), diabetes (Couce et al., 1996), infertility (Oppenheimer et al., 1970) and liver disease (Colombo et al., 2002) (Figure 1.2). The main problems encountered by CF patients are briefly outlined below.

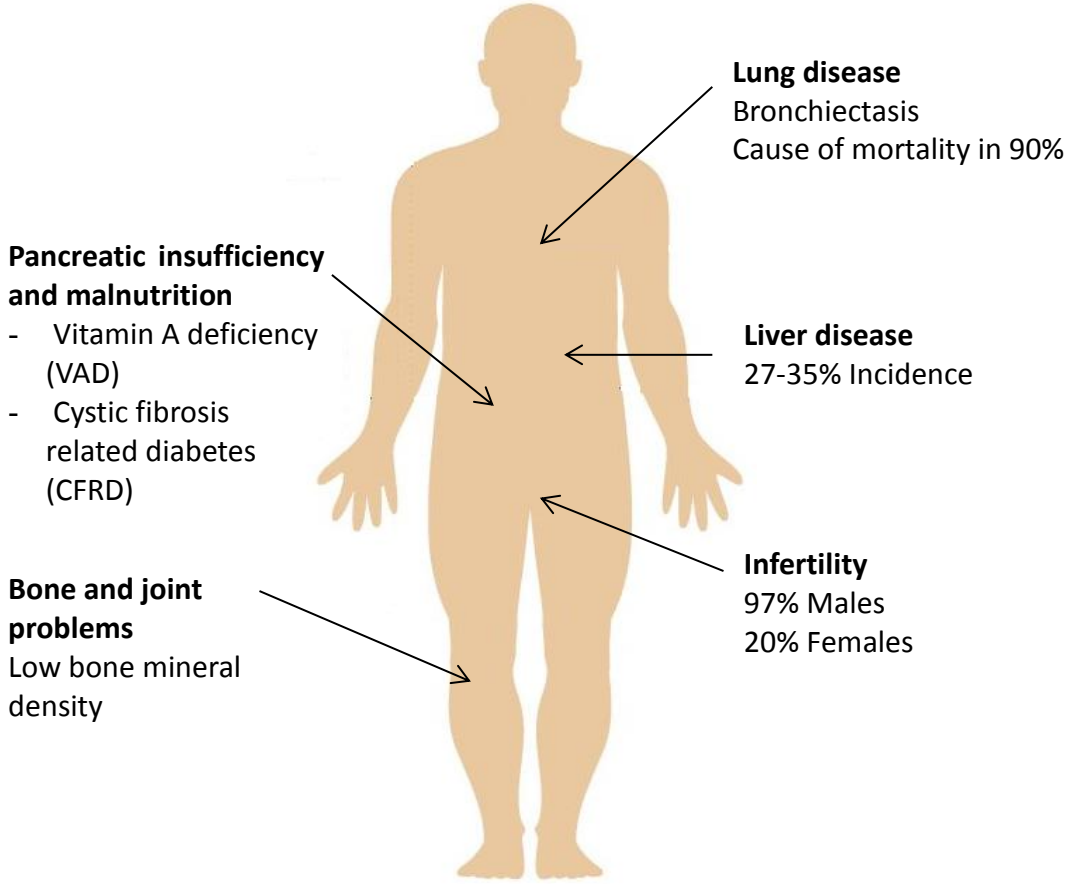

Figure 1.2 A summary of the health complication associated with CF

1.2.3.1 Lung disease

Pulmonary disease in CF is believed to stem from a reduction in the airway surface layer (ASL), caused by defective CFTR processing. Thinning of the ASL in CF produces a highly viscoelastic, adhesive material which traps infectious bacteria and provides the perfect medium for pathogen growth (Worlitzsch, Tarran and Ulrich, 2002). This, combined with the consecutive breakdown of mucociliary transport and subsequent mucous stasis (Matsui et al., 1998) causes infection from the trapped bacteria, neutrophillic inflammation and fibrosis.

Clinically, this causes chronic bacterial bronchitis, which evolves into a syndrome of bronchiectasis (widening of the airways associated with excess mucous), and ultimately leads to respiratory failure. Pulmonary complications are the most common cause of mortality in CF patients, accounting for up to 90% of all CF deaths (Boucher, 2007).

1.2.3.2 Pancreatic insufficiency and malnutrition

Up to 90% of CF patients suffer from pancreatic insufficiency as a direct result of the absence or dysfunction of CFTR at the apical membrane of pancreatic epithelial cells (Dodge and Turck, 2006). This leads to highly concentrated protein-containing secretions, causing obstruction of the pancreatic ducts and ultimately results in organ damage secondary to the formation of fibrotic tissue (Scheele et al., 1996). Combined with a reduction in the volume of the bicarbonate-rich fluid which is essential for the transport of enzymes, this results in reduced levels of pancreatic enzymes reaching the small intestine. A reduction of these enzymes, which are vital for the absorption of fat, protein and fat soluble vitamins, can cause malnutrition, even when patients are administered exogenous enzymes (Karlet, 2000).

1.2.3.2.1 Vitamin deficiency

Fat-soluble vitamin deficiency (A, D, E and K), particularly vitamin A deficiency (VAD) has been associated with CF since the earliest descriptions of the disease (Anderson, 1939), and is now known to be attributed to fat maldigestion secondary to pancreatic insufficiency. However, it is hypothesised that there may also be specific defects of vitamin A metabolism, involving its absorption from the bowel and mobilisation from the liver (Ahmed et al., 1990). Despite supplementation with vitamin A and pancreatic enzymes, sporadic deficiency and persistent or recurrent deficiency can still occur, highlighting the need for regular monitoring of serum vitamin concentration (Morton, 2009). Along with poor growth and increased mortality (West, 2003), clinical consequences of VAD also include impaired dark adaptation (Fulton et al., 1982), and conjunctival and corneal xerosis (Sommer, 1989; Vernon et al., 1989; Brooks, Driebe and Schemmer, 1990; Campbell et al., 1998). Determination of true vitamin A status is difficult; circulating serum vitamin A levels are often a poor indicator of true vitamin A status, as vitamin A is mostly stored in the liver, bound to tissue membrane (Underwood and Denning, 1972; Lindblad et al., 1997). Additionally, research has shown that serum vitamin A levels can remain low despite adequate liver stores, suggesting defective vitamin A release from the liver in CF (Underwood and Denning, 1972; Tsinopoulos et al., 2000).

1.2.3.3 Cystic Fibrosis Related Diabetes

Cystic fibrosis related diabetes (CFRD) was first recognised as a distinct disease, separate from type 1 and type 2 diabetes, in 1955 (Shwachman, Leubner and Catzel, 1955). Whilst the pathogenesis of CFRD is not completely understood, increasing evidence suggests that insulin-deficiency, exacerbated by peripheral insulin resistance, is the primary cause (O'Riordan et al., 2009). Insulin-deficiency results from β-cell apoptosis in the pancreas (Kopelman et al., 1985; Couce et al., 1996) in conjunction with defective insulin secretion by the remaining β-cells (Mohan et al., 2009). Other key factors known to be involved in the development of CFRD include genetic variations (Blackman et al., 2009), diminished pancreatic blood flow, chronic pancreatic inflammation and oxidative stress (Stecenko and Moran, 2010). Insulin resistance is exacerbated by respiratory infection and corticosteroid treatment, and therefore fluctuates over time (Moran et al., 1999; Mackie, Thornton and Edenborough, 2003).

Latest reports indicate increasing prevalence of CFRD with advancing age, from 3% in children to 45-50% in those over thirty years (Moran et al., 2009), with the mean age of diagnosis in the mid-twenties (Milla, Billings and Moran, 2005). Three large scale studies (Koch et al., 2001; Marshall et al., 2005; Moran et al., 2009), and several smaller studies (Finkelstein et al., 1988; Lanng et al., 1992; Cawood et al., 2006; Bismuth et al., 2008) have shown that the presence of CFRD is associated with worse clinical status in CF, specifically, more severe pulmonary disease and poorer nutritional status. This has been attributed to both the influence of hyperglycaemia on inflammation and infection, and the effect of insulin deficiency on protein catabolism and malnutrition (Moran et al., 2009). Although mortality rates still remain higher for patients with CFRD, compared to those without, the gap has considerably narrowed (Moran et al., 2009), with improvements related to earlier disease detection and aggressive treatment regimes.

Currently, as CFRD is often asymptomatic, CF patients are screened for CFRD yearly using the recommended oral glucose tolerance test (OGTT) (Mohan et al., 2009; O'Riordan et al., 2009). Patients are categorised into different groups (Table 1.2), depending on the results of the OGTT. Glycosylated haemoglobin (HbA1c), a test accepted for use to diagnose diabetics in the general population, cannot be used in CF patients as measurements are often falsely low (Lanng et al., 1995; Solomon et al., 2003). However, HbA1c is useful to monitor the level of glucose control in CFRD (Brennan et al., 2004).

Table 1.2 Categories of glucose tolerance based on OGTT in CF. Table adapted from Nathan, Laguna and Moran (2010)

Category of glucose tolerance / intolerance	Fasting plasma glucose (mmol/l)	2 hour glucose (mmol/l)
Normal glucose tolerance	< 7.0	< 7.8
Abnormal glucose tolerance: Indeterminate glucose tolerance*	< 7.0	<7.8
Abnormal glucose tolerance: Impaired glucose tolerance	< 7.0	7.8 – 11.1
CFRD without fasting hyperglycaemia (CFRD FH-)	< 7.0	≥ 11.1
CFRD with fasting hyperglycaemia (CFRD FH+)	≥ 7.0	≥ 11.1
Impaired fasting glucose	5.6 – 6.9	Not applicable

* Mid-OGTT glucose ≥ 11.1

1.2.3.4 Low bone mineral density

Low bone mineral density (BMD) is a common characteristic in patients with CF, and has been termed CF-related bone disease (Hahn et al., 1979; Mischler et al., 1979; Buntain et al., 2004; Aris et al., 2005). A comprehensive study has shown that BMD decreases with age, beginning as normal in children and progressing throughout adolescence to become significantly deficient in CF adults (Buntain et al., 2004). The pathogenesis of CF-related bone disease is multifactorial and likely to be due to several CF-related factors that also influence bone metabolism. These factors include vitamin D and K insufficiency, calcium malabsorption, malnutrition, reduced weight-bearing activity, hormonal, steroid use, delayed puberty, pulmonary infection/systemic inflammation and the effect of CFTR dysfunction on bone cell activity (Aris et al., 2005).

1.2.3.5 Infertility

Infertility in women with CF is relatively uncommon, though the true fertility rate is unknown (Lyon and Bilton, 2002). Although the cause of the reduction in fertility in women remains unclear, it is suggested that the accumulation of thick and tenacious cervical mucous (Oppenheimer et al., 1970; Kopito et al., 1973), caused by CFTR dysfunction, acts as a barrier

to sperm penetration. In contrast to the low levels of infertility in women, the rate of infertility in men is very high; at least 97% of men with CF are infertile due to congenital bilateral absence of the vas deferens, with resultant obstructive azoospermia (Welsh et al., 1995; Wong, 1998). The pathological basis for the structural changes in the genital tract may be either developmental abnormalities of the reproductive tract (Kaplan et al., 1968), or in-utero obstruction of the tract by dehydrated secretions (di Sant'Agnese, 1968), caused by lack of or a reduction of functional CFTR.

1.2.3.6 Liver Disease

Liver disease in CF most commonly presents in the first decade of life; however, a small percentage of patients develop decompensated cirrhosis during adulthood (Colombo et al., 2002). Whilst the incidence of CF liver disease ranges from 27-35%, progression to cirrhosis and consequent liver failure is uncommon and only occurs in 3-7% of all patients (Nash et al., 2008). Though the pathogenesis of liver disease has long been questioned, more recent studies suggest that defective CFTR causes liver cell injury or death, leading to activation of hepatic stellate cells, which in turn contributes to the development of tissue fibrosis (Kinnman et al., 2000).

1.2.4 *Diagnosis of CF*

Most cases of CF are identified during childhood, with the median age of diagnosis three months, and with over 70% of cases being recognised within one year (UK CF Registry, 2013). An accurate and timely diagnosis is important, enabling implementation of an appropriate treatment regime in order to maximise the lifespan of the patient (Dankert-Roelse and Merelle, 2005; Rosenfeld, 2005).

In 1996, the Cystic Fibrosis Foundation gathered a panel of experts to develop the criteria for the diagnosis of CF. The panel stated that the diagnosis of CF should be based on: the presence of one or more characteristic phenotypic features; a history of CF in a sibling, or a positive newborn screening test; plus, confirmation through laboratory evidence of CFTR dysfunction (Rosenstein and Cutting, 1998). In the majority of cases, neonatal screening for CF is based on the immunoreactive trypsinogen assay, which is relatively inexpensive and adaptable to large numbers (Crossley et al., 1981). Acceptable evidence of CFTR abnormality includes biological evidence of CFTR dysfunction through elevated sweat chloride concentrations (considered to be the ‘gold standard’ in CF diagnosis) (Gibson and Cooke,

1959), or identification of mutations in each CFTR gene through DNA analysis (Comeau et al., 2004). For patients in whom sweat chloride concentrations are normal or borderline and in whom two CF mutations are not identified, an abnormal nasal potential difference (PD) measurement recorded on two separate days can be used as evidence of CFTR dysfunction (Rosenstein and Cutting, 1998).

1.2.5 *Treatment of CF*

In the 1960's three pillars of treatment were established (Matthews et al., 1964):

- relief of airway obstruction
- nutritional replacement
- antibiotic therapy

When implemented, this treatment strategy caused dramatic improvements in survival and quality of health in CF (Davis, 2006). Over the years, although the ways in which these aims are met have changed as new treatments have become available, aggressive treatment remains the foundation of care. A fourth pillar of treatment has also been added (Davis, 2006); the suppression of inflammation through use of pharmacologicals, which have been seen to reduce the rate of decline in pulmonary function (Eigen et al., 1995; Konstan et al., 1999). The ways in which these aims are met are outlined below.

1.2.5.1 Airway clearance techniques

Airway clearance techniques are used to promote mucociliary clearance of the thick airway mucous which is produced as a direct result of malfunctioning CFTR (Robinson and Bye, 2002). This is of upmost importance as accumulation of this mucous can obstruct the airways, trapping bacteria and cellular debris which can cause airway inflammation. Airway clearance techniques include percussion and postural drainage, positive expiratory pressure (PEP) (Groth et al., 1985), active cycle of breathing techniques (Pryor et al., 1979), oscillatory PEP, high frequency chest compression (Hansen and Warwick, 1990), autogenic drainage and exercise (Schoni, 1989).

1.2.5.2 Nutrition and Supplements

Chronic malnutrition with significant weight retardation and growth failure has been recognised as a characteristic of CF patients for many years. Maintenance of good nutrition is

key in preserving good pulmonary function, with some studies showing strong correlation between the degree of malnutrition and the severity of pulmonary disease (Sproul and Huang, 1964; Kraemer et al., 1978). It has been suggested that patients may require approximately 110% of the recommended daily calorie allowance to ensure normal growth (Roy, Darling and Weber, 1984; Bentur et al., 1996), with 30-40% of the energy consumed to be in the form of fat to prevent negative energy balance. Oral supplements can be prescribed for patients with poor diets, or alternatively, enteral feedings (feeding through a nasal tube to the stomach) or parenteral nutrition (feeding a patient intravenously) can provide additional support. Fat soluble vitamin supplementation (vitamins A, D, E and K) is standard clinical practice in CF (Borowitz et al., 2009), with the aim to maintain vitamin plasma levels within the normal range (Borowitz, Baker and Stallings, 2002). Additionally, supplementation with pancreatic enzymes is mandatory in all patients with pancreatic insufficiency to avoid malnutrition caused by maldigestion and malabsorption.

1.2.5.3 Pharmaceutical Therapy

The majority of CF-related morbidity and mortality is a result of chronic respiratory infection. Therefore, the basis of CF management is to control respiratory infection in order to reduce lung fibrosis and maintain lung function. Therapeutic progress has been realised in the last two decades, with improvements seen in health, quality of life, and overall survival (Cystic Fibrosis Foundation, 2011). An aggressive approach to CF care is supported by two epidemiological studies which show that CF centres which achieve high median pulmonary function test results see patients more frequently, obtain more frequent respiratory-tract cultures, and use more oral and intravenous antibiotics than centres that achieve lower median lung function results (Johnson et al., 2003; Padman et al., 2007). Many different pharmaceutical agents are used in the care of CF patients including antimicrobials (e.g. β-lactam antibiotics such as penicillin and inhaled tobramycin) (Ramsey et al., 1999), anti-inflammatories (e.g. steroids and ibuprofen) (Eigen et al., 1995), mucolytics (e.g. inhaled recombinant human DNAse) (Fuchs et al., 1994) and osmotic agents (e.g. saline) (Donaldson et al., 2006).

1.2.5.4 Protein Repair

An understanding of the molecular basis of CFTR mutations has led to the development of therapeutic treatment strategies based on the mutation classification. This type of therapy is known as ‘protein repair therapy’ (Zeitlin, 2007; Sloane and Rowe, 2010). There are two main classes of protein repair drugs available: ‘correctors’, which correct the localisation of CFTR

from the endoplasmic reticulum (ER) to the apical cell membrane, and 'potentiators' which increase the function of CFTR which is already correctly positioned at the apical cell membrane (Sloane and Rowe, 2010). The progress which is being made in finding potential compounds that target CFTR paves the way for targeted therapy of the molecular defect in the future.

1.2.5.5 Gene Therapy

Gene therapy involves insertion of healthy, functioning genes, into an individual's cells and biological tissues to replace malfunctioning genes, independent of the class of genetic mutation. As CF is essentially a monogenic disorder, it is a good candidate for gene therapy based treatment, and offers the hope of a cure for CF. Although the concept of gene therapy is straight forward, in practice gene therapy has proven to be particularly difficult, with the delivery of the gene to the lungs a complex task (Proesman et al., 2008). Despite this difficulty, clinical trials have achieved delivery of the gene to cells, but significant and long lasting effects on CFTR function have yet to be seen (Griesenbach and Alton, 2009; Burney and Davies, 2012; Griesenbach and Alton, 2013). The prospect of gene therapy correcting the defect in CF, and sustaining long-term effects remains a realistic hope for the future, with ongoing clinical trials examining the efficacy of a new formulation (Alton et al., 2013).

1.2.5.6 Lung Transplants

Bilateral lung transplantation is the predominant operative approach to end-stage CF lung disease. However, it is not an option that is available to every patient due to a shortage of organs available, with up to 25% of CF patients dying of progressive lung disease whilst awaiting lung transplantation (Quattrucci et al., 2008). Perioperative mortality is low, and CF recipients have significant survivals and functional benefits following transplantation. Three year-survival rates following lung transplantation in CF now stands at 70% in the UK, dropping to 50% at 10 years (Meachery et al., 2008). Whilst long term results post transplantation are good, increasing comorbidities and graft dysfunction occur with time (Meachery et al., 2008; Mordant et al., 2010).

1.2.6 *Prognosis and life expectancy*

With the advent of earlier and more aggressive treatments for underlying pulmonary and gastrointestinal disease, life expectancy continues to improve. Median life expectancy is now

41.5 years (UK CF Registry, 2013), a stark improvement compared to survival in the 1950's when life expectancy was just 5 years of age (Proesman et al., 2008).

1.2.7 *CFTR and the eye*

Active trans-epithelial transport of Cl^- is known to provide the driving force for subsequent osmotically driven fluid secretion, such as basal tear production (Yang et al., 2000; Dartt, 2002), and subretinal space volume regulation (Ueda and Steinberg, 1994). Abnormal secretion of Cl^-, caused by malfunctioning CFTR is the known pathogenesis of CF. To date, CFTR has been localised to human corneal (Itoh et al., 2000; Cao et al., 2010) and conjunctival epithelium (Itoh et al., 2000), corneal endothelium (Sun et al., 2001; Cao et al., 2010) and retinal pigment epithelium (Wills et al., 2000; Wills et al., 2001; Weng et al., 2002; Blaug et al., 2003) (Table 1.3).

The following sections review Cl^- transport across the corneal (section 1.2.1) and conjunctival epithelia (section 1.2.2), the corneal endothelium (section 1.2.3) and the RPE (section 1.2.4), and discuss the contribution of CFTR in ocular fluid regulation.

Table 1.3 CFTR in ocular epithelia

Reference	Sample	Method	Observations
Corneal Epithelium			
Itoh et al. (2000)	Human corneal cDNA	RT-PCR	CFTR mRNA expression confirmed
Al-Nakkash and Reinach (2001)	Rabbit corneal epithelial cells	RT-PCR	CFTR mRNA expression and function confirmed
Levin and Verkman (2005)	Wild type mice	Ocular surface PD in the presence of CFTR agonists and inhibitors	CFTR function identified
	Homozygous G551D-CFTR mutant mice		Evidence of CFTR involvement in ocular surface Cl^- transport
Cao et al. (2010)	Human corneal epithelial cells	RT-PCR, Western blot analysis, and IS	CFTR mRNA and protein expression confirmed CFTR expression highest at the apical membrane
Conjunctival Epithelium			
Itoh et al. (2000)	Human corneal cDNA	RT-PCR	CFTR expression confirmed
Turner and Candia (2001)	Rabbit and pig	IS and RT-PCR	CFTR expression confirmed
Shiue et al. (2002)	Rabbit	Western blot analysis, IS and RT-PCR	CFTR expression confirmed
Turner, Bernstein and Canada (2002)	Rabbit, rat and pig	Immunolocalization by staining with CFTR antibodies	CFTR expression confirmed and located to the apical surface in all three species
	Rabbit	RT-PCR	CFTR expression confirmed
Levin and Verkman (2005)	Wild type mice	Ocular surface PD in the presence of CFTR agonists and inhibitors	CFTR function identified
	Homozygous G551D-CFTR mutant mice		Evidence of CFTR involvement in ocular surface Cl^- transport

Corneal Endothelium			
Sun et al. (2001)	Human, rabbit and bovine endothelium	RT-PCR	CFTR expression confirmed in all samples
Sun and Bonanno (2002)	Cultured and fresh bovine corneal endothelial cells	Immunoprecipitation and indirect IS	CFTR protein expression confirmed and localized to the apical membrane
		Measuring Cl^- permeability with a CFTR agonist	CFTR localized to the apical membrane
Cao et al. (2010)	Human corneal cells	IS	CFTR expression confirmed
Retinal Pigment Epithelium			
Peterson et al. (1997)	Bovine Cells	RT-PCR, western blot analysis, and immuno-cytochemistry	CFTR expression confirmed and localized to the basal membrane
Wills et al. (2000)	Human foetal cells	Immuno-cytochemistry	CFTR expression confirmed
Wills et al. (2001)	Human adult cells	Immuno-cytochemistry and RT-PCR	CFTR expression confirmed
Weng et al. (2002)	Human adult cells	Western blot analysis and RT-PCR	CFTR expression confirmed and localized to the apical membrane and the lateral cell margins of the basal membrane
Blaug et al. (2003)	Human foetal cells	Immuno-histochemistry by western blot analysis and electrophysiology	CFTR expression confirmed and located to the basal and apical membranes, though dominant functional effect at the basolateral membrane
Loewen et al. (2003)	Canine Cells	Ussing chamber electrophysiology	CFTR contribution to Cl^- and fluid transport indicated

Key: cDNA, complementary DNA; RT-PCR, reverse transcription polymerase chain reaction; PD, potential difference; IS, immunofluorescence staining; mRNA, messenger RNA.

1.2.7.1 Chloride transport across the corneal epithelium

Historically, the function of the corneal epithelium has been that of a protective barrier, with no role in fluid transport and no capacity to contribute to the maintenance of corneal deturgescence. However, it is now accepted that the corneal epithelium has comparatively large osmotic and diffusional permeabilities (Fischbarg and Montoreano, 1982), along with Cl^- secretory mechanisms (Klyce and Crosson, 1985). Hence the corneal epithelium participates in the regulation of corneal hydration and maintainence of corneal clarity.

Cl^- secretion provides the primary driving force to elicit osmotic movement of water across the apical membrane of the corneal epithelium into the tear film. The basolateral membrane of the corneal epithelium contains the Na^+:K^+:2Cl^- co-transporter, which functions in parallel with the Na^+:K^+ pump to cause Cl^- influx. The rate of Cl^- influx at the basolateral membrane is regulated by the chloride conductance at the apical membrane. Cl^- channels located to the apical membrane of the human corneal epithelium and involved in Cl^- efflux include CFTR (Al-Nakkash and Reinach, 2001; Levin and Verkman, 2006; Cao et al., 2010), and the calcium activated chloride channel, CLCA2 (Itoh et al., 2000) (Figure 1.3). Current evidence suggests that CFTR has a functional involvement in ocular surface Cl^- secretion (Levin and Verkman, 2005). Recently, Cao et al. 2010, discovered through the use of reverse transcription polymerase chain reaction (RT-PCR), Western blot and immunofluorescence staining (IS) that human corneal epithelial cells also express the chloride channel (ClC) family of voltage gated Cl^- channels ClC-2, ClC-3, ClC-4, ClC-6 (Cao et al., 2010).

Aquaporins (AQPs) are believed to provide the principle pathway for water transport across the corneal epithelium (Levin and Verkman, 2006). AQP5, a water-selective aquaporin, and AQP3, a water-and glycerol-transporting aquaglyceroporin, expression has been identified in the corneal epithelium (Levin and Verkman, 2006). AQP5 appears to provide a significant epithelial pathway for stromal water uptake and extrusion, with one study showing that AQP5-deficient corneas are approximately 20% thicker than wild-type corneas (Levin and Verkman, 2004).

The expression patterns of AQPs and CFTR, along with other Cl^- channels in the corneal epithelium, suggest their involvement in tear film homeostasis. Thus, it is hypothesised that dysfunction of CFTR may cause deficient tear volume, and thus symptoms of dry eye in CF patients.

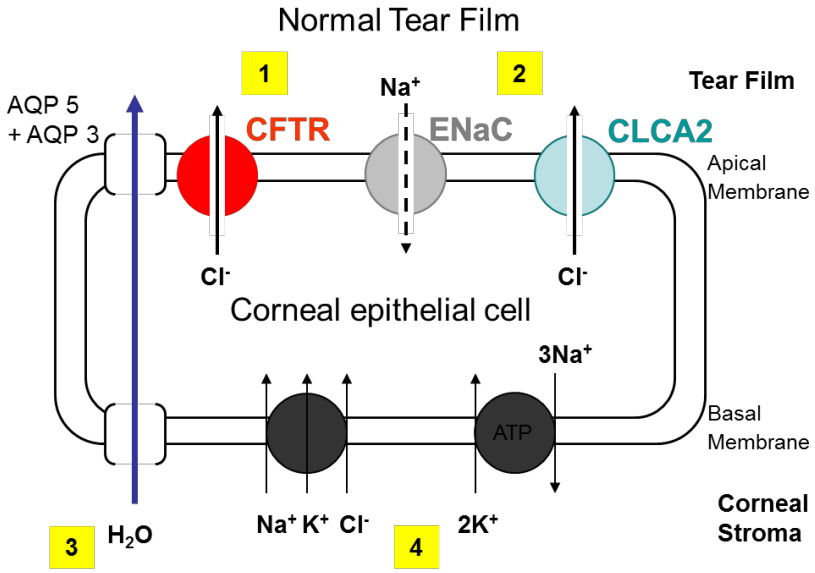

Figure 1.3 A simplified diagram showing the ion channels involved in electrolyte and water movement across the corneal epithelium. Efflux of Cl^- via CFTR and CLCA2 on the apical membrane (1), together with Na^+ influx via ENaC (2) causes H_2O to move out of the corneal stroma into the tear film via AQP5 and AQP3 (3). The basolateral Na^+:K^+:2Cl^- co-transporter and Na^+:K^+ pump load the epithelial cell with Cl^- (4) to maintain the electrochemical driving force for Cl^- efflux at the apical membrane.

1.2.7.2 Chloride transport across the corneal endothelium

Maintenance of corneal transparency requires precise regulation of corneal hydration to ensure regular organisation of collagen fibres (Sun and Bonanno, 2002). As the corneal stroma has a tendency to swell, the corneal endothelium must continuously secrete water out of the cornea to maintain transparency.

Transendothelial fluid secretion is dependent on the presence of HCO_3^- (Hodson, 1974; Riley et al., 1997) and Cl^- (Winkler et al., 1992; Riley et al., 1997) within the corneal endothelial cells. HCO_3^- and Cl^- are loaded into corneal endothelial cells from the stroma by basolateral endothelial membrane co-transporters Na^+:2HCO_3^- (Jentsch et al., 1984), and Na^+:K^+:2Cl^- (Jelamskii et al., 2000), respectively. This causes the intracellular concentration of Cl^- and HCO_3^- to rise above the electrochemical equilibrium (Sun et al., 2003), suggesting there is potential for apical anion efflux through anion channels (Sun et al., 2001). The mechanisms involved in Cl^- and HCO_3^- secretion at the apical membrane are yet to be fully elucidated. However, research suggests that chloride channels, including CFTR, CLCA1, and the anion

exchanger Cl^-/HCO_3^- (Bonanno et al., 1998; Shepard and Rae, 1998; Sun et al., 2001), contribute to the secretion and absorption of Cl^- and HCO_3 (Figure 1.4).

Despite the different roles of the corneal epithelium and endothelium in corneal homeostasis, they share expression of at least seven different Cl^- channel mRNAs (Davies et al., 2004). This finding may suggest that no particular Cl^- channel has a key role in epithelial or endothelial fluid transport, although this has yet to be discovered. AQPs (AQP1) are also expressed in the corneal endothelium, facilitating the movement of water down the osmotic gradient (Thiagarajah and Verkman, 2002).

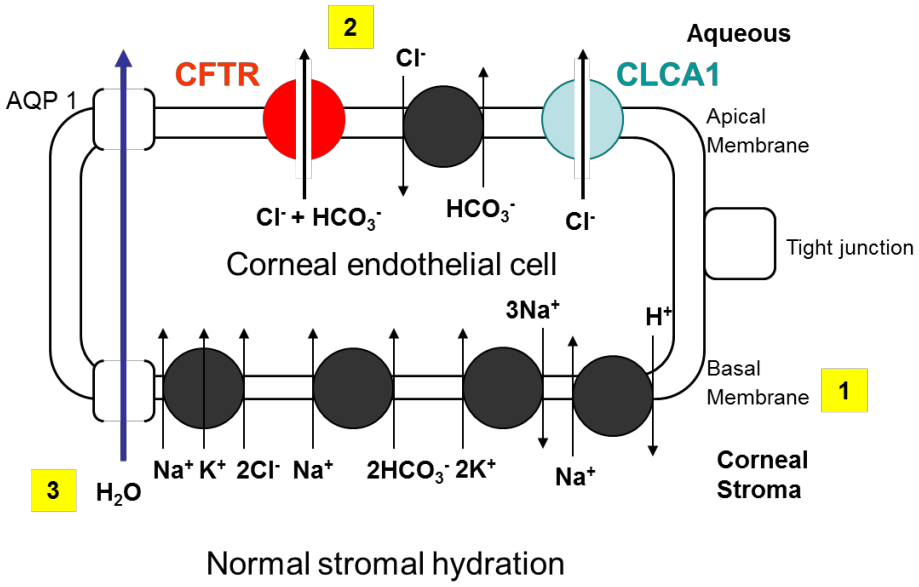

Figure 1.4 A simplified diagram showing the ion channels involved in electrolyte and water movement across the corneal endothelium. Cl^- and HCO_3^- are loaded into the endothelial cell across the basolateral membrane via the Na^+:K^+:$2Cl^-$ and Na^+:$2HCO_3^-$ co-transporters respectively (1). Efflux of Cl^- and HCO_3^- at the apical membrane via CFTR, CLCA1 and the HCO_3^-/Cl^- exchanger, occurs down the electrochemical gradient (2), and generates an osmotic gradient for H_2O, drawing it out of the stroma and into the aqueous via AQP1 (3).

1.2.7.3 Chloride transport across the conjunctival epithelium

The conjunctival epithelium lines the exposed surface of the sclera (bulbar conjunctiva), and eyelids (palpebral conjunctiva) and is a mucus-secreting stratified epithelium. Electrolyte and accompanying fluid transport by conjunctival cells may contribute to and be important in the maintenance of the ocular tear film.

The Na^+:K^+:2Cl^- co-transporter and the Na^+:K^+ pump mediate Cl^- influx at the basolateral membrane of conjunctival epithelial cells in order to maintain intracellular Cl^- above equilibrium (Turner et al., 2000; Turner and Candia, 2001), a property which is necessary to allow apically directed efflux. CFTR, which has been localised to the apical surface of bulbar and palpebral conjunctival epithelia (Turner et al., 2002), then facilitates Cl^- efflux (Figure 1.5). Voltage gated chloride channels ClC-1, ClC-2, ClC-3, ClC-4, ClC-6 and ClC-7 have been identified in the conjunctival epithelium, along with CLCA2 (Itoh et al., 2000), which may contribution to Cl^- transport. An outwardly-rectifying chloride channel (ORCC), which is modulated by CFTR, may also be present in the conjunctival epithelium (Itoh et al., 2000) and be involved in Cl^- transport. Active movement of Cl^- out of the conjunctival epithelial cells creates an osmotic gradient, drawing H_2O out of the cell and into the tear film.

AQP3 is expressed in the conjunctival epithelium (Hamann et al., 1998; Levin and Verkman, 2004), providing a pathway for the movement of water into and out of the conjunctival epithelial cell. However, Levin and Verkman (2004), found that osmotically induced water movement across the conjunctiva was not AQP3 dependent, and concluded that AQP3-facilitated water transport does not play a role in transconjunctival fluid movement.

The conjunctival epithelium has sufficient water permeability and the transporters necessary to significantly contribute to production of the tear film (Levin and Verkman, 2006). As CFTR plays a role in electrolyte transport across the conjunctival epithelium, it is possible that it has a direct effect on tear secretion (Levin and Verkman, 2005), and therefore malfunction may contribute to conditions such as dry eye (Dartt, 2002).

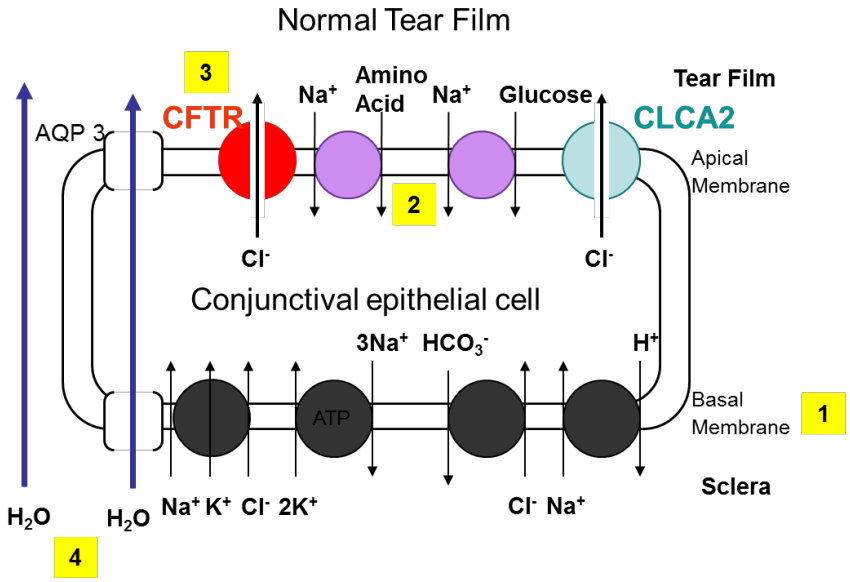

Figure 1.5 A simplified diagram showing the ion channels involved in electrolyte and water movement across the conjunctival epithelium. At the basolateral membrane, the Na^+:K^+:$2Cl^-$ co-transporter and the Na^+:K^+ pump mediate Cl^- influx (1) in order to maintain intracellular Cl^- above equilibrium. At the apical membrane, Na^+ is transported into the cell via Na^+-glucose and Na^+-amino acid co-transporters (2). Cl^- moves out of the cell across the apical membrane via CFTR and CLCA2 down the electrochemical equilibrium (3). This generates an osmotic gradient for H_2O, drawing it out of the stroma and into the tear film via AQP3, and other pathways (4).

1.2.7.4 Choride transport across the RPE

The RPE is a monolayer of densely packed hexagonal cells that forms a diffusion barrier between the photoreceptors in the retina and the choroidal blood supply. The apical membrane of the RPE is separated from the photoreceptors by the subretinal space (SRS), which is occupied by the inter-photoreceptor matrix (IPM). The IPM is an integral part of the retina, permitting communication between the RPE and the photoreceptors. It may also play a part in photoreceptor maintenance. It is the responsibility of the RPE to regulate the transport of metabolites, electrolytes and fluid between the IPM and the choroidal blood supply. This movement of ions is essential in maintaining the correct chemical composition and volume of the SRS and the extraceullular choroidal space (Marmor and Wolfensberger, 1998; Strauss, 2005). Studies on RPE epithelial cells indicate Cl^- transport across the RPE is important in several RPE functions, including fluid absorption (Miller and Edelman, 1990), volume

regulation (Ueda and Steinberg, 1994), and ligand-regulated ion and fluid transport (Peterson et al., 1997).

Current evidence suggests Na^+-K^+-ATPase activity at the apical membrane of RPE cells generates a Na^+ gradient across the membrane. Na^+/HCO_3^- co-transporter is also present at the apical membrane (Hughes et al., 1989). High levels of extraceullular Na^+ are then able to drive the uptake of Cl^- and K^+ against the concentration gradient, via a coupled Na^+-K^+-$2Cl^-$ co-transporter located at the apical membrane, and via a Cl^-/HCO_3^- exchanger at the basolateral membrane. This mechanism allows concentrations of intracellular K^+ and Cl^- to be maintained above equilibrium. Movement of Cl^- out of the RPE cell occurs at the basolateral membrane via CFTR and CLCA1 down the electrochemical gradient. Cl^- conductance at the basolateral membrane is believed to be controlled by intracellular levels of secondary messenger molecules including cAMP (Hipper et al., 1995) and Ca^{2+} (Ueda and Steinberg, 1994) (Figure 1.6). Cl^- efflux is accompanied by the outward flow of Na^+ in order to maintain electroneutrality. The direction of fluid transport across the RPE is dependent upon the relative magnitude of the absorptive and secretory Cl^- fluxes, with water passively following the net movement of Cl^- ions, due to the generated osmotic forces. Cl^- secretion at the basolateral membrane is initiated by endogenously generated ATP, which initiates purinergic signalling at the $P2Y_2$ receptor on the apical membrane. Signalling triggers elevation of Ca^{2+} within RPE cells, which likely causes an increase in basolateral Cl^- conductance, generating flux of ions and fluid across the RPE at a higher rate (Peterson et al., 1997). It has been postulated that CFTR enhances RPE fluid transport indirectly by generating the ATP needed to induce the autocrine purinergic signalling (Reigada and Mitchell, 2005).

Expression of CFTR has been reported in human RPE cells, along with CLCA1 and the ClC chloride channels ClC-2, ClC-3 and ClC-5 (Miller et al., 1992; Wills et al., 2000; Blaug et al., 2003). ClC-3 and ClC-5 have been principally detected at the apical membrane of the RPE (Weng et al., 2002). Evidence suggests that the ClC family of voltage gated chloride channels may be crucial for retinal function, with transgenic mice deficient in ClC-2, ClC-3 or ClC-7 shown to develop retinal degenerations and blindness (Bosl et al., 2001; Kornak et al., 2001; Stobrawa et al., 2001), though the pathogenesis is yet to be elucidated. ENaC has also been discovered throughout the RPE, however, it's function is not yet fully understood (Golestaneh et al., 2000). As in the cornea and conjunctiva, AQPs are also present in the human RPE.

AQP1 has been localised to human RPE cells by immunofluorescence (Stamer et al., 2001), though its function in the RPE remains unknown.

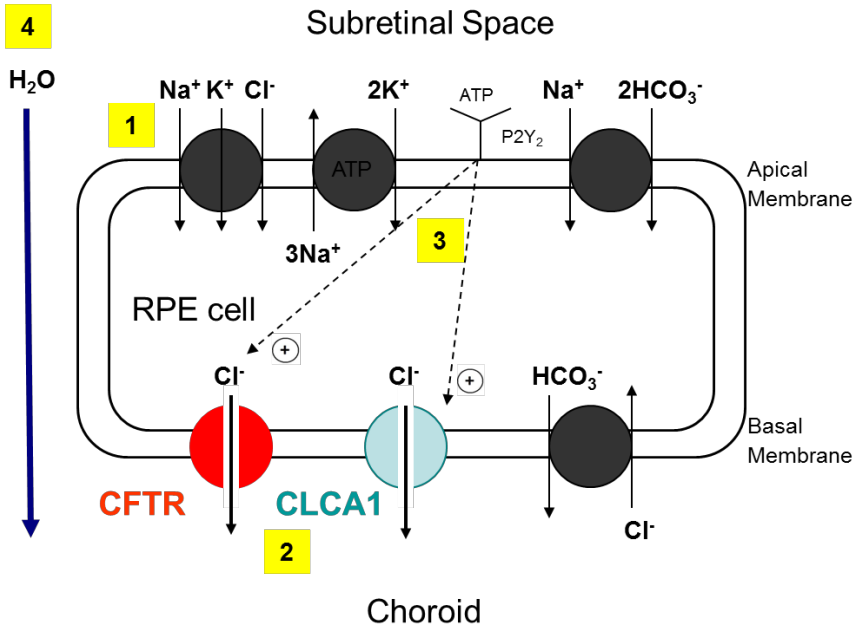

Figure 1.6 A simplified diagram showing the ion channels involved in electrolyte and water movement across RPE cells. Na^+-K^+-ATPase activity at the apical membrane generates a Na^+ gradient across the membrane (1), driving the uptake of Cl^- and K^+ against the concentration gradient, via a coupled Na^+-K^+-$2Cl^-$ co-transporter at the apical membrane, and via a Cl^-/HCO_3^- exchanger at the basolateral membrane. Movement of Cl^- out of the RPE cell occurs at the basolateral membrane via CFTR and CLCA1 down the electrochemical gradient (2). ATP enhances Cl^- efflux through purinogenic signalling via $P2Y_2$ (3). H_2O follows the net movement of Cl^- out of the cell due to the generated osmotic forces (4).

1.2.8 *Ocular Features of Cystic Fibrosis*

To date, numerous studies have investigated and reported upon the ocular abnormalities associated with CF. Whilst these studies provide valuable insight into the scope of the ocular abnormalities associated with CF, many were conducted prior to the discovery of CFTR within the eye. They were therefore unable to discuss the possibility of the abnormalities being a primary manifestation of the disorder; due to CFTR malfunction. Rather, the defects were generally believed to be secondary manifestations of CF, including VAD and CFRD. Herein follows a comprehensive review of current literature available on the ocular abnormalities associated with CF, along with discussion of the probable cause of the ocular defect. Due to the

nature of this study, particular emphasis will be given to the complications observed in the posterior segment.

1.2.8.1 Anterior Eye

1.2.8.1.1 Blepharitis

There is a significant degree of variance in the reported frequency of clinically significant blepharitis in CF between different studies (Table 1.4). Although all studies show an increased prevalence of blepharitis in CF subjects compared to controls, the difference only reached significance in two studies, and cohort numbers were small in all cases. Shepphard et al. (1989) suggested that the prevalence of blepharitis within their study may have been even more pronounced without the use of antimicrobial antibiotics, which are commonly used in CF, and were being used at the time of examination by 60% of the cohort. It is suggested that an increased prevalence of blepharitis in the CF population may be indicative of lipid dysfunction, which could contribute to ocular surface abnormalities (Sheppard et al., 1989; Mrugacz, Tobolczyk and Minarowska, 2005b). Lipid abnormalities, most likely caused by meibomian dysfunction, is consistent with a generalised glandular defect in CF (Sheppard et al., 1989).

Table 1.4 Frequency of blepharitis in CF

Authors	Subjects	Frequency	Statistical significance
Sheppard et al. (1989)	17 CF 17 Controls	88% CF 29% Controls	**p = 0.001**
Kalayci et al. (1996)	23 CF 20 Controls	13% CF 5% Controls	NS*
Mrugacz et al. (2005b)	15 CF 15 Controls	60% CF 7% Controls	**p = 0.032**
Mrugacz et al. (2007a)	24 CF 24 Controls	21% CF 17% Controls	NS*
Mrugacz et al. (2007b)	25 CF 25 Controls	20% CF 16% Controls	NS*
Evans (2009)	30 Juvenile CF 30 Juvenile Controls	29% Juvenile CF 7% Juvenile Control	p = 0.347
	28 Adult CF 28 Adult Controls	28% Adult CF 18% Adult Control	p = 0.422

Key: NS, not significant; *, no p-values stated; bold and shaded cells indicate significance

1.2.8.1.2 The tear film

The production and turnover of the preocular tear film is essential in providing tissues with the necessary nourishment and lubrication in order to maintain ocular health (Tiffany, 2008). Classically, the tear film is reported to consist of three layers: an outer lipid layer, a middle aqueous layer and an inner mucous layer. Each individual component of the tears is important, with a deficiency or abnormality in any one layer causing problems leading to dry eye (Rolando and Zierhut, 2001). The lipid layer, which is secreted primarily by the meibomian glands, is essential in providing a smooth optical surface for the cornea and in retarding evaporation of aqueous from the eye (Mishima and Maurice, 1961; Bron et al., 2004). The aqueous layer, which is composed of proteins, electrolytes, enzymes, metabolites and water (Mrugacz et al., 2005b) is principally thought to be produced by the lacrimal and accessory lacrimal glands, though a small proportion of electrolytes and water is secreted by the cornea and conjunctiva, via ion channels (Levin and Verkman, 2006). CFTR channels in the cornea and conjunctiva may contribute to aqueous tear production as it has been seen to be a major

pathway for Cl^- and subsequent water secretion (Levin and Verkman, 2005). Conjunctival goblet cells are responsible for secreting the majority of the mucins required to produce the inner-most mucous layer which is necessary to facilitate wetting of the cornea and thus allow tear film adherence (Tiffany, 2008).

Tears can be classified as either reflex or basal, depending on the secretion type. Reflex tears are produced in response to an irritant which stimulates secretion mainly by the lacrimal gland. Basal tear secretion occurs normally without the need for stimulation. Basal tears were originally believed to be produced mainly from the accessory glands of Krause and Wolfring, however, more recent evidence suggests that corneal and conjunctival epithelial fluid transport may also be of importance in basal tear production (Shiue et al., 2000; Yang et al., 2000; Li et al., 2001b; Candia, 2004).

1.2.8.1.2.1 ***Dry eye***

Dry eye can be divided into two sub groups; tear deficiency or evaporative, depending on the mechanism of tear disruption (Kaercher and Bron, 2008). The causes of dry eye are multifactorial and can be related to deficiencies in any of the three components of the tear film (Baudouin, 2001). Inflammation is known to play an important role in pathogenesis of dry eye (Baudouin, 2001; Pflugflder, 2004). Diagnosis of dry eye is based upon the patient's history and symptoms along with the application of specific tests including ocular surface staining with fluorescein, lissamine green or rose bengal, Schirmer's, tear break up time (TBUT), tear ferning and impression cytology. Some of these techniques have been used to evaluate tear volume and quality in CF patients, with widely varying results being obtained (Table 1.5).

Several studies report increased prevalence of sodium fluorescein staining in CF subjects compared to controls (Botelho, Goldstein and Rosenlund, 1973; Sheppard et al., 1989; Kalayci et al., 1996; Mrugacz et al., 2005b). However, this difference only reached significance in one case (Sheppard et al., 1989). In this instance, it was suggested that the most likely cause for the increased prevalence of corneal fluorescein staining was aqueous deficiency (Sheppard et al., 1989). An increased prevalence of abnormal Schirmer's test result in CF subjects compared to controls, as found in four studies (Sheppard et al., 1989; Mrugacz et al., 2005a; Mrugacz et al., 2007a; Mrugacz et al., 2007b), further suggests that CF patients suffer from aqueous tear deficiency. Castagna et al. (2001), found that Schirmer's test results and TBUT were correlated to the vitamin A status of patients, with subjects who had more severe vitamin A deficiency

(VAD) having lower levels of wetting and reduced TBUTs. These results would suggest that VAD is the cause of a reduction in aqueous tear secretion in CF, yet, reduced tear section levels have also been noted in CF subjects who were vitamin A sufficient (Morkeberg et al., 1995; Mrugacz et al., 2007a; Mrugacz et al., 2007b).

Given the evidence of tear film abnormalities and dry eye in patients with CF, both with and without VAD, and in light of the localisation of CFTR to the conjunctival and corneal epithelium, it is highly possible that dry eye is a primary manifestation of CF. Additional evidence from tear ferning studies which have found abnormal tear ferning patterns in CF, believed to be caused by altered electrolyte levels in the tears, also adds strength to this theory (Rolando, Baldi and Calabria, 1988; Kalayci et al., 1996; Evans, 2009). As survival rates continue to improve, eye care practitioners may begin to see more CF patients developing signs and symptoms of dry eye later in life.

Table 1.5 Dry eye in CF

Authors	Subjects	Tests Conducted	Observations	Statistical Significance
Sheppard et al. (1989)	17 CF 17 Controls	Schirmer's	Wetting after 5 minutes with anaesthetic: 9.5mm CF; 16mm Controls.	**p = 0.002**
		TBUT	Mean (seconds): 17 CF; 17 Controls	NS*
		Fluorescein staining	Frequency: 82% CF; 11.8% Controls	**p = 0.002**
		Rose Bengal staining	Frequency: 19.4% CF; 14.3% Controls	NS*
		Copenhagen	Frequency of dry eye: 18% CF, 12% Controls	-
Morkeberg et al. (1995)	25 CF 0 Controls	Schirmer's	31% CF abnormal (Where abnormal is defined as less than 5mm wetting in 5 minutes)	-
		TBUT	49% CF reduced (Reduced TBUT defined as less than 10 seconds)	-
		Rose Bengal	23% CF showed increased staining	-
		Copenhagen	Frequency of dry eye: 26% CF	-
Kalayci et al. (1996)	13 CF 19 Controls	Schirmer's Test	Wetting in 5 minutes without anaesthetic: 19.1mm CF, 23.1mm Controls	NS*
		Fluorescein staining	Frequency: 9% CF 0% Controls	NS*
Ansari et al. (1999)	28 CF 25 Controls	Rose Bengal staining	Frequency: 7% CF 0% Controls	-
		Schirmer's	Frequency of abnormality: 0% CF, 0% Controls	-
		TBUT	Frequency of reduced TBUT: 7% CF, 0% Controls	-
		Copenhagen	Frequency of dry eye: 7.1% CF	-
Castagna et al. (2001)	40 CF 24 Controls	Schirmer's	Reduced wetting in CF subjects	-
		TBUT	Reduced TBUT in CF, worse with VAD	-

Mrugacz et al. (2005b)	15 CF 15 Controls	Fluorescein staining	Frequency: 60% CF, 13.3% Controls	NS*
		Schirmer's	Frequency of abnormality: 33.3% CF, 0% Controls	NS*
		TBUT	Frequency of reduced TBUT: 53.5% CF, 13.3% Controls	NS*
		Copenhagen	Frequency of dry eye: 33.3% CF, Controls not noted	-
Mrugacz et al. (2005a)	18 CF 18 Controls	Schirmer's	Frequency of abnormality: 81% CF	**Yes***
Mrugacz et al. (2007b)	25 CF 25 Controls	Schirmer's	Wetting in 5 minutes without anaesthetic: 9.68mm CF, 25.21mm Controls	**p < 0.0001**
		TBUT	Mean (seconds): 5.3 CF, 9.9 Controls	**p < 0.0001**
		Copenhagen	Frequency of dry eye: 48% CF, Controls not noted	-
Mrugacz et al. (2007a)	24 CF 24 Controls	Schirmer's	Wetting in 5 minutes without anaesthetic: 9.65mm CF, 25.15mm Controls	**p < 0.001**
		TBUT	Mean (Seconds): 5.4 CF, 9.7 Controls	**p < 0.0001**
Evans (2009)	58 CF 58 Controls	NIBUT	Marginally reduced in CF juveniles and adults	p = 0.357; p = 0.509
		FBUT	Marginally reduced in CF juveniles and adults	p = 0.154; **p < 0.05**
		Fluorescein staining	Frequency: 25% juvenile CF, 22% controls 53% Adult CF, 32% controls	p = 0.794; p = 0.079

Key: NS, not significant; *, p-value not stated; -, statistical tests not performed; TBUT, tear break-up time; NIBUT, non-invasive tear break-up time; FBUT, fluorescein tear break-up time; Copenhagen criterion, standard used to confirm presence or absence of dry eye based on two abnormal findings from TBUT, rose bengal and schirmer's; bold and shaded cells indicate significance.

1.2.8.1.3 Xerophthalmia

Xerophthalmia refers to the entire clinical spectrum of ocular manifestations caused by VAD (Suan et al., 1990). It is the leading cause of childhood blindness worldwide, but is uncommon in developed countries (Sommer, 1998). The primary manifestation of xerophthalmia is extreme dryness of the conjunctiva and cornea due to failure of the secretory activity of the conjunctival goblet cells. Xerophthalmia also encompasses night blindness, retinopathy, Bitot spots and corneal ulceration or keratomalacia (Brooks et al., 1990). Early descriptions of CF found a high prevalence of xerophthalmia (Gamble, 1940; Phillipsborn, Lawrence and Lewis, 1944), however, with improvements in vitamin A supplementation, reports of xerophthalmia in CF were described as 'almost eliminated' in the 1990s (Brooks et al., 1990). Nevertheless, in a study carried out in 2000, mild xerophthalmia was noted in 71% of CF subjects examined (Tsinopoulos et al., 2000). In cases of adequate vitamin A supplementation in CF patients who present with xerophthalmia, it is likely that vitamin A levels are still reduced due to a combination of poor adherence to therapy, CF associated liver disease and liver malabsorption (Campbell et al., 1998).

Conjunctival xerosis (Figure 1.7) presents as dryness of the conjunctiva in the interpalpebral zone with loss of goblet cells and squamous metaplasia. This finding has previously been noted during slit lamp examination of CF subjects in many case studies (Sommer, 1989; Vernon et al., 1989; Brooks et al., 1990; Campbell et al., 1998). In all instances conjunctival xerosis was associated with low vitamin A levels, and signs, along with any associated symptoms were resolved upon increasing vitamin A supplementation.

Whilst reports of xerophthalmia are now less commonplace due to vast improvements in nutritional supplementation, previous findings highlight the importance of considering VAD in CF patients who present with ocular complications (Campbell et al., 1998). It also demonstrates the importance of regular eye examinations for those with CF, with any patients found to have conjunctival or corneal xerosis being referred on for further ophthalmological assessment including dark adaptation (DA) and/or electoretinography to confirm clinical vitamin A deficiency before treatment is commenced (Vernon et al., 1989).

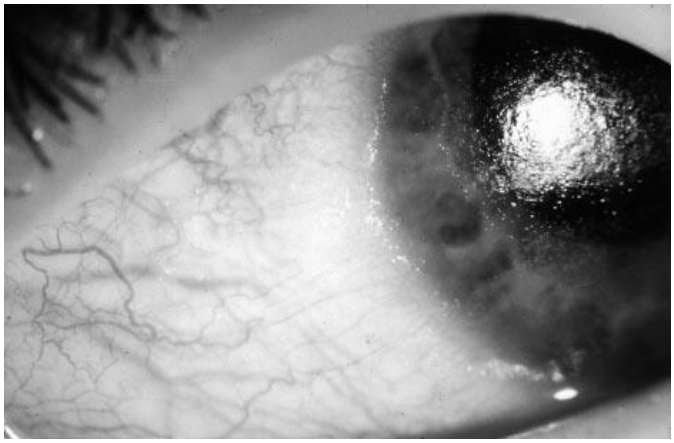

Figure 1.7 Conjunctival and corneal xerosis with punctuate epithelial keratopathy and corneal haze. Image from Campbell et al. (1998)

1.2.8.1.4 The cornea

CFTR expression has previously been localised to the apical membrane of the corneal endothelium (Sun et al., 2001; Sun and Bonanno, 2002; Cao et al., 2010), where it is known to facilitate fluid efflux in order to maintain corneal desturgesence (Sun et al., 2001). It is therefore reasonable to predict that loss of CFTR function in CF could cause an increase in corneal thickness and a decrease in transparency, unless other Cl^- channels provide a certain level of compensation. To date, only two studies have been identified which have investigated corneal thickness in CF, with conflicting results being found. The older study found corneal thickness to be increased in CF, as determined using corneal video specular microscopy (Lass et al., 1985). Conversely, the most recent study which used the Oculus Pentacam, found no significant difference in either central or peripheral corneal thickness in CF subjects compared to healthy controls (Evans, 2009). This lack of increase in corneal thickness in CF may indicate that there is a certain degree of corneal endothelial compensation for CFTR dysfunction in CF by other Cl^- channels. Morphological changes including reduced endothelial cell area, increased endothelial cell density, increased endothelial cell permeability and increased relative endothelial pump rate (Lass et al., 1985) may also compensates for impaired Cl^- transport via CFTR. Further investigations are needed to give a more detailed view of corneal changes in CF

1.2.8.2 <u>The Posterior Eye</u>

1.2.8.2.1 The Crystalline lens

Crystalline lens transparency has been reported to be significantly reduced in CF subjects (Fama et al., 1998; Castagna et al., 2001), when measured with Opacity Lens Meters, despite

slit lamp examinations reveal no clinical signs of cataract. Lens transparency in CF has been correlated to the level of digestive insufficiency, with those patients with the most severe digestive insufficiency having the most reduced levels of lens transparency (Fama et al., 1998). A decrease in lens transparency has also been associated with an increase in the level of conjunctival xerosis (Fama et al., 1998; Castagna et al., 2001). Additionally, measures of maximal lens density and anterior lens thickness have been found to be higher in CF subjects compared to controls (Evans, 2009).

The occurrence of cataract is known to be associated with reduced intake of vitamins and minerals, with vitamins C and E providing a protective function against cataract development and progression (Varma et al., 1984; Leske, Chylack and Wu, 1991; Chiu and Taylor, 2007). Therefore, reduced lens transparency in CF may be due to vitamin deficiency secondary to malabsoprtion of nutrients caused by pancreatic insufficiency. The role of oxidative stress in the etiology of cataract formation has also been clearly established (Chiu and Taylor, 2007). Persistent pulmonary infection in CF is known to increase the levels of oxidative stress (Brown and Kelly, 1994). This, combined with decreased levels of antioxidants which usually protect the crystalline lens (Fama, Castagna and Salmeri, 1993), will contribute to the development of decreased lens transparency in CF. Fama et al. (1998) postulated that low concentrations of vitamin A in the aqueous humour of CF patients could induce a lowering of ascorbic acid concentration in the aqueous humour and lens, which may precipitate a reduction in lens transparency.

Diabetes and steroid use are known risk factors for the development of cataract in the normal population (Hollister and Bowyer, 1987; Klein, Klein and Lee, 1998; Beneyto et al., 2007). Development of posterior subcapsular cataracts following administration of prednisone in CF patients has previously been documented (Majure, Mroueh and Spock, 1989). One study which investigated the effect of CFRD on lens density whilst there was a trend towards increased lens density in CFRD compared to controls, statistical significance was not reached (Evans, 2009).

To date, whilst chloride ion currents have been recognised, the presence of CFTR has not been detected in the lens epithelium and fluid transport within the lens remains widely uncharacterised (Candia, 2004); therefore, it is impossible to speculate whether reduced lens transparency in CF is a primary manifestation of the disorder. Reduced lens transparency in

CF is most likely attributed to a combination of vitamin deficiency and increased levels of oxidative stress, along with CFRD and steroid use.

1.2.8.2.2 Diabetic retinopathy in CFRD

Previously, due to the increased mortality of CF patients with CFRD, life expectancy was considered to be too short for the development of diabetic complications, including diabetic retinopathy. However, increasing longevity of CF patients has been accompanied by increasing reports of microvascular complications (Dolan Jr, 1986; Sullivan and Denning, 1989).

The frequency of diabetic retinopathy (DR) in CFRD, as found in several studies, is outlined in Table 1.6. DR in CFRD is predominantly seen in patients with a duration of diabetes of at least 10 years (Yung et al., 1998; Andersen et al., 2006; Schwarzenberg et al., 2007). DR has generally been reported to be less common in CFRD than in type 1 and 2 diabetes (Fong et al., 2004). One study found the frequency of DR in type 1, insulin dependent diabetics, to be 60% after 10 years duration, in comparison to 16-36% frequency after 10 years in CFRD patients (Yung et al., 1998; Andersen et al., 2006; Schwarzenberg et al., 2007). In a study by van den Berg et al. (2008), microvascular complications were examined in CFRD patients who were matched to type 1 diabetics for age and duration of insulin dependence (van den Berg et al., 2008). Retinopathy was present in 10% of CFRD patients, in comparison to 24.3% of type 1 diabetics, providing a statistically significant difference. Several factors may account for the reduced frequency of retinopathy in CFRD; firstly, hyperglycaemia is less severe in CFRD as patients retain variable degrees of endogenous insulin secretion. Secondly, there appears to be a role for dislipoproteinemia in the pathogenesis of DR (Lyons et al., 2004), but cholesterol levels are low in CF. Van den Berg (2008), concluded that the difference in frequency of retinopathy was best explained by the tendency towards better diabetic control in CF patients.

In light of increasing life expectancy in CF, more patients are likely to develop CFRD, and associated diabetic changes, including DR. It is therefore prudent that the importance of regular ocular screening for all patients with CFRD is stressed. Andersen et al. (2008), suggested that CFRD patients follow identical retinopathy screening programmes as patients with type 1 diabetes.

Table 1.6 Frequency of DR in CFRD

Author and Year	CFRD patients examined	Frequency of DR
Rodman, Doershuk and Roland (1986)	24 Unknown treatment	2 subjects (8.3%) had DR; 1 background, 1 maculopathy
Sullivan and Denning (1989)	19 All insulin treated	3 subjects (15%) had DR, all of which progressed to proliferative DR
Lanng et al. (1994)	41 70% of patients on insulin	2 subjects (4.9%) had DR; both background
Yung et al. (1998)	32 All insulin treated	5 subjects (15.6%) had DR; 3 background, 1 proliferative and 1 maculopathy. 16% incidence DR in CFRD duration ≥ 5 years; 23% incidence DR in CFRD duration ≥ 10 years
Andersen et al. (2006)	38 All insulin treated	9 subjects (23.7%) had DR; 6 mild, 1 moderate, 2 proliferative. 36% incidence DR in CFRD duration ≥ 10 years
Schwarzenberg et al. (2007)	84 CFRD FH+ All insulin treated 57 CFRD FH- Majority not insulin treated	6 subjects (7%) with CFRD FH+ had DR; 16% incidence of DR in CFRD FH+ duration > 10 years 0 CFRD FH- subjects had DR
van den Berg et al. (2008)	79 All insulin treated	7 subjects (10%) had DR

Key: DR, diabetic retinopathy; CFRD, CF-related diabetes; CFRD FH+, CFRD with fasting hyperglycaemia; CFRD FH-, CFRD w ithout fasting hyperglycaemia.

1.2.8.2.3 Macular pigment density

Although supplementation of the major vitamins is common practice in patients with CF, carotenoids are often neglected, resulting in low carotenoid concentrations (Winklhofer-Roob et al., 1996; Rust et al., 2000). Carotenoids, including lutein and zeaxanthin, are antioxidant micronutrients (Krinsky and Yeum, 2003), and are particularly important in CF patients who,

due to persistent pulmonary infection, are susceptible to higher levels of oxidative stress (Brown and Kelly, 1994).

Lutein and zeaxanthin accumulate at the macula and are believed to play a major part in protecting the retina from free-radicals, by absorbing the phototoxic effects of short-wavelength light and through their action as free radical scavenging antioxidants (Snodderly, 1995; Mitchell et al., 2002c). Previously, it has been discovered that low plasma concentrations of lutein and zeaxanthin is associated with an increased incidence of macular degeneration (Marse-Perlman et al., 2001). Additionally, patients with macular degeneration have been reported to have 32% lower concentrations of macular pigment (a measure which is related to macular carotenoid levels), compared to normals (Bernstein et al., 2002). As CF patients are known to have a low concentration of carotenoids, along with increased levels of oxidative stress, it is postulated that their serum levels of carotenoids would be reduced. CF patients would therefore be more likely to exhibit an acceleration of normal age-related changes in visual function.

Schupp et al. (2004) investigated these hypotheses by measuring the plasma and retinal concentrations of lutein and zeaxanthin, and their correlation with visual performance in CF subjects (n=10; aged 21-47 years). CF subjects were found to have significantly lower serum concentrations of lutein and zeaxanthin compared to normal controls, with these low concentrations correlating with low retinal concentrations at all retinal locations, as measured by macular pigment density. However, the severe degree of retinal carotenoid depletion was not associated with any visual abnormalities as tested by contrast sensitivity, colour discrimination and multi-focal electroretinogram. Considering these results, although no visual abnormalities were found in this study, as the life expectancy of CF patients increases, it is reasonable to predict that CF patients may increasingly show signs of decreased retinal carotenoid concentrations, including age-related macular degeneration (AMD). Drusen (as found in macular degeneration) have been noted previously in two CF subjects in one particular study (Evans, 2009). Interestingly, both subjects were between the ages of 20-25 years old, and suffered from CFRD.

CFTR is known to mediate transport of glutathione, a major antioxidant peptide. Several studies have shown that glutathione depletion increases the risk of oxidative injury (Thor et al., 1982; Wefers and Sies, 1983). Exogenous supply of glutathione to the RPE is known to protect

against oxidative damage (Sternberg et al., 1993), and recently a positive relationship has been found between macular pigment and blood glutathione levels (Qin et al., 2011). Blood plasma levels of glutathione have been observed to be reduced in CF patients (Roum et al., 1993). It could be hypothesised that impairment in glutathione transport by malfunctioning CFTR may further contribute to an increased risk of premature AMD in CF.

Considering the findings of reduced macular pigment in CF patients, as the survival age of CF patients increases, CF patients may increasingly show signs of premature onset AMD, secondary to retinal carotenoid depletion. It may therefore be appropriate to recommend dietary supplementation of lutein and zeaxanthin to help reduce the possible increased risk of AMD development in patients with CF. Additionally, with impaired trans-epithelial RPE transport implicated in AMD pathogenesis (Strauss, 2005) dysfunctional CFTR at the RPE may contribute to the development of premature age-related macular changes.

1.2.8.3 Visual Function

Several measures of visual function have been noted to be reduced in patients with CF. These measures are discussed below.

1.2.8.3.1 Visual acuity, refractive error and binocular vision

A number of studies have reported reduced visual acuity (VA) in individuals with CF (Table 1.7), with the cause of loss attributed to diabetic retinopathy (Spaide et al., 1987), optic neuropathy secondary to chloramphenicol use (Spaide et al., 1987), and VAD (Campbell et al., 1998). Conversely, other studies have found the vast majority of CF subjects to have normal VA (Fulton et al., 1982; Morkeberg et al., 1995; Fama et al., 1998; Castagna et al., 2001; Schupp et al., 2004; Whatham et al., 2009).

Refractive error in CF has been reported in a number of studies (Table 1.7). Fama et al. (1998) and Castagna et al. (2001) found 27.5% of its CF cohort to be myopic, and 12.5% to be hypermetropic. These results agree with those found by Morkeberg et al. (1995) and Evans (2009), who found 31% and 36% of CF patients to be myopic respectively. The only study to make direct comparisons between CF and healthy controls found a small but significant reduction in VA, but no difference in binocular status or refractive error between the two (Evans, 2009). A number of studies have reported the presence of strabismus and/or amblyopia in CF subjects (Fulton et al., 1982; Morkeberg et al., 1995). In light of these findings, it

appears that normal emmetropisation and orthophorisation occurs in CF subjects , however, larger scale studies would be useful to confirm these conclusions.

Table 1.7 Visual acuity and refraction in CF

Authors	Subjects	Visual Acuity	Refractive Error
Fulton et al. (1982)	56 CF	All patients VA 6/6 (Excluding two patients with congenital strabismus)	Not noted
Spaide et al. (1987)	32 CF	23 patients VA 6/7.5 or better; 9 patients VA < 6/7.5, 3 of which had VA < 6/30	Not noted
Morkeberg et al. (1995)	35 CF	All patients VA 6/6 or better (Excluding one eye with amblyopia and VA 6/60)	11 patients (31%) myopic (range – 0.38 dioptres (D) to – 6.25 D; median – 1.75 D)
Fama et al. (1998)	40 CF	All patients VA 6/6	11 patients (27.5%) myopic, 5 patients (12.5%) hypermetropic
Castagna et al. (2001)	40 CF	All patients VA 6/6	11 patients (27.5%) myopic, 5 patients (12.5%) hypermetropic
Schupp et al. (2004)	10 CF	All patients VA 6/6 or better (Excluding one with a retinal vein occlusion and one with previous ocular trauma)	Maximum refractive error -2.00 D
Evans (2009)	28 CF 28 Controls	VA significantly better in controls compared to CF subjects ($P < 0.05$)	36% CF subjects myopic 0% CF hypermetropic

1.2.8.3.2 Dark adaptation

The visual system in humans is able to function over a wide range of light intensities, covering more than $10\log_{10}$ units, by means of light and dark adaptation (DA). Light adaptation occurs extremely rapidly, allowing adjustment to different levels of illumination within a few seconds. However, this relationship breaks down when entering the dark following exposure to an

intense light source, which 'bleaches' a large proportion of visual photopigment. The process by which the eye recovers visual sensitivity following this exposure is known as 'dark adaptation'. The recovery of sensitivity can be plotted onto a graph (Figure 1.8), which measures the log threshold of perceivable light against time. (The processes involved in dark adaptation are discussed in detail in section 1.3.2.2.)

Throughout this thesis several parameters will be used to evaluate and describe the recovery of sensitivity during DA. Definitions of these parameters are given in Table 1.8, and example curves are shown with corresponding values in Figure 1.9.

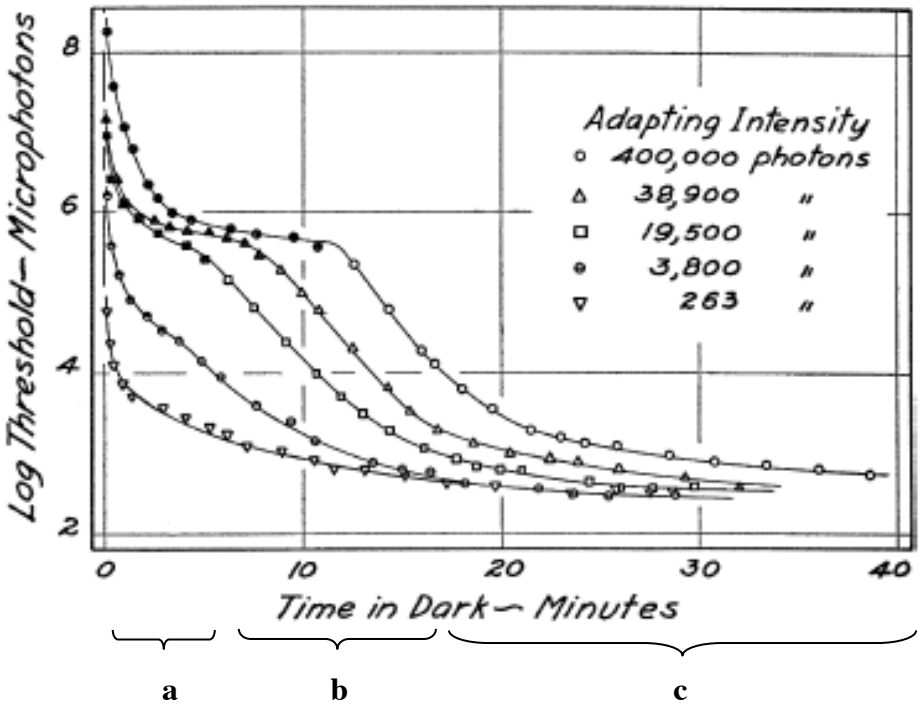

Figure 1.8 Dark adaptation curve for a normal subject. The normal DA curve features an initial rapid recovery in sensitivity which is mediated by the cone system (a). This recovery then reaches a plateau, until there is a 'rod-cone break' at approximately 10 minutes (b), where rod sensitivity exceeds that of the cones. The threshold gradually falls over the next 20 minutes (c), until the absolute threshold is achieved. Image adapted from: Hecht (1937).

Table 1.8 DA recovery parameters

Parameter	Definition
Cone constant	The time constant of cone recovery, representing the cone decay characteristics. A larger number represents a slower rate of recovery.
Final cone threshold	The lowest threshold value reached by the cone component of recovery
Rod-cone break time	The inflection point between the cone and rod components of recovery. This point represents the time when rod-sensitivity first exceeds that of cone-sensitivity
Rod-rod break time	The inflection point between the first and second rod components of recovery
Final rod threshold	The lowest threshold value reached by the rod component of recovery

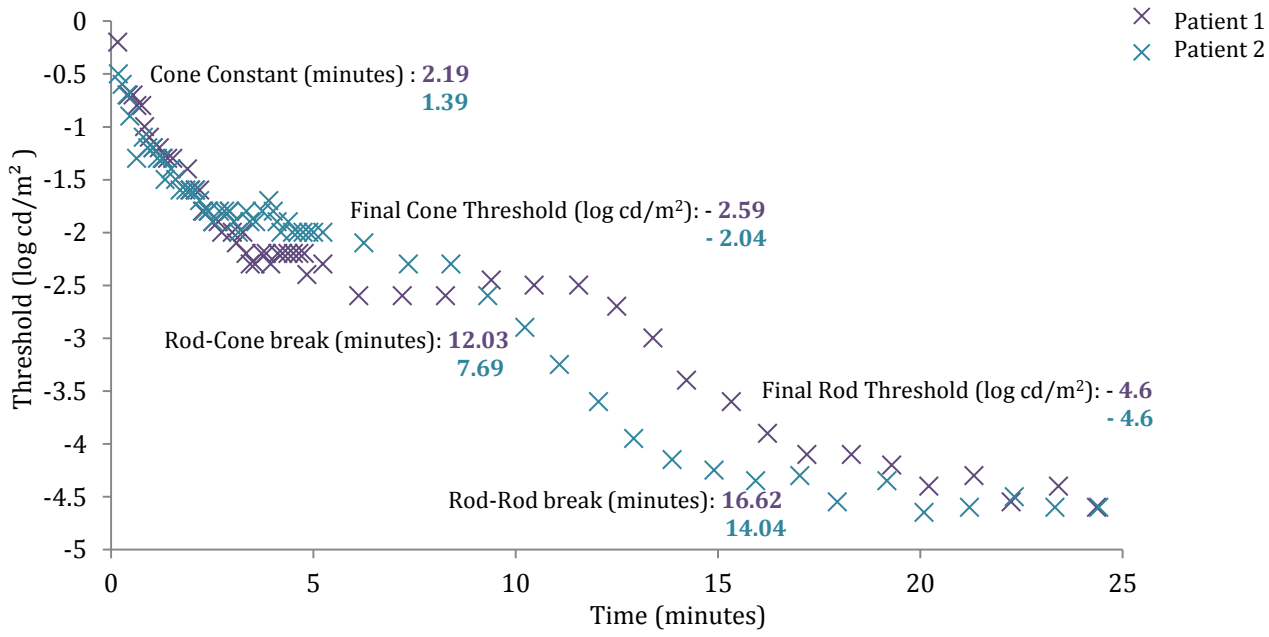

Figure 1.9 Example dark adaptation curves obtained from two healthy subjects on a computerized dark adaptometer showing the parameters as described in Table 1.8.

It has long been established that vitamin A deficiency (VAD) results in impaired DA (Wald, Jeghers and Arminio, 1938), with nyctalopia being the earliest clinical feature of xerophthalmia (Campbell et al., 1998). As vitamin A levels become deficient, there is a decrease in the rate of pigment regeneration and thus DA (Kemp, Faulkner and Jacobson, 1988). However, given

sufficient adaptation time, a normal DA threshold can still be achieved. The effects of VAD can be reversed by oral supplementation of vitamin A. Kemp et al. (1988) found dark adaptation to return to almost normal within one week of vitamin A supplementation, and another study found restoration of dark adaptation after only one day (Cideciyan et al., 1997). The rapid recovery of dark adaptation thresholds upon supplementation with vitamin A makes it unlikely that VAD causes structural abnormalities in the photoreceptors or RPE. Instead, the recovery has been attributed to the restoration of the concentration of 11-cis-retinal, a product of vitamin A in the RPE (Lamb and Pugh, 2004).

As VAD is a known characteristic of CF, several studies have investigated DA in CF subjects, both with and without VAD (Table 1.9). Results demonstrate that DA is reduced in CF patients with reduced plasma retinol concentrations with one study showing a correlation between low plasma retinol levels and an elevated DA threshold (Fulton et al., 1982). As with healthy subjects, retinal sensitivity can recover to normal levels in CF patients through high-dose supplementation of vitamin A (Fulton et al., 1982; Rayner et al., 1989). However, high dose vitamin A supplementation should be given with caution due to the risk of hepatotoxicity and intracranial hypertension (Huet et al., 1997). It was previously thought that supplementation with zinc alone may not resolve night blindness, but only act to potentiate vitamin A. However, supplementation with zinc alone has also been shown to improve nyctalopia in CF patients (Tinley et al., 2008). This may be due to the involvement of zinc in modifying plasma membranes in photoreceptors, regulating the light-rhodopsin reaction within the photoreceptor, and acting as an anti-oxidant in the RPE and retina (Grahn et al., 2001).

Table 1.9 Dark adaptation in CF

Authors	Subjects	Method	Observations
Fulton et al. (1982)	56 CF 8 Controls	Two-alternative forced-choice procedure. Full DA curves for 15 CF and 7 controls using a Maxwellian-view adaptometer	6 CF patients (10.7%) had abnormal DA thresholds* Mean DA thresholds significantly higher in CF. Mean retinol values lower in CF patients. Low plasma retinol levels correlated to elevated DA value in CF.
Rayner et al. (1989)	43 CF 4 Controls	Modification of Friedman Field Analyser and a computer system	8 CF patients (18.6%) had abnormal DA thresholds* Abnormal DA associated with significantly lower serum vitamin A and retinol binding protein
Neugebauer et al. (1989)	31 CF 28 Controls	Friedman Field Analyser and a computer system	6 CF subjects (19%) had abnormal DA thresholds* CF patients with vitamin A levels <30 microgm/dL had raised DA ($p<0.02$)
Morkeberg et al. (1995)	35 CF	Goldmann-Weekers Adaptometer	DA normal for all CF patients No reduction in serum retinol concentration in CF patients
Huet et al. (1997)	10 CF	Beyne Optometer	3 CF subjects (30%) had reduced DA[#]; 2 CF subjects (20%) had pathological DA No significant statistical correlation between DA and serum retinol
Ansari et al. (1999)	28 CF 25 Controls	Friedman Field Analyser	DA normal for all CF patients (No patients with VAD) No statistical correlation between DA and serum retinol
Evans (2009)	26 CF 28 Controls	Goldmann-Weekers Adaptometer	DA thresholds significantly higher in CF ($P < 0.005$) Abnormal DA* in 9 CF subjects (35%), but no controls DA thresholds significantly higher in VAD CF patients compared to controls ($P <0.0001$) DA significantly worse in ΔF508 homozygote group compared to controls DA significantly worse in CFRD subjects compared to controls

* Abnormal DA defined as two standard deviations above the normal mean

[#] Reduced DA defined as dark adaptation 0.12 to 0.23 candela/hectometer^2

[^] Pathological DA defined as dark adaptation ≥ 0.23 candela/hectrometer^2

The correlation of reduced DA with decreased serum retinol levels suggests that DA is not a primary manifestation of CF, rather a secondary consequence caused by maldigestion and malabsoprtion of nutrients. In more recent years, the incidence of abnormal DA in CF appears to have decreased (Morkeberg et al., 1995; Ansari et al., 1999). This is likely to be due to the improvement in care of CF as knowledge on correct nutrition and supplementation has increased.

It is well documented that DA is also adversely affected in type 1 and type 2 diabetes. Specifically, there have been reports of slowed DA and an elevated final threshold, even in the absence of DR (Henson and North, 1979; Arden, Wolf and Tsang, 1998; Arden et al., 2005; Holfort, Jackson and Larsen, 2010). The only study to investigate the effect of CFRD on DA, found comparable results to those of type 1 and type 2 diabetic subjects: DA appeared to be significantly worse in subjects with CFRD compared to healthy controls ($p < 0.0001$), and to non-CFRD subjects ($p < 0.005$) (Evans, 2009). It is likely that DA is particularly affected by diabetes, as scotopic conditions are known to greatly increase the metabolic demands of rod photoreceptors (Arden et al., 2005).

It has been postulated that DA is impaired in type 1 and type 2 diabetes due to increased levels of retinal hypoxia (Arden et al., 1998; Drasdo et al., 2002). Findings of abnormal DA thresholds in diabetes have led to experiments investigating the effect of oxygen inhalation on the DA in diabetic subjects. Results indicate that inhalation of oxygen improves cone and rod sensitivity in diabetic patients (Kurtenbach et al., 2006). It would be of considerable interest to repeat the oxygen inhalation experiments as carried out by Kurtenbach et al. (2006) on CF subjects both with and without CFRD, to further the understanding of the cause of the visual deficit in CF and CFRD. If, like in type 1 and type 2 diabetes, oxygen inhalation improves DA in subjects with established CFRD who are receiving treatment, this would prove that hypoxia is present at the level of the retina. Similarly, if improvements are also seen in patients diagnosed as having impaired glucose tolerance, it may be beneficial to commence more intense diabetic therapy diabetic. Conversely, if no improvement in DA is seen upon oxygen inhalation in CFRD subjects, this would point to another cause for the deficit, which would further distinguish CFRD from type 1 and type 2 diabetes.

1.2.8.3.3 Electrophysiology

Electro-diagnostic techniques can be used as non-invasive, objective methods for assessing the integrity of the visual pathway, from the retina to the visual cortex. Electrodiagnostic tests include the electro-oculogram (EOG), the electroretinogram (ERG) and the visual evoked potential (VEP). A summary of electrophysiological studies in CF subjects is presented in Table 1.10.

The EOG measures the standing electrical potential that exists between the cornea and the posterior pole of the eye during dark and light adaptation whilst the subject alters fixation between two horizontal lights separated by 30 degrees. It measures the function and integrity of the RPE-photoreceptor complex (Steinberg, Linsenmeier and Griff, 1985). The Arden ratio, a ratio of the light peak to dark trough, is the preferred clinical measure obtained by the EOG, with a value of approximately 1.8 being considered normal (Arden, 2006). The Arden ratio has been shown to be reduced in certain ocular dystrophies before any clinically apparent fundus changes have been observed (Arden, 2006). Certain parameters of the EOG have been noted to be abnormal in CF, including the Arden ratio (Leguire et al., 1992; Constable, Lawrenson and Arden, 2006) and the fast oscillations (FO) (Miller et al., 1992). FO are produced following movement of Cl^- in response to light (Gallemore and Steinberg, 1993). Reduction in FO in CF has previously led to claims that CFTR forms the basis of basal chloride conductance (Miller et al., 1992). However, in more recent studies, the FO were found to be normal in CF (Constable et al., 2006), therefore, it is likely that there is an alternative mechanism that does not rely solely on CFTR to produce FO (Wu, Marmorstein and Peachey, 2006). Results from EOGs in CF patients suggest that CFTR is most likely interacting with other ion channels to modulate the time-course of the EOG, but does not appear to be responsible for the alteration in the RPE's electrical potential (Constable et al., 2006).

The ERG measures the current flowing within and across the retina in response to stimulation. It is a physiological measure which provides an objective assessment of retinal function, providing information regarding the integrity of a variety of retinal structures, from the RPE through to the ganglion cell layer (Weisinger, Vingrys and Sinclair, 1996). The ERG may detect early cone and rod dysfunction. Several studies have found abnormal ERG's in patients with CF (Willison et al., 1985; Leguire et al., 1991; Suttle and Harding, 1998; Tsinopoulos et al., 2000; Schupp et al., 2004), with the abnormality generally associated with VAD and seen to improve following vitamin supplementation. The scotopic ERG appears to be most affected

in CF, suggesting abnormal rhodopsin function, and relatively normal cone function (Suttle and Harding, 1998). However, in the most recent study, results from photopic and scotopic ERGs in CF were comparable to those from normal controls (Whatham et al., 2009).

The VEP is the electrophysiological response to visual stimulation, recorded from encephalographic activity (Fishman and Sokol, 1990). It is useful to determine the macula function in patients with dense media opacities, and also to evaluate the integrity of the visual pathways and cortex in non-verbal or un-cooperative patients (Arden, 2006). The VEP has been noted to be abnormal in CF (Messenheimer et al., 1984; Willison et al., 1985; Spaide et al., 1987; Kaplan et al., 1988). A significant latency in VEP response has been noted in patients previously on chloramphenicol therapy (Spaide et al., 1987). This supports the concept that chloramphenicol causes optic nerve disease in CF. Vitamin E deficiency is also seen to have a detrimental effect on the VEP, with abnormal results normalising upon vitamin E supplementation (Messenheimer et al., 1984; Willison et al., 1985; Kaplan et al., 1988). These results show the importance of vitamin E in normal visual functioning.

Table 1.10 Electrophysiology in CF

Authors	Subjects	Method	Observations
Messenheimer et al. (1984)	1 CF	VEP	VEP initially abnormal when the patient was vitamin A, D and E deficient. Normalised following vitamin E supplementation.
Willison et al. (1985)	1 CF	VEP and ERG	Patient severely vitamin E deficient VEP bilaterally delayed and degraded ERG not detectable following pattern reversal and very degraded following flash stimulation.
	10 CF	VEP and ERG	2 patients had abnormal flash ERGs, 1 of the two also had prolonged VEP latencies. Both cases were vitamin E deficient, but vitamin A sufficient
Spaide et al. (1987)	17 CF	VEP	29% of patients had delays of the VEP. Mean latency of the P100 wave significantly delayed in patients who had previously used chloramphenicol. Abnormality in VEP associated with chloramphenicol optic neuropathy.
Kaplan et al. (1988)	10 CF	VEP	30% had abnormal VEPs All subjects were vitamin E deficient
Leguire et al. (1991)	1 CF	Scotopic and photopic ERG	Scotopic and photopic ERG abnormal when patient had VAD; results normalised following vitamin A supplementation
(Leguire et al., 1992)	1 CF	EOG	Abnormal Arden ratio when patient had VAD; results normalised following vitamin A supplementation
Miller et al. (1992)	13 CF 15 Controls	EOG	FO significantly reduced in CF subjects compared to controls
Suttle and Harding (1998)	1 CF	Scotopic and photopic ERG; VEP	Photopic and fast-flicker ERG within normal range. Scotopic ERG absent until 6 weeks after treatment for CF. VEP abnormal both before and after treatment.

Tsinopoulos et al. (2000)	41 CF 41 Controls	Scotopic and photopic ERG	No significant difference in ERG responses between CF and control groups. 65.7% CF patients had abnormally low serum retinol concentrations
Schupp et al. (2004)	10 CF 10 Controls	Multifocal ERG	20% CF patients showed delayed latencies but normal response densities
Constable et al. (2006)	6 CF 9 Controls	Light-EOG Alcohol-EOG	Alcohol and light-EOG amplitude normal. Ratio of light peak to dark trough alcohol-EOG significantly higher ($p = 0.0297$) in CF than controls. ΔF508 homozygotes showed no significant difference in DR:LT ratio or timing. DR:LT ratio significantly greater in ΔF508 heterozygotes compared to controls and ΔF508 homozygotes; time to FO's was significantly slower in ΔF508 heterozygotes compared controls, but not ΔF508 homozygotes.
Whatham et al. (2009)	41 CF; 29 PI, 12 PS	Scotopic and photoptic flash ERG	No significant difference between ERG measures in PI and PS groups. Results broadly similar to data from healthy subjects in another study.

Key: FO, fast oscillation; DR:LT, dark rise: light trough; PI, pancreatic insufficient; PS, pancreatic insufficient

1.2.8.3.4 Colour vision

Colour vision (CV) begins at the level of the retina, with three cone types maximally sensitive to short, medium or long wavelengths. It is then mediated throughout the rest of the visual system by parallel neural pathways. Normal ageing is known to be associated with overall losses in the sensitivity of the cone pathway (Werner, Bieber and Schefrin, 2000), whereas retinal and optic nerve disorders can cause selective losses (Krastel and Moreland, 1991). Congenital CV deficiency affects approximately 8% of males and 0.4% of females in the normal Caucasian population (Birch, 1998; Swanson and Cohen, 2003). Very little literature on CV in CF is available, however, that found is summarised in Table 1.11. Spaide et al. (1987)

and Morkeberg et al. (1995) found a similar prevalence of CV abnormalities in CF subjects, reporting 16% and 14% respectively. In the study carried out by Spaide et al. (1987) all patients found to have CV abnormalities had a history of chloramphenicol use, and had associated VEP delays. Therefore, the CV abnormalities were attributed to optic neuropathy secondary to chloramphenicol use. In a study carried out by Morkeberg et al. (1995), three CF patients were found to have abnormal red-green CV, including one deuteranomal, one deuteranope and one protanope. It was not noted whether these defects were acquired or congenital, so unfortunately results do not offer any insight on the effect of CF on CV. The most recent study which investigated CV in CF found all CF patients to have colour vision within the normal range, with no significant difference found between CF and normal subjects (Evans, 2009).

VAD would be expected to affect colour vision due to the importance of vitamin A in the regeneration of photopigment. One study which investigated the effect of VAD on CV, showed that some measures of CV were significantly reduced in vitamin A deficient CF subjects compared to controls, suggesting there may be subtle levels of cone dysfunction (Evans, 2009). Type 1 and type 2 diabetes is also known to have a detrimental effect on CV, even in the absence of DR (Di Leo et al., 1992; North et al., 1997). It is unknown whether this relationship is similar in CFRD, as the only study to investigate the effect of diabetic status on CV, found there to be no significant reduction in measures of CV in subjects with CFRD compared to healthy controls (Evans, 2009).

Table 1.11 Colour vision in CF

Authors	Subjects	Method	Observations
Spaide et al. (1987)	31 CF	Ishihara*	5 CF patients (16%) had CV defects. Type not specified.
Leguire et al. (1991)	Case study: 1 CFRD	Not noted	No CV abnormality
Morkeberg et al. (1995)	35 CF 0 Controls	Ishihara and American Optical Hardy Rand Ritler Nagel's anomaloscope	Three men (14% of men) had abnormal red-green CV. One deuteranomal, one deuteranope and one protanope.
Schupp et al. (2004)	10 CF 10 Controls	Cambridge Colour Test Presented Landolt C patterns on a computer monitor	CF patients had colour discrimination well within the normal range. No significant difference between CF patients and control subjects for protan, deutan or tritan defects.
Evans (2009)	27 CF 28 Controls	Saturated and desaturated Farnsworth D15	No acquired CV defects. Some measures of CV significantly reduced in VAD subjects

* Result considered abnormal if 3 or more plates incorrect

1.2.8.3.5 Contrast sensitivity

Several studies have investigated the effect of CF on the contrast sensitivity function (CSF) (Table 1.12). In the earlier studies, optic nerve dysfunction secondary to chloramphenicol use was believed to be the cause of reduced CS in CF patients, as CS was seen to be reduced at all spatial frequencies (SF) (Spaide et al., 1987). However, the CSF remained reduced in patients who had not received chloramphenicol therapy. It was therefore concluded that other factors, such as iatrogenic, nutritional or primary effects of the disease must contribute to the loss of CS in CF.

It is well established that vitamin A is essential for photoreceptor function (Sommer, 1983). Reduction of CS in CF has been previously attributed to subtle losses of photoreceptor function

associated with VAD (Leguire et al., 1991). This hypothesis is supported by the improvement in CS seen in a 16 year old boy with CF following an increase in vitamin A supplementation (Leguire et al., 1991). In contrast, in two studies carried out by Ansari et al. (1999), and Morkeberg et al. (1995) CS was still seen to be reduced in CF patients who were considered to be vitamin A sufficient, as measured by their serum retinol concentration. These results would suggest that the cause of low contrast sensitivity in CF is not to be found in the retina (Morkeberg et al., 1995). However, problems exist in establishing if a patient is vitamin A sufficient or deficient as VAD may exist even when serum retinal A levels are measured to be normal (Wechsler, 1979). Morkeberg at al. (1995), suggested that tear film abnormalities in CF may cause a CSF defect, as the tear film forms the anterior refracting surface of the optical system. However, no significant correlation was found between the occurrence of dry eye and decreased CS.

Additional factors which have not been addressed in previous studies could contribute to the reduction of CS in CF. A reduction in CS has been noted previously in subjects with type 1 and type 2 diabetic subjects, in the absence of diabetic retinopathy (North et al., 1997). Similar results have been found in subjects with CFRD, with CS measuring significantly lower ($p < 0.0001$) in CFRD subjects compared to controls (Evans, 2009). Retinal hypoxia, caused by abnormal retinal perfusion and ischaemia in diabetes is believed to be responsible for this defect (North et al., 1997; Kurtenbach et al., 2006).

Table 1.12 Contrast sensitivity in CF

Authors	Subjects	Method	Observations
Spaide et al. (1987)	29 CF 12 Controls	Bekesy interactive CS technique, with 6 SF from 0.5-22.8 cpd	CS significantly lower at all SF in CF, even with exclusion of subjects with reduced VA or using chloramphenicol ($P < 0.01$).
Leguire et al. (1991)	Case report 1 CF 15 Controls	Wall mounted CS chart, 8 contrast levels at 5 SF	CSF decreased at all SF in CF during VAD. CSF improved by 94% following vitamin A supplementation
Morkeberg et al. (1995)	35 CF	Mesoptometer, 8 levels, CS determined at 2 luminance levels (0.1 and 0.03 cd/m^2), and following blinding glare	CF patients had significantly decreased CS in all tests ($P < 0.001$) compared to a reference population. CS was most reduced following blinding glare
Ansari et al. (1999)	28 CF 25 Controls	Vistech chart, 5 SF from 1.5-1.8 cpd	29% of CF patients had reduced CS at intermediate and high SF
Schupp et al. (2004)	10 CF 10 Controls	Sinusoidal gratings on a computer monitor at optical infinity at 6 SF from 0.55-18 cpd and a luminance of 45 cd/m^2	No significant difference in CS at all SF ($P < 0.05$)
Evans (2009)	28 CF 28 Controls	Pelli-Robson at 3m, SF of 3 cpd, luminance 160 cd/m^2	CS significantly lower in CF ($P < 0.005$) CS significantly worse in CFRD compared to controls ($P < 0.0001$)

Key: SF, spatial frequency; cpd, cycles per degree; CSF, contrast sensitivity function

1.2.8.3.6 Summary: CF and visual function

The hypothetical aetiology for changes in visual function suggests that any changes observed are primary manifestations of CF. CFTR has been localised to the RPE where it is believed to contribute to Cl^- efflux (Reigada and Mitchell, 2005). Unless this fundamental CFTR dysfunction is compensated by other Cl^- channels, normal photoreceptor function may be affected by altered IPM composition. This could potentially result in photoreceptor dysfunction and reduced visual function.

It is well established that vitamin A is essential for normal photoreceptor function (Sommer, 1983). VAD in CF has therefore been identified as a causative factor for impaired measures of visual function including CS (Leguire et al., 1991), dark adaptation (Fulton et al., 1982; Neugebauer et al., 1989; Rayner et al., 1989), and electrophysiological findings (Messenheimer et al., 1984; Leguire et al., 1991; Leguire et al., 1992). Though low serum concentrations may reflect hepatic depletion (Olson and Tanumihardjo, 1998; Tsinopoulos et al., 2000), they do not adequately mirror the concentrations of vitamin A in the liver, which is the main site of storage (Underwood and Denning, 1972; Lindblad et al., 1997). It is therefore difficult to draw clear conclusions based upon the serum A concentrations. The observed relationship between abnormal dark adaptation and decreased serum retinol levels (Fulton et al., 1982; Rayner et al., 1989) in CF subjects suggests that dark adaptation is not a primary manifestation of CF, but a secondary consequence of maldigestion and malabsorption of nutrients. However, elevated DA thresholds despite normal VA serum concentrations (Huet et al., 1997; Ansari et al., 1999) may suggest another cause for the abnormality.

With the presence of dysfunctional CFTR at the RPE in CF patients, it is possible that normal RPE Cl^- efflux function is disrupted. Without compensation by other apical chloride channels, altered IPM composition could have an impact on normal RPE and photoreceptor function. With the RPE's involvement in several functions important for the maintenance of normal visual function, including transport of nutrients to photoreceptors, recycling of substances involved in the visual cycle and retinal regeneration (Strauss, 2005), it seems clear that RPE impairment could result in photoreceptor degradation and reduced visual function. If this were the case, those patients with the most severe CFTR mutations would be expected to show the most severely impaired measures of visual function. This was demonstrated by Evans (2009), when ΔF508 homozygous subjects showed significantly reduced VA, CS and DA compared to controls, whilst less severe ΔF508 heterozygotes showed no difference.

There is substantial evidence that dark adaptation, (Henson and North, 1979; Arden et al., 1998; Arden et al., 2005; Holfort et al., 2010) colour vision (Di Leo et al., 1992; North et al., 1997), and contrast sensitivity (North et al., 1997) are adversely affected in type 1 and type 2 diabetes, even in the absence of DR. Retinal hypoxia, secondary to abnormal retinal perfusion and ischaemia in diabetes has been identified as the cause of this defect (North et al., 1997; Kurtenbach et al., 2006). As DA has similarly been seen to be reduced in CFRD subjects compared to both NGT CF subjects and healthy controls, it is reasonable to predict that abnormal retinal perfusion and ischaemia is also the cause of visual functional problems in CFRD. Further work is needed to determine whether this is the case.

1.2.8.4 CF and the Eye Summary

To date, CFTR has been localised to the corneal and conjunctival epithelium, corneal endothelium and the RPE, where it is believed to play an important role in Cl^- conductance. The movement of Cl^- across epithelia is known to be important in the maintenance of electrolyte and fluid balance of cells. CFTR is therefore likely to facilitate a number of ocular processes which rely upon Cl^- transport to establish an electrochemical gradient, thereby allowing the passive movement of fluid. These processes include: basal tear production from the cornea and conjunctival epithelium, maintenance of normal corneal integrity by the corneal endothelium, and maintenance of the SRS by the RPE. It is therefore, reasonable to predict that malfunction of CFTR in CF may have a direct influence on the ocular status and cause visual function abnormalities.

Previous studies into the effect of CF on the eye have identified a number of ocular characteristics of the disease including dry eye, conjunctival xerosis, reduced crystalline lens transparency, reduced macular pigment density, impaired dark adaptation, reduced contrast sensitivity and abnormal electrophysiological results (Figure 1.10). However, many of these studies have limitations due to small sample size, lack of healthy matched control patients, and failure to take into account confounding factors including VAD and CFRD which could impact the results. Also, as the majority of studies were conducted prior to the localisation of CFTR within the eye, little thought has been paid to the possibility of certain ocular abnormalities being primary manifestations of the disease.

Due to dramatic improvements in patient treatment and management, average life expectancy is now approaching 41.5 years (UK CF Registry, 2013) and is anticipated to further increase in the future (Cystic Fibrosis Foundation, 2009). As a consequence, ocular complications which may have previously gone undetected, may become more of a pressing concern. It is therefore important that not only do health practitioners understand the full breath of ocular complications associated with CF, but that practitioners also become more aware of their association with the general health of the CF patient. In this way, ocular complications may act as a biomarker, giving health care practitioners valuable insight into the patient's general CF status.

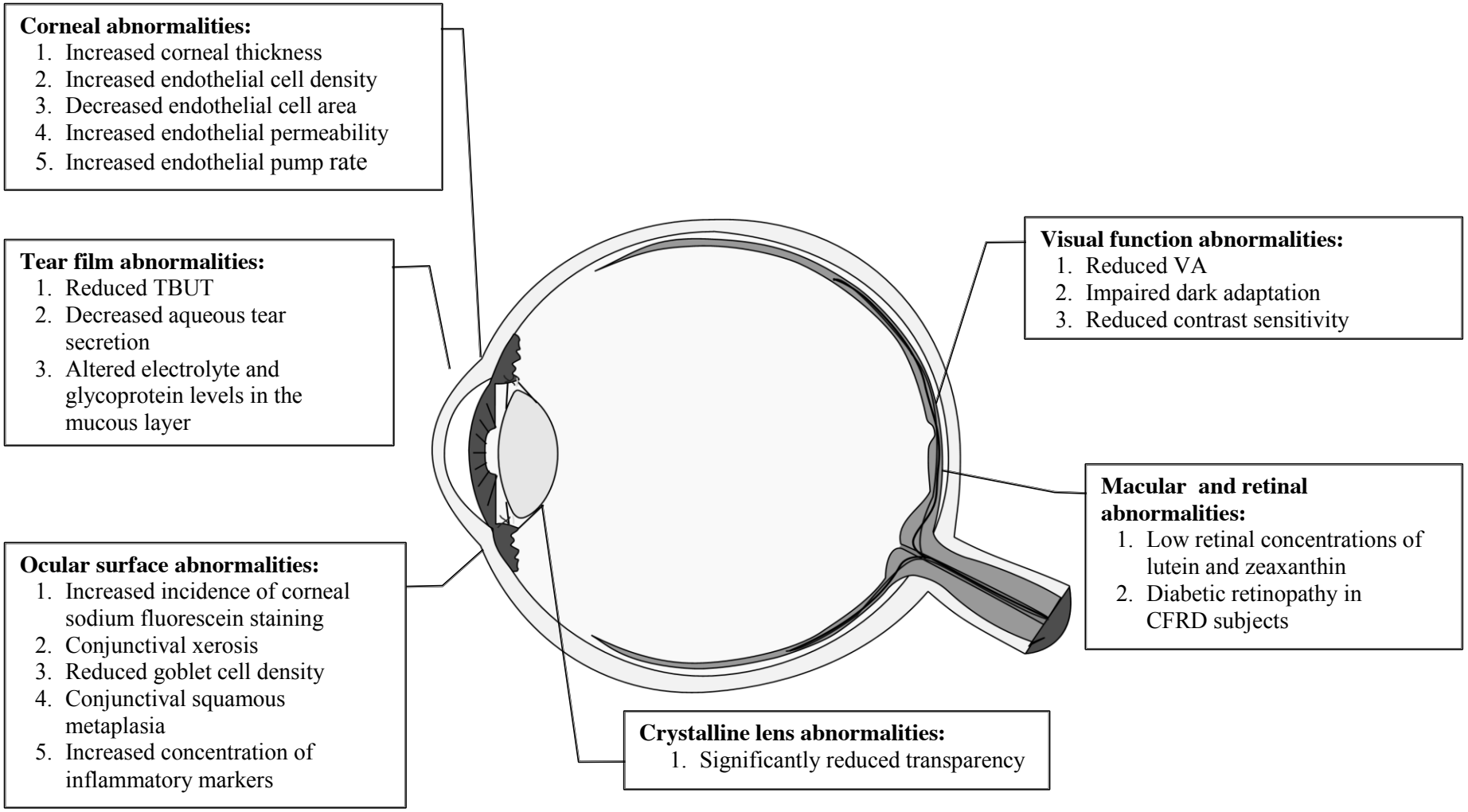

Figure 1.10 A summary of the ocular abnormalities in CF.

1.3 The Retina

1.3.1 *Investigating Retinal Structure*

CFTR has been localised to the basal membrane of the RPE (Wills et al., 2000; Wills et al., 2001; Weng et al., 2002; Blaug et al., 2003), where it may contribute to Cl^- flux from the SRS to the choroid (section 1.2.4). Studies on RPE epithelial cells indicate Cl^- transport across the RPE is important in several RPE functions, including fluid absorption (Miller and Edelman, 1990), volume regulation (Ueda and Steinberg, 1994) and ligand-regulated ion and fluid transport (Peterson et al., 1997). Disturbance of normal CFTR activity could cause complications such as oedema and serous retinopathy (Bird, 1994); however, there have been no reports of such complications in CF subjects to date. In addition to the dysfunction of CFTR at the RPE, the retina may also be compromised in CF due to increased levels of oxidative stress caused by chronic recurrent respiratory infection and decreased levels of protective antioxidants including lutein and zeaxanthin (Schupp et al., 2004). Furthermore, the observation of premature drusen in CF subjects could indicate an increased risk of premature age related macular degeneration (Evans, 2009).

An important part of understanding the aetiology of clinical differences in visual function in CF is to assess for differences in structure. Assessing the living retina *in vivo* has previously been limited to two-dimensional, surface retinal examination and photography. However, with the advent of optical coherence tomography (OCT) in the 1990s, visualization of the retinal structure in vivo is now possible, aiding in the early diagnosis of age-related macular degeneration and retinal oedema (Drexler, 2004). Retinal imaging by OCT in CF patients and healthy controls will allow for quantitative comparisons of the RPE/photoreceptor complex for the first time in this disease group. In addition, qualitative assessment will allow detection of inter-retinal signs of early age-related changes in CF, which may have previously gone un-noticed with less sophisticated fundus photography.

The following section explores the retinal structure, reviews the pathogenesis of AMD and introduces OCT, which will be used to investigate the retinal structure in CF.

1.3.1.1 <u>Retinal Structure</u>

The primary role of the retina is the detection of light and the subsequent translation of light into a neural signal for processing in the visual cortex. Observation of the retina by light microscopy (Figure 1.11) reveals a highly organised structure, made up by several distinct

layers according to the cell bodies and synapses contained within them (Figure 1.12). The retinal pigment epithelium, which lies just behind the retina, and the photoreceptor layer will be described below.

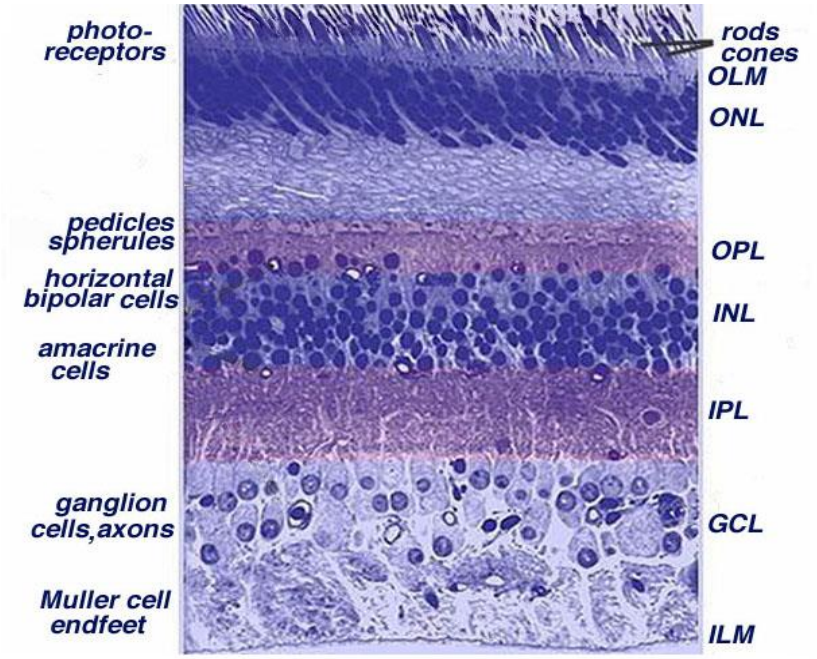

Figure 1.11 A light micrograph of a vertical section through a central portion of the human retina with retinal layers and cell types identified. Image from Kolb (1995). Key ILM, inner limiting membrane; GCL, ganglion cell layer; IPL, inner plexiform layer; INL, inner nuclear layer; OPL, outer plexiform layer; ONL, outer nerve fibre layer; OLM, outer limiting membrane.

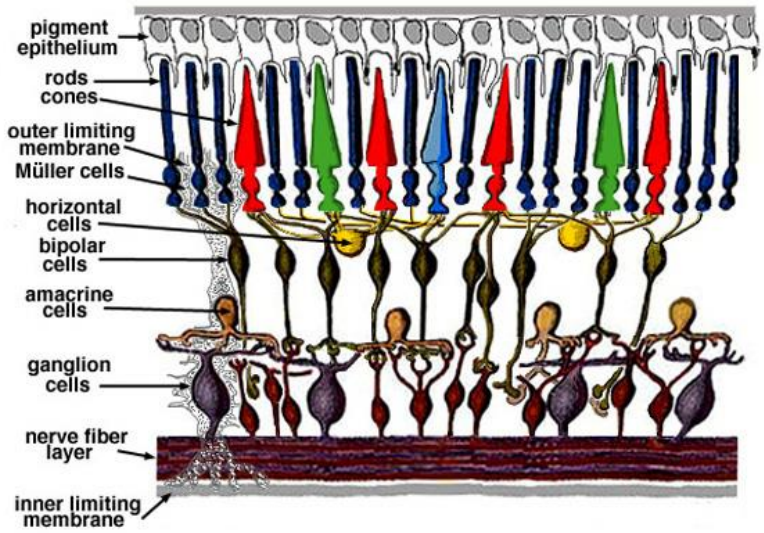

Figure 1.12 A schematic drawing of the neural retina, depicting the major retinal layers. Image from Kolb (1995)

1.3.1.1.1 The Photoreceptor Layer

The photoreceptor layer is made up of two types of photoreceptor cells; rods and cones. The distribution of these cells varies across the retina, with cone density maximal at the fovea, and rod density maximal at approximately 18° from the centre of the fovea (Osterberg, 1935; Curcio et al., 1987) (Figure 1.13). The average human retina contains approximately 4.6 million cones and 92 million rods (Curcio et al., 1990). Cone photoreceptors can be further divided into three sub-types based upon their spectral sensitivity, giving blue- (short wavelength), green- (medium wavelength) and red- (long wavelength) cones, and enabling high acuity, trichromatic vision at high levels of illumination. In contrast, rod-derived vision is monochromatic, and is optimised for much dimmer levels of illumination, and only provides a low visual acuity.

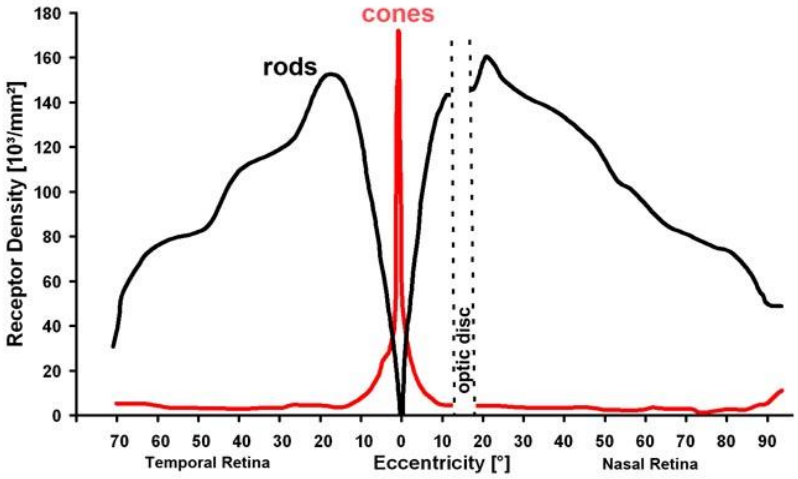

Figure 1.13 Rod and cone densities along the horizontal meridian. Image adapted from Osterberg (1935)

Both rods and cones are structurally similar; they both comprise:

1. an outer segment, which contains the visual pigment (iodopsin in cones and rhodopsin in rods) embedded upon membranous discs;
2. an inner segment containing mitochondria, ribosomes and golgi apparatus for the production of opsin and ATP energy;
3. a cell body containing the nucleus of the photoreceptor (this forms the outer nuclear layer); and
4. a synaptic terminal where neurotransmitter is released to second order retinal neurons (bipolar and horizontal cells).

However, whilst rods are slim 'rod-shaped' structures which stretch down to the RPE cells, cones have a 'conical' shape which tend to be shorter in length (Figure 1.14).

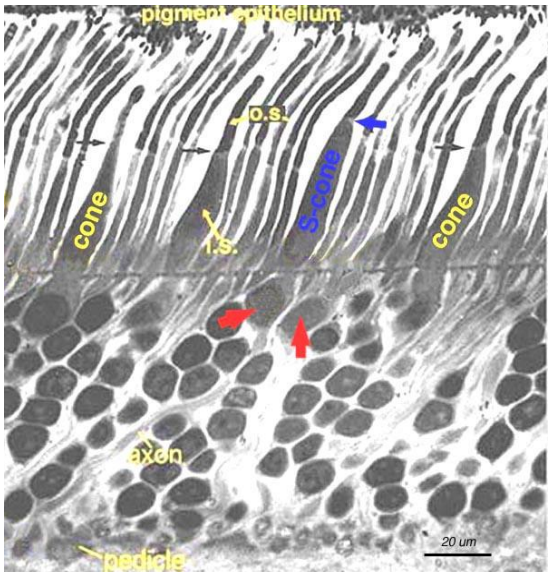

Figure 1.14 A histological section of the human outer retina, showing the thinner, longer rods and shorter, fatter cones. Short wavelength cones (blue arrows) are commonly found occurring next to a longer wavelength cone (red arrow). Image from (Kolb, 2013).

1.3.1.1.2 The Retinal Pigment Epithelium

The RPE is a monolayer of densely packed hexagonal pigmented cells. Each cell is bound to the next by a tight junction, forming a blood-retinal barrier. The apical membrane of the RPE contains surface microvilli which project inwards toward the photoreceptor outer segments. The RPE and photoreceptors are separated by the SRS, occupied by the inter-photoreceptor matrix (IPM), enabling interaction between the RPE and the outer segments (Strauss, 1995). The basolateral membrane of the RPE is in contact with Bruch's membrane, allowing interaction between the RPE and the choroidal bloody supply (Guymer, Luthert and Bird, 1999).

The RPE has many important functions (Strauss, 2005), with the main ones identified as (Figure 1.15):

- Absorption of stray light by pigment, improving optical quality and maintaining visual function
- Protection against photo-oxidative damage
- Transepithelial transport of nutrients, ions, water and metabolic waste products

- The isomerisation of all-trans-retinal to 11-cis-retinal as part of the visual cycle
- Maintenance of the ion composition of the SRS, a process which is essential for the maintenance of photoreceptor excitability
- Phagocytosis of shed photoreceptor outer segments
- Secretion of a variety of growth factors and immunosuppressant factors which help to maintain the integrity of the retina, choriocapillaries and the immune privilege of the eye

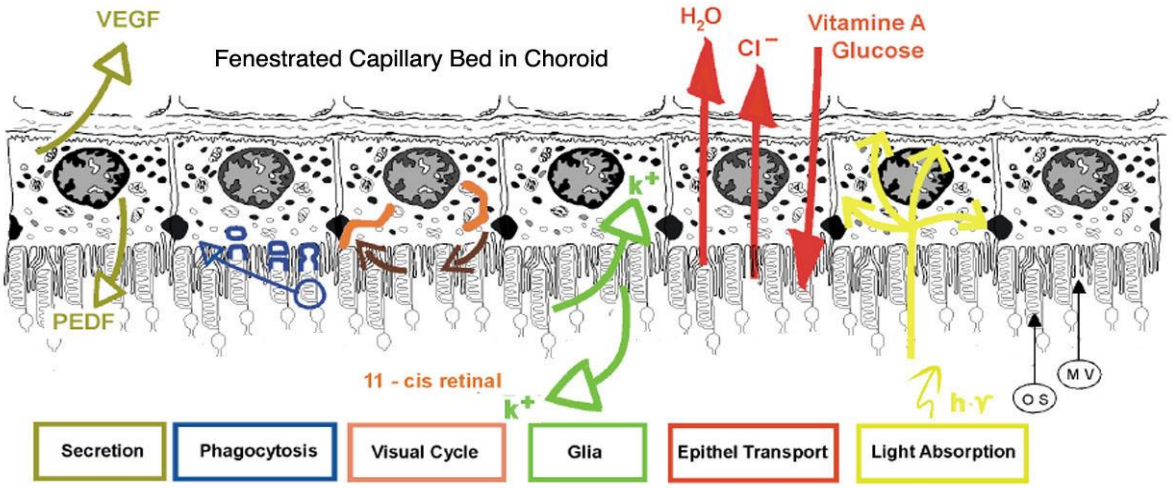

Figure 1.15 A summary diagram showing the main functions of the RPE. Image from Lamb and Pugh (2006). Key: VEGF, vascular endothelial growth factor; PEDF, pigment epithelium derived growth factor

1.3.1.2 Age-related Macular Degeneration

Age-related macular degeneration (AMD) is the principle cause of irreversible blindness among those aged over 65 years in the western world (Klein, Klein and Linton, 1992; Klein et al., 1995; Resnikoff et al., 2004). Currently, the prevalence of AMD in adults is approximately 3% (Klein R et al., 2010), however, this is likely to increase with increasing longevity, and a shift towards an ageing society (Williams et al., 1998). With the previous finding of early onset drusen in two patients with CF aged 23 and 24 years by fundus photography, it is pertinent that further research is carried out using more sophisticated instrumentation to determine whether sub-clinical signs of AMD are present in a larger proportion of the CF population. The clinical features and pathogenesis of AMD is explored herein.

1.3.1.2.1 Clinical features of AMD

AMD can be broadly classified into two states: wet and dry (Figure 1.16). Dry AMD, characterised by drusen within the macular region is the most common type, accounting for up to 90% of all cases of AMD (Ambati et al., 2003). It is generally accepted that dry AMD precedes wet AMD (Donoso et al., 2006), which is characterised by growth of new vessels from the choroid (choroidal neovascularisation) (Lim et al., 2012). Dry AMD causes gradual deterioration of central vision as a result of retinal and RPE atrophy, whereas visual loss is sudden in wet AMD due to neovascularisation and subsequent leakage from the new, weak vessels (Fine et al., 2000; Khandhadia et al., 2012b). Whilst both forms can cause significant visual loss, wet AMD accounts for approximately 75% of cases with severe vision loss (Klein et al., 1997). The characteristics of both wet and dry AMD are discussed below.

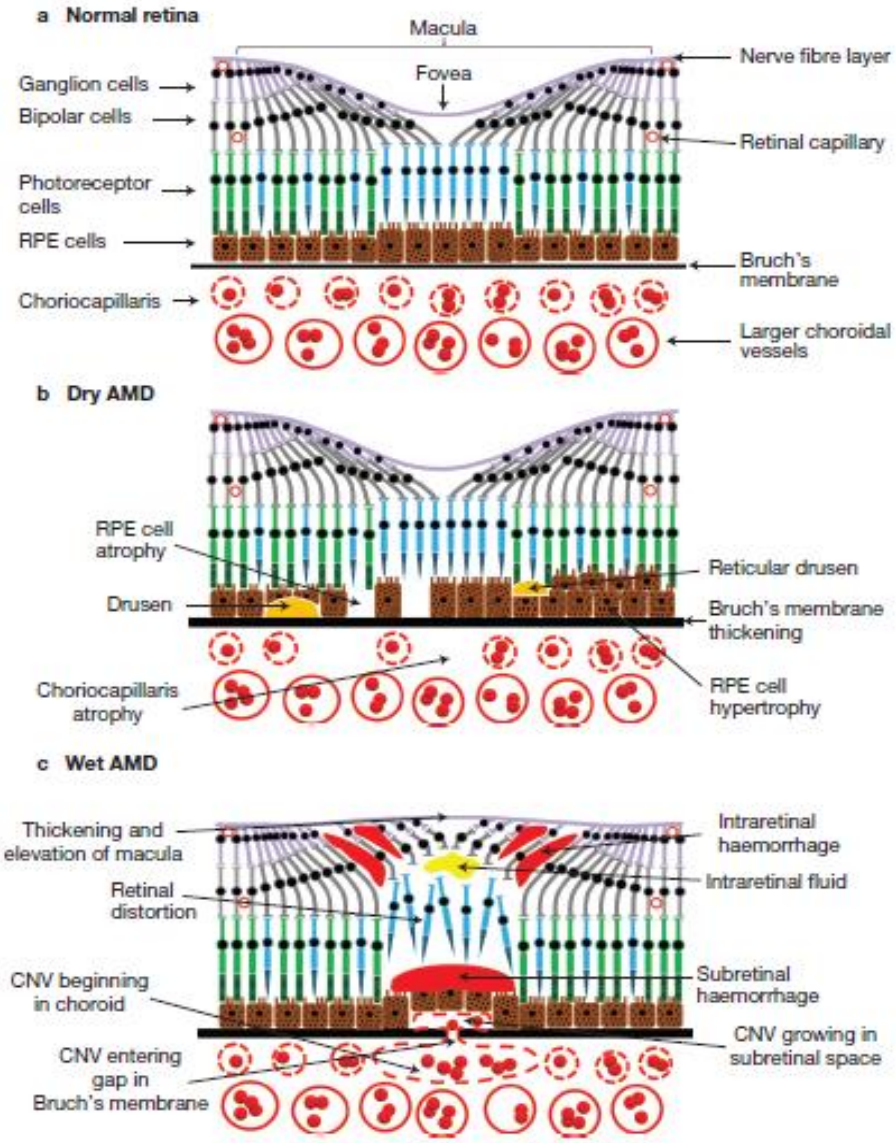

Figure 1.16 Retinal changes in AMD in comparison to the healthy retina (a). In dry AMD (b) specific anatomical changes occur including accumulation of drusen between RPE cells and Bruch's membrane, and the formation of reticular drusen between the RPE layer and photoreceptors. Bruch's membrane becomes thickened and atrophy and hyperatrophy of RPE cells occurs, along with choriocapillary atrophy. Wet AMD (c) is characterised by the presence of a choroidal neovascular membrane, which forms in the choroid and enters the RPE through a break in Bruch's membrane. Image from Khandhadia et al. (2012b).

1.3.1.2.1.1 *Drusen*

Drusen, the hallmark of AMD (Augood et al., 2006; Nowak, 2006), consist of extracellular deposits of material, collected between the basal lamina of the RPE and the inner layer of

Bruch's membrane (Ambati et al., 2003) (Figures 1.17 and 1.18b). Drusogenesis is a complex and multifactorial process, taking place over many years and resulting in the physical displacement of the RPE and photoreceptors (Nowak, 2006). Two main methods of drusen formation have been identified; entrapment of membrane bound bodies between the basement membrane of the RPE and the collagen fibrils of the inner collagenous zone of Bruch's membrane (McConnell and Silvestri, 2005), and deposits of plaques as focal excrescences on the inner surface of Bruch's membrane (Hageman et al., 2001). Common constituents of drusen include RPE remnants, complement, lipids, lipoproteins, dendritic cell processes, cholesterol esters, fibrinogen, class II antigens and immunoglobulins (Johnson et al., 2000; Mullins et al., 2000; Anderson et al., 2002; Donoso et al., 2006). The presence of inflammatory mediators, including complement, in drusen has led to the suggestion that immunological and inflammatory processes may contribute to the development of AMD (Klein et al., 2003b).

Drusen can be classified morphologically as either hard or soft (Ambati et al., 2003), depending on their size and shape (Algvere and Seregard, 2003). Hard drusen are typically smaller than 63μm in diameter, appearing as pinpoint yellow-white lesions with well demarcated edges. Whilst numerous hard drusen represent a risk factor for the development of visual loss from AMD, small numbers are common and can be found in at least 95% of the aged population (Fine et al., 2000), therefore they are not considered to be a risk factor for AMD development (Hageman et al., 2001). Soft drusen (Figure 1.18b), considered pathogonomic of AMD (Sarks, Sarks and Killingsworth, 1994), are typically larger than hard drusen (≥125-250μm) (Nowak, 2006) with less distinct boarders (Khandhadia et al., 2012b) and the tendency to coalesce and become confluent (Ambati et al., 2003).

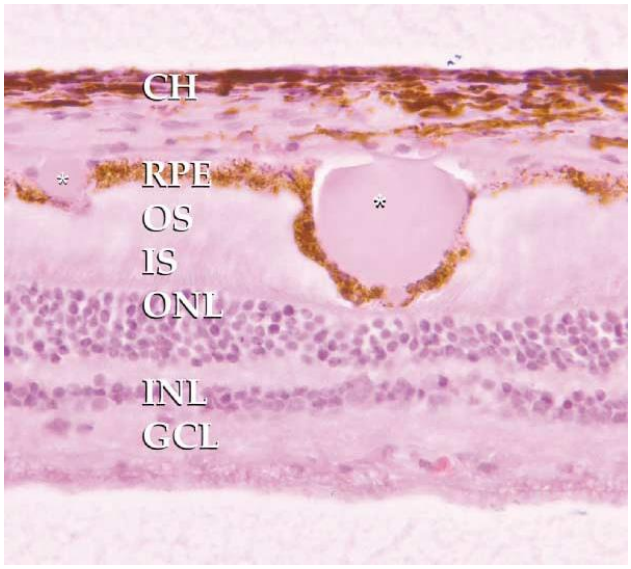

Figure 1.17 Light micrograph image depicting the appearance of hard drusen and their location between the basal lamina of the RPE and the inner layer of Bruch's membrane. The large drusen causes attenuation of photoreceptor outer segment layer. Image from Hageman et al. (2001). Key: * = drusen; CH = choroid; OS = outer segments; IS = inner segments; ONL = outer nuclear layer; INL = inner nuclear layer; GCL = ganglion cell layer.

1.3.1.2.1.2 *Pigmentation abnormalities*

Pigmentary irregularities in AMD are caused by hypertrophy, hyperplasia or atrophy of RPE cells (Khandhadia, Cherry and Lotery, 2012a). Pigmentary abnormalities present as focal areas of hyperpigmentation and hypopigmentation within the RPE (Figure 1.18c), and are a common sign of early AMD (Klein et al., 2004). Focal hyperpigmentation of the RPE has been identified as a risk factor for progression to wet AMD (Bressler et al., 1990). Hypopigmentation signifies areas of RPE cell loss (Green and Key, 1977).

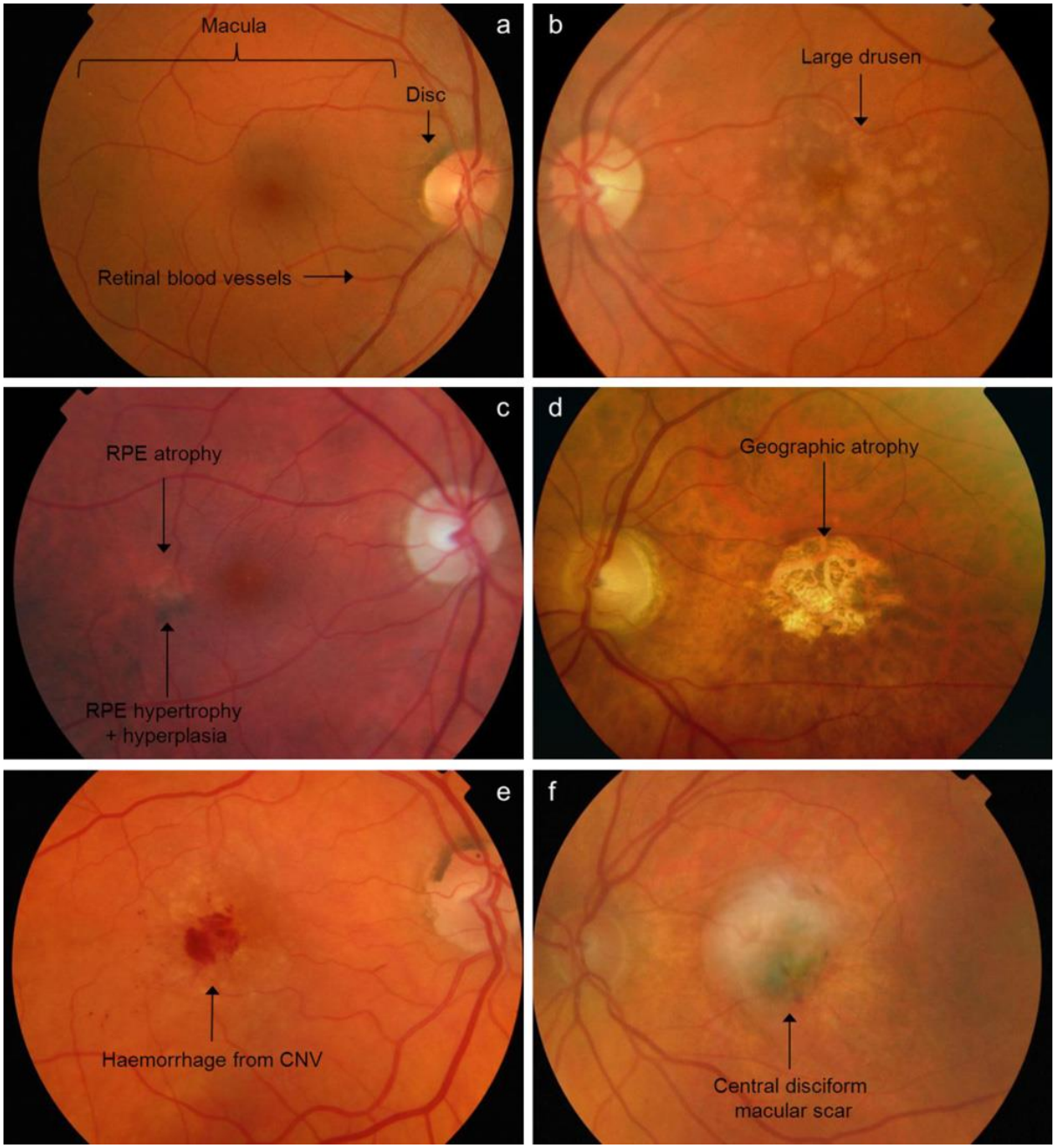

Figure 1.18 Fundus photographs showing features of AMD in comparison to a healthy retina (a). Soft drusen (b) and RPE pigmentary irregularities (c) in early dry AMD. Haemorrhage secondary to a choroidal neovascular membrane in acute wet AMD (c). A large area of sharply demarcated RPE atrophy and underlying choroidal vessel atrophy, representing geographic atrophy in late AMD (d). Retinal haemorrhage (e) caused by an underlying choridal neovascular membrane in wet AMD. A disciform scar (f) formed following involution of neovascularisation in wet AMD. Image from Khandhadia et al. (2012b)

1.3.1.2.1.3 ***Atrophy***

Atrophic AMD accounts for approximately 25% of cases with severe central visual loss (Klein et al., 1997). It is characterised by RPE dysfunction and death, leading to the loss of photoreceptors which are unable to survive without the nutritional and metabolic support of the RPE (Green and Key, 1977). Consequently, visual loss is often slowly progressive. Underlying choriocapillary atrophy often accompanies retinal atrophy (McLeod et al., 2002). Large areas (≥175μm diameter) of atrophy are termed 'geographic atrophy' (Figure 1.18d) (Green and Key, 1977; Klein et al., 2008), representing end-stage dry AMD and accompanied by severe visual loss. Geographic atrophy can develop following fading of drusen, involution of CNV or following a resolving pigment epithelium detachment (Ambati et al., 2003). It is characterised by sharply demarcated areas of depigmentation, with increased visualisation of underlying choroidal vasculature. Geographic atrophy often develops in the parafoveal region, sparing the fovea until late in the disease (Maguire and Vine, 1986; Sarks, Sarks and Killingsworth, 1988; Gass, 2003). Accumulation of RPE lipofuscin may be associated with the pathogenesis of geographic atrophy (Ambati et al., 2003).

1.3.1.2.1.4 ***Neovascularisation***

Development of choroidal neovascularisation is the hallmark of wet AMD, a stage found in approximately 10% of all AMD cases (Ambati et al., 2003). Choroidal neovascularisation (CNV) refers to the growth of new blood vessels from the choroid, which may remain beneath the RPE ("occult" CNV) or breach the RPE and enter the subretinal space ("classic" CNV) (Ambati et al., 2003). The neovascular processes in AMD are thought to result from a local imbalance of growth factors (Witmer et al., 2003; Roth et al., 2004), including anti-angiogenic pigment epithelial derived factor (PEDF) and angiopoetin 1, along with pro-angiogenic vascular endothelial growth factor (VEGF) and angiopoetin 2 (Hangai, Murata and Miyawaki, 2001; Roth et al., 2004; Nowak, 2006). In wet AMD, over expression of the pro-angiogenic VEGF from RPE cells (Lopez et al., 1996), potentially stimulated by hypoxia (Aiello et al., 1995) or inflammation (Anderson et al., 2002), induces development of new vessels (Roth et al., 2004).

Clinically, the earliest sign of CNV is often subretinal or sub-RPE haemorrhage due to the fragility of the new vessels (Figure 1.18e). Fluid and hard exudates may also be present (Khandhadia et al., 2012b). Patient symptoms include sudden onset of a significant reduction in central vision, and metamorphopsia (Lim et al., 2012) which can be clearly visualised with

an Amsler grid. This is caused by disruption to normal photoreceptor orientation and organisation (Khandhadia et al., 2012a). Repeated leakage of blood, serum, and lipid in wet AMD can stimulate fibroglial reorganisation leading to formation of a disciform scar (Figure 1.18f) (Khandhadia et al., 2012b).

Currently, whilst no treatment is available for dry AMD, anti-VEGF intravitreal injections (e.g. Bevacizumab and Ranibizumab), given via the sclera can be used in wet AMD, leading to an improvement in vision in up to 30% of patients (Brown et al., 2006; Rosenfeld et al., 2006).

1.3.1.2.2 Risk Factors for AMD

Epidemiological studies are responsible for determining the various risk factors associated with the development of AMD. Knowledge of the risk factors not only facilitates early detection, but also offers insight into the aetiology of the disease. A full review of the risk factors associated with AMD is beyond the scope of this work, therefore only the main risk factors are discussed below. For comprehensive reviews on the risk factors for AMD see Evans (2001), Chakravarthy et al. (2010) and Seddon and Chen (2004).

1.3.1.2.2.1 *Age*

The prevalence, incidence and progression of all forms of AMD have been demonstrated to rise steeply with advancing age across all races studied (Leibowitz et al., 1980; Klein et al., 1992; Klein et al., 1997; Seddon, Cote and Rosner, 2003; Friedman et al., 2004; Varma et al., 2004; Kawasaki et al., 2008). In the Beaver Dam Study, the prevalence of late ARM or AMD was 7.1% in people over 75 years of age, compared to 0.6% in those aged 55 to 64 years, and 0.1% in those aged 43 to 54 years (Klein et al., 1992).

1.3.1.2.2.2 *Gender*

Whist women are commonly believed to be at higher risk of developing AMD (Mitchell et al., 2002a), few studies have been able to demonstrate this finding with certainty (Evans, 2001). Pooled data from three large scale AMD studies (The Blue Mountains Eye Study, the Beaver Dam Eye Study and the Rotterdam Study) showed a slightly increased risk for AMD in women compared to men in the older age groups (Smith et al., 2001), however, all age effects may not have been excluded. Evans (2001) concurs with these findings, however a more recent meta-analysis by Chakravarthy et al. (2010), suggested there was no significant increase in

prevalence of late AMD in females. Due to varying conclusions, further research is required to determine if a true difference in prevalence exists across gender.

1.3.1.2.2.3 *Ethnicity*

The majority of current literature suggests that all forms of AMD are more common in whites than among black and Hispanic races (Sommer et al., 1991; Pieramici et al., 1994; Friedman et al., 1999; Klein et al., 2003a; Leske et al., 2004; Seddon and Chen, 2004). This has led to the suggestion that melanin may be protective against development of AMD, and specifically CNV (Ambati et al., 2003). However, a study by Berendschot et al. (2002) found no difference in macular or melanin pigment densities between eyes with and without early AMD (Berendschot et al., 2002), suggesting that racial differences in AMD prevalence may be due to factors other than pigmentation (Ambati et al., 2003), including genetics or differences in lifestyle between groups.

1.3.1.2.2.4 *Genetics*

There is considerable evidence from twin concordance studies (Klein, Mauldin and Stoumbos, 1994a; Meyers, Greene and Gutman, 1995; Gottfredsdottir et al., 1999; Grizzard, Arnett and Haag, 2003), familial aggregation (Seddon, Ajani and Mitchell, 1997; Klaver et al., 1998), genomewide scans (Weeks et al., 2000; Schick et al., 2003; Weeks et al., 2004) and candidate gene studies (Allikmets et al., 1997; Seddon et al., 2001a; Schmidt et al., 2002) implicating a genetic basic for AMD (Evans, 2001). However, due to difficulties associated with the investigation of the genetics behind AMD, the degree of heritability and its relative role against environmental factors is still unknown. It is likely that AMD inheritance is a complex trait which is controlled by many genes, rather than a single one (Ambati et al., 2003). Siblings of ARM sufferers are reported to have a three to six fold higher risk for developing ARM compared to non-sufferers (Feigl, 2009), and twin studies suggest greater than 90% concordance in monozygotic twins (Klein et al., 1994a; Meyers et al., 1995; Gottfredsdottir et al., 1999).

1.3.1.2.2.5 *Light exposure*

The relationship between light exposure and the risk of AMD remains unclear, possibly due to the difficulty associated with quantifying lifetime light exposure in humans (Evans, 2001). Numerous studies have examined the relationship between sunlight exposure and development of AMD (Hyman et al., 1983; Taylor et al., 1990; Taylor et al., 1992; The Eye Disease Case-

Control Study Group, 1992; Cruickshanks, Klein and Klein, 1993; Darzins, Mitchell and Heller, 1997). Results from the Beaver Dam Eye Study were conflicting; no association was found with lifetime exposure to ultraviolet light, however, increased leisure time spent outdoors in the summer was significantly associated with increased exudative AMD and late maculopathy (Cruickshanks et al., 1993). The Eye Disease Case Control Study Group showed no significant association between advanced AMD and cumulative sunlight exposure (The Eye Disease Case-Control Study Group, 1992). Darzins et al (1997) found that whilst controls had significantly greater average yearly ocular sun exposures, cases with AMD were more likely to report that they did not tan well, indicating that sensitivity to sunburn may be a risk factor (Darzins et al., 1997).

The suggested mechanistic hypothesis for the link between light exposure and AMD is that light stimulates photo-oxidative damage, leading to the production of reactive oxygen intermediates within the outer retina and choroid (see Section 6.3.3.1) (Gottsch et al., 1993).

1.3.1.2.2.6 *Diet*

In a study including over 70,000 men and women, total fat intake was found to be positively associated with risk of AMD, whilst higher intake of fish was associated with a lower risk of AMD (Cho et al., 2001). Specifically, high linolenic acid was associated with 49% increased risk of AMD, and high docosahexaenoic acid with a 30% reduced risk of AMD. Similar findings were made in another study (Seddon et al., 2001b). However, no association was found between dietary fat intake and AMD in another large cross sectional survey (Heuberger et al., 2001). High intake of fat may be associated with increased deposition of fat in Bruch's membrane, hindering the supply of nutrients and removal of waste from the RPE.

High intake of cholesterol has similarly been associated with a higher risk of AMD (Mares-Perlman et al., 1995; Smith, Mitchell and Leeder, 2000). The Eye Disease Case Control Study reporting a statistically significant fourfold increased risk of exudative AMD with high cholesterol (>6.75 mmol/L) compared to people with lower values of serum cholesterol (≤4.89 mmol/L). However, results are not consistent and other studies have found either a decreased risk of AMD with high cholesterol (Goldberg et al., 1988), or no association at all (Klein and Klein, 1982). The proposed mechanism by which high cholesterol would increase risk of AMD suggests that raised levels of cholesterol in the bloodstream increase the risk of atherosclerosis (Evans, 2001), which may in turn lead to choroidal vasculature deficiencies causing

deterioration of the RPE secondary to ischaemia or build up of waste products (Friedman et al., 1995).

1.3.1.2.2.7 *Smoking*

Smoking has been associated with an increased risk of both dry and wet AMD in many population based epidemiologic studies (Klein, Klein and Moss, 1998; Age-Related Eye Disease Study Reasearch Group, 2000; Smith et al., 2001; Mitchell et al., 2002c), with prior and current smokers developing AMD 5 to 10 years before non-smokers, respectively (Mitchell et al., 2002b). The Physicians Health Study was able to demonstrate a dose-response effect; men who smoked more than 20 cigarettes a day were at increased risk of AMD compared to those who smoked less than 20 cigarettes a day (Christen et al., 1996).

Two potential mechanisms have been identified by which smoke may lead to an increased risk of AMD; it may reduce the level of plasma antioxidants through oxidative damage (see section 6.3.3.1) or it may have direct effects on the choroidal blood flow (see section 6.3.3.3) as nicotine acts as a vasoconstrictor (Evans, 2001; Ambati et al., 2003). Additionally, nicotine has been found to stimulate neovascularisation by inducing endothelial cell proliferation and accelerating fibrofascular growth (Heeschen et al., 2001). This may account for the increased rates of recurrent CNV after laser photocoagulation in smokers (Macular Photocoagulation Study Group, 1986).

1.3.1.2.2.8 *Medications*

Use of certain medication may be associated with altered risk of developing AMD, however results are rather mixed. Whilst the Beaver Dam Eye Study found no association between any medication use and early AMD (Klein et al., 2001), other studies have shown a borderline statistically significant increased risk of early ARM with use of antihypertensive medications, particularly β-blockers (Hyman et al., 2000). Use of cholesterol lowering drugs such as statins have been reported to be associated with a decreased rate of CNV among AMD patients (Hall et al., 2001; Wilson et al., 2004). Conversely, in an Australian cohort study, statin use was associated with an increased risk of AMD (McCarty et al., 2001). Further work is required in this area before any concrete conclusions can be made.

1.3.1.2.3 Pathogenesis

AMD is recognised as a complex, multifactorial disease, with the true pathogenesis of the condition not fully understood, though it is likely to involve the disruption of multiple physiological pathways. The hypothesised pathogenesis models for AMD are discussed below.

1.3.1.2.3.1 *Oxidative Stress*

Cumulative oxidative damage has been implicated in the pathogenesis for many age-related pathologies, including AMD (Beatty et al., 2000). Oxidative damage is caused by reactive oxygen intermediates (ROI), or free radicals, including hydrogen peroxide (H_2O_2) and singlet oxygen ($^1O_2$).

In vivo, ROI are continually formed as normal by-products of cellular metabolism (Kukreja and Hess, 1992), photochemical reactions (Ambati et al., 2003) and by the immune system as a defence against pathogens (Khandhadia et al., 2012a). The major source of ROI production is the micochondira (Liang and Godley, 2003). Stimuli known to increase ROI production include aging, inflammation, irradiation and smoking (Borish et al., 1987; Machlin and Bendich, 1987). Oxidative damage by ROI leads to point mutations and deletions in mitochondrial DNA (Golden and Melov, 2001) and leads to earlier senescence, possibly due to damage of telomeric DNA (Rubio, Davalos and Campisi, 2004). The retina, and especially the macula, is particularly vulnerable to oxidative damage due to its high oxygen consumption (Alder and Cringle, 1985), high levels of cumulative irradiation (Beatty et al., 2000), high concentrations of polyunsaturated fatty acids in photoreceptor outer segments which are readily oxidised (Bazan, 1989), high levels of chromophores (Delmelle, 1978; Gaillard et al., 1995) and phagocytosis in the RPE which generates ROI (Tate, Miceli and Newsome, 1995). Oxidative stress may also promote neovascularisation; ROIs have been found to reduce the expression of PEDF (Ohno-Matsui et al., 2001) and upregulate VEGF in the RPE (Kuroki et al., 1996).

As antioxidants are important in scavenging ROI, many studies have investigated the effect of dietary supplementation of antioxidants on AMD development and progression. Most noticeably, the AREDS study (AREDS, 2001), a multicentre randomised double masked clinical trial including over 3600 participants with early signs of AMD, showed that supplementation with high doses of antioxidant vitamins and minerals (ascorbic acid, 500mg/d; vitamin E, 400IU/d; beta carotene, 15 mg/d; zinc oxide, 80 mg/d; and cupric oxide, 2mg/d)

reduced the risk of progression to advanced AMD from 29% to 20%, and the rate of at least moderate vision loss from 29% to 23%. A similar multicentre study also found a positive association between higher serum levels of catotenoids and antioxidants and a decreased risk of exudative AMD (EDCCS, 1993). Several other studies concur with these findings (Goldberg et al., 1988; Sanders et al., 1993; Seddon et al., 1994). These results indicate that not only may supplementation be beneficial in preventing progression of AMD, but also that oxidative damage may be involved in progression of AMD. However, numerous other large scale studies show no evidence for the protective effect of dietary antioxidants or supplementation for AMD (Smith et al., 1999).

1.3.1.2.3.1.1 Lipofuscin formation

Lipofuscin, a lipid-protein aggregate of phagosomal, lysosomal and photoreceptor origin (Nowak, 2006), accumulates in the lysosomal compartment of the RPE (Delori et al., 1995; Kennedy, Rakoczy and Constable, 1995) with age due to the incomplete phagocytosis of photoreceptor outer segment discs (Roth et al., 2004). This implicates malfunction of lysosomal activity with age (Roth et al., 2004). The lipofuscin content of RPE cells has been shown to increase from 1% in the first decade of life, to 19% in the eighth decade (Feeney-Burns, Hilderbrand and Eldridge, 1984). Histopathological studies have shown an association between high levels of lipofuscin and degeneration of RPE cells and adjacent photoreceptors (Dorey et al., 1989), indicating that lipofuscin may play a role in compromising RPE function (Beatty et al., 2000). Holz et al. (2001) also showed by autofluorescence imaging that lipofuscin accumulation in RPE cells was directly associated with the development of geographic atrophy (Holz et al., 2001). Lipofuscinogenesis has therefore been implicated in the pathogeneiss of AMD.

1.3.1.2.3.2 *Inflammation*

AMD is associated with chronic inflammation in the RPE, Bruch's membrane and the choroid (Anderson et al., 2002). The theory of inflammation in the pathogenesis of AMD was proposed by Hageman et al. (1999) following the discovery of inflammatory mediators within drusen deposits (Hageman and Mullins, 1999). Although intraocular inflammation is not clinically apparent in AMD, the presence of HLA-DR and immunoglobulins in drusen, suggest that inflammatory immune processes are involved in drusen biogenesis (Hageman et al., 1999; Johnson et al., 2000; Crabb et al., 2002). The complement system is known to play a key role in host defence against pathogens, the elimination of apoptotic cells and adaptive immune

responses (Walport, 2001). Several studies have found evidence of compliment components in drusen (Johnson et al., 2000; Mullins et al., 2000; Johnson et al., 2001; Nozaki et al., 2006), and there is growing evidence that the complement system plays a vital role in the pathogenesis of AMD (Khandhadia et al., 2012b), with drusen acting as a focus for chronic inflammation (Anderson et al., 2002). Specifically, fragments of C3a and C5a have been found in drusen and are known to induce VEGF expression in RPE cells (Nozaki et al., 2006). The presence of inflammatory cells within Bruch's membrane has also been demonstrated through anatomical studies (Hageman et al., 2001).

Macrophage distribution has been found to correlate with arborizing CNV in both human (Grossniklaus et al., 2000) and animal models (Nishimura et al., 1990), suggesting a possible role in the pathogenesis of wet AMD (van der Schaft et al., 1993; Grossniklaus et al., 2002). Activated macrophages, along with other inflammatory cells secrete enzymes that can damage cells of Bruch membrane (Oh et al., 1999). Thus breaks in Bruch's membrane are likely to be the result, not the cause of CNV (Heriot et al., 1984).

1.3.1.2.3.3 ***Hemodynamic changes and ischemia***

AMD pathogenesis was attributed to impairment of choroidal blood flow as early as 1937 (Verhoeff and Grossman, 1937). Evidence suggests that choroidal blood flow is impaired in patients with AMD, however, the exact nature of this impairment is not fully understood Impaired choroidal blood flow may lead to hypoxia and impaired retinal metabolism (Stefansson, Geirsdottir and Sigurdsson, 2011), causing waste material to accumulate in the outer part of Bruch's membrane (Ambati et al., 2003). Vascular defects have been identified in both dry and wet AMD patients by fluorescein angiography (Pauleikhoff et al., 1999), laser Doppler flowmetry (Grunwald et al., 1998), indocyanine green angiography (Grunwald et al., 2005), histology (Sarks, 1976) and pulsatile ocular blood flow methods (Ciulla, Harris and Martin, 2001; Ambati et al., 2003; Stefansson et al., 2011).

Laser Doppler imaging has shown reduced flow velocities in the posterior ciliary arteries in dry AMD, suggesting abnormal choroidal perfusion (Ciulla et al., 1999). With changes also seen in the central retinal artery, it is suggested that there may be a more generalised perfusion abnormality in AMD (Stefansson et al., 2011). In-vivo findings are supported by histological evidence showing choriocapillaris dropout adjacent to areas of neovascularisation in eyes with wet AMD (McLeod et al., 2009). Vascular dropout will presumably lead to RPE hypoxia,

which may result in increased VEGF production by the RPE, stimulating CNV (McLeod et al., 2009). Similarly, lower pulsatile ocular blood flow in subjects with wet AMD, will likely also play a role in inducing neovascularisation via stimulation of angiogenic factors by hypoxia (Mori, 2001; Mori et al., 2001).

1.3.1.2.4 AMD in Cystic Fibrosis

Pancreatic insufficiency and reduced bile production result in malabsorption of fab-soluble nutrients, vitamins A, D, E and K, and antioxidants beta (β)-carotene and coenzyme Q_{10}. Despite supplementation with multivitamins and pancreatic enzymes as standard in CF, deficiencies of vitamins D and K and antioxidants have been demonstrated (Feranchak et al., 1999; Grey et al., 2008; Laguna et al., 2008; Maqbool and Stallings, 2008). Additionally, due to chronic infection and inflammation associated with CF lung disease, CF patients experience elevated levels of oxidative stress and increased free radical production (van der Vliet et al., 1997; Lezo et al., 2012). A recent study has even shown oxidative stress markers to be elevated in stable clinical conditions, and with antioxidants within the normal range (Lezo et al., 2012). Consequently, the antioxidant/oxidant balance is impaired in CF. This imbalance is thought to contribute to disease progression in CF (Back et al., 2004).

CFTR is known to mediate transport of glutathione, a major antioxidant peptide. Several studies have shown that glutathione depletion increases the risk of oxidative injury (Thor et al., 1982; Wefers and Sies, 1983). Exogenous supply of glutathione to the RPE is known to protect against oxidative damage (Sternberg et al., 1993), and recently a positive relationship has been found between macular pigment and blood glutathione levels (Qin et al., 2011). Blood plasma levels of glutathione have been observed to be reduced in CF patients (Roum et al., 1993). It could be hypothesised that impairment of glutathione transport by malfunctioning CFTR may contribute to increased risk of AMD in CF.

Drusen have previously been noted in two young CF patients (aged 20-25 years old). With oxidative stress identified as having a potential role in the development of AMD, it is reasonable to predict that due to increased oxidative stress and reduced antioxidant status in CF, that patients may show signs of early onset AMD.

1.3.1.3 Optical Coherence Tomography

OCT is a non-invasive, non-contact, transpupillary imaging technique, able to produce high resolution images of retinal structures *in vivo*. OCT generates cross-sectional or three-dimensional images by utilising low coherence interferometry to detect and measure the depth and magnitude of back scattered (reflected) light (Drexler and Fujimoto, 2008).

Since OCT was first demonstrated in 1991 (Huang et al., 1991), it has rapidly developed as the only non-invasive diagnostic technique able to provide images of the retinal microstructure, which directly relate to the histological structure of the retina (Figure 1.19) (Anger et al., 2004).

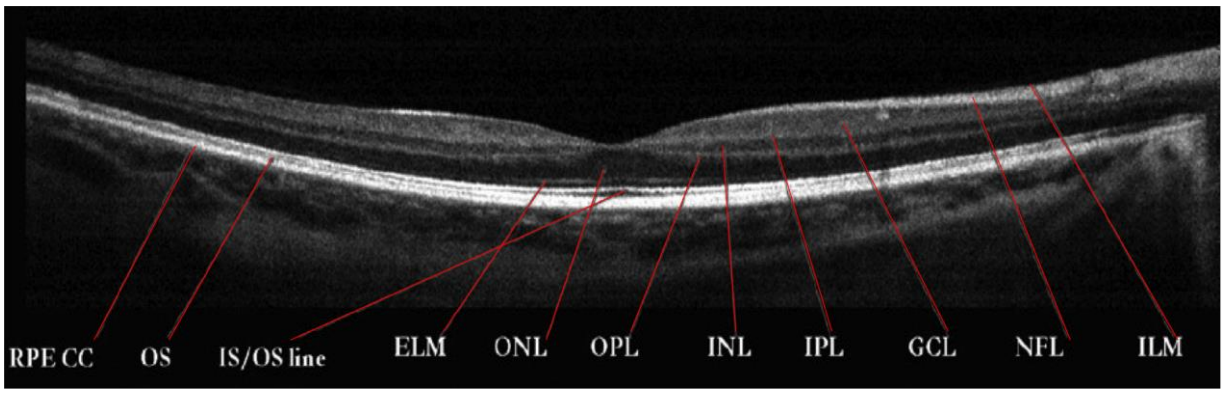

Figure 1.19 OCT of a healthy macular showing the retinal layers. Image from Sheth, Rush and Natarajan (2012). Key: RPE CC, retinal pigment epithelium chorio capillary complex; OS, outer segment; IS, inner segment; ELM, external limiting membrane; ONL, outer nuclear layer; OPL, outer plexiform layer; INL, inner nuclear layer; IPL, inner plexiform layer; GCL, ganglion cell layer; NFL, nerve fiber layer; ILM, internal limiting membrane.

1.3.1.3.1 Operating Principles

Optical coherence tomography is based upon the principles of Michelson interferometry (Huang et al. 1991). Low coherence near-infrared light (typically 800-1400nm) is emitted from a superluminescent diode laser (Guedes et al. 2003), and travels to the interferometer where it is split into two equal components by a semi-transparent mirror. One component is then directed towards the retina through the ocular media (the measurement beam), whilst the other component is directed to a reference mirror (the reference beam). The distance between the beam-splitter and the reference mirror is continuously varied until the distance between the light source and the retinal tissue is equal to the distance between the light source and reference mirror. When this occurs the reflected light from the retinal tissue being imaged, and the light from the reference mirror interact to produce an interference pattern which is detected by a

photosensitive detector and processed into a signal (Figure 1.20). Light reflected from deeper retinal layers have longer time-delays than that reflected from more superficial layers (Figure 1.21). The amplitude of reflected light is dependent upon the tissue reflectivity, and can be plotted against the time delay to produce an a-scan (Costa et al., 2006).

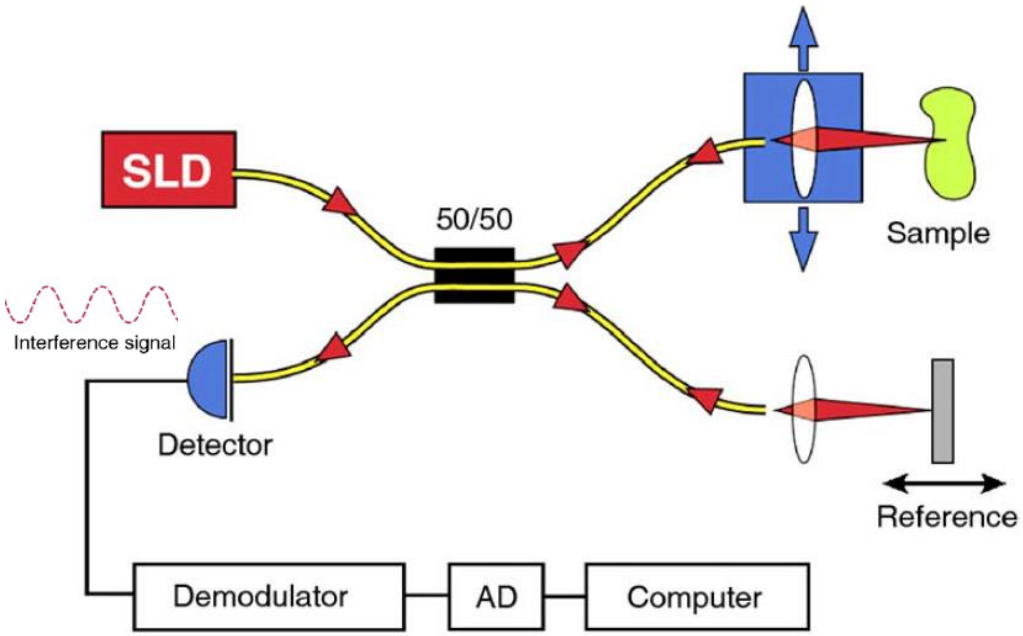

Figure 1.20 A simplified depiction of an OCT system. Output from the superluminescent diode (SLD) is split into the sample and reference arms. Sample and reference reflections are recombined to create an interference pattern which is detected and processed into a signal. Image adapted from Huang, Tan and Fujimoto (2005).

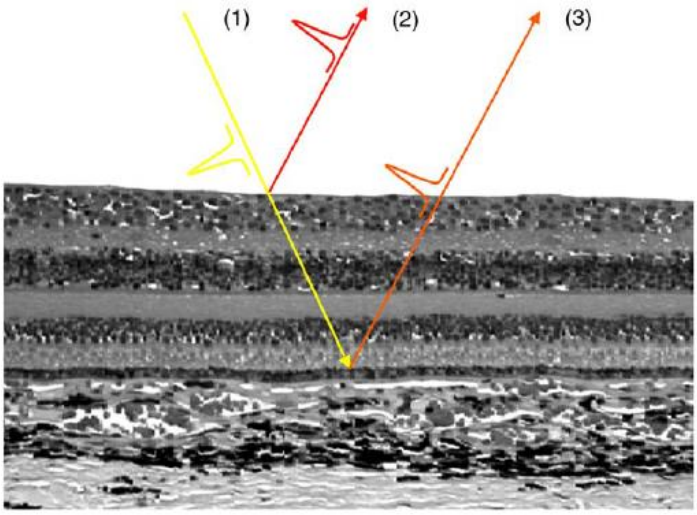

Figure 1.21 OCT time delay of retinal layers. The OCT measurement beam (1) is directed towards the retina. The delay of a superficial reflection (2) is shorter than that of a deeper reflection (3). Image from Huang et al. (2005).

A two-dimensional, cross-sectional retinal image is produced as the light source scans across the retina, stacking and aligning consecutive axial-scans (A-scans) side by side to produce a two-dimensional transverse-scan (B-scan) (Figure 1.22 and Table 1.13) (Costa et al., 2006). Eye movements are corrected by digital processing (cross-correlation scan registration) to align the A-scans, and digital smoothing techniques are used to further reduce image noise (Swanson et al. 1993). The image produced resembles that of a histological section, with contrast produced by differences in the refractive index and scattering properties of the different retinal layers.

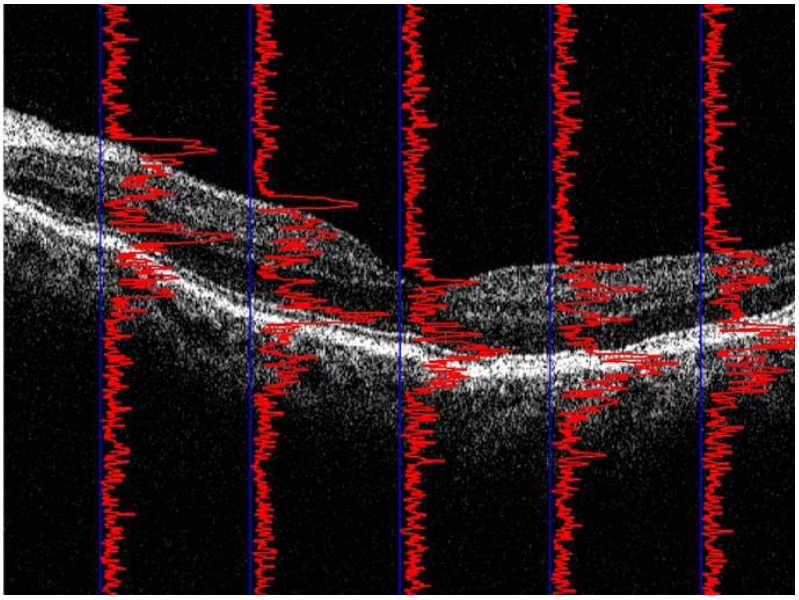

Figure 1.22 Representation of how an OCT B-scan (grey-scale image) is generated by building up and aligning multiple A-scans (red plot lines). Image from Huang et al. (2005).

Table 1.13 Definitions of terms used in OCT

Term	Definition
Pixel	A pixel represents an individual data point within an OCT image
a-scan	The a-scan represents the reflectivity of the sample with increasing depth. It comprises a series of adjacent pixels.
b-scan	The b-scan is a cross sectional tomograph generated by laterally combining a series of adjacent a-scans to generate a 2D cross section of the sample.
c-scan	A c-scan is a 3D image generated by stacking adjacent b-scans.

1.3.1.3.2 Time Domain and Fourier Domain OCT

Since its introduction in 1991, technological OCT parameters have progressed significantly, enabling a substantial improvement in retinal imaging. Original OCT instruments required manual adjustment of the reference mirror to sequentially measure the echo time delay of reflected light. These systems are classed as Time Domain OCT (TD-OCT). Due to the manual nature of image capture with these early devices, acquisition speed was rather limited, resulting in a maximum capture speed of 400 A-scans per second and axial resolutions of approximately 10μm.

More recently, the advent of Fourier Domain OCT (or Frequency Domain OCT; FD-OCT) has enabled data acquisition speeds of up to 18,000-50,000 A-scans per second (Potsaid et al., 2008; Srinivasan et al., 2008)., and a resolution of 2-3μm (Ultrahigh resolution OCT, UH-OCT), enabling in vivo sub-cellular resolution of the intraretinal structure (Drexler and Fujimoto, 2008). In contrast to TD-OCT, FD-OCT employs the use of a stationary reference mirror to obtain an interference spectrum. This spectrum then undergoes computer operated Fourier transformation allowing simultaneous assessment of all the echo time delays (Wojtkowski, Leitgeb and Kowalczyk, 2002).

The significantly higher acquisition speeds achieved by FD-OCT reduces eye motion artefacts in B-scans and enables better delineation of the intraretinal layers due to higher axial resolution, smaller speckle size, and an increase in the number of A-scans (Drexler and Fujimoto, 2008). High acquisition speeds of FD-OCT also enables in vivo three-dimension ultrahigh resolution OCT (3D-OCT) (Figure 1.23).

The improvements gained in axial resolution can be attributed to advances in broad-bandwidth light source technology, providing enhanced image contrast and tissue penetration. Significant improvements in transverse resolution have also been achieved by simultaneous measurements of all light echoes from different axial depths, and through coupling OCT with emerging adaptive optics technologies, moving OCT closer towards cellular resolution imaging (Leitgeb, Hitzenberger and Fercher, 2003). Adaptive optics (AO) improves transverse resolution and reduces granular artifacts by correcting for ocular aberrations (e.g. coma, spherical aberration) in real time through computer manipulation of a deformable mirrors and liquid crystal spatial light modulators (Drexler and Fujimoto, 2008). Integration of adaptive optics into OCT has

enabled an improvement in transverse resolution from 15-20μm to 5-10μm (Hermann et al., 2004).

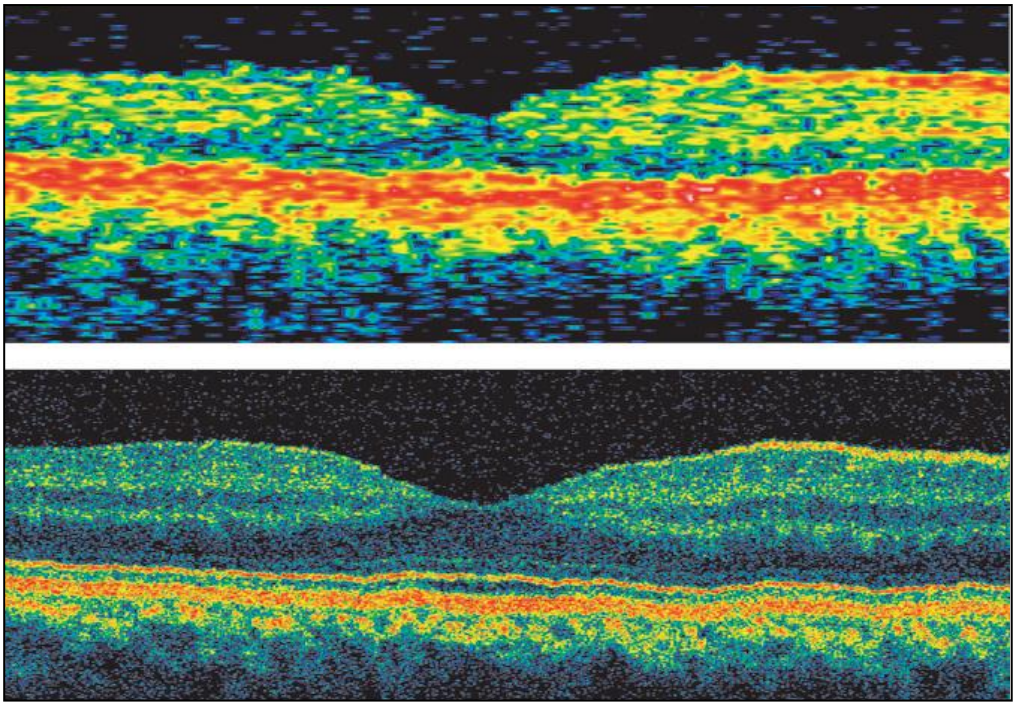

Figure 1.23 Standard resolution OCT (upper picture) versus ultrahigh-resolution OCT (lower picture) of the human retina. Image from Drexler and Fujimoto (2008)

1.3.1.3.3 Transverse image magnification

Whilst the axial component of an OCT image is laser dependent, and is therefore unaffected by magnification effects of varying axial length, transverse parameters are affected by optical magnification. Therefore, correction should be applied when measuring along the transverse direction of an OCT image. Littmann (1982) first proposed a method which could correct for transverse magnification in retinal imaging, which has since been modified by Bennet et al. (1994) to give the following equation:

$$t = pqs \qquad \textit{Equation 1}$$

Where t = true size of retinal feature, μm

p =correction factor based on the optics of the imaging devise

q = correction factor based on the optical dimensions of the eye

s = measured size of retinal feature, μm

Research by Bennett et al. (1994) found that whilst q can be calculated according to the

ametropia, keratometery, refractive indices and the lens curvature of the eye, that axial length has the largest effect on value *q*. Thus q can be defined by the following equation, known as the 'adjusted axial length method':

$$q = 0.01306(x - 1.82) \qquad \textit{Equation 2}$$

Where q = eye correction factor

x = axial length (mm)

The value of p has been calculated for OCT systems as 3.3822 through the use of telecentric devices (Leung et al. 2007). This gives the following equation, which should be used to correct for transverse measurements in OCT images:

$$t = 3.3822(0.01306(x - 1.82))s \qquad \textit{Equation 3}$$

Where: t = true size of retinal feature, μm

x = axial length, mm

s = measured size of retinal feature, μm

1.3.1.3.4 Establishing normal retinal thickness

OCT has become increasingly popular for real-time quantitative and objective evaluation of retinal thickness (RT), due to its ability to detect the inner and outer retinal boundaries to a high degree of accuracy, automatically producing a retinal thickness value. However, different OCT instruments give different measures of RT (Table 1.14). A study that compared the RT values obtained by six different instruments, found a variation of up to ±175μm may exist when measuring the same area of retina (Giani et al., 2010). However, the eyes measured within this experiment not only included healthy eyes, but also those with exudative and non-exudative age-related macular degeneration (AMD), epiretinal membranes, cystoid macular oedema, macular hole and branch retinal vein occlusion. Other studies investigating RT with different instruments have also observed considerable disparity. Using Bland-Altman analysis, Leung et al. (2008) found the largest value for the limit of agreement to be 38.6μm, demonstrating a relatively poor level of agreement between different OCT instruments.

The main cause of this disparity is likely to be that different instruments employ different automated segmentation protocols, and define RT using different retinal boundaries. For example, the Zeiss Stratus, delineates the outer retinal boundary at the photoreceptor inner/outer segment junction (Giani et al., 2010), whereas the Topcon 3D-OCT 1000 identifies the outer boundary at the level of the photoreceptor outer-segment tip (Sull et al., 2010). Whilst this is an important source of variability, instruments that use identical boundaries still measure retinal thickness differences (Huang et al., 2009; Giani et al., 2010).

Table 1.14 Retinal thickness (RT) in healthy subjects at the central area of the Early Treatment Diabetic Retinopathy Study (ETDRS) grid

Authors	Subjects	Instrument	RT (μm) Mean ± SD
Huang et al. (2011a)	n = 60; 33 Males, 27 Females Ethnicity: Chinese Mean age: 40.87 ± 10.17 years	Topcon 3D-OCT 1000	222 ± 16
		Zeiss Cirrus HD	244 ± 19
		Zeiss Stratus	191 ± 17
Sull et al. (2010)	n = 40; 21 Males, 19 Females Ethnicity: 22 White, 13 Asian, 3 Hispanic, 2 Black Mean age: 36.1 ±15.9 years	Topcon 3D-OCT 1000	231 ± 16
		Zeiss Cirrus HD	262 ± 16
		Optovue RTVue-100	267 ± 15
		Stratus OCT	203± 17
Wolf-Schnurrbusch et al. (2009)	n = 20; 9 Males, 11 Females Ethnicity: Not stated Mean age: 37.1 ± 12.8 years	Stratus OCT	213 ± 19
		Heidelberg Spectralis	288 ± 16
		Spectral OCT / SLO	243 ± 25
		Zeiss Cirrus HD	276 ± 17
		SOCT Copernicus	246 ± 23
		Optovue RTVue-1000	245 ± 28
Bruce et al. (2009)	n = 10; 7 Males, 3 Females Ethnicity: Not stated Mean age: 32 years	Topcon 3D-OCT 1000	244 ± 17.84
Sayanagi, Sharma and Kaiser (2009)	n = 8; Gender not stated Ethnicity: Not stated Mean age: 37.0 ± 11 years	Topcon 3D-OCT 1000	222 ± 23
Leung et al. (2008)	n = 35; Gender not stated Ethnicity: Not stated Mean age: 36.4 ± 12.6 years	Topcon 3D-OCT 1000	260 ± 12.2
		Stratus OCT	195.6 ± 17.2
Witkin et al. (2006)	n = 36; 11 Males, 25 Females Ethnicity: Not stated Mean age: 43 years	Stratus OCT	228.4 ± 15.6
Chan et al. (2006)	n = 37; 11 Males, 26 Females Ethnicity: Not stated Median Age: 43 years	Stratus OCT	212 ± 20
Paunescu and Schuman (2004)	n = 10; 6 Males, 4 Females Ethnicity: 8 White, 2 Other Mean Age: 30.5 ± 7.4 years	Stratus OCT	203.8 ± 19.5

1.3.1.3.4.1 ***Repeatability of retinal thickness measures***

The repeatability of any test is important to ensure diagnostic accuracy. Repeatability, as defined by ISO standards, and according to the British Standards Institute, refers to "test conditions that are as constant as possible" and indicates "the strength of agreement between repeated measures", respectively. It is a measure of the precision of the instrument.

Repeatability can be defined by several parameters:

- Coefficient of variation (CoV): the ratio of the standard deviation to the mean
- Intraclass correlation coefficient (ICC): a measure of the correlation and similarity of two different groups
- Coefficient of repeatability (CoR): defined as 1.96 x the standard deviation of differences between visit 1 and 2. CoR represents the value below which approximately 95% of the absolute differences between two repeated tests would be expected to lie.

Several studies have investigated the intra-session repeatability of retinal thickness measures using the Topcon 3D-OCT 1000 (Table 1.15). Leung et al. (2008) found that the Topcon 3D-OCT 1000 demonstrated high repeatability of macular thickness measurements, with the ICC ranging from 92% to 99% in normal eyes for all areas measured within the Early Treatment Diabetic Retinopathy Study (ETDRS) grid (Figure 1.24). All macular measurements had CoV at or less than 1%, with the exception of foveal thickness, which had a CoV of 2.42%. This equates to total macular thickness measures repeatable to within 6.3μm in 95% of cases. Bruce et al. (2009) obtained similar results, concluding that repeatability of macular thickness measures with the Topcon 3D OCT-1000 was within ± 6μm for a single scan. However, repeatability appeared to reduce with age.

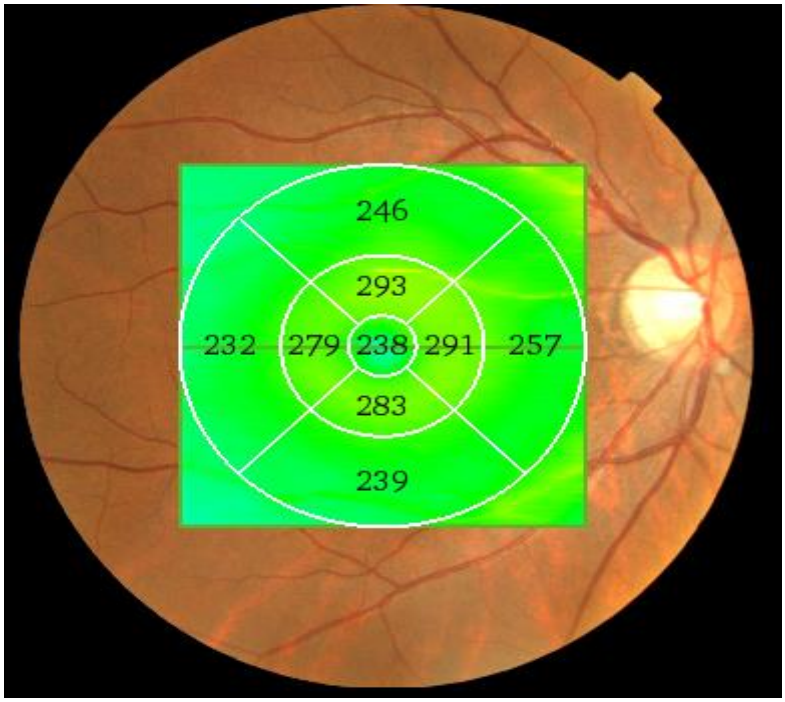

Figure 1.24 Circular ETDRS macular thickness map superimposed upon a fundus photograph. The central area represents the fovea and has a diameter of 1mm.

Repeatability of measurements with the Topcon 3D OCT 1000 appears to remain acceptable even in the presence of ocular abnormality (Ho et al., 2009; Menke et al., 2009). In a study of 52 patients with varying ocular pathologies, the Topcon 3D-OCT 1000 demonstrated excellent repeatability at the central foveal region with an ICC of 96% (Ho et al., 2009). However, the parafoveal and perifoveal regions had greater variability, with ICCs reaching 21% and 54% in the superior parafoveal and inferior perifoveal areas, respectively. Greater variability at these regions may be attributed to the presence of eccentric fixation, leading to higher rates of retinal layer segmentation errors, and hence inaccurate measures of retinal thickness (Ho et al., 2009). It has been suggested that inter-test variability in measurements as a result of eccentric fixation may potentially be minimised by registration of OCT scans to landmarks features, such as retinal vessels (Sull et al., 2010).

Menke et al. (2009) investigated the repeatability of retinal thickness in dry and wet AMD. The mean CoV for the dry and wet AMD groups were 1.8% and 3.6% respectively, indicating a good level of repeatability, particularly in the dry AMD cohort. Increased thickness variability in wet AMD is attributed to the severe morphological changes that occur in wet AMD, making differentiation of retinal layers by the OCT software more difficult (Menke et al., 2009). It has been suggested that this problem can be tackled by manually correcting

segmentation errors, or by employing specially developed software programs for error correction and quantitative subanalysis (Sadda et al., 2007). Repeatability was found to be highest in peripheral macular areas, compared to the central macular, regardless of AMD type. This finding is in contrast to those of Ho et al. (2009). It is suggested that decreased repeatability in the central region could be associated with this area being most severely affected by morphological changes, making correct segmentation of retinal layers more difficult. Lack of manual correction for errors in fixation in the study by Menke et al. may account for the differences in repeatability seen over different retinal areas compared to the study by Ho et al. (2009). Despite significantly higher CoV, repeatability was also deemed acceptable in wet AMD.

Table 1.15 Intra-session repeatability of macular thickness measures for the Topcon 3D-OCT 1000 in healthy and pathological eyes

Authors	Subjects	Scan Type	CoV (%)	ICC (%)
Huang et al. (2011a)	60 Healthy	Macular cube^	0.95 ± 0.55*	97.70*
Sull et al. (2010)	40 Healthy	Macular cube^	-	96.59*
		Radial (6 mm) 1024 A scans per line	-	97.88*
Leung et al. (2008)	35 Healthy	Macular cube^	2.42*	91.80*
Menke et al. (2009)	10 Dry AMD	Macular cube^	1.8 ± 0.6α	-
	12 Exudative AMD		3.6 ± 1.4α	-
Pierro et al. (2010)	18 Healthy	Macular cube^	-	78.0*
Ho et al. (2009)	52 Range of ocular pathology	Macular cube^	-	96.0*

^ Macular cube scan: 512×128 (6×6 mm)

* All values relate to Area 1 of the ETDRS plot (Figure 2.6)

α All values relate to the mean of the macular scan area

1.3.1.3.4.2 *The contribution of intrinsic and external factors on OCT retinal thickness measurements*

1.3.1.3.4.2.1 Age

Song et al. (2010) investigated the relationship between age and macular thickness with the Cirrus HD-OCT in 198 healthy subjects (age range 17-83 years). Results demonstrated an overall decrease in macular thickness and volume with increasing age, except in the central foveal subfield (ETDRS area 1) (Song et al., 2010). These results concur with those by Manassakorn et al. (2008) who found a significant negative correlation between macular thickness and age in all ETDRS areas except the centre (Manassakorn et al., 2008). Eirksson and Alm (2009), also reported a significant negative correlation between macular thickness and age for all ETDRS areas (Eriksson and Alm, 2009). Histological retinal studies similarly show a decrease in the density of photoreceptors, ganglion cells, and RPE cells with age (Gao and Hollyfield, 1992; Panda-Jonas, Jonas and Jackobczyk-Zmija, 1995).

In contrast, a number of other OCT studies have reported the absence of any significant relationship between retinal thickness and age (Gobel, Hartmann and Haigis, 2001; Massin et al., 2002; Wakitani et al., 2003; Wong, Chan and Hui, 2005; Chan et al., 2006; Lam et al., 2007; Sull et al., 2010). However, these studies either contained small sample sizes or failed to control for confounding factors, which may have masked any relationship between retinal thickness and age. Additionally, the study carried out by Lam et al. (2007) utilised the Stratus OCT, which generates a macular thickness map from only six linear line scans over 360°. Results therefore require interpolations to generate thickness estimations for the spaces, which could mask areas of retinal thickening or thinning, leading to inaccurate results.

1.3.1.3.4.2.2 Axial Length / Refractive error

Histopathological studies have demonstrated that axial myopia is associated with increased scleral and retinal thinning (Yanoff and Fine, 1982). This increased thinning is believed to be caused by stretching beyond normal ocular dimensions and is secondary to elongation of the globe. In a recent study investigating the correlation between AL and macular thickness, average outer macular thickness, overall macular thickness and overall macular volume were seen to decrease as AL increased (Song et al., 2010). However, there was no such relationship between AL and central foveal thickness. These results confirm findings by Lam et al. (2007) who observed a significant negative correlation between total macular thickness and AL, and a positive correlation between central foveal thickness and AL. This positive correlation was also noted by Lim et al. (2005), but was attributed to poor fixation in highly myopic eyes.

Conversely, Lam et al. (2007) suggested this increase in central foveal thickness in myopia could be due to photoreceptor outer segment elongation or early vitreoretinal traction.

Earlier studies investigating the relationship between AL and macular thickness utilised first and second generation OCT instruments. The majority of these studies identified no association between macular thickness and AL of the eye, or myopia (Wakitani et al., 2003; Lim et al., 2005). This lack of association could stem from lack of control of possible confounding factors including patient age and gender. Additionally, the relatively low scanning resolution and sampling density of earlier instruments is likely to impact on the accuracy of averaged thickness measures. However, Wakitani et al. (2003) suggest no association was found in their study due to exclusion of eyes with pathological myopia, which have a greater tendency to exhibit decreased thickness (Yanoff and Fine, 1982).

It has been proposed that the periphery, rather than the central retina, is thinner in myopic eyes due to reduced resistance of the peripheral retina to traction and stretch (Wakitani et al., 2003). Decreased peripheral retinal thickness may compensate for the stretching force applied over the whole retina in order to preserve central macular thickness, which is critically important for visual function. Although previous studies have not reached a common consensus on the effect of refractive error and axial length on retinal and macular thickness, observations suggest that AL should be taken into consideration in the interpretation of RT values generated by OCT. This can be achieved by using linear regression analysis to correct raw data when a significant relationship is found (Wood et al., 2011).

1.3.1.3.4.2.3 Ethnicity

The most recent study to investigate the relationship between RT and ethnicity found no significant difference in macular thickness according to race (Sull et al., 2010). These findings contradict those from earlier studies which suggest there is an association between macular thickness and ethnicity. Kelty et al. (2008) investigated macular thickness using the Stratus OCT in 83 healthy subjects. Mean foveal thickness was discovered to be 32μm thinner in African-Americans compared to Caucasians, a value which reached statistical significance. A number of other studies, have also reported central and inner macular thickness (according to the ETDRS plot) to be significantly thinner in blacks and Asians than in Caucasians (Asefzadeh, Cavallerano and Fisch, 2007; El-Dairi et al., 2009; Duan et al., 2010; Wagner-Schuman et al., 2010).

1.3.1.3.4.2.4 Gender

Several studies have reported findings of significantly reduced macular thickness in women, in comparison to men (Massin et al., 2002; Wakitani et al., 2003; Wong et al., 2005; Lam et al., 2007; Kelty et al., 2008; Duan et al., 2010; Kashani et al., 2010; Song et al., 2010; Wagner-Schuman et al., 2010), suggesting an influence of gender on central retinal thickness measurements. A finding of reduced macular thickness in females is synonymous with increased risk of macular hole (Evans et al., 1998), development of which is known to begin with retinal thinning.

1.3.1.3.4.2.5 Diurnal variation

Few studies have investigated the effect of diurnal variation on macular thickness in healthy subjects using OCT. Polito et al. (2006) investigated diurnal variation in diabetic macula oedema compared to healthy controls with the Stratus OCT. All healthy subjects, along with diabetic patients with a baseline foveal thickness of <300μm, were found to have no significant variation in macular thickness throughout the day. Results concur with those by Larsen et al. (2005) who reported that macular thickness remains stable throughout the night in healthy subjects (Larsen, Wang and Sander, 2005). Conversely, diabetic patients with baseline foveal thickness of ≥300μm were found to display a significant decrease in retinal thickness throughout the day, with an average decrease of 9.4% (Polito et al., 2006). This finding is consistent with results from studies performed by Danis et al. (2006), and Larsen et al. (2005). However, it was concluded that the diurnal reduction of retinal thickness is generally of small magnitude, and only occasionally achieves levels that would be considered clinically relevant (Danis et al., 2006). Patients suffering from central retinal vein occlusion have also demonstrated decreasing levels of macula oedema throughout the course of the day (Gupta et al., 2009). Changes in macular thickness throughout the day in patients with macular oedema are thought to be caused by postural changes (mean decrease by 20% when upright) (Polito et al., 2007), arterial pressure (Paques et al., 2005), and/or increased nocturnal retinal metabolism (Gupta et al., 2009).

1.3.1.3.4.2.6 Inter-ocular differences

No significant difference in central retinal thickness has been noted between eyes (Massin et al., 2002; Kelty et al., 2008; Wolf-Schnurrbusch et al., 2009; Duan et al., 2010). Similarly,

ocular dominance has been shown to have no significant effect on macular and retinal thickness (Samarawickrama et al., 2009).

1.3.2 *Investigating retinal function*

Impaired dark adaptation (DA) has been observed in CF subjects with VAD (Fulton et al., 1982; Neugebauer et al., 1989; Rayner et al., 1989; Evans, 2009) and with CFRD (Evans, 2009). However, DA was significantly worse in ΔF508 homozygotes compared to heterozygotes suggesting function is similarly affected by genotype (Evans, 2009). Therefore, it remains unclear if impaired DA in CF subjects can be considered secondary to VAD or CFRD, or if it is actually a primary manifestation of the disease directly related to CFTR dysfunction.

It is well documented that DA is adversely affected in type 1 and type 2 diabetes. Specifically, there have been reports of slowed DA and an elevated final threshold, even in the absence of DR (Henson and North, 1979; Arden et al., 1998; Arden et al., 2005; Holfort et al., 2010). It has been postulated that DA is impaired in type 1 and type 2 diabetes due to increased levels of retinal hypoxia associated with micro vascular abnormalities (Arden et al., 1998; Drasdo et al., 2002), and oxygen inhalation in diabetic subjects has demonstrated temporary normalisation of DA thresholds (Kurtenbach et al., 2006). Repeating oxygen inhalation studies in CF subjects with and without CFRD should further understanding of the aetiology of impaired DA in CF. An absence of improvement in DA with oxygen inhalation in CF subjects would provide support for the hypothesis that impaired DA is a primary manifestation of the disease.

The following section discusses current knowledge on retinal haemodynamics, retinal oxygen consumption and the processes involved in dark adaptation.

1.3.2.1 <u>Retinal haemodynamics</u>

The retina is one of the most metabolically active tissues in the body, consuming oxygen more rapidly than the brain (Ames, 1992). The human retina is supplied by two sources: the central retinal artery (CRA) and the choroidal blood vessels, both of which originate from the ophthalmic artery (Figure 1.25).

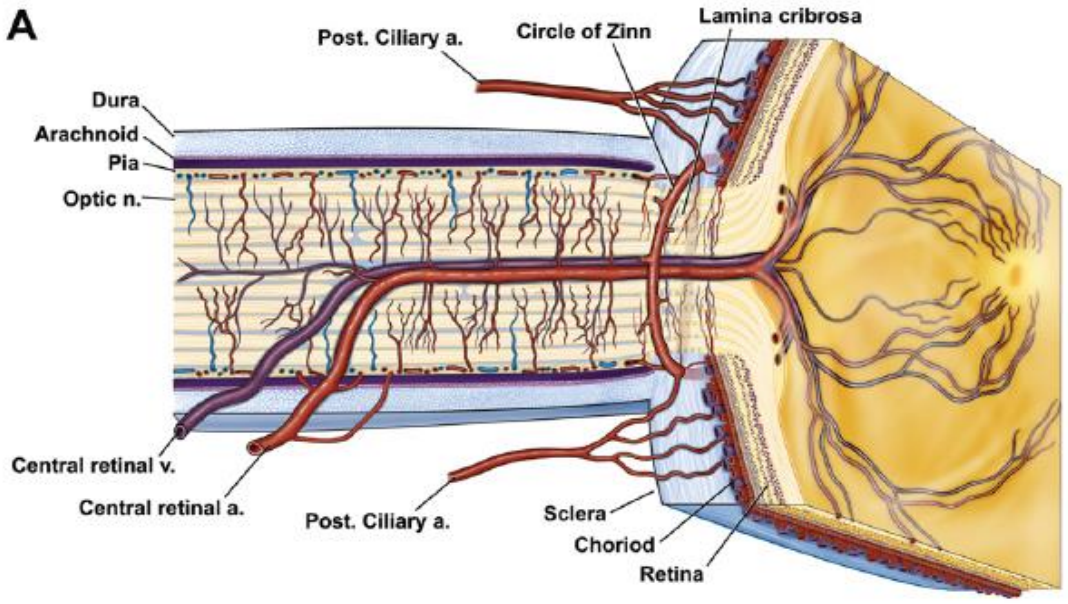

Figure 1.25 The retinal and choroidal blood supply. Image from Anand-Apte and Hollyfield (2009)

The inner retina is supplied by the CRA which receives 20-30% of the total ocular blood flow (Kolb, 1995) and enters the eye at the optic nerve head where it divides into two major branches. These branches in turn divide into arterioles (superior, inferior, nasal and temporal) which extend away from the optic disc to supply separate areas of the retina (Figure 1.26).

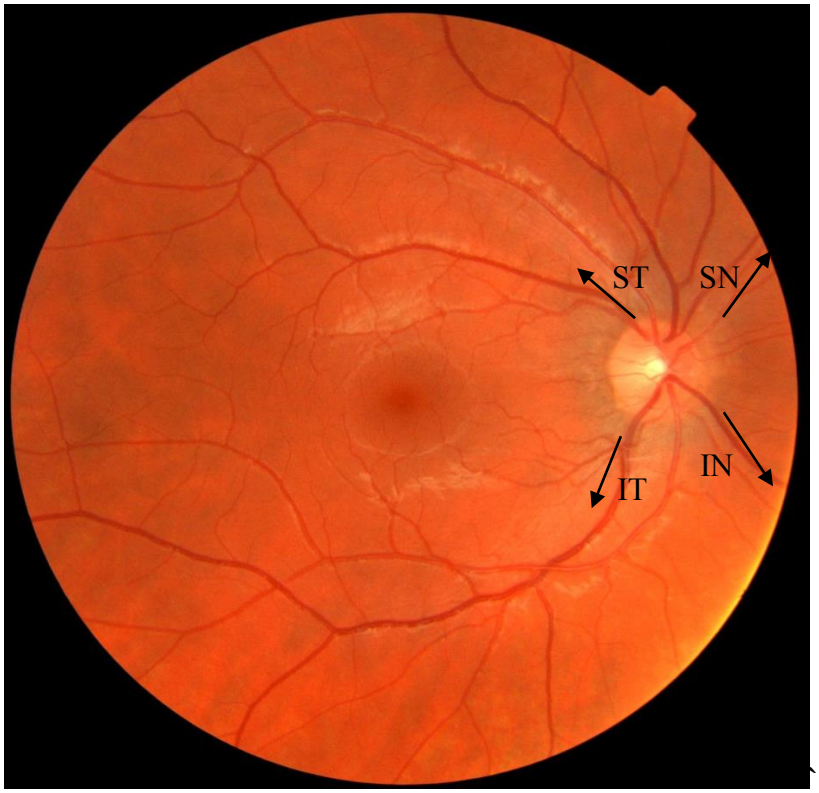

Figure 1.26 The retinal blood supply showing the superior temporal (ST), superior nasal (SN), inferior temporal (IT) and inferior nasal (IN) arcades.

The larger retinal arteries lie in the retinal nerve fibre layer, just beneath the internal limiting membrane. Retinal arterioles give rise to a plexus of capillaries which form an interconnecting network: the first capillary layer is located in the retinal nerve fibre layer and ganglion cell layer, whilst the second capillary layer extends down to the inner nuclear layer (Figure 1.27) (Pournaras et al., 2008).

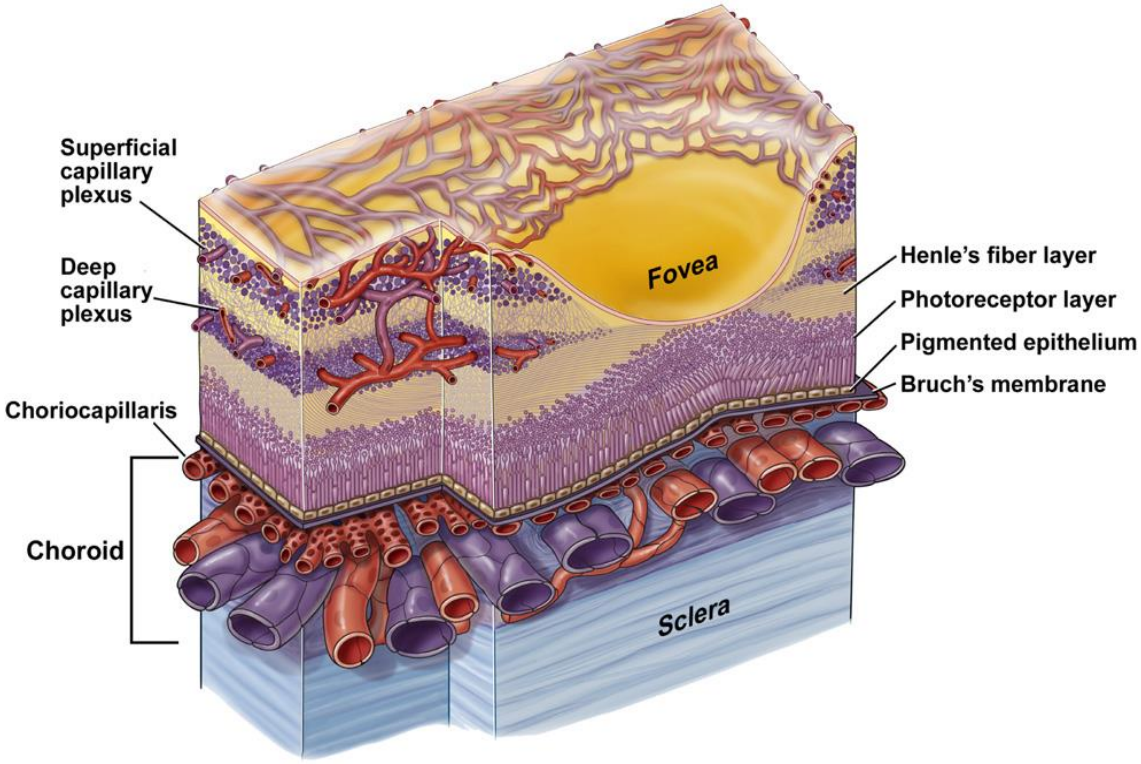

Figure 1.27 Retinal and choroidal blood supply to the various retinal layers. Image from Anand-Apte and Hollyfield (2009)

The retinal vasculature has a relatively low blood flow rate and a high oxygen extraction ratio, resulting in a high arteriovenous oxygen saturation difference and a low venous oxygen tension (Hickam, Sieker and Frayser, 1959; Lange and Bainbridge, 2012).

The choroid receives 65-85% of ocular blood flow (Kolb, 1995) and is vital for the maintenance of the avascular outer retinal layers, particularly the photoreceptors. It has the highest perfusion rate of any vascular bed within the human body, reflecting the high metabolic activity of the photoreceptors (Maleki et al., 2011). The vascular bed of the choriocapillaries lies adjacent to Bruch's membrane and is supplied primarily by the long and short posterior ciliary arteries (both of which are branches of the ophthalmic artery), with minor contribution from the anterior ciliary arteries. Each posterior ciliary artery supplies a localised region of the choroid by breaking up into fan-shaped lobules of capillaries (Hayreh, 1975). The choroidal circulation has a very low rate of oxygen extraction resulting in a low arteriovenous oxygen saturation difference and a high venous oxygen tension (Alm and Bill, 1972; Lange and Bainbridge, 2012). Choroidal blood is thought to be drained exclusively through the vortex veins (Ruskell, 1997)

1.3.2.1.1 Retinal Oxygen Consumption

The retinal oxygen distribution varies across the retina in accordance with the retinal cell class and their associated level of metabolic activity (Figure 1.28). The highest oxygen tension is found in the choroid, and the lowest at the level of the photoreceptor inner segments, reflecting the high oxygen consumption rate of the tightly packed mitochrondria in this region (Cringle et al., 2002). Whilst the choroid has a high oxygen tension, the extraordinarily high oxygen demand of the photoreceptors, combined with the avascular nature of the outer retina, results in a substantially increased risk of these cells experiencing hypoxic episodes. This risk is further increased in dark adapted conditions when oxygen consumption at the inner segments is at its highest in order to produce the ATP necessary to maintain the dark current. Oxygen tension has been shown to drop to to 0 mmHg at the outer nuclear layer in rats in dark adapted conditions (Kimble, Svoboda and Ostroy, 1980; Linsenmeier, 1986; Lange and Bainbridge, 2012).

Studies show that the choroid contributes approximately 90% of the oxygen consumed by the photoreceptors in the darkness, and all of the oxygen consumed during light adaptation (Linsenmeier and Braun, 1992). In order to maintain sufficient oxygenation , the outer retina may increase oxygen utilisation from the deep retinal capillaries (Caprara and Grimm, 2012), suggesting a dynamic regulation of the outer retinal oxygen supply.

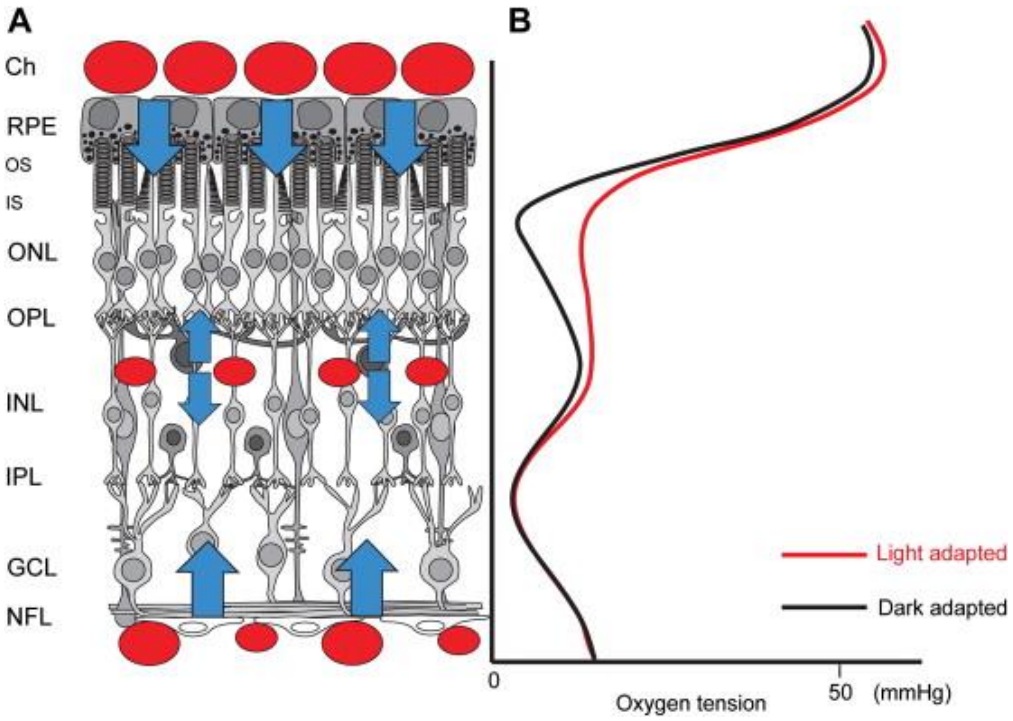

Figure 1.28 Oxygen distribution throughout the retina. (A) Schematic representation of the rat retina. Red circles represent blood vessels, blue arrows show the direction of oxygen diffusion. (B) Intraretinal oxygen distribution profile of a rat retina in light and dark adapted conditions. Image from Caprara and Grimm (2012). Key: ch, choroid; RPE, retinal pigment epithelium; os, outer segments; is, innger segments; ONL, outer nerve fibre layer; OPL, outer plexiform layer; INL inner nuclear layer; IPL, inner plexiform layer; GCL, ganglion cell layer; NFL, nerve fibre layer.

1.3.2.1.2 Autoregulation

Autoregulation describes the ability of the blood vessels to control the level of blood flow in accordance with the metabolic demands of the tissue through release of local factors including nitric oxide and endothelin, to modulate the tone of the vessels (Pournaras et al., 2008). Local factors may be either ionic or molecular, or related to arterial blood gas modifications, and released by the vascular endothelium and/or neural tissue surrounding the vessels (Pournaras et al., 2008). Autoregulation is achieved by compensatory changes in artierial and arteriolar diameter, a response which also serves to protect microvasculature from blood-pressure induced damage (Justesen et al., 2010).

With the potential influence of the autonomic innervation excluded (Ye, Laties and Stone, 1990), and the contribution of hormones and neurotransmitters negligible due to the blood-retinal barrier (Delaey and Van De Voorde, 2000), the retinal vasculature is believed to have well-developed, intrinsic autoregulatory mechanisms (Flammer and Mozaffarieh, 2008).

Hyperoxia (increased partial pressure of oxygen (PaO_2) in arterial blood), achieved through the inhalation of 100% oxygen has been shown to result in retinal vasoconstriction in healthy subjects (Hickam and Sieker, 1960; Riva et al., 1983b; Grunwald et al., 1984a; Jean-Louis, Lovasik and Kergoat, 2005; Gilmore et al., 2007a; Gilmore et al., 2007b). Conversely, hypercapnia (increased partial pressure of carbon dioxide ($PaCO_2$)) and hypoxia (decreased PaO_2) induce vasodilation of the retinal arterioles causing an increase in retinal blood flow (Pournaras, Tsacopoulos and Chapuis, 1978; Venkataraman et al., 2006). It is thought that the autoregulatory abilities of the retinal blood supply compensate for the increased oxygen demand in dark adapted conditions in healthy subjects (Caprara and Grimm, 2012).

The choroidal circulation is controlled by autonomic innervation, with blood flow mediated by activation of sympathetic and parasympathetic innervation of the smooth muscle cells (Kawarai and Koss, 1998; Kur, Newman and Chan-Ling, 2012). Human choroidal vasculature has demonstrated little reactivity to changes in PaO_2 (Schmetterer et al., 1995; Geiser et al., 2000), and its autoregulatory capacity is thought to be negligible (Wangsa-Wirawan and Linsenmeier, 2003).

1.3.2.1.2.1 ***Retinal effects of hyperoxia***

An increase in PaO_2 through inhalation of 100% O_2 has consistently shown to induce vasoconstriction of retinal vessels in humans (Grunwald et al., 1984b; Fallon, Maxwell and Kohner, 1985; Sponsel, DePaul and Zetlan, 1992; Langhans, Michelson and Groh, 1997; Kiss et al., 2002; Werkmeister et al., 2012), with the effect most marked in the inner retinal arterioles (Jean-Louis et al., 2005). These findings suggest that arterioles are the main site of the autoregulatory response (Riva, Grunwald and Sinclair, 1983b; Kiss et al., 2002). Venular and arterial constriction have been reported in the range of 11-14.9%, and 9.2-14.9%, respectively (Hickam, Frayser and Ross, 1963; Riva et al., 1983b; Kiss et al., 2002; Jean-Louis et al., 2005).

All vasoconstriction induced by hyperoxia has been shown to occur within the first five minutes of onset of inhalation and was negatively correlated with baseline vessel diameter (Kiss et al., 2002). These findings support the notion that the small pre-capillary arterioles and small post-capillary venules play a key role in the increase in vascular resistance during hyperoxia (Kiss et al., 2002). Vasoconstriction in response to hyperoxia serves to maintain retinal PaO_2 at a constant level (Pournaras et al., 1989). As the retinal oxygen tension gradient

from the choroid is much steeper during hyperoxia following inhalation, a greater portion of the retina's demands can be supplied via the choroid during hyperoxia, compared to periods of normoxia (Wangsa-Wirawan and Linsenmeier, 2003).

1.3.2.1.3 Effect of illumination on ocular haemodynamics

1.3.2.1.3.1 *Retina*

Elevation of oxygen consumption by photoreceptors in the dark compared to light has been established in animal models both *in vitro* (Zuckerman and Weiter, 1980; Haugh-Scheidt, Linsenmeier and Griff, 1995) and *in vivo* (Linsenmeier, 1986; Linsenmeier and Braun, 1992; Birol et al., 2007). Given the autoregulatory ability of the retinal blood supply, changes in retinal haemodynamics would be expected to meet any increased oxygen demand that results during dark adaptation.

Retinal haemodynamic studies investigating the effect of illumination have previously utilised a range of techniques, including measurements of blood velocity in the main retinal arteries, retinal vessel diameter and tissue oxygen saturation. Measurement of blood velocity and vessel diameter by laser Doppler flowmetry in two studies have shown an increase in retinal blood flow of 40-70% upon transition from light to dark conditions (Feke et al., 1983; Riva, Grunwald and Petrig, 1983a). This active haemodynamic response has been attributed to an increase in blood flow velocity rather than to a change in retinal vessel diameter. Observations by Havelius and colleagues, that systolic and diastolic blood flow velocities in the CRA were markedly increased in dark conditions, support this view (Havelius et al., 1999). However, these results are inconsistent with findings from a more recent study utilising laser Doppler velocimetry, which demonstrated only a transient rise in blood flow (Hardarson et al., 2009) suggesting that earlier observations may have been a consequence of the transition from light itself, rather than the effect of darkness (Riva, Petrig and Grunwald, 1987; Hardarson et al., 2009).

1.3.2.1.3.2 *Choroid*

Recent investigations have shown that transition from light to dark in humans is associated with a considerable decrease in choroidal blood flow of up to 15% (Longo, Geiser and Riva, 2000; Fuchsjager-Mayrl et al., 2001; Fuchsjager-Mayrl et al., 2003), with the reduction reported in both eyes when only one was subjected to dark adaptation (Fuchsjager-Mayrl et al., 2001). The change in choroidal blood flow was attributed to local vasoconstriction of the

choriocapillaris (Longo et al., 2000). It is unlikely that this change in choroidal blood flow during dark adaptation is secondary to increased oxygen consumption in the outer retina as choroidal circulation has been shown to be insensitive to PaO_2 changes (Geiser et al., 2000), and no change would be observed in the contralateral eye. In addition, increased oxygen consumption in the dark by photoreceptors would be expected to lead to an increase in choroidal blood flow, rather than the decrease observed. Furthermore, a change in oxygen consumption of the photoreceptors would only occur in the stimulated eye (Kur et al., 2012). The contralateral eye response to light stimulation suggests a neuronal mechanism is involved. This theory supports previous findings which indicate that the choroid is under tight neural control (Kiel, 1999). This neural circuit, which is believed to mediate this response, has not been identified in humans to date (Longo et al., 2000).

1.3.2.1.4 Retinal changes and blood flow in diabetes

Retinal diabetic pathophysiology involves pericyte loss (Ejaz et al., 2008), vascular leakage, retinal vessel angiogenesis, changes to inner and outer retinal neurones, and alteration to the structure and function of glial cells (Rungger-Brandle, Dosso and Leuenberger, 2000; Phipps et al., 2006). Whether or not retinal blood flow differs in diabetic patients compared to healthy controls remains controversial, with observations appearing contradictory (for a thorough review see Pournaras et al. (2008) and Clermont and Bursell (2007)). However, the combination of vascular wall damage and impaired rheological blood properties suggest that regulation of retinal blood flow would be affected in diabetes (Pournaras et al., 2008).

Blood flow speeds in retinal arteries of type 1 diabetic patients have been found to be significantly slower compared to healthy subjects, even before the clinical appearance of diabetic retinopathy (Arend et al., 1991; Feke et al., 1994; Bursell et al., 1996). Konno et al. (1994) found arterial blood flow speeds reduced with increasing duration of diabetes, a finding which is consistent with previous studies (Rimmer, Fallon and Kohner, 1989; Feke et al., 1994). This decrease in blood flow is an effect of increasing resistance in the retinal vascular network with increasing duration of diabetes. This is in line with findings of abnormal synthesis or action of vasodilators, and increased expression and action of vasoconstrictors, resulting in a net vasoconstrictory effect in early diabetes (Clermont and Bursell, 2007).

As retinopathy progresses and becomes more severe, retinal blood flow in major arteries ceases to decrease and begins to increase (Konno et al., 1996). It is suggested that this increase

represents a decrease in the resistance to blood flow secondary to the development of anastomoses (Konno et al., 1996), a hypothesis which is supported by histological findings (Cogan and Kuwabara, 1963). Chronic hyperglycaemia in diabetes is associated with decreased total retinal blood flow, even in the absence of diabetic retinopathy (Bursell et al., 1996). However, as the disease progresses, bulk retinal blood flow is generally above normal, as confirmed by laser Doppler flowmetry and video fluorescein angiography (Grunwald et al., 1993).

1.3.2.1.4.1 ***Retinal oxygenation in diabetes***

Diabetes causes a series of circulatory/vascular changes throughout the body including: stiffening of red blood cell walls which reduces the ease of transport through capillaries, and vessel basement membrane thickening (Arden et al., 2005). Additionally, within the retina, retinal capillaries show loss of pericytes and endothelial cells, changes which are expected to impair the quality of retinal perfusion (Trick and Berkowitz, 2005). These changes are hypothesised to result in a reduction in the retinal oxygen supply. In diabetic cats, inner retinal oxygen tension is reduced by half even in the absence of capillary dropout (Linsenmeier et al., 1998), and in rat models of diabetes, hypoxia is evident via magnetic resonance imaging oximetry (Trick and Berkowitz, 2005). Similarly, in humans with diabetes, oxygen tension in the mid vitreous (which is believed to mirror oxygenation of the inner retina) (Wangsa-Wirawan and Linsenmeier, 2003) is reduced, as measured using an optical oxygen probe (Lange et al., 2011)

There are various lines of evidence to suggest rod-driven hypoxia triggers the development of diabetic retinopathy (DR). DR does not occur in patients with diabetes and retinitis pigmentosa, where rod outer segments are reduced (Arden 2001). DR is often successfully treated with pan-retinal photocoagulation, which is believed to work by destroying rods and consequently reducing the retinal oxygen demand (Yu and Cringle, 2001). Furthermore, some studies show that oxygen inhalation can reverse early functional deficits including impaired colour vision (Dean, Arden and Dornhorst, 1997), dark adaptation (Drasdo et al., 2002; Kurtenbach et al., 2006) and contrast sensitivity (Harris et al., 1996), along with reducing macular oedema (Nguyen et al., 2004) . It is hypothesised that these deficits are secondary to relative retinal oxygen desaturation caused by abnormal retinal perfusion and ischaemia, which is seen in early diabetes.

1.3.2.1.4.2 ***Autoregulation in diabetes***

It is understood that diabetes impairs retinal autoregulation (Ciulla et al., 2002). Previous studies have shown a reduction in the autoregulatory constriction response of the retinal arteries and veins in diabetics following inhalation of 100% oxygen, even in those with no DR (Hickam and Sieker, 1960; Grunwald et al., 1984a). One of the earliest defects in diabetes is the loss of perictyes (Ansari et al., 1998) which regulate retinal vascular tone (Shepro and Morel, 1993). Damage to these cells causes disruption to retinal haemodynamics (Ciulla et al., 2002). Diabetic patients have been shown to suffer from impaired autoregulatory capacity in proportion with the disease severity (Ciulla et al., 2002). Subjects with proliferative retinopathy showed a 24% reduction in retinal vessel bulk upon inhalation of oxygen compared to those with background retinopathy who had a 38% reduction (Grunwald et al., 1984a). Magnetic resonance imaging retinal oximetry has demonstrated that patients with diabetes show an exaggerated rise in retinal PaO_2 following exposure to hyperoxia, suggesting abnormal retinal autoregulation (Trick et al., 2006).

1.3.2.1.4.3 ***Retinal effects of hyperoxia in diabetes***

Numerous studies show that the arteriolar vasoconstrictor response to breathing 100% oxygen is reduced in patients with type 1 diabetes compared to non-diabetic controls (Hickam and Sieker, 1960; Grunwald et al., 1984b; Justesen et al., 2010). Reduced arterial constriction in response to hypoxia indicates defective reactivity of retinal arterioles in diabetes. The mechanism that causes reduced artieriolar reactivity to hyperoxia is not yet fully understood. However, is has been suggested that hyperglycaemia may play a role in the impaired response to hyperoxia in diabetes (Justesen et al., 2010) following the finding that induced hyperglycaemia reduced vasoconstriction in response to hyperoxia in non-diabetic subjects (Gilmore et al., 2008).

In contrast, venules appear to show no significant response to hyperoxia (Hickam and Sieker, 1960; Justesen et al., 2010), except in those subjects with retinopathy or with co-existing hypertension, in which case vasoconstriction was observed (Hickam and Sieker, 1960).

1.3.2.1.4.4 ***Retinal effects of hyperglycaemia***

Hyperglycaemia mediates endothelial cell dysfunction, and thus affects vascular reactivity, causing impairment in vasodilation. Increased extracellular glucose concentrations in hyperglycaemia leads to an increase in the intracellular glucose concentration and the

metabolic rate. This increase in intracellular glucose may initiate abnormalities including increased oxygen consumption (Clermont and Bursell, 2007).

Previous studies have demonstrated increased retinal blood flow during hyperglycaemia in diabetes through examination by Doppler velocimetry and video fluorescein angiography (Grunwald et al., 1987; Bursell et al., 1996). This increase is related to the duration of diabetes, with those individuals with the shortest duration showing the greatest increase, hence demonstrating retained autoregulatory capacity, whilst those with the longest duration lacked this ability (Tiedeman et al., 1998). Further research by Tiedeman et al. (1998), provided substantial evidence that increased blood flow during acute hyperglycaemia is related to increased retinal oxygen consumption.

Other studies examining the retinal vascular response to hyperglycaemia report no change in the retinal blood flow (Fallon et al., 1987; Gilmore et al., 2007b). The disparity in these results may be partly attributed to the various methods used to measure retinal haemodynamics, the varying glycaemic control of participants, and the various methods used to induce hyperglycaemia. Furthermore, the lack of blood flow response to hyperglycaemia in diabetic patients in these studies may be explained by a loss of vascular reactivity (Gilmore et al., 2007b).

1.3.2.2 Dark adaptation

As discussed in section 1.2.8.3.2, the human visual system is able to function over a wide range of light intensities, covering more than $10\log_{10}$ units, by means of light and dark adaptation (DA). Light adaptation occurs extremely rapidly, allowing individuals to adjust to different levels of illumination within a few seconds. However, this relationship breaks down upon entering the dark following exposure to an intense light source which 'bleaches' a large proportion of visual photopigment. The process by which the eye recovers visual sensitivity following this exposure is known as 'dark adaptation' and typically takes 30-40 minutes.

1.3.2.2.1 The retinoid cycle

Recovery of visual sensitivity following exposure to an intense light is associated with the 'retinoid cycle' of visual pigment regeneration (Lamb and Pugh, 2004). The retinoid cycle refers to the biochemical processes involved in removing the products of light absorption from

the photoreceptors and the regeneration of visual photopigments. Figure 1.29 and Table 1.16 summarise the sequence of events involved in the retinoid cycle.

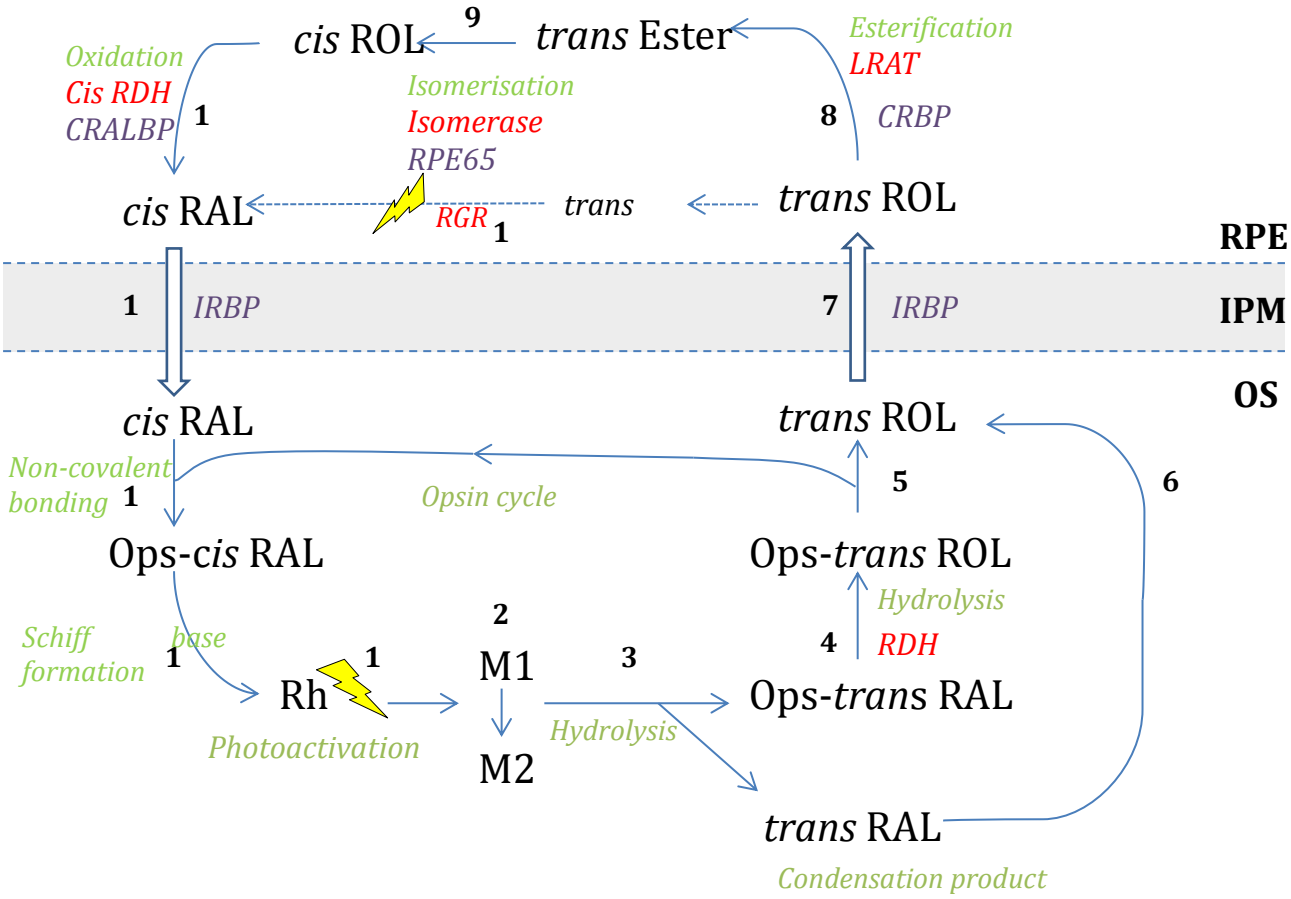

Figure 1.29 The retinoid cycle of vision. Numbers relate to the different steps involved in the retinoid cycle as outlined in Table 3.1. Image adapted from Lamb and Pugh (2004). Key: Rh = rhodopsin; RAL = retinal; ROL = retinol; IRBP = interphotoreceptor retinol binding protein; CRBP = cellular retinol binding protein; LRAT = lecithin retinol acyl transferase; CRALBP = cellular retinaldehyde-binding protein; RGR = retinal G-protein coupled receptor; OS = outer segment; IPM = inter-photoreceptor matrix; RPE = retinal pigment epithelium

Table 1.16 Steps of the retinoid cycle. Adapted from Lamb and Pugh (2004)

Step	Process	Enzyme	Chaperone protein
1	Photoactivation of photopigment		
2	Opsin protein re-arrangement		Opsin (metarhodopsin)
3	Hydrolysis of the covalent bond between all-trans retinal and opsin		Opsin (metarhodopsin)
4	Reduction of the retinal aldehyde	RDH	Opsin (Ops-trans RAL)
5	Release of all-trans retinol		Opsin (Ops-trans RAL)
6	Flippase	ABCR	
7	Transport across the IPM and RPE		IRBP CRBP
8	Esterification	LRAT	CRBP
9	Isomerisation	Isomerase	RPE65
10	Oxidation of the alcohol	cis RDH	
11	Transport across the RPE and IPM		CRALBP IRBP
12	Non-covalent binding of opsin to 11-cis-retinal to form opsin-11-cis retinal		
13	Spontaneous formation of Schiff-base bond and conformation change to yield rhodopsin		
14	Photoisomerisation – a subsidiary step of the retinoid cycle which requires light energy	RGR	

Key: RDH = retinol dehydrogenase; RAL = retinal; CRALBP = cellular retinaldehyde-binding protein; IRBP = interphotoreceptor retinol binding protein; CRBP = cellular retinol binding protein; LRAT = lecithin retinol acyl transferase; RGR = retinal G-protein coupled receptor.

Photopigment molecules comprise a protein, opsin, which is covalently bound to the chromophore, 11-cis-retinal (Schertler, Villa and Henderson, 1993). Absorption of a photon of light by a photopigment molecule triggers photoisomerisation of 11-cis-retinal to its all-trans form and begins the cycle of bleaching and regeneration of photopigment. This reaction is the initial stage of phototransduction (see section 1.3.2.2.3), which leads to visual perception (McBee et al., 2001). The photopigment protein molecule known as 'metarhodopsin' can exist in a number of interchangeable forms (M_1,M_2, M_3). Metarhodopsin 1 (M_1) is rapidly converted into metarhodopsin 2 (M_2), which causes a shift in the λ_{max} towards the near UV range, resulting in loss of visual pigment colour, hence why light is said to 'bleach' photopigment.

Once in the M_2 state, rhodopsin becomes susceptible to hydrolysis, producing Opsin-all-trans retinal. Retinol dehydrogenase is then able to reduce the aldehyde to all-trans retinol. At this stage it is believed that all-trans retinol is still bound to opsin at an 'exit site' (Heck et al., 2003; Schadel et al., 2003). Evidence suggests that all-trans retinol can only be released from opsin once the entrance site is again occupied by 11-cis-retinal (Schadel et al., 2003).

Once released, all-trans-retinol is chaperoned across the inter-photoreceptor matrix (IPM) by interphotoreceptor retinol binding protein (IRBP) (Qtaishat, Wiggert and Pepperberg, 1999), one of the most abundant proteins in the photoreceptor/RPE layers (Liou, Geng and Baehr, 1991). All-trans-retinol is then chaperoned by cellular retinol binding protein (CRBP) within the RPE, and undergoes esterification by lecithin retinol acyl transferase (LRAT) to form retinyl esters (Trehan, Canada and Rando, 1990). A steady supply of fatty acid is essential for this esterification reaction (Lamb and Pugh, 2004). All-trans-retinol ester, formed by LRAT, is chaperoned by RPE65 (Gollapalli, Maiti and Rando, 2003; Mata et al., 2004), a protein which is essential for the production of 11-cis-retinal (Redmond et al., 1998). Isomerisation of the retinyl ester by isomerohydrolase produces 11-cis-retinol which then inhibits further acitivity of isomerohydrolase (Gollapalli and Rando, 2003). Oxidation of 11-cis-retinol by 11-cis retinol dehydrogenase (RDH) is the final step in the production of the 11-cis-retinal chromophore. Studies suggest that IRBP is then able to facilitate the release of 11-cis-retinal from the RPE and chaperone it across the IPM (Carlson and Bok, 1992; Edwards and Adler, 2000). No chaperone molecule for 11-cis-retinal has been identified within the photoreceptor outer segments (OS), therefore 11-cis-retinal is believed to move unchaperoned through the water space to reach rod discs where the opsin is bound (Lamb and Pugh, 2004). Opsin and 11-cis-retinal spontaneously recombine (de Grip, Daemen and Bonting, 1972), at opsins 'entrance site' (Schadel et al., 2003) before a Schiff base bond is formed between the two, causing transformation to reform rhodopsin.

1.3.2.2.2 The iodopsin visual cycle

Whilst light exposure bleaches rod and cone pigment at equal rates (Harosi, 1975), their quantum efficiency is identical (Dartnall, 1972), and their excitation coefficients are very similar (Shichida et al., 1994), cone recovery is much more rapid in comparison to rods (3-4 minutes versus 30 minutes, respectively) (Hecht, Haig and Chase, 1937; Wang and Kefalov, 2011). As pigment regeneration is essential for the restoration of dark adapted sensitivity, these differences in recovery times between cones and rods suggest that cone photopigment is

regenerated substantially faster than that of rods. Pigment regeneration is rate-limited by the supply of 11-cis-retinal to the photoreceptors (Lamb and Pugh, 2004), therefore, rapid cone recovery suggests chromophore is supplied significantly faster to cones than rods, possibly by a different, cone-specific retinoid cycle (Wang and Kefalov, 2011).

1.3.2.2.2.1 ***The Müller cell hypothesis***

There is increasing evidence of an alternate processing pathway for the regeneration of cone photopigment, separate to the RPE (Wang and Kefalov, 2009; Wang and Kefalov, 2011). The expression of retinoid binding proteins CRBP and CRALBP within Müller cells, allowing the conversion of all-trans retinol to 11-cis-retinol within the retina, suggests Müller cells might be involved in a separate chromophore processing pathway (Bok, Ong and Chytil, 1984; Eisenfeld, Bint-Milam and Saari, 1985; Mata et al., 2002). In further studies, only cone cells have demonstrated ability to regenerate pigment by oxidation of 11-cis-retinol to 11-cis-retinal, suggesting the Müller cell pathway is only available to cones, and not rods (Wang and Kefalov, 2009; Wang and Kefalov, 2011).

A summary of the cone-specific visual pathway based upon current knowledge is shown in Figure 1.30. Following photolysis, all-trans retinal is reduced to all-trans retinol within the cone outer segment. All-trans retinol is then transported across the IPM to Müller cells, possibly chaperoned by IRBP (Jin et al., 2009; Parker et al., 2009). Once within the Müller cells, all-trans retinol is chaperoned by CRBP and undergoes isomerisation to 11-cis-retinol (Mata et al., 2002). 11-cis-retinol is then transported to the cone inner segment (Parker et al., 2009), where it can then move freely to the outer segment, where oxidisation to 11-cis-retinal completes pigment regeneration (Mata et al., 2002; Miyazono et al., 2008). This additional pathway for cone photopigment regeneration facilitates rapid photopigment regeneration during photopic conditions.

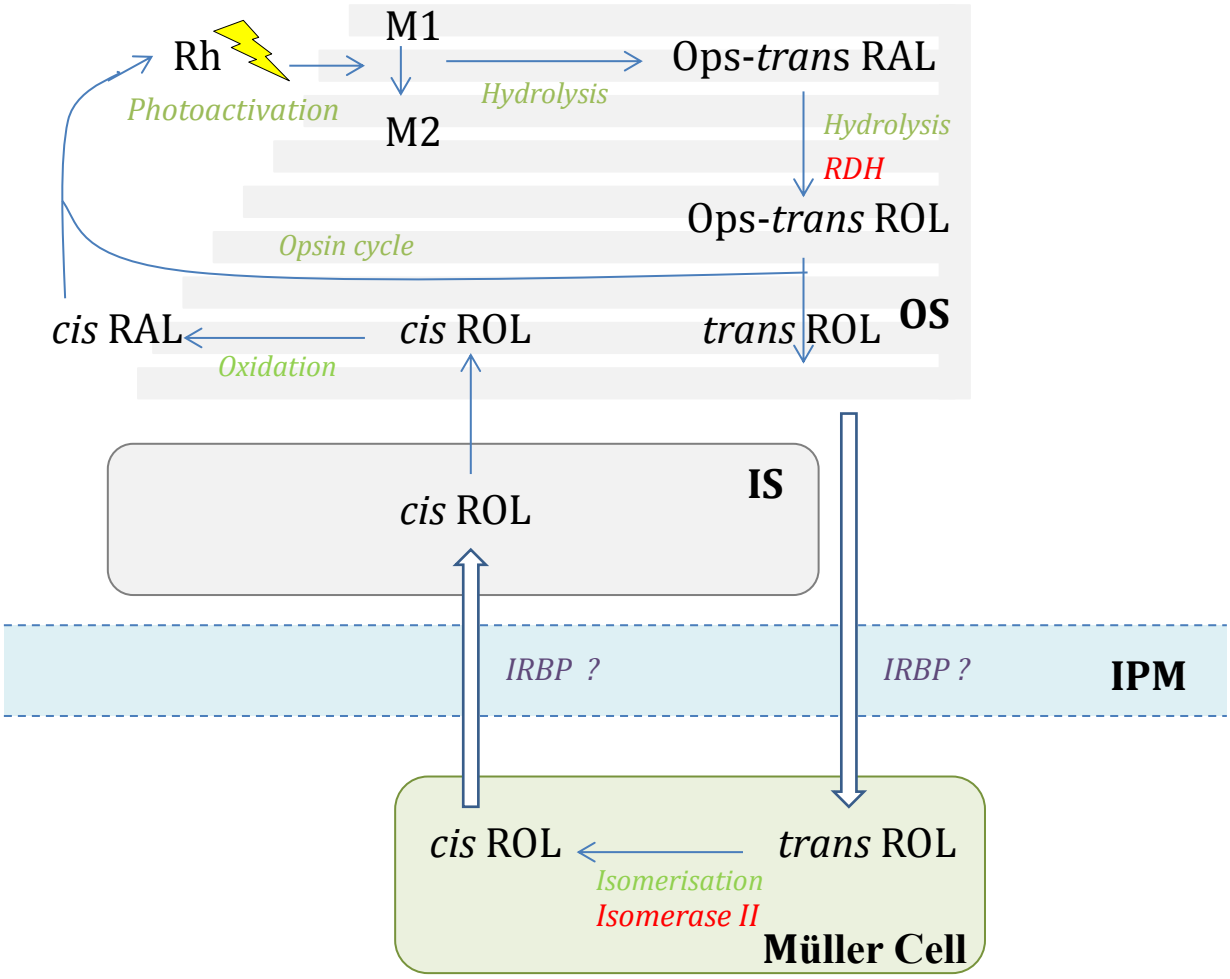

Figure 1.30 The cone-specific retinoid cycle. Image adapted from Wang and Kefalov (2011) Key: Rh = rhodopsin; RAL = retinal; ROL = retinol; IRBP = interphotoreceptor retinol binding protein; OS = outer segment; IS = inner segment; IPM = inter-photoreceptor matrix; RDH = retinol dehydrogenase)

1.3.2.2.3 Phototransduction

In dark adapted conditions, cyclic guanosine monophosphate (cGMP) binds to and holds open light sensitive ion channels found in the plasma membrane of outer semgments, allowing influx of Na^+ and Ca^+ ions from the extracellular matrix, down the electrochemical gradient (Figure 1.31) (Baylor, Lamb and Yau, 1979; Fesenko, Kolesnikov and Lyubarsky, 1985; Lamb and Pugh, 2006). This inward current, known as "dark current", causes partial depolarisation of the photoreceptor, and triggers the release of the neurotransmitter glutamate from their synaptic terminals, to second order neurones in the retina (i.e. bipolar and horizontal cells). Complete depolarisation is prevented by a Ca^{2+}/K^+ ion exchanger in the outer segment, pumping Ca^{2+} and K^+ out and Na^+ in along the concentration gradient (Bauer, 2002).

When exposed to light, cGMP levels drop, causing closure of cation channels in the photoreceptor outer segments, leading to photoreceptor hyperpolarisation. The extent of hyperpolarisation is proportional to the intensity of retinal illumination, and leads to a graded reduction in the release of glutamate.

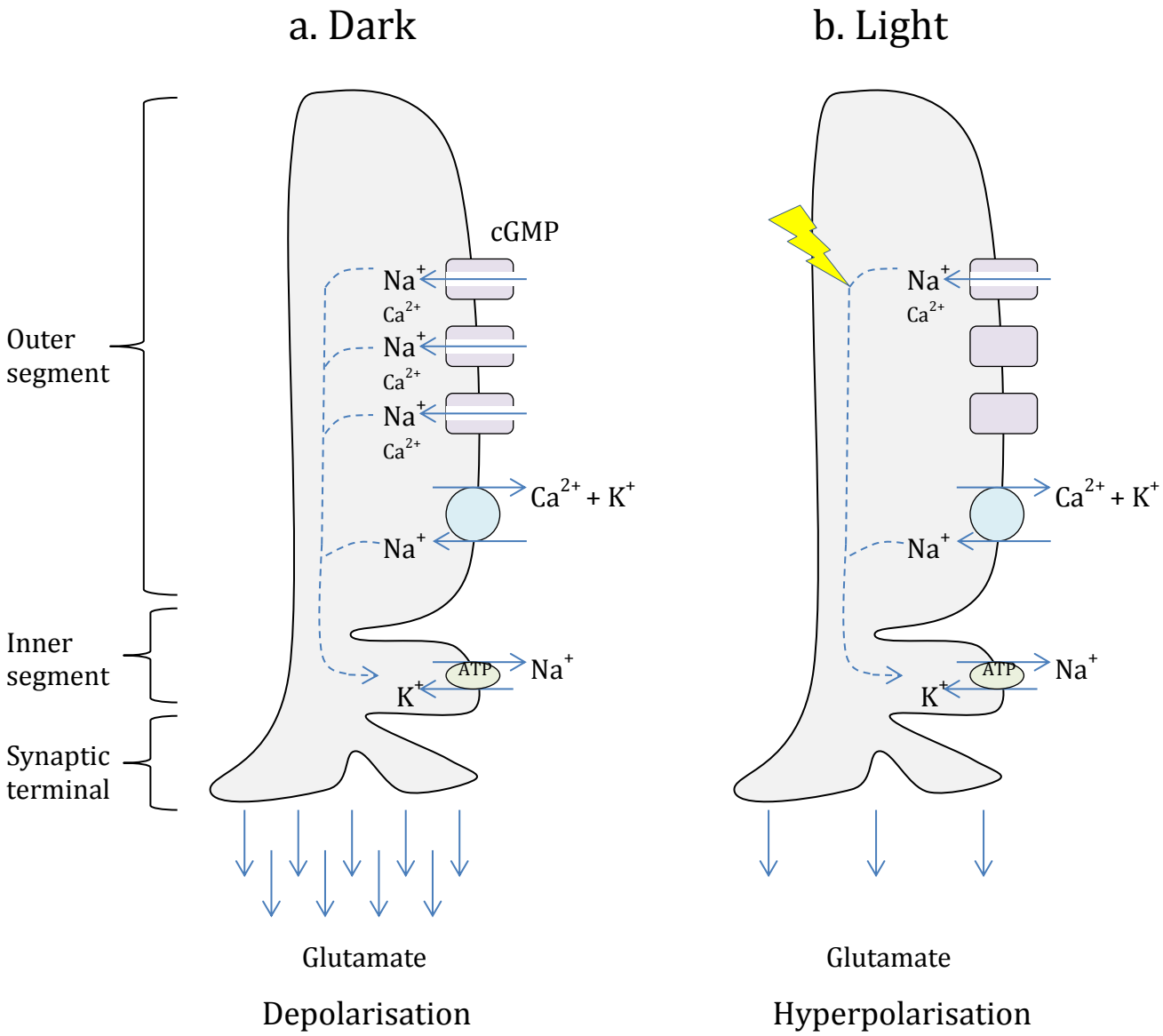

Figure 1.31 Ion circulation across a rod photoreceptor. In the dark (a), cGMP gated channels are open, allowing Na^+ and Ca^{2+} influx and cell membrane depolarisation. The Na^+/Ca^{2+} exchanger maintains Ca^{2+} balance, and the Na^+/K^+ ATP driven exchanger maintains Na^+ balance. In light (b), a proportion of cGMP channels close, resulting in hyperpolarisation, since the Na^+/K^+ pump continues to operate. Hyperpolarisation causes a proportional decrease in glutamate release. Image adapted from Smith (2006).

Phototransduction refers to the process by which light is converted into electrical neural signals within the outer segment of a rod or cone photoreceptor (Wang and Kefalov, 2011). The process of phototransudction can be summarised in 5 steps (Figure 1.32). Upon absorption of a photon of light by rhodopsin, isomerisation of the 11-cis-retinal chromophore occurs, converting rhodopsin to its active form, metarhodopsin II (R*) (step 1). R* is then able to transiently bind to and activate the G-protein transducing to G-GTP, which is found at the surface of the rhodopsin outer segment disc membrane, before dissociation occurs (step 2). R* is not altered in any way by this interaction, so whilst it remains active it is able to repeat this process indefinitely. Activated tranducin (G*) in turn activates the phosphodiesterase enzyme (PDE) (step 3), which catalyses hydrolysis of the intracellular messenger cGMP, and results in a subsequent drop in cGMP concentration (step 4). This reduced concentration causes cGMP to unbind from the ion channels within the cell's plasma membrane (Yau, 1994), resulting in channel closure and causing a reduction in the circulating current and a consequent hyperpolarisation (step 5). As a result, glutamate release is reduced, thus converting the light signal to postsynaptic neurons as an electrical signal (Yau and Hardie, 2009).

In order to maintain responsiveness, the phototransduction cascade must be terminated. This is achieved by the protein arrestin inactivating all the transduction components, and recovering the levels of cGMP, thereby allowing the ion channels to re-open and depolarisation to occur (Wang and Kefalov, 2011).

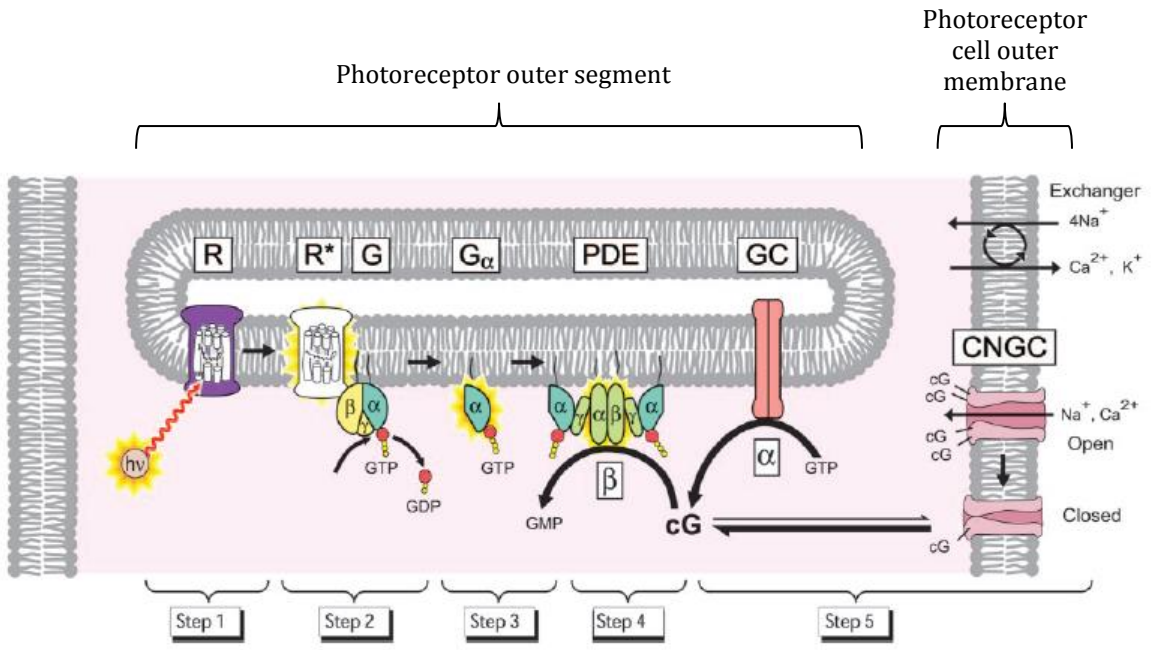

Figure 1.32 The phototransduction cascade. Image from Lamb and Pugh (2006) Key: h*ν*, photon; R, rhodopsin; R*, activated rhodopsin; G, G protein; Gα, G protein α sub-unit; PDE, phosphodiesterase; GTP, guanine tri-phosphate; GDP, guanine di-phosphate; GMP, guanine mono-phosphate; cG, cyclic GMP; GC, guanylyl cyclase; CNGC, cyclic nucleotide-gated channels.

1.3.2.2.4 Theories behind threshold elevation in dark adaptation

1.3.2.2.4.1 *The photochemical hypothesis*

The photochemical explanation of dark adaptation states that threshold following a bleaching light was directly proportional to the concentration of unbleached photopigment (Hecht et al., 1937). If this theory were to be true, 50% regeneration of rhodopsin would result in 50% recovery of threshold. The increase in threshold predicted by this method dramatically underestimates the threshold elevation measured during dark adaptation, and the theory was later disproved with retinal densitometry results showing that when 90% rhodopsin was regenerated, threshold was still elevated by three log units (Campbell and Rushton, 1955; Leibrock, Reuter and Lamb, 1998).

Following research, it was proposed that there is a linear relationship between the log threshold and the concentration of bleached rhodopsin (Dowling, 1960; Rushton, 1961). This relationship is known as the Dowling-Ruston relationship (*Equation 1*). This relationship has since been verified for rhodopsin (Rushton and Powell, 1972) and cone photopigment (Hollins and Alpern, 1973), however, it only holds true for almost total bleaches, and is incorrect for

small bleaches (Rushton and Powell, 1972; Pugh, 1975). In addition, the constant, *a*, has been shown to vary with bleaching intensity (Pugh, 1975).

$$\log(I_t/I_a) = \alpha B \qquad \textit{Equation 1}$$

Where I_t is the visual threshold at a given time, I_a is the final dark adapted threshold, α is a constant and *B* is the proportion of pigment bleached.

1.3.2.2.4.2 ***The equivalent background theory***

Stiles and Crawford (1932) proposed the 'equivalent background theory' which stated that at any given time during dark adaptation, the visual threshold is equivalent to that caused by adaptation to an 'equivalent background' light . This theory suggests that during dark adaptation, the visual system experiences a source of light (the 'equivalent background') that is equivalent to a real background light (Blakemore and Rushton, 1965). During the course of dark adaptation the equivalent background slowly 'fades away' as the threshold decreases (Leibrock et al., 1998). This equivalent background is proposed to be due to the presence and decay of a metarhodopsin photoproduct, free-opsin (Lamb, 1981; Leibrock et al., 1998; Lamb and Pugh, 2004). The proposed mechanism behind threshold elevation involves the photoproducts generating 'photon-like-fluctuations', causing direct activation of phototransduction (Okada, Nakai and Ikai, 1989; Leibrock et al., 1998; Lamb and Pugh, 2004). The recovery time course during rod dark adaptation is therefore determined by the removal of free-opsin as it recombines with 11-cis retinal to regenerate rhodopsin.

1.3.2.2.5 Dark adaptation in diabetes

There is evidence of rod malfunction in diabetic subjects: diabetic subjects show subnormal rates of DA and higher absolute thresholds compared to healthy controls (Figure 1.33) (Amemiya, 1977; Henson and North, 1979; Greenstein et al., 1993; Arden et al., 1998; Kurtenbach et al., 2006). This is observed even in patients with little or no retinopathy (Greenstein et al., 1993; Kurtenbach et al., 2006). Elevation of final rod threshold is positively correlated with duration of diabetes (Henson and North, 1979). However, there is a wide spread of results, with some subjects showing significantly elevated thresholds after only a few years of diabetes and others showing no elevation many years after disease onset. It has been postulated that this variation may be due to varying levels of glycaemic control between individuals and variation of sensitivity across different retinal areas in each subject (Henson

and North, 1979). Studies also show that rod threshold is sensitive to the serum glucose level; patients with a lower serum glucose of around 60 mg/dl show a threshold that is approximately 1 log cd/m^2 higher that than of a subject with a serum glucose of around 150 mg/dl (Kurtenbach et al., 2006).

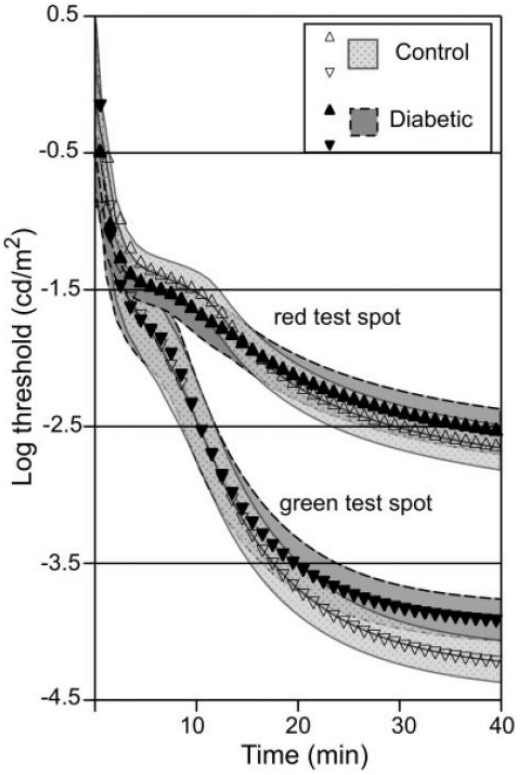

Figure 1.33 Mean dark adaptation curves for diabetic and control subjects under normal conditions, with the shaded regions showing the 95% confidence intervals. The final rod threshold for diabetic subjects was significantly raised compared to controls. Image from Kurtenbach et al. (2006).

1.3.2.2.5.1 ***Effect of oxygen inhalation on dark adaptation***

It has been hypothesised that rod-driven hypoxia, present at the inner photoreceptor level during DA, is responsible for the development and progression of diabetic retinopathy. This hypothesis is supported by the absence of diabetic retinopathy in retinitis pigmentosa (Arden, 2001), by the efficacy of pan-retinal photocoagulation, which reduces the retinal oxygen demand, and increases available retinal PaO_2, and by the reduction in progression of DR seen when dark adaptation is prevented by implementation of light therapy (Arden et al., 2010; Arden et al., 2011). Retinal hypoxia in diabetes is hypothesised to result from both

abnormalities in oxygen delivery secondary to altered retinal blood flow, and from decreased oxygen release from haemoglobin (Ditzel, 1972; Greenstein et al., 1993).

Kurtenbach et al. (2006), examined the effect of 100% oxygen inhalation on dark adaptation in 12 Type 1 diabetic subjects with no or mild retinopathy. Whilst the final rod sensitivity was unaffected by 100% oxygen breathing in healthy controls, there was a significant improvement in diabetic subjects, with recovery of the rod threshold to within the normal range (Figure 1.34). Whilst this change in sensitivity only occurred in 6 of the 12 patients examined, in general it occurred in those with the lowest rod sensitivities. These result support the hypothesis that the retina becomes hypoxic early in diabetes due to the large energy requirements of rods in their dark adapted state (Kurtenbach et al., 2006). This hypoxia, along with oxidative stress (Brownlee, 2005), is believed to contribute to the development of DR (Curtis, Gardiner and Stitt, 2009) through hypoxia driven up-regulation of vascular endothelial growth factor (VEGF) (Arden et al., 2011).

Oxygen inhalation in both diabetic and healthy control subjects results in improved final cone thresholds (0.15 log cd/m^2 and 0.27 log cd/m^2, respectively). This finding is in contrast to that seen in the rod system in control subjects. It is suggested that the different behaviour of the two photoreceptor systems indicates two distinct metabolic processes (Kurtenbach et al., 2006). In monkeys, cones have been shown to have a volume of mitochondira that is 10 times higher than that of rods (Hoang et al., 2002). It is therefore proposed that under normal conditions, maximal metabolic rates may have been reached in rods which already use most of the oxygen available from the circulation (Wangsa-Wirawan and Linsenmeier, 2003), but not cones, allowing them to increase their sensitivity during oxygen inhalation (Kurtenbach et al., 2006). The cone-specific Muller-cell pathway of photopigment regeneration may also contribute to the sensitivity increase gained by oxygen inhalation (Kurtenbach et al., 2006), enabling a faster regeneration rate of 11-cis-retinal (Lamb and Pugh, 2004). The reduced response of cone threshold to oxygen inhalation in the diabetic subjects compared to controls may reflect impaired vascular reactivity to hyperoxia that has been demonstrated in diabetic subjects (Grunwald et al., 1984a; Justesen et al., 2010).

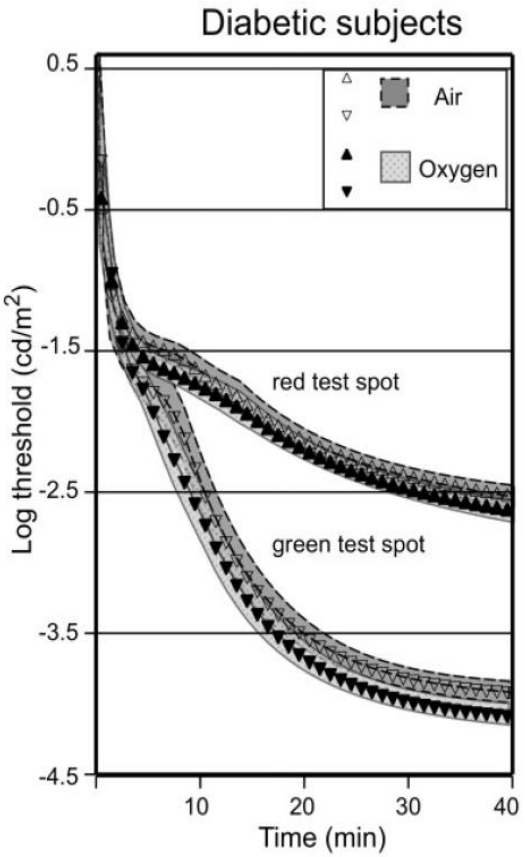

Figure 1.34 Mean dark adaptation curves for diabetic subjects during the inhalation of air and oxygen, with the shaded regions showing the 95% confidence intervals. The final rod threshold for diabetic subjects was significantly reduced on inhalation of oxygen compared to air. Image from Kurtenbach et al. (2006).

1.4 Thesis Aims

To date, there has been little investigation into the ocular effects of CF at a retinal level. With the localisation of CFTR to the apical membrane of the RPE, and the importance of Cl^- transport for regulation of the SRS, it is hypothesized that abnormalities may be present at the level of the photoreceptors and RPE in CF, including increased SRS volume. Additionally, reduced levels of antioxidants at the macular region in CF patients, combined with increased levels of oxidative stress, is likely to make CF patients more susceptible to early onset age related changes such as AMD. Through the use of sophisticated imaging techniques such as Optical Coherence Tomography (OCT), the RPE can be directly observed *in-vivo* in order to investigate these theories through quantitative and qualitative analysis. If structural retinal differences are noted between CF patients and controls, there is potential that this difference could be utilised in the future as a non-invasive outcome measure to test the efficacy of new CF therapies.

Impaired DA has been observed in CF subjects with VAD and CFRD; however, DA is also affected by CF genotype. Therefore, it is unclear if impaired DA in CF is secondary to VAD or CFRD, or if it is a primary manifestation of the disease caused by CFTR dysfunction. Reduced DA in Type 1 and Type 2 diabetes is thought to be caused by retinal hypoxia, and oxygen inhalation in diabetic subjects has shown temporary improvement in DA thresholds. Repeating oxygen inhalation studies in CF subjects (with known vitamin A sufficiency), with and without CFRD will further our understanding of the cause of impaired DA in CF.

Established CFRD is difficult to diagnose as glucose tolerance fluctuates with periods of disease exacerbation. The decision to commence treatment for CFRD is therefore difficult. The investigation of the effect of oxygen inhalation on DA thresholds in CF subjects with known diabetic status could provide support for CFRD diagnosis and management, and act as an indicator of the presence or absence of retinal hypoxia.

Therefore, the main objectives of this thesis are:

1. Quantitative and qualitative investigation of the retina and RPE with OCT to determine the primary and secondary effects of CF at a retinal level.
2. To identify if abnormal dark adaptation in CF is a primary manifestation of the disease caused by CFTR dysfunction, or is secondary to VAD or CFRD, through use of oxygen inhalation studies on subjects with known vitamin A and diabetic status. Through conducting these investigations, further knowledge may be gained which could improve the diagnosis and management of CFRD.

Chapter 2 Development of an OCT Protocol

2.1 Introduction

This chapter describes the development of the OCT protocol to be used in this thesis for the investigation of retinal structure in CF.

2.2 Experimental Aims

- Refine an OCT protocol for retinal imaging which can later be used for the quantitative and qualitative examination of the retina in CF patients.
- Determine the least number of OCT scans required in order to minimise data variability and subject participation time.
- Establish the intra-session and inter-session repeatability of retinal thickness measures using the Topcon 3D OCT-1000 for a particular operator.
- Investigate the effect of diurnal variation on retinal thickness measures using the Topcon 3D OCT-1000.
- Verify a suitable scan protocol in order to produce high resolution retinal scans which can be used to accurately measure the RPE/photoreceptor layer thickness.

2.3 Subjects

Twenty[1] healthy Caucasian adults were recruited from School of Optometry and Vision Sciences, Cardiff University. Inclusion criteria comprised: best-corrected visual acuity (VA) of 6/7.5 or better, age range between 18-40 years, and no known disease of the retina or visual pathways. Exclusion criteria included any ocular or systemic condition known to affect retinal thickness and composition, pregnancy, spherical equivalent refraction (SER) exceeding ±6.00D, media opacities, or any previous ocular trauma.

Informed consent was obtained from all subjects. Ethical approval was given by the Human Science Research Ethics Committee, School of Optometry and Vision Sciences, Cardiff University. All procedures conformed to the tenets of the Declaration of Helsinki.

2.4 Methods

2.4.1 *Phase 1 - Investigating the effect of multiple OCT scans on the standard deviation of retinal thickness.*

Ten consecutive 256x256 (vitreous reference) scans were performed with the Topcon 3D OCT-1000 (Topcon, Tokyo, Japan) on one randomly selected eye in five subjects (two males, three females, age range 22-32 years, mean age ± SD, 25.6 ± 3.78 years). Each scan was performed by the same examiner with room lights extinguished and without pupillary dilation.

2.4.2 *Phase 2 – Investigating intra-session and inter-session repeatability and the effect of diurnal variation on macular thickness.*

Twenty subjects were recruited (8 males, 12 females, age range 21-34 years, mean age ± SD, 26.6 ± 3.9 years). Each subject was required to attend on three separate occasions.

Session one – Conducted on all participants between 9 and 11am. Each patient answered questions regarding their age, gender, ethnic origin, personal and family general and ocular health. Distance vision or VA (right and left) was recorded with a LogMAR ETDRS chart (Precision Vision, La Salle, IL, USA) at three meters (luminance 160 candelas/meter^2 (cdm^2)).

[1] Power calculations were based upon data from Sull et al. (2010) and numbers were calculated using the Altman Nomogram for paired t-tests
Retinal thickness in healthy subjects = 231 ± 16μm
Smallest clinical difference = 10μm (Calculated as twice the axial resolution of the Topcon 3D OCT-100)
Standardised difference 2x10/16 = 1.25
Subject number = 20 paired observations

Axial length was determined as the average of five readings using the IOLMaster (Zeiss, Germany) and objective refraction was determined for each eye using an auto-refractor (Topcon KR-7500; Topcon, Newbury, UK), and the average of three readings recorded.

Three consecutive 256x256 resolution (vitreous reference) macular OCT scans were obtained for the right eye using the Topcon 3D-OCT 1000. Scans with quality measures below 40 were rejected then repeated (Ho et al., 2009). Images with artefacts, or missing parts due to fixation errors or patient blinking were rejected and scans repeated. For each scan, the ETDRS grid (Figure 1.15) was placed onto the scan using the automated software algorithms and average retinal thickness and volume was recorded for each area.

Session Two - Carried out five days after session one at approximately the same time of day (± one hour). A single 256x256 macular OCT scan was performed on the right eye and retinal thickness and volume recorded.

Session Three - Conducted five hours after the commencement of session two. A single 256x256 macular OCT scan was performed on the right eye, and retinal thickness and volume recorded.

2.4.3 *Phase 3 – Determination of the optimal OCT scan type for imaging the RPE/photoreceptor layer*

Twelve different raster scan types were consecutively performed on one randomly selected eye of ten subjects (six males, four females, age range 22-40 years, mean age 27.4 ± 5.66) (Table 2.1). For each subject, scan order was randomised and images were coded. A study group of four experienced observers viewed all scans and selected the two scans which most clearly delineated the photoreceptor and RPE layers for each patient. Scans were then decoded to determine which scan type was identified most frequently as producing the clearest image.

Table 2.1 Scan protocols used for imaging the RPE/photoreceptor layer

Scan	Resolution	Reference	B-Scan length (mm)	Number of Averages
1	4096	Vitreous	6	0

2	4096	Choroid	6	0
3	4096	Vitreous	4.5	0
4	4096	Choroid	4.5	0
5	1024	Vitreous	6	4
6	1024	Vitreous	6	8
7	1024	Choroid	6	4
8	1024	Choroid	6	8
9	1024	Vitreous	4.5	4
10	1024	Vitreous	4.5	8
11	1024	Choroid	4.5	4
12	1024	Choroid	4.5	8

2.4.4 *Phase 4 – Investigating repeatability of manual measures of RPE/Photoreceptor layer thickness*

Measurement of the RPE/photoreceptor layer thickness was conducted over three days. Measurements were taken using the calipers integrated into the Topcon 3D OCT-1000 software (Figure 2.1), and using the scan type determined in phase 3 for each of the 10 subjects. Measurements were taken using the B-scan with the greatest macular dip for each patient, at the point of minimum retinal thickness. Computer monitor and mouse settings were adjusted to optimize image quality and pointer sensitivity.

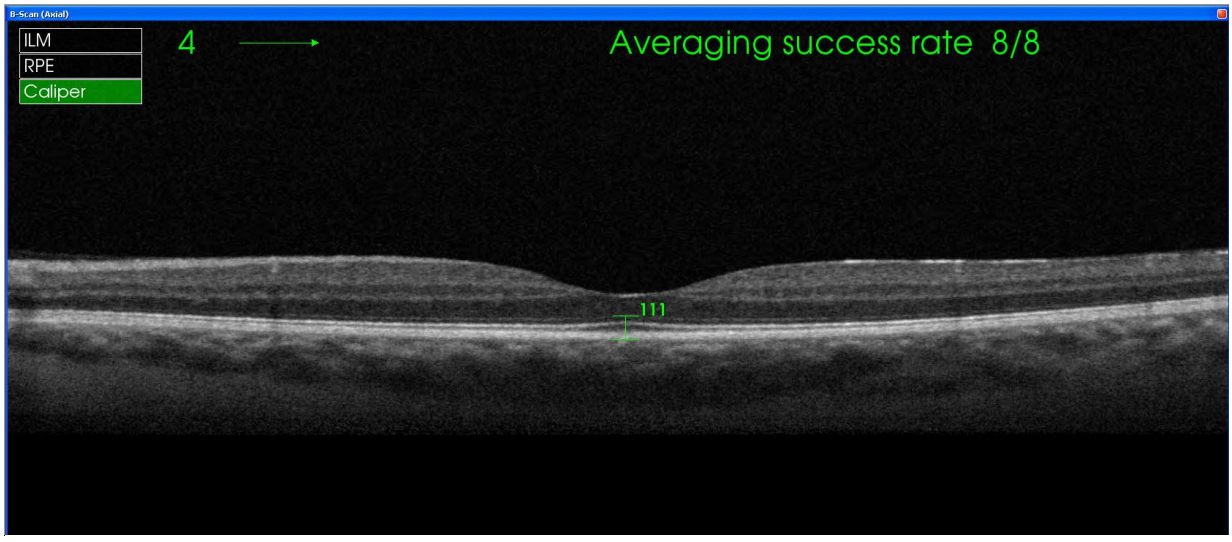

Figure 2.1 Caliper measurement of the RPE/Photoreceptor layer on the Topcon 3D OCT-1000

2.4.5 *Statistical Analysis*

All results were analysed with SPSS 20 software (IBM, Armonk NY). Results for the retinal thickness values were normally distributed (Shapiro-Wilk; $p = 0.200$). As data was normally distributed, parametric statistical analysis was applied.

One-way repeated measures analysis of variance (ANOVA), interclass correlation coefficient (ICC) and coefficient of repeatability (CoR) were used to assess the intra-session repeatability of retinal thickness values, and manual measures of photoreceptor and RPE layer thicknesses. Paired-samples (2-tailed) t-tests and CoR was used to determine the inter-session repeatability, and to establish the effect of diurnal variation on macular thickness values. Significance was set at the 0.05 level.

2.5 Results

2.5.1 *Phase 1 – The effect of multiple OCT scans on the cumulative standard deviation of retinal thickness values*

Figure 2.2 shows the effect of multiple retinal thickness measures on the cumulative standard deviation (SD). Results demonstrate that repeated retinal thickness measures had limited clinical effect on the cumulative SD for the central ETDRS area. The SD of three repeated scans was approximately 3µm. In order not to compromise instrument repeatability against patient comfort and chair time it was agreed that three scans would be used to assess the within-session repeatability at session one.

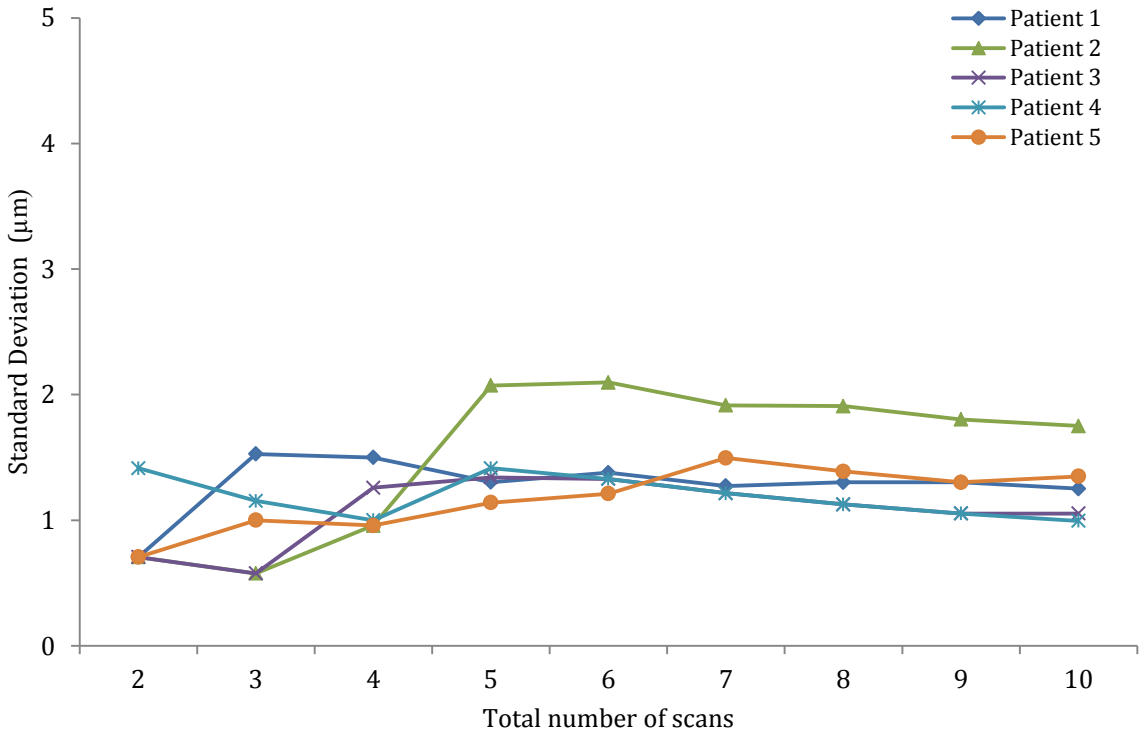

Figure 2.2 The effect of repeated measures of retinal thickness on the cumulative standard deviation

2.5.2 *Phase 2 - Investigating intra-session and inter-session repeatability and the effect of diurnal variation on macular thickness.*

2.5.2.1 Intra-session analysis

Twenty eyes from 20 healthy subjects (8 males, 12 females, age range 21-34 years, mean age ± SD, 26.6 ± 3.9; mean axial length ± SD, 23.85 ± 0.98; mean refractive error ± SD, -1.44 ± 1.68) were analysed.

There was no significant difference in retinal thickness measures for all ETDRS areas (paired-samples (2-tailed) t-test, $0.43 < p < 1.00$) (Table 2.2). Retinal thickness measures were highly repeatable for all ETDRS areas, with ICCs exceeding 0.9 in all cases, and CoR between 4.13μm and 7.66μm.

Table 2.2 Intra-session repeatability of retinal thickness

ETDRS area	Scan number	Retinal Thickness Mean ± SD (*µ*m)	ANOVA	ICC	CoR (µm)
CS	1	250.95 ± 17.90	0.55	0.97	7.45 2.99%
	2	249.00 ± 13.20			
	3	249.15 ± 13.25			
NI	1	313.55 ± 15.18	0.58	0.98	7.29 2.33%
	2	312.75 ± 17.04			
	3	314.30 ± 14.46			
TI	1	295.95 ± 14.30	0.55	0.97	7.62 2.58%
	2	294.55 ± 15.03			
	3	295.80 ± 13.56			
SI	1	308.15 ± 16.71	0.43	0.98	5.04 1.64%
	2	308.45 ± 16.38			
	3	209.50 ± 14.06			
II	1	304.20 ± 20.44	0.91	0.96	7.66 2.53%
	2	303.35 ± 14.83			
	3	303.90 ± 18.49			
NO	1	284.25 ± 13.63	0.87	0.99	4.13 1.45%
	2	284.10 ± 14.25			
	3	284.00 ± 13.63			
TO	1	246.20 ± 12.11	0.84	0.95	4.51 1.83%
	2	245.55 ± 13.33			
	3	246.80 ± 11.73			
SO	1	262.35 ± 12.30	0.66	0.97	5.85 2.24%
	2	261.70 ± 11.89			
	3	262.95 ± 12.04			
IO	1	255.30 ± 11.06	1.00	0.92	7.64 2.99%
	2	255.25 ± 12.29			
	3	255.20 ± 9.65			

Key: CS, central; NI, nasal inner; TI, temporal inner; SI, superior inner; II, inferior inner; NO, nasal outer; TO, temporal outer; SO, superior outer; IO, inferior outer; ANOVA, analysis of variance; ICC, interclass correlation coefficient; CoR, coefficient of repeatability

2.5.2.2 Inter-session analysis

No significant difference was noted between the retinal thickness values obtained at session one and session two for any of the ETDRS areas (Paired-samples (2-tailed) t-test; $0.13 < p < 0.94$) (Table 2.3). CoR ranged from 3.68µm to 8.05µm, and the mean difference between visits was close to zero for all areas, with a maximum difference of 2.10µm (Figure 2.3).

Table 2.3 Inter-session repeatability of retinal thickness

ETDRS area	Retinal Thickness Session 1 (μm) (Mean ± SD)	Retinal Thickness Session 2 (μm) (Mean ± SD)	Paired T-test	CoR (µm)	
CS	250.95 ± 17.90	251.60 ± 20.74	0.67	6.89	(2.78%)
NI	313.55 ± 15.18	313.45 ± 13.77	0.92	6.59	(2.09%)
TI	295.95 ± 14.30	295.60 ±12.57	0.70	7.92	(2.68%)
SI	308.15 ± 16.71	306.60 ± 13.34	0.52	7.06	(2.30%)
II	304.20 ± 20.44	300.30 ± 17.64	0.38	7.81	(2.59%)
NO	284.25 ± 13.63	283.70 ± 14.86	0.21	3.68	(1.30%)
TO	246.20 ± 12.11	246.25 ± 11.30	0.94	6.08	(2.47%)
SO	262.35 ± 12.30	260.25 ± 12.34	0.13	8.05	(3.08%)
IO	255.30 ± 11.06	258.10 ± 17.61	0.20	6.87	(2.69%)

Key: CS, central; NI, nasal inner; TI, temporal inner; SI, superior inner; II, inferior inner; NO, nasal outer; TO, temporal outer; SO, superior outer; IO, inferior outer; CoR, coefficient of repeatability.

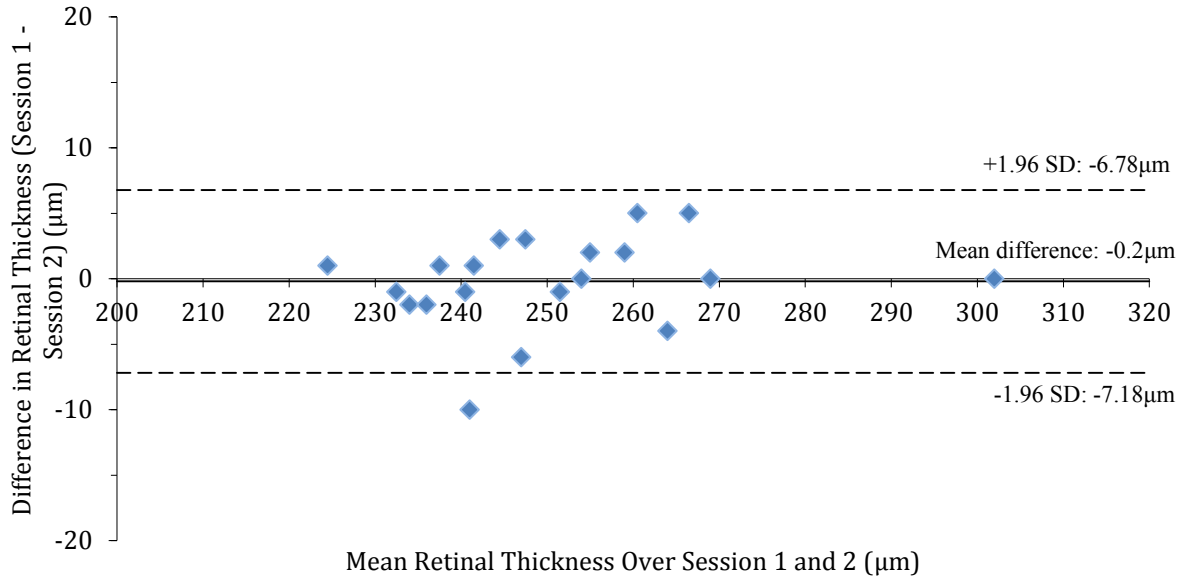

Figure 2.3 Bland-Altman plot for inter-session repeatability of the central ETDRS area. The mean difference between session 1 and 2 is shown by the solid horizontal line, whilst the dotted lines indicate the 95% limits of agreement.

2.5.2.3 Diurnal variation analysis

Retinal thickness appeared to show no significant diurnal variation from the morning to the afternoon for all ETDRS areas, apart from SO, which was significantly thicker in the afternoon (Paired-samples (2-tailed) t-test, $p < 0.05$) (Table 2.4). However, as the difference in thickness (1.95µm) is smaller than the CoR, it is of limited clinical relevance. CoR ranged from 4.47µm to 7.31µm, and the mean difference between visits was close to zero for all areas, with a maximum difference of 1.20µm (Figure 2.4).

Table 2.4 Diurnal variation of retinal thickness

ETDRS area	Retinal Thickness AM (Mean ± SD)	Retinal Thickness PM (Mean ± SD)	Paired-samples t-test	CoR (µm)
CS	251.60 ± 20.74	251.75 ± 20.92	0.93	6.95 (2.76%)
NI	313.45 ± 13.77	312.30 ± 12.94	0.15	6.74 (2.15%)
TI	295.60 ±12.57	294.90 ± 12.74	0.29	5.69 (1.93%)
SI	306.60 ± 13.34	305.25 ± 15.52	0.19	7.31 (2.39%)
II	300.30 ± 17.64	301.85 ± 13.75	0.38	7.07 (2.04%)
NO	283.70 ± 14.86	284.20 ± 14.58	0.34	4.47 (1.58%)
TO	246.25 ± 11.30	246.85 ± 11.76	0.48	7.26 (2.95%)
SO	260.25 ± 12.34	262.20 ± 12.23	0.00	5.26 (2.01%)
IO	258.10 ± 17.61	257.50 ± 18.11	0.67	5.28 (2.06%)

Key: CS, central; NI, nasal inner; TI, temporal inner; SI, superior inner; II, inferior inner; NO, nasal outer; TO, temporal outer; SO, superior outer; IO, inferior outer; CoR, coefficient of repeatability.

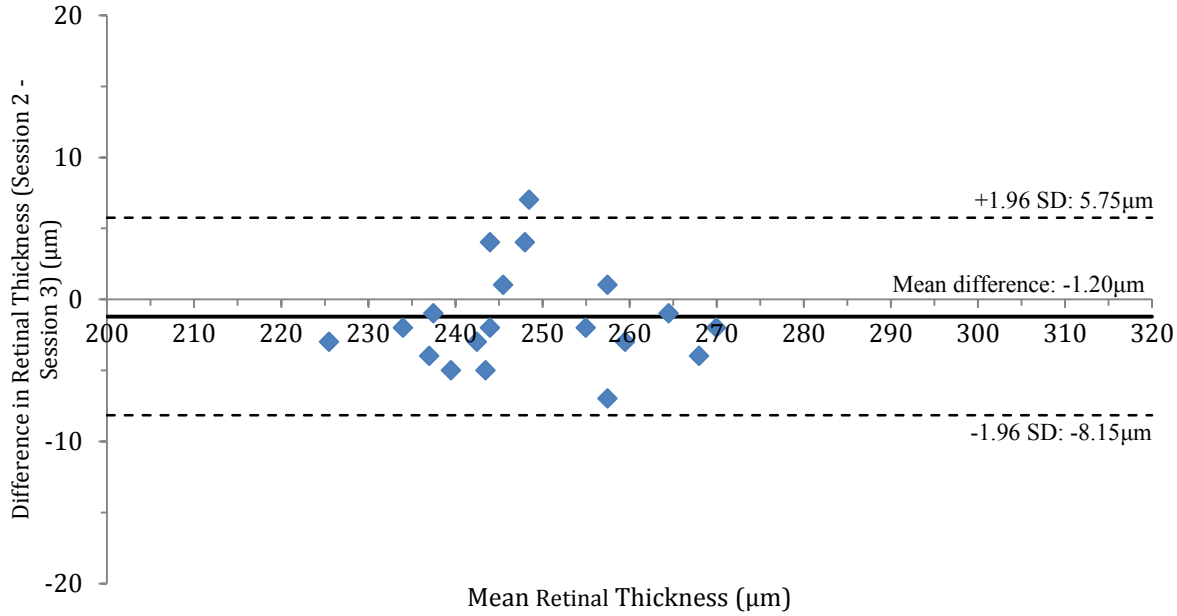

Figure 2.4 Bland-Altman plot for diurnal variation of the central ETDRS area. The mean difference between session 2 and 3 is shown by the solid horizontal line, whilst the dotted lines indicate the 95% limits of agreement.

2.5.3 *Phase 3 – Determination of the best OCT scan type for imaging the RPE/photoreceptor layer*

The scan protocol identified by the study group to produce the best image of the RPE/photoreceptor layer had the following parameters (Figure 2.5):

- Transverse resolution: 1024 A scans per B scan
- B-scan length: 6mm
- Reference: choroid
- Averaging: 8

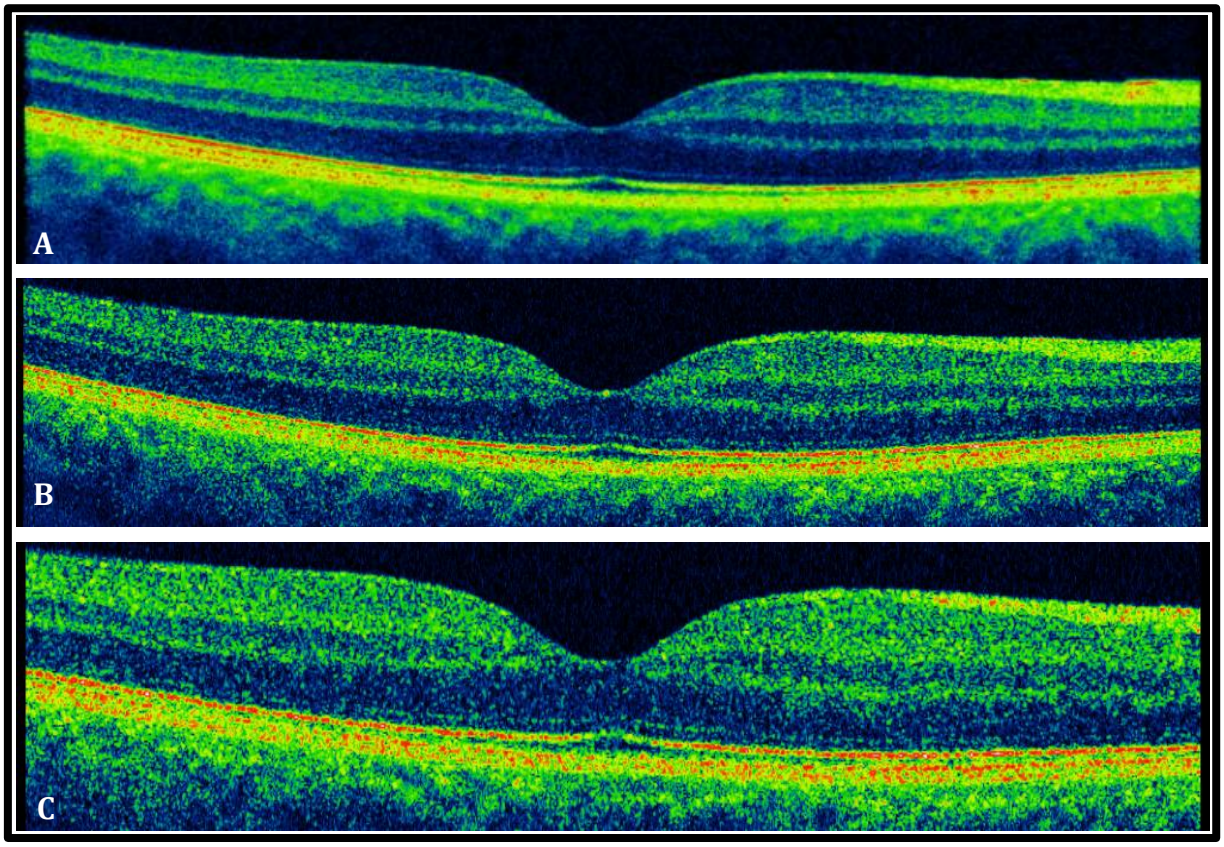

Figure 2.5 Example of OCT scans obtained in phase 3. **(A)** Optimal scan protocol; **(B)** Poor visualisation of external limiting membrane; scan parameters: resolution 4096 A scans per B scan, choroid reference, 0.15mm pitch, 6mm scan length, no averaging; **(C)** Poor visualisation of RPE limits; scan parameters: resolution 4096 A scans per B scan, vitreous reference, 0.15mm pitch, 4.5mm scan length, no averaging.

2.5.4 *Phase 4 –Repeatability of manual measures of RPE/Photoreceptor layer thickness*

Table 2.5 shows the mean and standard deviation of manual photoreceptor and RPE layer thickness measurements (Figure 2.6) obtained over three sessions using the scan protocol outlined above. There was no significant difference in thickness measures over the three collection sessions (One-way repeated measures ANOVA; p = 0.422).

Table 2.5 Repeatability of RPE/Photoreceptor layer thickness measurements

Session	RPE/Photoreceptor thickness (*µ*m) (Mean ± SD)	ANOVA	ICC	CoR (µm)
1	106.60 ± 3.95	0.422	0.905	3.90 (3.55%)
2	110.10 ± 2.85			
3	109.60 ± 2.76			

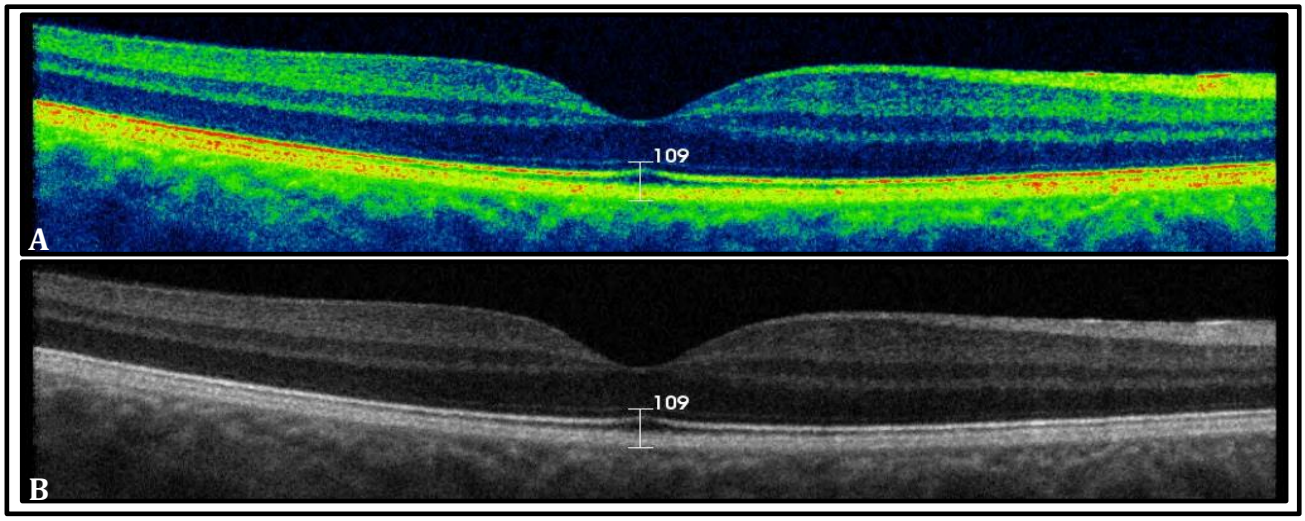

Figure 2.6 Manual measures of photoreceptor and RPE layer thickness using integrated calipers. Measurements were made with both pseudo-colour (A), and grey scale (B) scans.

2.6 Discussion

High measurement repeatability is of paramount importance in the quantitative application of OCT for retinal research in cystic fibrosis. The repeatability of macular thickness measures for healthy eyes using the Topcon 3D-OCT has been reported in a number of previous trials (Leung et al., 2008; Pierro et al., 2010; Sull et al., 2010; Huang et al., 2011a). The results of this study strongly concur with past studies, finding intra-session repeatability to be very high, with ICC's in excess of 0.90, and CoR lower than 7.66μm for all ETDRS areas. Similarly, inter-session repeatability was also high, with no significant difference being found in thickness values obtained over session one and two, and CoR lower than 7.92μm for all ETDRS areas. These results are highly favourable, as they permit the use of a reduced number of OCT scans on patients, without the loss of reliability. High levels of repeatability for the Topcon 3D-OCT 1000 may be attributable to its fast scan rate and increased sampling frames, which allow for detailed mapping of the macular in a short period of time and require less estimation of retinal thickness in areas between scans. It is likely that repeatability was found to be so high in this study due to the exclusion of eyes with any pathology, which is known to decrease OCT instrument repeatability (Menke et al., 2009), additionally, the subject cohort was young with good VA, allowing accurate fixation. As the retinal changes hypothesized to occur in CF are unlikely to disrupt retinal architecture to such a degree that retinal segmentation is compromised, it is expected that repeatability of retinal thickness measures will remain high.

The high levels of intra-session and inter-session repeatability observed in this study suggest that one OCT scan would be sufficient for the majority of patients to ensure macular measurement accuracy. However, there were some clear outliers that showed significant degrees of variation in retinal thickness measures. Higher degrees of variation in these subjects may be attributed to fixation errors, or insufficient OCT image quality (Huang et al., 2011b). Therefore, it may be of benefit to conduct three OCT scans on CF patients, who may present with ocular pathology. This measure should ensure recorded measures of macular thickness are reliable.

Inter-ocular difference in retinal thickness was not investigated in this study as previous research indicates there is no significant difference (Massin et al., 2002; Kelty et al., 2008; Wolf-Schnurrbusch et al., 2009; Duan et al., 2010). Although this suggests that only one eye

of CF patients requires imaging in order to evaluate macular thickness, both eyes will be scanned to allow a larger sample of images for qualitative retinal assessment.

Earlier research has demonstrated that females have areas of significantly reduced macular thickness in comparison to men (Massin et al., 2002; Wakitani et al., 2003). It is therefore pertinent that in the following experiments, all subjects are gender matched to eliminate the risk of any relationship having an impact on results.

Whilst diurnal variation significantly affected retinal thickness in patients suffering from diabetic macular oedema (Larsen et al., 2005; Danis et al., 2006; Polito et al., 2006) and other retinal diseases (Gupta et al., 2009), healthy subjects have displayed no evidence of true diurnal variation (Larsen et al., 2005; Polito et al., 2006). In line with these findings, healthy subjects in the present study displayed no diurnal variation in retinal thickness, except in the SO area, which increased from 260.25μm in the morning, to 262.20μm in the afternoon. Despite statistical significance, the mean difference is within the instrument repeatability and can be considered clinically irrelevant. Additionally, this apparent relationship is likely attributed to one subject who displayed a large change in retinal thickness from the morning to the afternoon, possibly due to poor fixation and subsequent errors in ETDRS grid placement. It is likely that with a larger sample size of patients, that the effect of this outlier would significantly reduce. These results are comparable to those of Jo et al. (2011), who observed a 3.5μm increase in retinal thickness over the day in healthy subjects when measured with a time domain (TD)-OCT (Stratus OCT). However, this trend was not observed with a more advanced spectral-domain OCT instrument (Cirrus HD-OCT). The increase in retinal thickness observed with the Stratus OCT was therefore attributed to poor equipment repeatability, rather than any "true" diurnal variation (Jo et al., 2011).

As retinal thickness in patients with retinal diseases has been noted to decrease throughout the day, it seems reasonable to hypothesise that CF patients (particularly those with CFRD) will display similar changes. Whilst it would be of considerable interest to examine this hypothesis fully by imaging CF patients in the morning and evening, this will not be viable due to restrictions in appointment times caused by intense treatment regimes. To maximize the possibility of observing differences between the two cohorts, whenever possible, CF patients will be examined in the morning, when any potential retinal oedema is likely to be exacerbated.

With the localisation of CFTR to the apical membrane of the RPE, and the importance of Cl^- transport for the regulation of the SRS, it is hypothesised that abnormalities will be present at the level of the RPE/photoreceptor layer in CF, including increased SRS volume. In order to determine if the SRS is increased in thickness in CF patients compared to controls, any measurements of these areas must be highly repeatable. Within this study, manual measures of RPE/photoreceptor layer thickness were seen to be highly repeatable. This is an important finding as it suggests that any difference between controls and CF patients will be identified using the same equipment and techniques employed by the observer in this instance.

In line with the findings discussed above, the following protocol is suggested to investigate retinal integrity in CF: three retinal thickness scans per eye, each with a quality score of > 60 and one high quality RPE/photoreceptor layer scan per eye. All CF patients will be age, gender and ethnicity matched to controls to account for any relationships with retinal thickness, and where possible all CF patients will be imaged in the morning when any potential oedema will be maximal. As axial length matching would be unrealistic, raw retinal thickness data will be corrected using linear regression analysis.

Chapter 3 Development and Verification of a Computerised Dark Adaptometer

3.1 Introduction

The Goldmann-Weekers (GW) adaptometer is considered to be the 'gold standard' method for the investigation of dark adaptation. However, it is no longer commercially available, and its repeatability has recently been questioned (Gaffney, Binns and Margrain, 2011).

Extensive research of available literature revealed that whilst other dark adaptometers exist and are in use (for example, AdaptDx (Holfort et al., 2010), SST-1 by LKC technologies (Abbott-Johnson et al., 2011), modified Humphrey Visual Field Analyser (Haimovici et al., 2002), and the modified Friedmann Field Analyser (Rayner et al., 1989)), currently none are commercially available which meet the requirements of this experiment. In vitamin A deficiency (Fulton et al., 1982; Neugebauer et al., 1989) and diabetes (Henson and North, 1979; Arden et al., 1998; Arden et al., 2005; Holfort et al., 2010), the final rod threshold is most noticeably affected, therefore a dark adaptometer is required which is able to measure over the full threshold range. Other researchers have tackled these problems by using custom made dark adaptometers (Hecht, 1937; Jackson, Owsley and McGiwin, 1999), using computer programming and cathode ray tube computer screens to present the stimuli (Dimitrov et al., 2008).

The aim of this study was to create a computer controlled dark adaptometer using Matlab (R2012b; MathWorks Ltd; Massachusettes, USA) programming and a cathode ray tube computer screen. This chapter presents the development and verification of a suitable computerised dark adaptometer (CDA)

3.2 Computerised Dark Adaptometer Development

Cathode ray tubes (CRTs) have served as useful stimulus generators in vision research since as early as 1971 (Sperling, 1971). They are universally available and offer the ability to create a variety of static or mobile stimuli, with accurate rendering when correctly calibrated and used within their operating limits (Metha, Vingrys and Badcock, 1993; Brainard, Pelli and Robson, 2002; Zele and Vingrys, 2005).

CRT monitors produce light by electron beam excitation of phosphor, which is applied as a coating to the front of the monitor (Figure 3.1) (Brainard et al., 2002). Images are formed by the sequential activation of discrete pixel elements in a raster scan pattern across the screen, from left to right and top to bottom during each frame (Brainard et al., 2002; Zele and Vingrys, 2005). The time taken to complete a scan of the screen determines the frame rate. Electron beam intensity is modulated during a raster scan so that the amount of light varies with the spatial position on the monitor.

Colour CRT monitors contain three different phosphor types – red, green and blue – which are interleaved, arranged as dots or stripes across the monitor. These dots or stripes are finer than a pixel, so observers are unable to resolve the pattern at a typical viewing distance. Three separate electron beams and a shadow mask are arranged within an evacuated glass tube so that each beam only illuminates one of the three phosphor types (Figure 3.1) (Metha et al., 1993; Brainard et al., 2002). Electron beams are focused and deflected by precise internal electromagnetic fields.

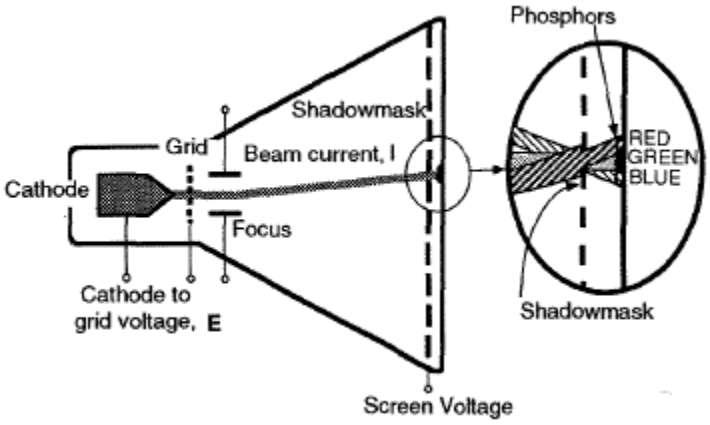

Figure 3.1 A representation of a colour CRT monitor. The shadow mask principle is displayed on the far right, whereby the spatial arrangement of the electron guns and the shadow mask ensure that each gun excites only one phosphor type. Image from Metha et al. (1993).

Whilst, as stated, CRTs offer the ability to produce a flexible and user specific stimulus, several drawbacks exist. The entire range of cone and rod recovery spans five to six log units (Lamb and Pugh, 2004), however, CRTs only operate over approximately three log units (Travis, 1991), leaving a shortfall of three log units. Additionally, the lowest achromatic luminance of standard CRT hardware is approximately 0.08 cd/m^{-2}, which is three-four log

units above the normal rod absolute threshold (Dimitrov et al., 2008). In order to expose the full range of cone and rod recovery, neutral density filters can be used over the CRT monitor to further attenuate luminance.

It has been shown that CRT luminance can vary by as much as ±1% over a period of eight hours. This is an acceptable level of fluctuation for most experimental applications, as the changes in output are not abrupt, therefore will not be perceived (Metha et al., 1993). However, up to 6% fluctuation in luminance can occur during CRT warm up, with a stable luminance only achieved after 60 and 150 minutes following warm (restart after 20 minutes off following a three hour on period) and cold (off period greater than 14 hours) starts, respectively (Metha et al., 1993). It is therefore recommended that CRTs are given a suitable warm-up period to ensure output is stable before any experiments proceed.

Properties of a CRT may vary across the space of the monitor. Luminance at the edge of a CRT screen has been found to be 20% less than that in the centre (Brainard, 1989). Whilst Brainard (1989) found that this spatial inhomogeneity of a monitor could be characterised by a light-attenuation factor at each location, this was not necessary for the purposes of this study, where the stimulus was only presented centrally, with calibration measures calculated according to the used stimulus.

CRTs do not behave as linear devices; the voltage applied to the guns is not linearly related to the luminance output or number of photons emitted. The cathode supplies an electron beam current (*I*), which is regulated by the cathode to grid voltage (*E)*, resulting in a power function relationship, known as the gamma function, such that $I \propto E$ (Metha et al., 1993; Brainard et al., 2002). Each CRT monitor has a different gamma function, therefore the gamma function for the CRT monitor used throughout these experiments was determined as an initial step in the experimental process. The Matlab code used can be found in Appendix A.

3.2.1 *Matlab script*

Matlab software with Psychophysical Toolbox (PTB_3) (Brainard, 1997) extensions was used to develop a programme which would present the CRT stimulus required for this study. The full DA Matlab code can be found in Appendix B. All CDA stimulus parameters were based upon the GW adaptometer, in order to mimic the current 'gold standard' as closely as possible.

3.2.1.1 Stimulus presentation

Due to luminance variations across the CRT screen (Brainard, 1989) the stimulus was presented centrally, indicated by four peripheral luminescent fixation markers (Figure 3.2). An achromatic spot target of 10.8° diameter was utilised so that with the patient viewing straight ahead, both cone and rod photoreceptors would be stimulated and that the full range of dark adaptation could be measured (Hecht, Haig and Wald, 1935). The stimulus was programmed to flash for a period of one second every two seconds (i.e. 0.5Hz). For the first five minutes, during cone recovery, threshold was measured continuously. After five minutes, threshold was measured every 50 seconds, with the commencement of measurement signalled by a computerised 'beep'.

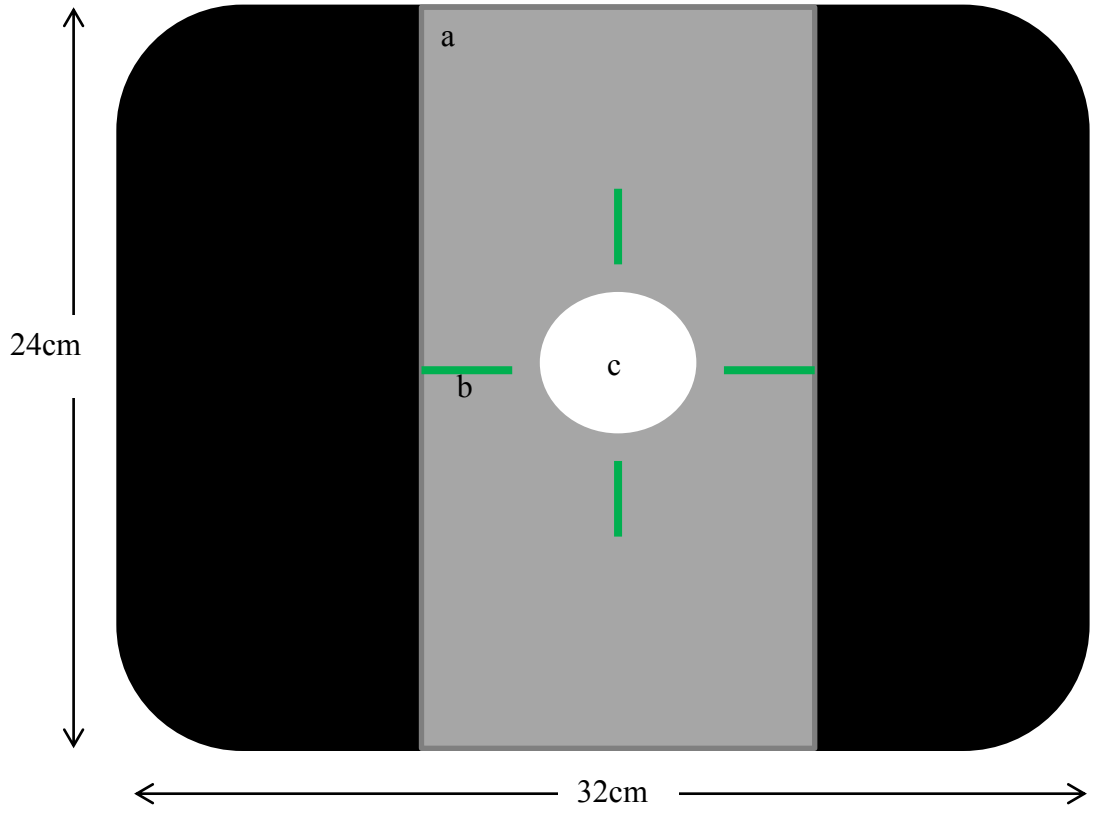

Figure 3.2 A diagram showing the CRT display. The CRT monitor positioned at a distance of 30cm from the subject, with a neutral density filter (a) fixed over the central area, surrounded by card. Subjects were instructed to fixate at the centre of the screen, marked by four 6.5° x 1° luminescent fixation markers (b). The 10.8° achromatic stimulus (c) was presented in the middle of the fixation markers.

3.2.1.2 Psychophysical technique

Two different psychophysical techniques were used during the course of the computerised dark adaptation programme. The first, used over the first five minutes to measure rapid cone recovery, was a modified staircase procedure, based on a method previously described by Jackson et al. (1999). If the subject reported perception of the stimulus, by depressing a key on the keyboard within a 600 milli-seconds (msec) response window, stimulus luminance was reduced by 0.3 log units for the next presentation. If the subject took longer than 600msec to respond to the stimulus, or failed to respond, stimulus intensity was increased by 0.1 log units for the next presentation. Threshold was recorded as the first visible stimulus on an ascending staircase.

The second psychophysical procedure was used after the first five minutes to measure slower rod photoreceptor recovery. In order to mimic the GW, a computer adapted method of ascending limits was employed, whereby stimulus intensity was gradually increased in 0.05 log unit steps, from 0.6 log units below the last recorded threshold. Threshold was recorded when the subject first reported perception of the stimulus within a 600 msec response window. If the subject took longer than 600 msec to respond to the stimulus, or failed to respond, stimulus intensity was increased by a further 0.05 log units until threshold was recorded. Once threshold was recorded, a 50 second break would be given before threshold was measured again. All threshold measures were exported to an Excel spreadsheet (2007; Microsoft; Washington, USA) following completion of the programme.

3.3 Retinal Bleach

In order to bleach a constant and known portion of photopigment for dark adaptation experiments, the retinal illuminance and duration of exposure must be under stringent control. Such control is obtained using a Maxwellian view system (Margrain and Thomson, 2002), which allows efficient light transmission and strict control over light source parameters (Leibowitz, 1954).

3.3.1 *Maxwellian-View*

In Maxwellian viewing, instead of directly viewing a source of light, the light source is imaged in the pupil of the eye using a lens (Westheimer, 1966). Provided the image of the light source is smaller than the pupil, all of the light enters the eye (Beer, MacLeod and Miller, 2005). As

all light emerging from the viewing system enters the pupil, the quantity of light reaching the retina is greatly increased. The principle advantage of the Maxwellian view technique is that whilst the retinal illuminance remains the same as in a standard viewing system, a larger retinal area is illuminated (Leibowitz, 1954) (Figure 3.3). Maximum illumination is achieved when the lenses in the Maxwellian viewing system remain unobstructed (Westheimer, 1966).

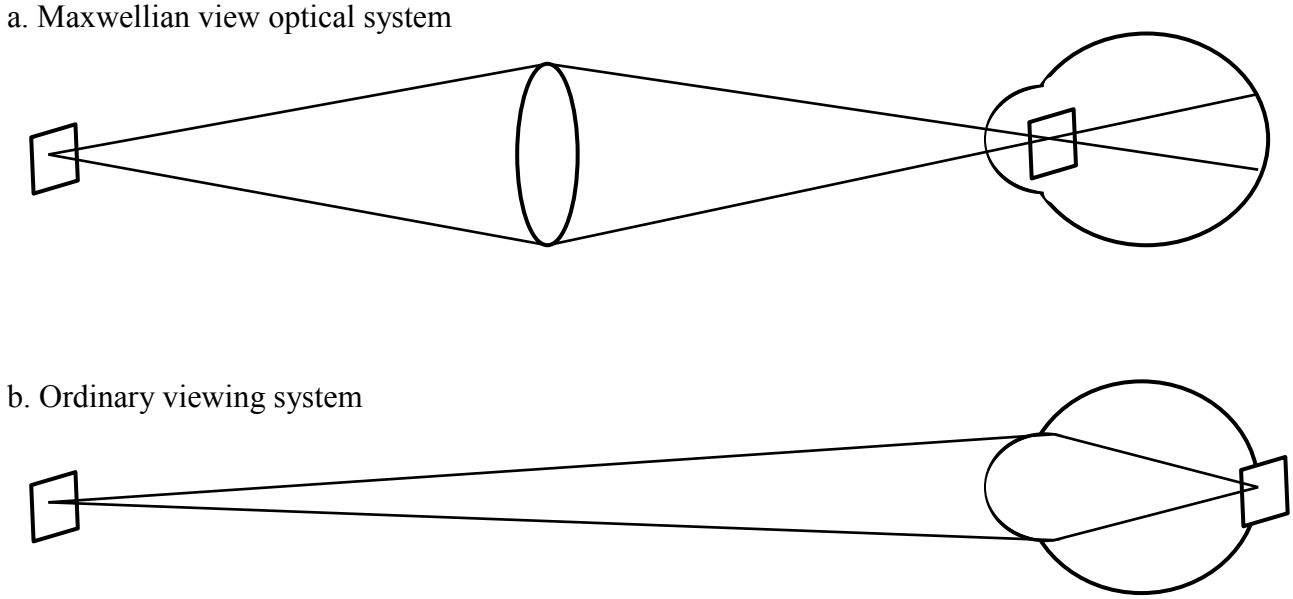

Figure 3.3 A schematic diagram showing the principles of Maxwellian viewing. A larger area of retina is illuminated under Maxwellian view conditions (a), in comparison to an ordinary viewing system (b).

3.3.2 *Calibration of retinal bleach*

The Maxwellian view optical system used to administer retinal bleach in these experiments consisted of a super bright white LED source and two 15 dioptre (D) lenses (Figure 3.4). An eyepiece was positioned so that the image of the source would fall in the pupil plane. Retinal illuminance was calculated by measuring the luminance (B) of a perfectly diffusing surface of known reflectance (r mL), at a set distance (x m) beyond the source image that would normally be in the plane of the eye, using the equation below, given by Westheimer, 1966.

$$Retinal\ illuminance\ (td) = 10^7 B\, x^2 / r \qquad \textit{Equation 2}$$

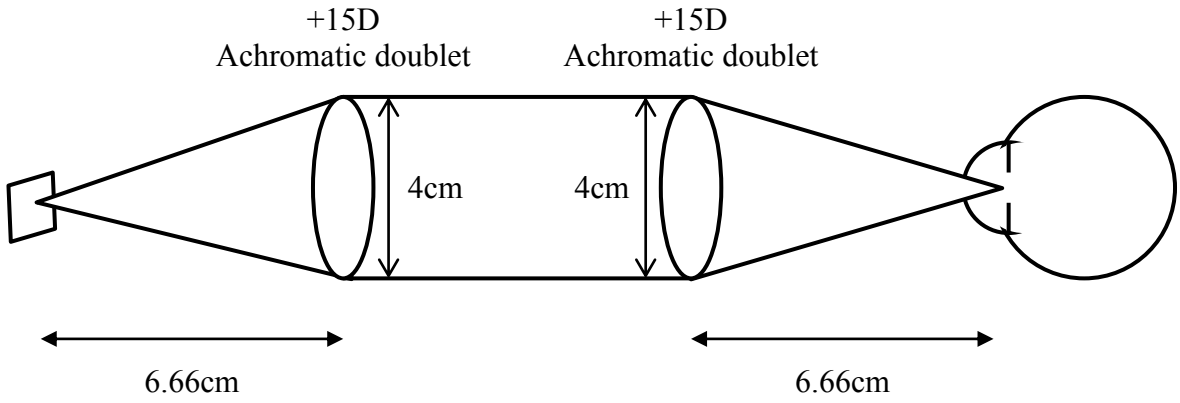

Figure 3.4 Diagram of the set-up of the Maxwellian view

The Maxwellian view was set up with the image projected onto a uniform surface of reflectance 84.2% at 0.185m. The luminance of the surface was measured with a photometer (LS-110; Konica Minolta, Osaka, Japan) at a range of different voltages until a luminance of 1.14 cd/m^2 was achieved, which, using *Equation 2* (Westheimer, 1966), gives a retinal illuminance of 145593.64 td which would give the desired level of rhodopsin and iodopsin photopigment bleach (see Section 3.3.3). The Maxwellian view was set at this luminance throughout all dark adaptation experiments, with luminance checked before every bleach.

3.3.3 *Calculating photopigment bleach*

3.3.3.1 Rhodopsin Bleach

The level of rhodopsin bleach obtained by the Maxwellian view system was calculated using *Equation 3,* given by Thomas and Lamb (1999).

$$B = \frac{I}{I+I_{Rh}}\left(1 - exp\left(1 + \frac{I}{I_{Rh}}\right)\frac{t}{\tau_{Rh}}\right) \qquad \textit{Equation 3}$$

Where B is the percentage of rhodopsin photopigment bleached, I is the retinal illuminance, t is the exposure duration in seconds, I_{Rh} is the bleaching constant and τ_{Rh} is the time constant of rhodopsin regeneration.

When rhodopsin is bleached by a steady light of illuminance I, it regenerates according to a first order reaction with a time constant (τ_{Rh}) of 420 seconds (Thomas and Lamb, 1999). The bleaching constant (I_{Rh}) has previously been measured by retinal densitometry and is within the

range of 6.8-7 Log_{10} Td.s (Rushton and Powell, 1972; Thomas and Lamb, 1999). For these calculations a value of 7.0 log Td.s was used. Using these two time constants, I_{Rh} can be calculated using *Equation 4*, giving a value of 23,809 td.

$$I_{Rh} = \frac{L_{Rh}}{\tau_{Rh}} \qquad \textit{Equation 4}$$

Where I_{Rh} is the light intensity at which half the rhodopsin is bleached, L_{Rh} is the rhodopsin bleaching constant, and τ_{Rh} is the time constant of rhodopsin regeneration. (Thomas and Lamb, 1999)

When:

I 145,593.64 td

I_{Rh} 23,809 td

t 120 s

τ_{Rh} 420 s

Rhodopsin bleach = 74.7%

3.3.3.2 Iodopsin bleach

The level of rhodopsin bleach obtained by the Maxwellian view system was calculated using *Equation 5*, given by Paupoo et al. (2000) (originally described by Thomas and Lamb (1999)) for rhodopsin bleach.

$$B = \frac{I}{I+I_P}\left(1 - exp\left(1 + \frac{I}{I_P}\right)\frac{t}{\tau_P}\right) \qquad \textit{Equation 5}$$

Where B is the percentage of iodopsin photopigment bleached, I is the retinal illuminance, t is the exposure duration in seconds, I_P is the bleaching constant and τ_P is the time constant of iodopsin regeneration.

For a total bleach, the cone bleaching constant (I_P) has been measured as 30,000 Td, with a time constant of cone regeneration (τ_P) of 105 seconds for equilibrium bleaches (Hollins and Alpern, 1973).

When:

I 145,593.64 td

I_P 30,000 td

t 120 s

τ_P 105 s

Iodopsin bleach = 82.8%

3.3.3.3 Bleach duration

A bleach time of two minutes was employed for these experiments in order to achieve suitable levels of rhodopsin and iodopsin bleach whilst utilising a light source which would not be uncomfortably bright for patients (Hollins and Alpern, 1973; Lamb and Pugh, 2004). With an equilibrium bleach of this kind, transient fixation losses and blinking are unlikely to have a large impact on the level of photopigment bleached (Figure 3.5), ensuring a constant level of bleach is obtained for each study participant.

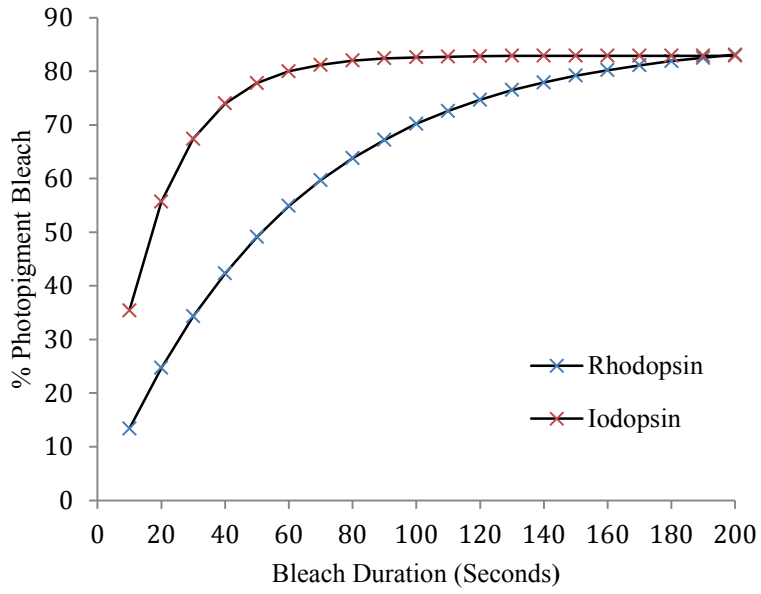

Figure 3.5 Percentage of rhodopsin and iodopsin photopigment bleached against time, calculated using *Equation 3* and *Equation 5*.

3.3.3.4 Extent of retinal bleach

The total area of retinal bleach was calculated as shown in Figure 3.6. Retinal distances are described as an angular measure of the eyes object space. The length of the eye was based upon Bennett-Rabbetts schematic eye model (2.409 cm) (Bennett and Rabbetts, 1998).

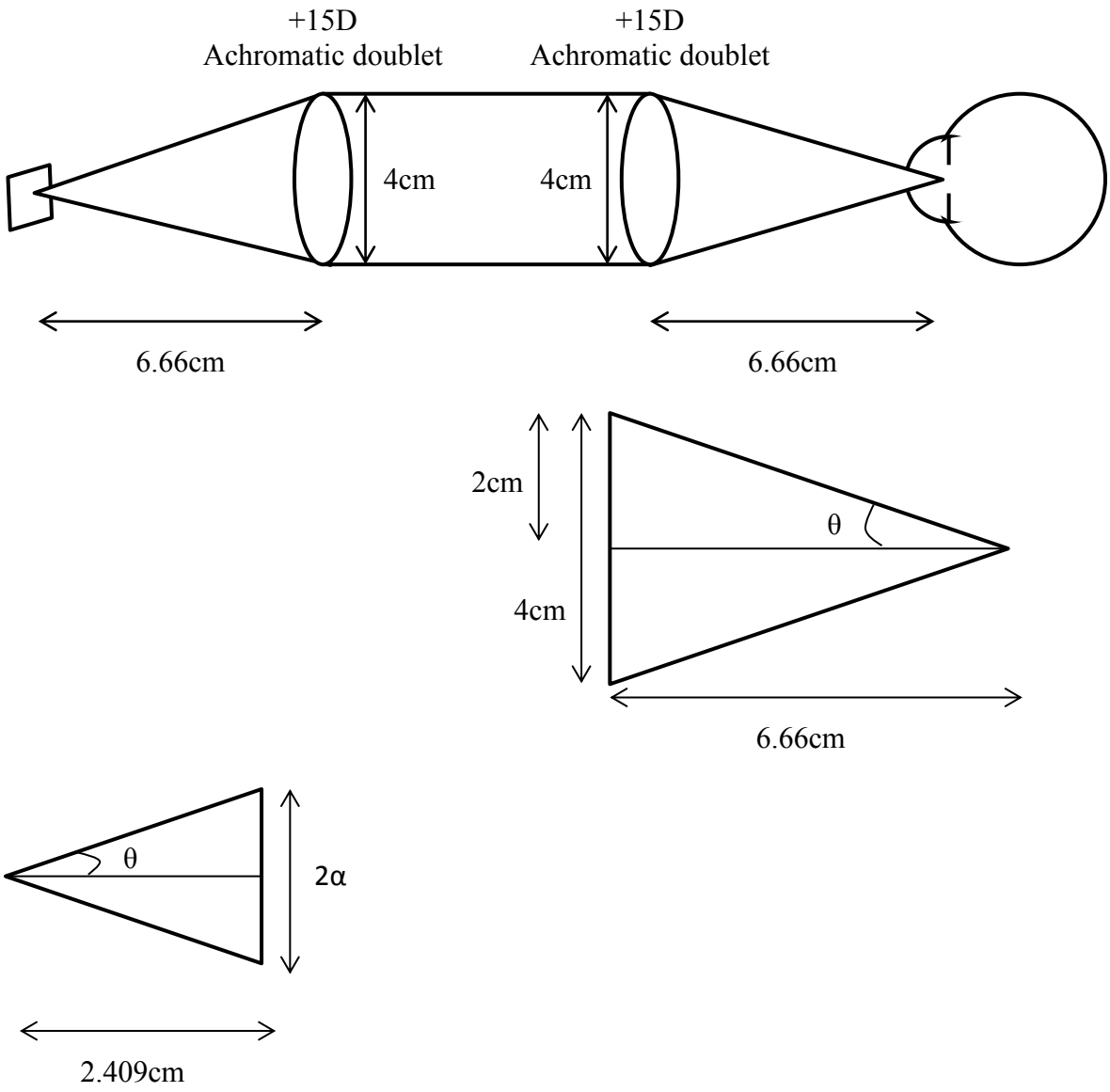

$\theta = \text{Tan}\ \frac{2}{6.66} = 16.72°$

$\alpha = \text{Tan}\ 16.72 \times 2.409 = 7.234\text{cm}$

$2\alpha = 14.468\text{cm}$

$1° = 288\mu\text{m}$ (Drasdo and Fowler, 1974)

Retinal area bleached = $14.468 \times 2.88 =$ **41.6°**

Figure 3.6 Calculation of the total area of retinal bleach.

3.3.4 *Comparison of the GW and CDA*

This section describes methods used for the comparison of the CDA to the GW, as the gold-standard for DA, to ensure comparable results were obtained.

3.3.4.1 Subjects

Dark adaptation curves were obtained from 11 eyes of 11 healthy adults[2] (8 males, 3 females, age range 21-34 years, mean age 25.8 ± 3.5 years) recruited from School of Optometry and Vision Sciences, Cardiff University. Inclusion criteria comprised: age range between 18- 40 years, and no known disease of the media, retina or visual pathways. Exclusion criteria included any ocular or systemic condition known to affect dark adaptation, diabetes, photosensitive epilepsy, pregnancy, a Van Herrick anterior chamber angle of grade 1 or less or any history of a previous attack of acute angle closure glaucoma following Tropicamide use.

Informed consent was obtained from all subjects. Ethical approval was given by the Human Science Research Ethics Committee, School of Optometry and Vision Sciences, Cardiff University. All procedures conformed to the tenets of the Declaration of Helsinki.

3.3.4.2 Methods

Subjects were required to attend a single session for 1.5 hours. Each subject answered questions regarding their age, ethnic origin, gender, medication, family general and ocular history and personal general and ocular history. Distance vision and/or VA (right and left) was recorded with a LogMAR ETDRS chart (Precision Vision, La Salle, IL, USA) at three meters (luminance 160 candelas/meter^2 (cd/m^2)). Anterior chamber depth was assessed by Van Herrick assessment (Friedman and He, 2008) with a slit lamp biomicroscope and intraocular pressure was determined using a non-contact tonometer (CT-80, Topcon, Tokyo, Japan) for both eyes.

---

[2] Power calculations were based upon data from Gaffney et al. (2011) and numbers were calculated using the Altman Nomogram for paired t-tests
GW final cone threshold = -1.81 ± 0.21 cd/m^2
CDA final cone threshold = -2.05 ± 0.62 cd/m^2
Difference in means 2.05 – 1.81 = 0.24
Standardised difference 2 x 0.24/0.21 = 2.29
Subject number = minimum 8 paired observations

One drop of Tropicamide 1% (Bausch and Lomb Pharmaceuticals; Florida, USA) was instilled into one randomly selected eye and pupil size was monitored until it equalled or exceeded 7mm diameter. Whilst waiting for adequate dilation, the two dark adaptometers were demonstrated to the patient and clear instructions given on their use. Once dilation was adequate, the non-dilated eye was patched and a long duration 'equilibrium' bleach was provided to the dilated eye with a Maxwellian-view optical system providing a white light of 5.16 log td for a period of two minutes, which bleached approximately 74.7% rhodopsin and 82.8% iodopsin. Upon bleach cessation, the subject was randomly allocated to either the GW or CDA where dark adaptation was monitored for 25 minutes in the dilated eye. A wash out period of 15 minutes after completion of the first adaptation measurement was given before the second bleach to avoid carry-over effects. Immediately after the second bleach, dark adaptation was measured on the second dark adaptometer (Figure 3.7).

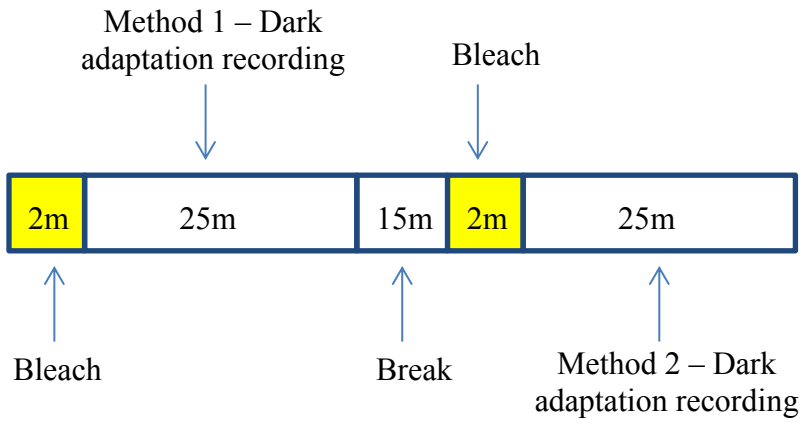

Figure 3.7 Timeline for assessment of dark adaptation

3.3.4.2.1 Goldmann-Weekers

The GW adaptometer (Figure 3.8) employed a method of ascending limits and recorded the dark adaptation function directly onto logarithmic paper (Figure 3.9). The investigator manually increased the intensity of the 10.8° diameter achromatic spot stimulus until the subject reported that it was just seen by tapping the table. Threshold was recorded at this point by marking the recording paper, before the stimulus intensity was reduced and the procedure repeated. Threshold was determined continuously for the first 5 minutes. After this, threshold was measured every minute for the remaining 20 minutes. The subject was instructed to focus straight ahead throughout the test.

Figure 3.8 The Goldmann-Weekers adaptometer. 1 = patient chin rest; 2 = light stimulus; 3 = examiner controls to adjust stimulus illumination; 4 = rotating drum and logarithmic paper.

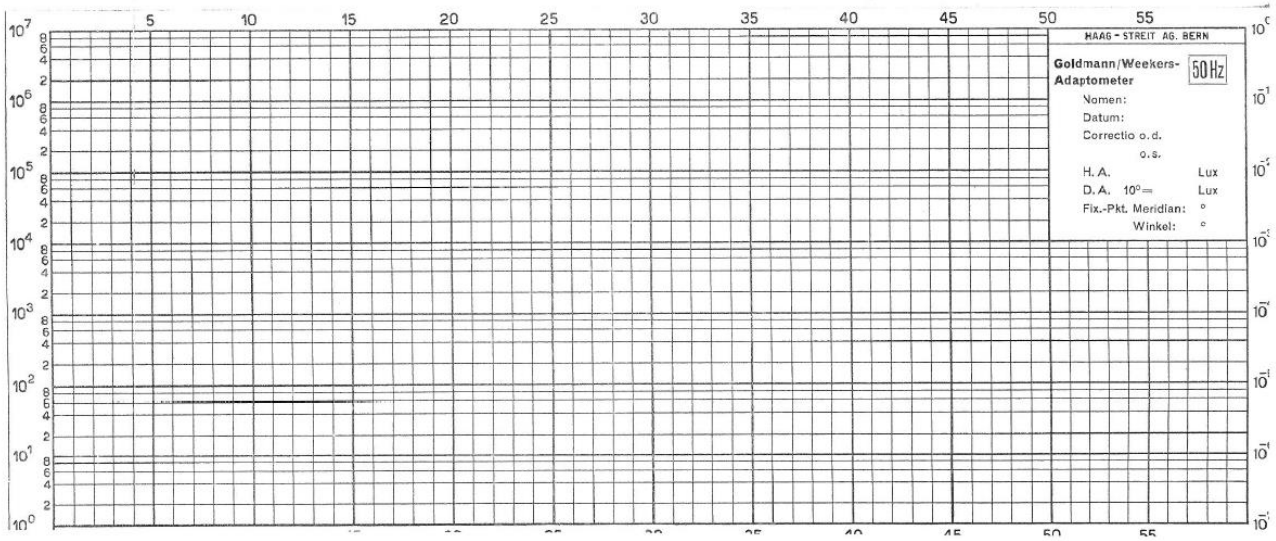

Figure 3.9 The logarithmic paper used by the Goldmann-Weekers adaptometer, enabling immediate recording of the visual threshold.

3.3.4.2.2 CDA

The computerised dark adaptometer presented a flashing stimulus on a calibrated cathode ray tube (CRT) monitor, driven by a graphics board under software control (Matlab). The monitor luminance was γ-corrected and modified by three neutral density filters (2.0 ND, 1.2 ND and

2.4 ND) mounted on the screen at specific points throughout the experiment in order to expose the full range of visual recovery. In order to avoid any fluctuations in luminance having an impact on dark adaptation results, the CRT was given at least 1.5 hours to warm up before dark adaptation recordings began. The programme utilised a modified staircase procedure to determine threshold, with threshold recorded when the stimulus first became visible on the ascending staircase. Threshold was measured continuously for the first five minutes. After this, threshold was measured every minute up to 25 minutes. The subject was instructed to focus straight ahead as indicated by four peripheral fixation markers. Threshold results were automatically transferred to an Excel spreadsheet upon programme completion.

3.3.4.2.3 Calibration

The GW adaptometer records luminance in units of log microapostilbs, rather than cd/m^2. In order to convert measurements to log cd/m^2 accurately, the luminance of the GW stimulus was calibrated using a photometer (LS-110; Konica Minolta, Osaka, Japan). The luminance output of the GW was measured at 0.2 log microapostilbs increments with the phototometer, and an average taken from three readings. The relationship between the measured luminance output and the log microapostilbs value was described by an equation which was then used to calculate the log cd/m^2 luminance value from any given log microabostilbs value.

3.3.5 *Repeatability of the CDA*

To further assess the suitability of the CDA for the assessment of DA, the intra-session repeatability was examined. All procedures were carried out as described in sections 3.4.1.2 and 3.4.1.2.2, except each measurement of dark adaptation was taken on the CDA.

3.3.5.1 Subjects

Dark adaptation curves were obtained from five eyes of five healthy adults (2 males, 3 females, age range 23-26 years, mean age 24.6 ± 1.14 years) recruited from School of Optometry and Vision Sciences, Cardiff University. Inclusion criteria comprised: age range between 18- 40 years, and no known disease of the retina or visual pathways. Exclusion criteria included any ocular or systemic condition known to affect dark adaptation, diabetes, photosensitive epilepsy, pregnancy, a Van Herrick anterior chamber angle of grade 1 or less or any history of a previous attack of acute angle closure glaucoma following Tropicamide use.

Informed consent was obtained from all subjects. Ethical approval was given by the Human Science Research Ethics Committee, School of Optometry and Vision Sciences, Cardiff University. All procedures conformed to the tenets of the Declaration of Helsinki.

3.3.5.2 Statistical Analysis

The parameters of both cone and rod recovery were determined by fitting a multiple component exponential function (*Equation 6)* (McGwin, Jackson and Owsley, 1999), on a least squares basis using the Solver Function in Microsoft Excel (2010).

$$T(t) = \left[a + \left(b.exp^{(-t/\tau)}\right)\right] + \left[c.\left(max(t - rcb, 0)\right)\right] + \left[d.\left(max(t - rrb, 0)\right)\right] \quad \textit{Equation 6}$$

Where T = threshold (log cd/m^2) at time t after cessation of bleach

a = final cone threshold (log cd/m^2)

b =change in cone threshold from t = 0

τ = time constant of cone recovery (minutes)

c = slope of the second component of rod recovery

max = a logic statement

rcb = time from bleach offset to the rod-cone break

d = slop of the third component of rod recovery

rrb = time from bleach offset to the rod-rod break

Data was analysed with SPSS (Version 18.0; PASW for Windows; Chicago, USA). Final cone threshold, cone time constant, rod-cone break time, rod-rod break time, final rod threshold and area under the curve (AUC) were all normally distributed (Shapiro-Wilk; $p > 0.05$ for all parameters). Therefore, parametric statistical analysis was applied.

Paired samples (2-tailed) t-test was used to assess differences in final cone threshold, cone time constant, rod-cone break time, rod-rod break time, final rod threshold and AUC between the GW and CDA. The repeatability of the CDA was assessed by evaluating the data from each visit using established statistical techniques (Bland and Altman, 1986; McAlinden, Khadka and Pesudovs, 2011) and by calculating the coefficient of repeatability (CoR). Significance was set at the 0.05 level.

3.4 Results

3.4.1 *Comparison of GW and CDA*

There was no significant difference in the cone constant, rod-cone break and rod-rod break between the two devices (Paired-samples (2-tailed) t-test, $0.338 < p < 0.858$) (Table 3.1 and Figure 3.10). A statistically significant difference was observed between final cone threshold, final rod threshold and AUC between the GW and CDA (Paired samples t-test; $p = 0.001$, $p = 0.000$ and $p = 0.004$ respectively). The final cone threshold for the CDA was significantly lower than the GW with a mean difference of 0.20 log cd/m^2. The final rod threshold decreased from the GW to the CDA by a mean of 0.52 log cd/m^2. The AUC also decreased from the GW to the CDA by 6.18 log cd/m^2.min.

Table 3.1 Comparing the GW and CDA

Parameter	GW (Mean ± SD)	CDA (Mean ± SD)	Paired t-test	95% CI	
				Lower	Upper
Final cone threshold (log cd/m^{-2})	-2.25 ± 0.82	-2.45 ± 0.14	**< 0.005**	0.102	0.278
Cone Constant (minutes)	1.93 ± 0.36	1.82 ± 0.48	0.620	-0.345	0.550
Rod-Cone break (minutes)	12.05 ± 1.16	11.99 ± 0.87	0.858	-0.717	0.846
Rod-Rod break (minutes)	18.73 ± 2.43	17.88 ± 1.17	0.338	-1.026	2.719
Final rod threshold (log cd/m^2)	-4.17 ± 0.07	-4.69 ± 0.12	**< 0.005**	0.466	0.565
AUC (log cd/m^2.min)	-55.77 ± 43.10	-61.95 ± 46.54	**< 0.005**	2.47	9.90

Key: GW, goldmann-weekers; CDA, computerized dark adaptometer; CI, confidence interval; AUC, area under the curve; bold and shaded cells indicate significance.

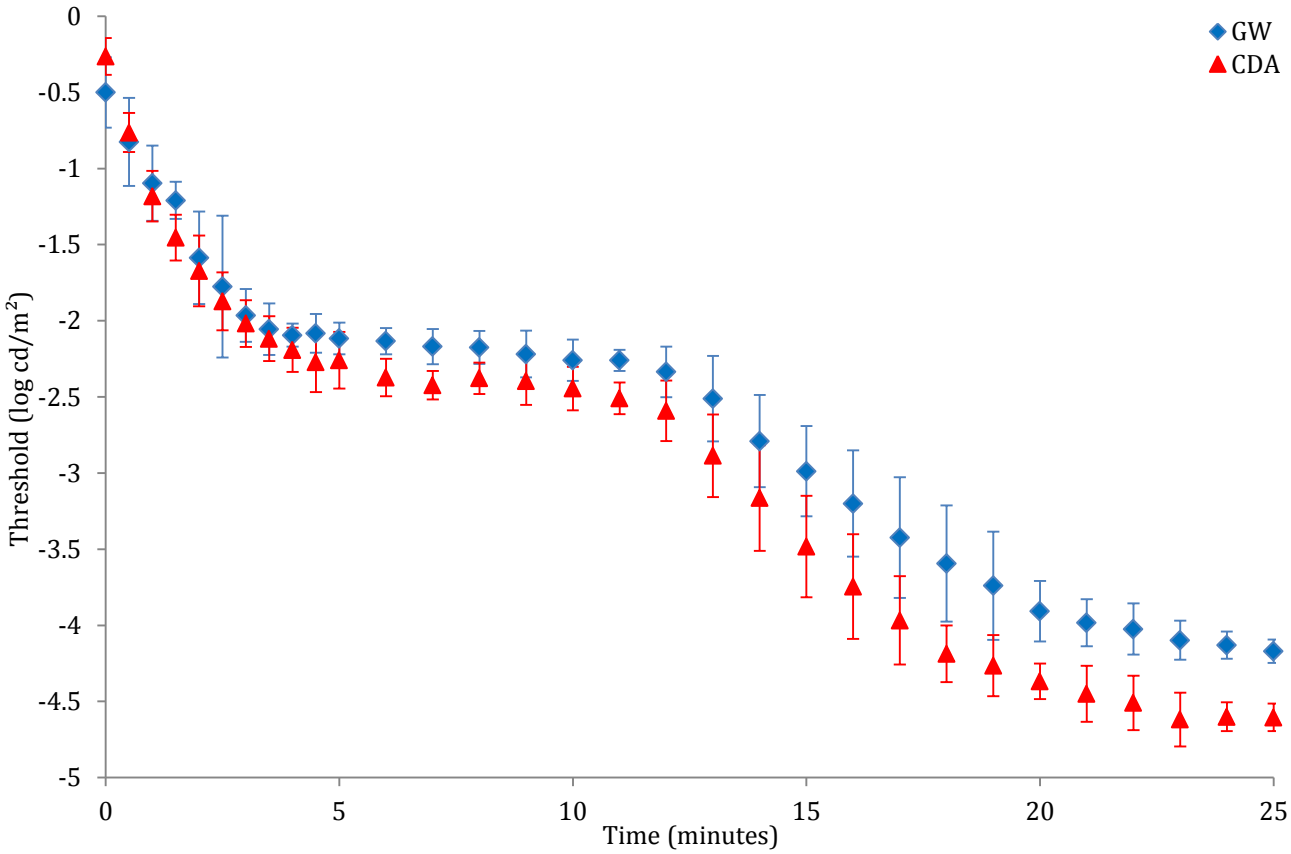

Figure 3.10 Mean dark adaptation functions for the Goldmann-Weekers (GW) and the computerised dark adaptometer (CDA). Error bars represent ± SD.

3.4.2 *Repeatability of the CDA*

There was no significant difference in the final cone threshold, cone constant, rod-cone break, rod-rod break, final rod threshold and AUC between measurement 1 and measurement 2 on the CDA (Paired-samples (2-tailed) t-test, $0.592 < p < 0.966$) (Table 3.2 and Figure 3.11). The difference between all parameters recorded during measurement 1 and measurement 2 are plotted as a function of the mean in Bland-Altman plots (Figure 3.12).

Table 3.2 Repeatability of the CDA

Parameter	M 1 (Mean ± SD)	M 2 (Mean ± SD)	Paired T-Test	95% CI		COR	COR%
				Lower	Upper		
Final cone threshold (log cd/m^{-2})	-2.33 ± 0.12	-2.33 ± 0.13	0.966	-0.120	0.124	0.19	8.15
Cone Constant (minutes)	1.62 ± 0.56	1.52 ± 0.27	0.592	-0.377	0.577	0.85	54.14
Rod-Cone break (minutes)	10.56 ± 1.32	10.52 ± 1.06	0.945	-1.476	0.1556	2.43	23.06
Rod-Rod break (minutes)	17.90 ± 2.98	18.08 ± 2.51	0.768	-1.784	1.420	2.35	13.06
Final rod threshold (log cd/m^2)	-4.64 ± 0.65	-4.68 ± 0.22	0.726	-0.256	0.336	0.51	10.94
AUC (log cd/m^2.min)	-76.92 ± 4.33	-77.45 ± 3.14	0.612	-2.16	3.23	4.79	6.21

Key: M1, measurement 1; M2, measurement 2; COR, coefficient of repeatability; CI, confidence interval; AUC, area under the curve

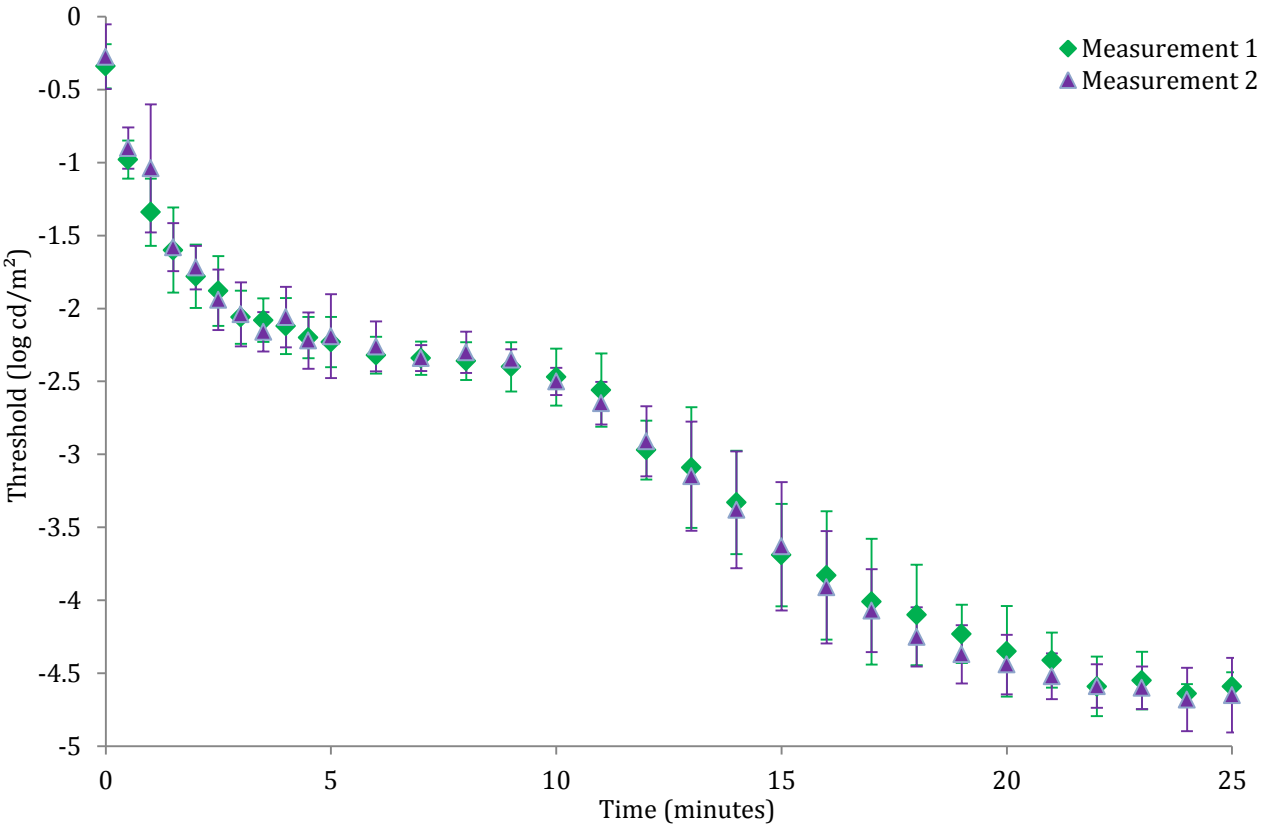

Figure 3.11 Mean dark adaptation functions for the CDA, showing results from measurement 1 and 2. Error bars represent ± SD.

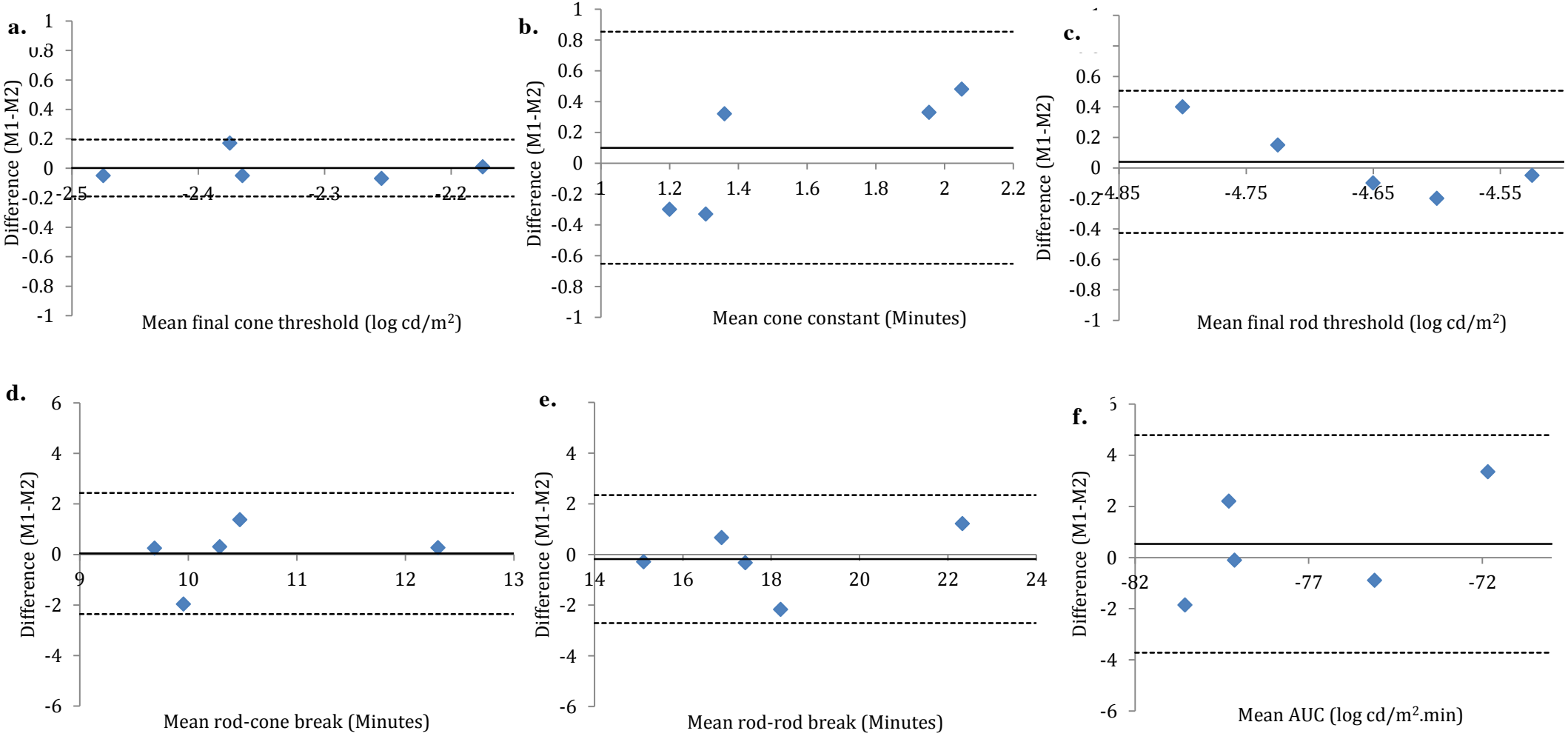

Figure 3.12 Bland-Altman plots for final cone threshold (a), cone constant (b), final rod threshold (c), rod-cone break (d), rod-rod break (e) and AUC (f). The difference between the values recorded during measurement 1 (M1) and measurement 2 (m2) is plotted as a function of the mean value for all subjects (solid line) and 95% limits of agreement, 1.96 × SD (dotted lines).

3.6 Discussion

Investigation of dark adaptation has traditionally been measured with the 'Gold standard' instrument, the Goldmann-Weekers dark adaptometer (Gaffney et al., 2011). With limited access to functioning Goldmann-Weekers dark adaptometers, the current trend in the measurement of dark adaptation involves the use of specially developed computerised dark adaptometers (Dimitrov et al., 2008). Before the data obtained from these custom made dark adaptometers can be considered reliable, it is important that the equipment is verified according to the current gold standard.

The CDA developed for this study was compared to the GW. Whilst previous reports on DA have used only rod thresholds and rod/cone break time as the primary outcome measures, more recent reports utilise non-linear regression analysis (McGwin et al., 1999) to accurately interpret DA parameters (Herse, 1995; Omar and Herse, 2004; Christoforidis and Zhang, 2011). Non-linear regression analysis was therefore used to analyse data for this experiment. Both the GW and the CDA were capable of monitoring and recording the changes in visual threshold that occurred during dark adaptation, with data successfully recorded from all participants. Results from both the GW and the CDA showed two distinct regions of recovery, dominated by the cones and rods, respectively. There was no significant difference in the cone constant, rod-cone break time, or rod-rod break time between the two techniques. This is reassuring as the parameters of dark adaptation are determined by the physiology of the visual cycle and should therefore be independent of equipment and psychophysical procedures used. However, final cone threshold and final rod threshold did show a significant difference between the two techniques. In both cases, the CDA produced lower measures of threshold. This may be attributed to the different psychometric procedure employed by the CDA, and the lack of examiner influence on the final result, as with the GW.

Repeatability of the CDA was found to be acceptable, with all parameters analysed showing no significant difference between measurement 1 and 2. No DA parameters demonstrated a learning effect between test and retest, an effect which is often a feature of ophthalmologic psychophysical procedures, but has not previously been shown to cause a problem when testing dark adaptation (Christoforidis and Zhang, 2011). Assessment of COR is important in the evaluation of a technique for clinical use, as it indicates the extent of inherent variability (Bland and Altman, 1986), giving the smallest change which may be considered clinically significant (Bland and Altman, 1986). The parameter which is of most importance for this

study is the final rod threshold, which has previously been shown to be significantly higher in CF subjects compared to controls (Fulton et al., 1982; Neugebauer et al., 1989; Rayner et al., 1989; Huet et al., 1997; Evans, 2009). The COR values found in this study for the CDA, are within a similar range to those previously found for the GW when measuring cone adaptation (0.85 and 1.32 minutes for cone τ for the CDA and GW, respectively) (Gaffney et al., 2011), suggesting the CDA has similar level of repeatability as the gold standard. Previous research showed mean differences greater than 1 log cd/m^2 between CF subjects and controls (Evans, 2009). These differences are greater than the final rod COR of 0.51 log cd/m^2, suggesting that the CDA is able to reliably differentiate between healthy controls and CF subjects with abnormal dark adaptation.

Chapter 4 Experimental Methods

This chapter outlines the methodology used throughout data collection for this thesis, bringing together the protocols developed in Chapters 2 and 3. All techniques were performed identically on CF subjects and controls, with all data collected between September 2011 and April 2013. Results are presented in Chapters 5 and 6.

4.1 Subjects

CF subjects were recruited from the All Wales Adult Cystic Fibrosis Centre, University Hospital, Llandough, Cardiff, in collaboration with Dr Ian Ketchell (FRCP PhD), Consultant Physician of Respiratory and General Medicine and Director of the All Wales Adult Cystic Fibrosis Centre. Healthy controls were recruited from undergraduates, postgraduates and staff from Cardiff University.

Ethical approval was gained from the Cardiff and Vale Trust Research and Development Office, South East Wales Research Ethics Committee (REC reference: 12/WA/0011; Protocol Number: SPON 1054-11)[1] and the Human Science Research Ethics Committee, School of Optometry and Vision Sciences, Cardiff University. All procedures conformed to the tenets of the Declaration of Helsinki. All subjects were provided with an information sheet and given the opportunity to discuss the study with the researchers prior to giving written consent.

---

[1] NHS ethics power calculations
Currently, 204 adult patients attend the CF clinic, approximately half of which have impaired glucose tolerance or CF related diabetes. For the sake of convenience, it is thought that only patients from within a reasonably close proximity will be interested in participating in the study; therefore, it is expected that a maximum of 50 patients will be recruited.

Power calculations for the DA experiments were based on a previous study by Fulton et al (1982) and numbers were calculated using the Altman Nomogram.
CF subjects; mean log threshold = 4.53 ± 0.42
Healthy Subjects; mean log threshold = 4.29 ± 0.18
Difference in means 4.53 - 4.29 = 0.24
Standardised difference: 0.24/0.42 = 0.57
Subject number = 44

Power calculations for the OCT experiments were based on a previous study by Oshitari et al. (2009). As retinal thickness has not previously been investigated in CF, instead results from diabetic patients were used. Number were calculated using the Altman Nomogram.
Healthy subjects; mean retinal thickness = 210.7 ± 28.6μm
Diabetic subjects; mean retinal thickness = 195.6 ± 23.3μm
Difference in means: 15.1μm
Standardised difference: 15.1/23.3 = 0.65
Subject number = 34 subjects per group

4.1.1 *Inclusion and exclusion criteria*

The inclusion criteria for CF volunteers required all subjects to be over 18 years of age, have a positive diagnosis of CF and to have given valid informed consent. CF subjects were excluded if they were pregnant or breast feeding, had a history of respiratory failure, chronic bronchitis, smoking, emphysema or previous chest surgery, suffered from photosensitive epilepsy, or previous acute angle closure following pupil dilation. Furthermore, subjects were excluded if Dr Ketchell advised that the patient was not well enough to participate, or that oxygen inhalation carried associated risks for the patient.

For gender-matched healthy controls, inclusion criteria required subjects to have a date of birth within 12 months of their CF match, no diagnosis of cystic fibrosis, be healthy and free from systemic problems, and to have given valid informed consent. Controls were excluded if they were pregnant, had an immediate family history of CF, suffered from diabetes, had a history of respiratory failure, chronic bronchitis, smoking, emphysema or previous chest surgery, suffered from photosensitive epilepsy or have previously had acute angle closure following pupil dilation.

4.2 Experimental Procedure

All subjects attended the School of Optometry and Vision Sciences, Cardiff University, for a single data collection session lasting two hours. The various tests and their order are shown in Figure 4.1. All subjects answered questions regarding current and previous ocular health, vision, and family ocular health. Medications and reports of general health were recorded in control subjects. The following information regarding the general health and medications taken by CF patients was obtained from their medical records via a member of the CF team at University Hospital, Llandough, with all identifiable patient information removed:

- Premature birth and gestation period
- Age at diagnosis of CF
- Genotype
- Medications and supplements
- Organ transplant history (as applicable)
- Forced Expiratory Volume in one second (FEV_1 %) – an indication of lung function expressed as a percentage of their personal predicted value

- CFRD status – classed as normal glucose tolerance (NGT), impaired glucose tolerance (IGT) or CF-related diabetes (CFRD)
- Glucose tolerance – determined by the oral glucose tolerance test (OGTT). (See Section 1.3.3 and Table 1.2)
- Glycosylated haemoglobin (HbA1c) – used to monitor glycaemic control (Brennan et al., 2004).
- Serum vitamin A concentration – an indication of vitamin A deficiency
- Northern Score – a chest radiograph scoring system based upon an anteroposterior chest radiograph, with a maximum score of 20, indicating the most severe level of disease (McCormick, Conway and Mehta, 2007)

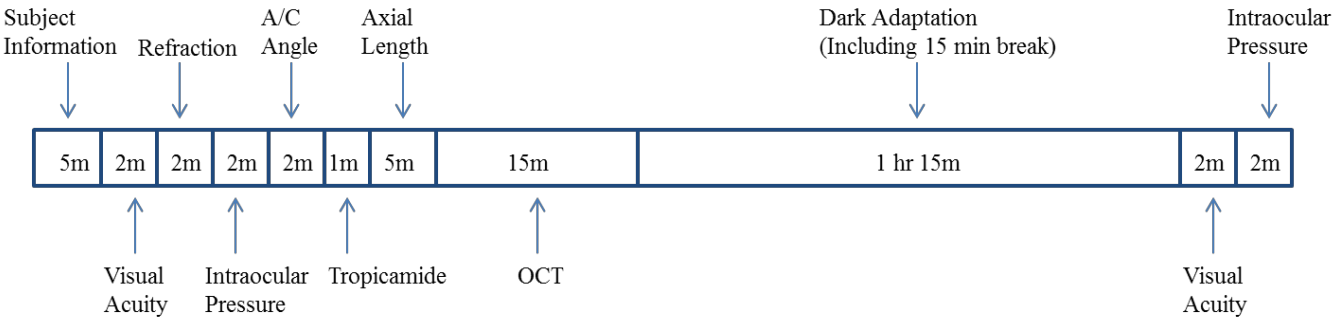

Figure 4.1 Timeline showing the order of data collection (m = minutes).

4.2.1 *Preliminary measurements*

Distance vision and/or visual acuity (VA) was recorded (right and left) with the patient's habitual correction in place using a LogMAR ETDRS chart (Precision Vision La Salle, IL, USA) at three meters (luminance 160 cd/m^2). Acuity was scored on an individual letter basis. Near visual acuity (right and left) was recorded with a Bailey-Lovie word near vision chart (Clement Clarke International Ltd., Essex, UK) chart at 25cm. Objective refraction was determined for each eye using an auto-refractor (Topcon KR-7500; Topcon, Tokyo, Japan), and the average of three readings was recorded.

Intraocular pressure was measured for each eye using a non-contact tonometer (CT-80, Topcon, Tokyo, Japan), and an average taken from four readings. Temporal anterior chamber angles were assessed by Van Herrick technique (Friedman and He, 2008) using a slip lamp biomicroscope and graded between 0-4. Any subjects who had a Van Herrick angle of grade 1

or less were excluded from this point forward due to increased risk of acute angle closure (Wolfs et al., 1997).

One drop of Tropicamide 1% (Bausch and Lomb, Laboratoire Chauvin, France) was instilled into the lower fornix of each eye and pupil size was monitored until it equalled or exceeded 7mm diameter. Tropicamide batch number and expiry date were recorded for each patient. Possible adverse reactions associated with Tropicamide were discussed and patients were advised on the appropriate action to take should they suspect an adverse reaction. Additionally, all patients were advised not to drive to the appointment and warned not to drive until they felt their vision was back to a normal level, which could take up to six hours.

Axial length was determined for each eye using the IOL Master (Zeiss, Germany). An average was taken from five readings, each with a signal to noise ratio (SNR) of five or above.

4.2.2 *Retinal Imaging*

Three consecutive 256x256 resolution (vitreous reference) macular Optical Coherence Tomography (OCT) scans were obtained for each eye using the Topcon 3D-OCT 1000 (Topcon, Tokyo, Japan). Scans with quality measures below 60 were rejected and repeated. Images with artefacts, or missing sections due to fixation errors or patient blinking were rejected and scans repeated. For each scan, retinal thickness and volume was recorded for each area of the ETDRS plot.

One high resolution OCT scan was obtained for each eye, using the following parameters: transverse resolution 1024, 6mm B scan length, choroid reference, 0.15mm pitch and 8 averages.

Qualitative and quantitative analysis of high resolution scans was undertaken at a later date. Each scan was evaluated and any abnormal features, including presence of drusen, were recorded. Measurements of RPE/photoreceptor layer thickness were taken using the callipers integrated into the Topcon 3D OCT-1000 software. Measurements were taken by an experienced examiner using the B-scan with the greatest macular dip for each patient, at the point of minimal retinal thickness and 1.1mm temporally and nasally. Computer monitor and mouse settings were adjusted to optimise image quality and pointer sensitivity prior to

measurements being taken. Manual measurements of RPE/photoreceptor layer thickness for all scans were conducted on the same day to reduce variation in examiner decision criteria.

4.2.3 *Dark Adaptation*

DA was assessed in the eye with the best VA for each patient, whilst the other eye was patched. If no difference in VA existed, the right eye was selected. Each patient was randomly allocated to receive either medical air (20% oxygen, 80% nitrogen) or 100% oxygen first from one of two concealed gas cylinders (British Oxygen Supplies, Cardiff, Wales). The patient was masked to which gas they were receiving. Both oxygen and medical air was administered via sterile disposable 60% venti masks (Intersurgical Ltd, Berkshire, UK), at a flow rate of 15 L/min (Drasdo et al., 2002). Inhalation of gases began two minutes prior to dark adaptation testing commencement (during light adaption), and continued throughout the duration of the experiment (Figure 4.2). Prior inhalation was necessary to allow time for retinal oxygenation, as the autoregulation response to oxygen inhalation occurs in less than 1.5 minutes (Riva, Grunwald and Sinclair, 1983b). Arterial oxygen saturation was recorded prior to gas inhalation, after two and five minutes of inhalation, then at five minute intervals up to 25 minutes using a fingertip pulse oximeter (Medisupplies Ltd, Dorset, UK).

A long duration 'equilibrium' bleach was provided to the selected eye with a Maxwellian-view optical system (Westheimer, 1966) (Figure 4.3), providing a white light of 5.16 log td for a period of two minutes, which bleached approximately 74.70% rhodopsin and 82.80% iodopsin (see section 3.3.3 for supporting calculations). Upon bleach cessation, the patient was immediately transferred to the chin rest in front of the dark adaptometer (Figure 4.4), and instructed to press any button on the keyboard to begin the dark adaptation programme.

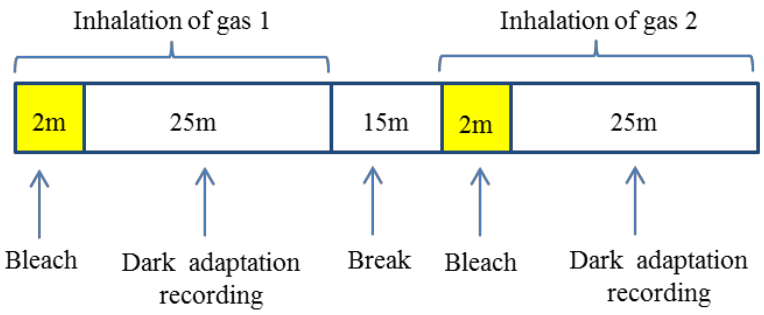

Figure 4.2 Timeline showing the order of dark adaptation data collection.

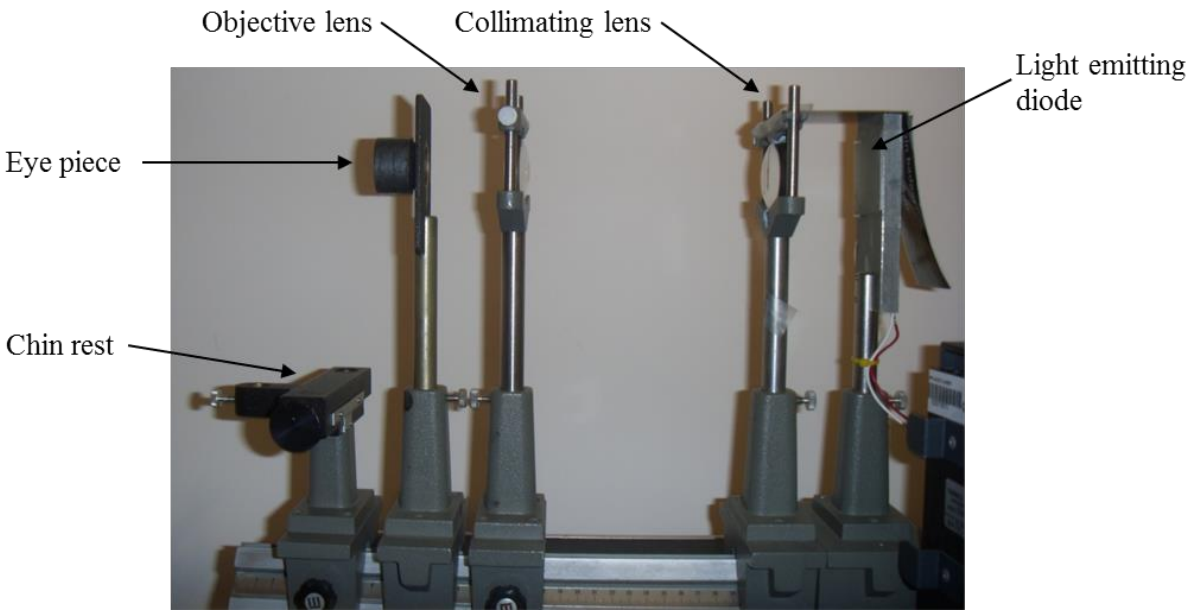

Figure 4.3 Photograph showing the Maxwellian View optical system used to administer an equilibrium bleach.

Figure 4.4 Photograph showing the set-up of equipment for testing dark adaptation whilst inspiring medical air or oxygen.

The computerised dark adaptometer presented a flashing stimulus on a calibrated cathode ray tube (CRT) monitor, driven by a graphics board under software control (Matlab) (see Appendix B for Matlab script). The monitor luminance was γ-corrected (Metha et al., 1993) and modified by three screen mounted neutral density filters (Dimitrov et al., 2008) (2.0 ND, 1.2 ND and 2.4 ND, respectively) at specific points throughout the experiment in order to expose the full range

of visual recovery. The programme utilised a modified staircase procedure to determine threshold (Jackson et al., 1999). Threshold was recorded when the stimulus first became visible on the ascending staircase Threshold was measured continuously for the first five minutes. After this, threshold was measured every 50 seconds for the remaining 20 minutes. The subject was instructed to focus straight ahead as indicated by four peripheral fixation markers. Each patient received full instructions, a demonstration and a practice session prior to threshold measurement. All results were automatically exported to Microsoft Excel following completion of the programme.

A 15 minute break and washout period followed the first measurement of dark adaptation, where the patient was provided with refreshments. The procedure was then repeated with the second gas, using the same eye. The parameters of both cone and rod recovery were determined by fitting a multiple component exponential function (*Equation 7)* (McGwin et al., 1999), on a least squares basis using the Solver Function in Microsoft Excel (2010).

$$T(t) = \left[a + \left(b.exp^{(-t/\tau)}\right)\right] + \left[c.\left(max(t - rcb, 0)\right)\right] + \left[d.\left(max(t - rrb, 0)\right)\right] \quad \textit{Equation 7}$$

Where T = threshold (log cd/m^2) at time t after cessation of bleach

a = final cone threshold (log cd/m^2)

b =change in cone threshold from $t = 0$

τ = time constant of cone recovery (minutes)

c = slope of the second component of rod recovery

max = a logic statement

rcb = time from bleach offset to the rod-cone break

d = slop of the third component of rod recovery

rrb = time from bleach offset to the rod-rod break

4.2.4 *Post-dilation measurements*

Distance vision/VA and IOP (methods as described in 4.1.2.1) were re-measured at the end of the data collection session to monitor for adverse effects following pupillary dilation.

4.2.5 *Statistics*

4.2.5.1 OCT data

All data was checked for normality using the Shapiro-Wilk test. All retinal thickness results were normally distributed (controls, $0.08 < p < 0.95$; CF, $0.14 < p < 0.90$). Some RPE/Photoreceptor complex thickness results were non-normally normally distributed for CF subjects ($0.00 < p < 0.513$). Despite a non-normal distribution of the RPE/Photoreceptor complex thickness data, the results are a small sample of continuous data, which is representative of a normal distribution. Therefore, parametric statistics were applied (Bland and Altman, 2009). Thickness measurements at each retinal location were assessed for a relationship with axial length using Pearson's correlation coefficient as CF and control groups were not matched for this factor. Where a statistically significant correlation was identified ($p < 0.05$), linear regression was used to correct retinal thickness values. Independent-samples (2-tailed) t-tests were used to assess the difference in retinal thickness between CF and controls. Whilst multiple comparisons increase the risk of type 1 error, this risk is reduced as retinal thickness values are correlated. Therefore, a conservative approach to multiple statistical testing, such as Bonferroni correction, was not appropriate (Bland and Altman, 1995). Significance was set at the 0.05 level.

4.2.5.2 Dark adaptation data

All data was checked for normality using the Shapiro-Wilk test. All parameters analysed were normally distributed. Paired-samples t-tests were used to compare the effect of oxygen inhalation within the CF and control groups. Independent-samples t-tests were used to compare data between CF and control groups. Two-tailed t-tests were used for all comparisons, excluding those where the hypothesis states a specified direction of change. One-tailed t-tests are indicated by a *. One-way repeated measures ANOVA was used to examine the effect of oxygen/air inhalation on SaO_2 in both CF and control groups. As multiple comparisons increase the risk of type 1 error, Bonferroni correction was applied where appropriate (Bland and Altman, 1995). One-way ANOVA was used to examine the effect of vitamin A status and genotype. Bonferroni's test was used for post-hoc comparisons. Correlation was assessed with Pearson's product moment correlation coefficient. Significance was set at the 0.05 level.

Chapter 5 Dark Adaptation and Oxygen Inhalation in Cystic Fibrosis

5.1 Introduction

This chapter presents the results of the study investigating the effect of oxygen inhalation on dark adaptation in cystic fibrosis. All methods were carried out as outlined in Chapter 4.

5.2 Experimental Hypothesis

Considering the literature as discussed in Chapter 1, if changes in DA in CF are only secondary complications of CFRD, the following hypotheses are proposed:

1. CFRD subjects will show raised final rod thresholds compared to controls when inhaling medical air. This impairment will be ameliorated during 100% oxygen breathing, indicating the presence of retinal hypoxia in CFRD subjects.
2. CFRD subjects will show a smaller improvement in cone threshold compared to controls during 100% oxygen breathing, demonstrating impaired vascular reactivity.
3. NGT CF patients will show no impairment in any DA parameters when inhaling medical air, and will therefore show no change during 100% oxygen breathing.

However, if changes in DA are a primary manifestation of the disease, caused directly by malfunction of CFTR at the RPE, it would be expected that:

1. All CF subjects will show impaired DA, both during the inhalation of air and oxygen, with impairment correlated to the severity of disease.
2. CFRD patients will show improvement in threshold upon inhalation of oxygen, but the final rod threshold will not recover to levels comparable to age-matched controls.

5.3 Results

5.3.1 *Subjects*

An overview of disease involvement in all subjects who took part in the DA experiment is shown in Table 5.1, then broken down into groups based upon diabetic status in tables 5.2-5.4, and based upon vitamin A status in tables 5.5-5.6 (Figure 5.1). Whilst a total of 28 CF subjects were recruited, DA was not carried out on 3 subjects due to programme errors and the results of 2 subjects were excluded due to unreliable data; it was apparent the subjects did not understand the examination. The average age of the 23 participants was 29.70 ± 8.72 years for

controls and 29.52 ± 8.34 years for CF subjects. Four females and 19 male controls and CF patients were examined. All controls were not diabetic and assumed to be vitamin A sufficient.

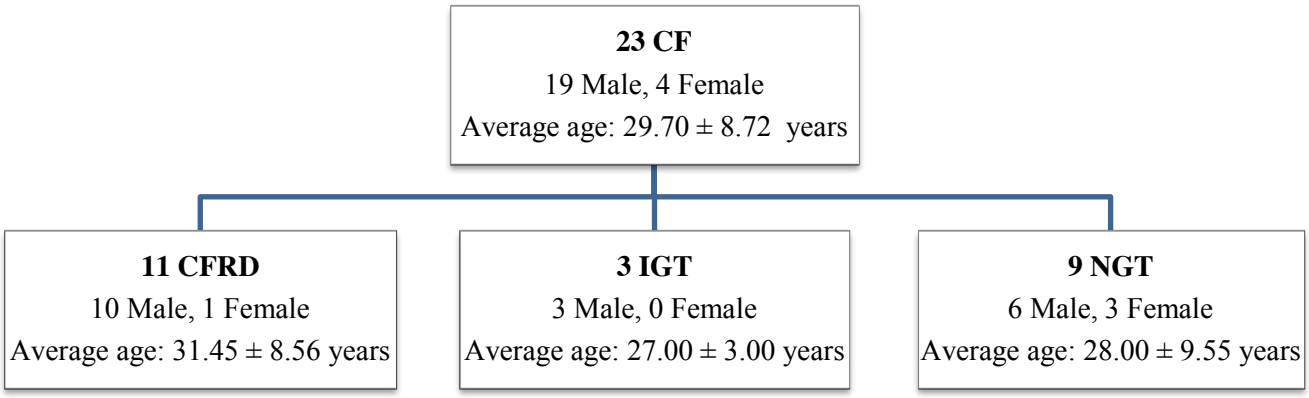

Figure 5.1 Diagram showing the diabetic distribution of CF subjects. (For guidelines on the classification of CFRD, IGT and NGT refer to Table 1.2)

Table 5.1 Disease characteristics of the CF subjects for DA (n = 23)

Variable	Description
Genotype	n = 14 ΔF508 homozygous n = 7 ΔF508 heterozygous n = 1 non-ΔF508 n = 1 unidentified
Pancreatic Function	n = 23 pancreatic insufficient
Serum Vitamin A concentration	Range: 0.78 – 1.97 µmol/L (Normal range: 1.10 – 2.60 µmol/L)* Mean ± SD: 1.37 ± 0.35 µmol/L
Vitamin A Status	n = 19 vitamin A sufficient n = 4 vitamin A deficient
CFRD status	n = 9 NGT; n = 3 IGT; n = 11 CFRD
HbA1c	Range: 28 – 111 mmol/mol (Normal range 26-48 mmol/mol)* Mean ± SD: 49.08 ± 18.59 mmol/mol
Predicted FEV_1	Range: 28 – 96% Mean ± SD: 59.83 ± 21.60 %
Northern Score	Range: 0 – 12 Mean ± SD: 6.26 ± 3.19
Age	Range: 18 – 49 years Mean ± SD: 29.52 ± 8.34
Gender	19 Male 4 Female

* Normal values obtained from laboratory

Key: NGT, normal glucose tolerance; IGT, impaired glucose tolerance; CFRD, cystic fibrosis related diabetes; HbA1c, glycosylated haemoglobin; FEV_1, forced expiratory volume in 1 second.

Table 5.2 Disease characteristics of the CFRD subjects for DA (n = 11)

Variable	Description
Genotype	n = 6 ΔF508 homozygous n = 4 ΔF508 heterozygous n = 1 unidentified
Pancreatic Function	n = 11 pancreatic insufficient
Serum Vitamin A concentration	Range: 0.78 – 1.97 μmol/L (Normal range: 1.10 – 2.60 μmol/L)* Mean ± SD: 1.51 ± 0.42 μmol/L
Vitamin A Status	n = 9 vitamin A sufficient n = 2 vitamin A deficient
HbA1c	Range: 35 – 111 mmol/mol (Normal range 26-48 mmol/mol)* Mean ± SD: 59.723 ± 22.09 mmol/mol
Predicted FEV_1	Range: 32 – 96% Mean ± SD: 67.23 ± 23.51 %
Northern Score	Range: 0 – 12 Mean ± SD: 5.77 ± 3.49
Age	Range: 18 – 44 years Mean ± SD: 31.45 ± 8.56
Gender	10 Male 1 Female

* Normal values obtained from laboratory

Key: NGT, normal glucose tolerance; IGT, impaired glucose tolerance; CFRD, cystic fibrosis related diabetes; HbA1c, glycosylated haemoglobin; FEV_1, forced expiratory volume in 1 second.

Table 5.3 Disease characteristics of the NGT subjects for DA (n = 9)

Variable	Description
Genotype	n = 5 ΔF508 homozygous n = 3 ΔF508 heterozygous n = 1 non-ΔF508
Pancreatic Function	n = 9 pancreatic insufficient
Serum Vitamin A concentration	Range: 0.92 – 1.82 μmol/L (Normal range: 1.10 – 2.60 μmol/L)* Mean ± SD: 1.25 ± 0.26 μmol/L
Vitamin A Status	n = 7 vitamin A sufficient n = 2 vitamin A deficient
HbA1c	Range: 28 – 51 mmol/mol (Normal range 26-48 mmol/mol)* Mean ± SD: 39.56 ± 6.29 mmol/mol
Predicted FEV_1	Range: 31 – 89% Mean ± SD: 52.33 ± 19.58 %
Northern Score	Range: 0 – 11 Mean ± SD: 6.67 ± 3.43
Age	Range: 20 – 49 years Mean ± SD: 28.00 ± 9.55
Gender	6 Male 3 Female

* Normal values obtained from laboratory

Key: NGT, normal glucose tolerance; IGT, impaired glucose tolerance; CFRD, cystic fibrosis related diabetes; HbA1c, glycosylated haemoglobin; FEV_1, forced expiratory volume in 1 second.

Table 5.4 Disease characteristics of the IGT subjects for DA (n = 3)

Variable	Description
Genotype	n = 3 ΔF508 homozygous
Pancreatic Function	n = 3 pancreatic insufficient
Serum Vitamin A concentration	Range: 1.20 – 1.29 µmol/L (Normal range: 1.10 – 2.60 µmol/L)* Mean ± SD: 1.24 ± 0.46 µmol/L
Vitamin A Status	n = 3 vitamin A sufficient
HbA1c	Range: 35 – 41 mmol/mol (Normal range 26-48 mmol/mol)* Mean ± SD: 38.67 ± 3.21 mmol/mol
Predicted FEV_1	Range: 50 – 89 % Mean ± SD: 69.67 ± 19.50 %
Northern Score	Range: 2 – 7 Mean ± SD: 4.67 ± 2.52
Age	Range: 24 – 30 years Mean ± SD: 27.00 ± 3.00
Gender	3 Male

* Normal values obtained from laboratory

Key: NGT, normal glucose tolerance; IGT, impaired glucose tolerance; CFRD, cystic fibrosis related diabetes; HbA1c, glycosylated haemoglobin; FEV_1, forced expiratory volume in 1 second.

Table 5.5 Disease characteristics of the vitamin A sufficient subjects for DA (n = 19)

Variable	Description
Genotype	n = 11 ΔF508 homozygous n = 7 ΔF508 heterozygous n = 1 unidentified
Pancreatic Function	n = 19 pancreatic insufficient
Serum Vitamin A concentration	Range: 1.10 – 1.97 μmol/L (Normal range: 1.10 – 2.60 μmol/L)* Mean ± SD: 1.47 ± 0.29 μmol/L
CFRD status	n = 7 NGT; n = 3 IGT; n = 9 CFRD
HbA1c	Range: 35 – 111 mmol/mol (Normal range 26-48 mmol/mol)* Mean ± SD: 50.21 ± 19.74 mmol/mol
Predicted FEV_1	Range: 32 – 91% Mean ± SD: 61.42 ± 20.06 %
Northern Score	Range: 0 – 12 Mean ± SD: 5.84 ± 3.11
Age	Range: 18 – 49 years Mean ± SD: 29.00 ± 8.71
Gender	15 Male 4 Female

* Normal values obtained from laboratory

Key: NGT, normal glucose tolerance; IGT, impaired glucose tolerance; CFRD, cystic fibrosis related diabetes; HbA1c, glycosylated haemoglobin; FEV_1, forced expiratory volume in 1 second.

Table 5.6 Disease characteristics of the VAD subjects for DA (n = 4)

Variable	Description
Genotype	n = 3 ΔF508 homozygous n = 1 non-ΔF508
Pancreatic Function	n = 4 pancreatic insufficient
Serum Vitamin A concentration	Range: 0.78 – 1.03 μmol/L (Normal range: 1.10 – 2.60 μmol/L)* Mean ± SD: 0.90 ± 0.10 μmol/L
CFRD status	n = 2 NGT; n = 2 CFRD
HbA1c	Range: 28 – 54 mmol/mol (Normal range 26-48 mmol/mol)* Mean ± SD: 43.75 ± 12.28 mmol/mol
Predicted FEV_1	Range: 31 – 96% Mean ± SD: 52.25 ± 30.26 %
Northern Score	Range: 5 – 11 Mean ± SD: 8.25 ± 3.20
Age	Range: 25 – 40 years Mean ± SD: 32.00 ± 6.78
Gender	4 Male

* Normal values obtained from laboratory

Key: NGT, normal glucose tolerance; IGT, impaired glucose tolerance; CFRD, cystic fibrosis related diabetes; HbA1c, glycosylated haemoglobin; FEV_1, forced expiratory volume in 1 second.

5.3.2 *The effect of oxygen inhalation on SaO_2*

As expected, both CF and control subjects exhibited a significant increase in mean SaO_2 during oxygen inhalation compared to air from two to 25 minutes (Table 5.7, paired-samples (1-tailed) t-test, $p < 0.005$, following Bonferroni correction). Comparing the groups, SaO_2 for CF subjects was significantly lower than controls when inhaling air from two to 25 minutes (independent-samples (2-tailed) t-test, $p < 0.05$, following Bonferroni correction), indicating CF subjects are hypoxic. Conversely, SaO_2 similar between CF subjects and controls with 100% oxygen inhalation (independent-samples (2-tailed) t-test, $p > 0.05$, following Bonferroni correction). There was no significant effect of time on SaO_2 during inhalation of air in controls and CF patients (one-way repeated measures ANOVA $p = 0.63$, $p = 0.21$ controls; ANOVA $p = 0.53$, $p = 0.065$ CF) (Figure 5.2 and 5.3). There was a significant effect of time on SaO_2 during inhalation of oxygen in controls (ANOVA $p < 0.005$; Bonferroni's $p < 0.005$) and CF patients (ANOVA $p < 0.005$; Bonferroni's $p < 0.005$) with a significant difference seen between pre-inhalation (0 minutes) and all other time points measured. When analysed according to diabetic status, there was no significant difference between mean SaO_2 during inhalation of air or oxygen between CFRD and NGT subjects (independent samples (2-tailed) t-test $p = 0.44$ and $p = 0.19$, respectively.

Table 5.7 SaO_2 during inhalation of oxygen and air in control and CF subjects

Time (Minutes)	SaO_2 (%)							
	Controls (n = 23)			CF (n = 23)			Independent-samples (2-tailed) t-test	
	Air	Oxygen	Paired samples (1-tailed) t-test	Air	Oxygen	Paired samples (1-tailed) t-test	Air: CF vs Controls	Oxygen: CFvs Controls
0	97.22 ± 1.68	97.61 ± 0.58	0.322	95.91 ± 1.95	96.22 ± 1.28	0.365	**0.019**	**< 0.005**
2	97.68 ± 0.48	98.91 ± 0.29	**< 0.005**	96.13 ± 1.98	98.43 ± 0.79	**< 0.005**	**< 0.005**	**0.040**
5	97.70 ± 0.47	99.00 ± 0.30	**< 0.005**	96.52 ± 1.41	98.78 ± 0.74	**< 0.005**	**0.001**	0.200
10	97.52 ± 1.04	98.86 ± 0.46	**< 0.005**	96.70 ± 1.18	98.78 ± 0.60	**< 0.005**	**0.016**	0.583
15	97.48 ± 0.73	99.13 ± 0.34	**< 0.005**	96.48 ± 1.59	98.78 ± 0.67	**< 0.005**	**0.010**	0.090
20	97.78 ± 0.52	98.96 ± 0.47	**< 0.005**	96.30 ± 1.29	98.78 ± 0.60	**< 0.005**	**< 0.005**	0.281
25	97.65 ± 0.57	98.96 ± 0.47	**< 0.005**	96.48 ± 1.34	98.87 ± 0.69	**< 0.005**	**< 0.005**	0.623

Key: SaO_2, arterial oxygen saturation; bold and shaded cells indicate significance.

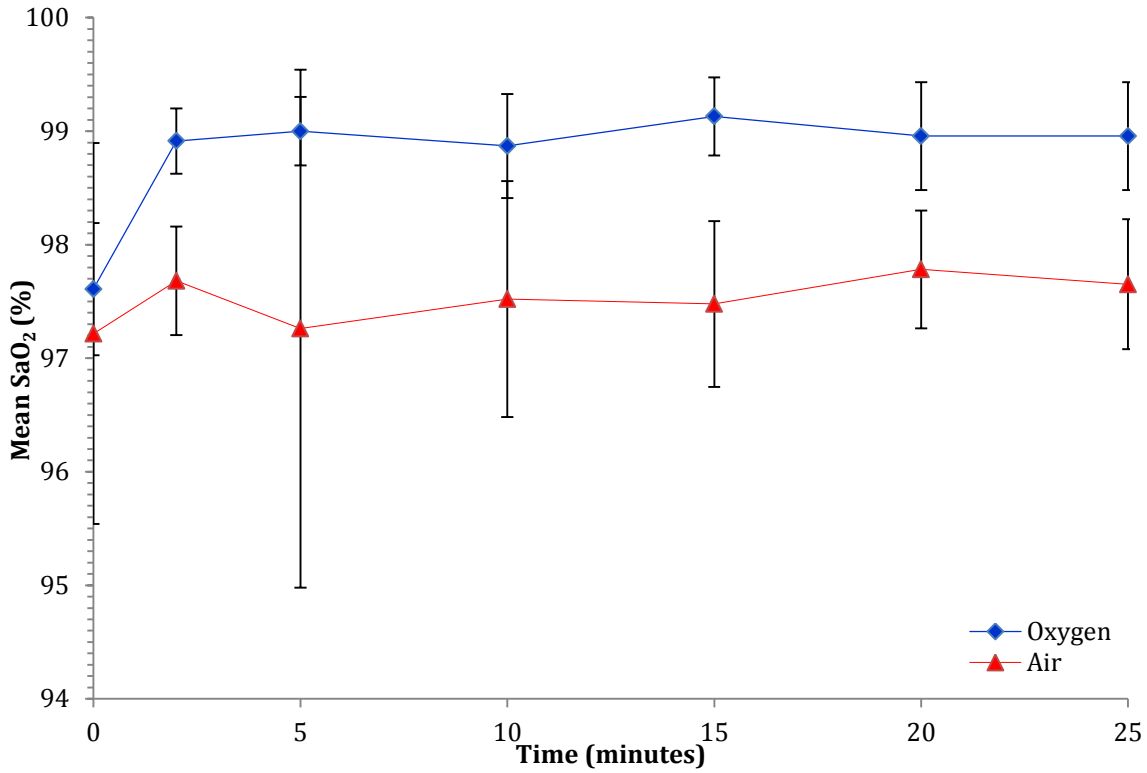

Figure 5.2 Mean SaO_2 for controls (n = 23) during inhalation of oxygen and air. Error bars show the standard deviation.

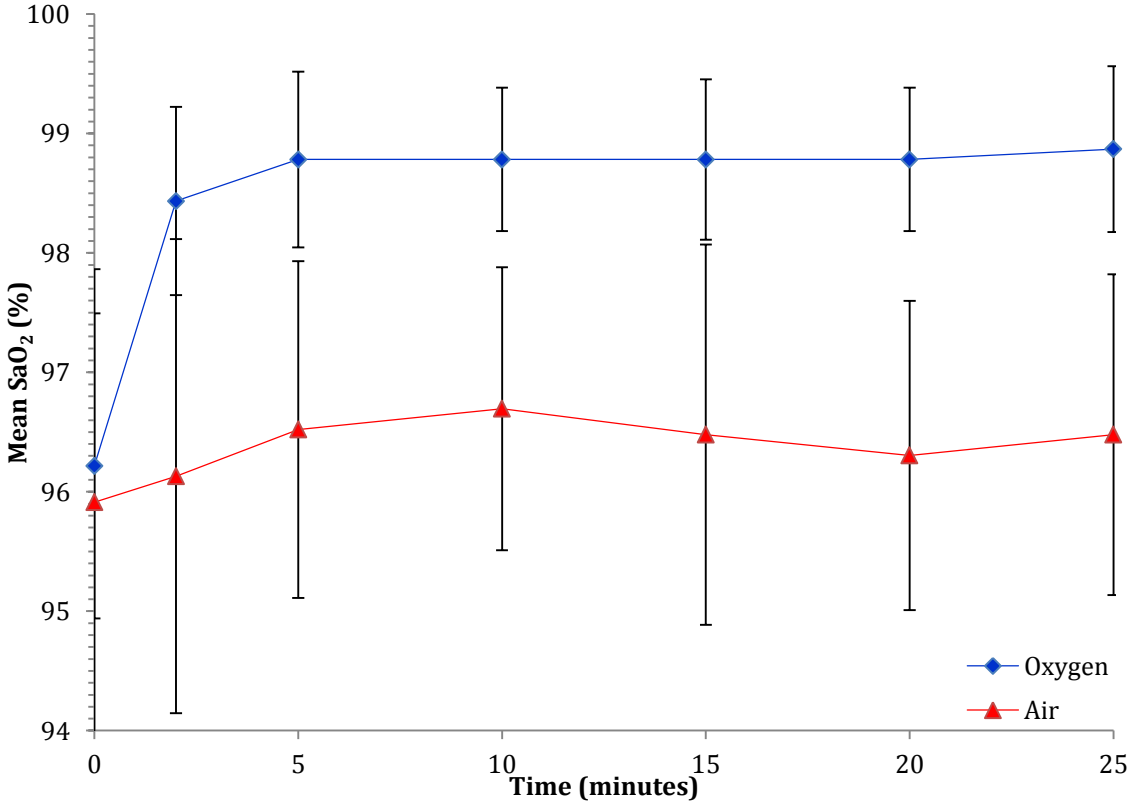

Figure 5.3 Mean SaO_2 for CF subjects (n = 23) during inhalation of oxygen and air. Error bars show the standard deviation.

5.3.3 *The effect of oxygen inhalation on DA*

5.3.3.1 Controls

For control subjects, inhalation of 100% oxygen was associated with significant reduction in the time to reach the rod-cone break (11.17 ± 1.12 minutes versus 10.53 ± 1.21 minutes respectively, paired-samples (2-tailed) t-test; p = 0.03). Changes in other parameters were evident but failed to reach statistical significance (Table 5.8 and Figure 5.4). The cone constant demonstrated a reduction upon inhalation of 100% oxygen, indicating an increase in the speed of cone recovery (1.85 ± 0.45 minutes versus 1.68 ± 0.50 minutes respectively), however, this failed to reach significance (paired-samples (2-tailed) t-test; p = 0.14).

Table 5.8 The effect of oxygen inhalation on DA in controls (n=23)

Parameter	Air (Mean ± SD)	Oxygen (Mean ± SD)	Paired t-test
Cone Constant (minutes)	1.85 ± 0.45	1.68 ± 0.50	0.14
Final Cone Threshold (log cd/m^2)	-2.34 ± 0.16	-2.28 ± 0.17	0.24
Rod- Cone Break Time (minutes)	11.17 ± 1.12	10.53 ± 1.21	**0.03**
Rod-Rod Break Time (minutes)	17.28 ± 1.41	17.44 ± 1.24	0.60
Final Rod Threshold (log cd/m^2)	-4.60 ± 0.15	-4.64 ± 0.19	0.21

Key: bold and shaded cells indicate significance

5.3.3.2 CF subjects

For CF subjects, inhalation of 100% oxygen was associated with a significant decrease in the final rod threshold from -4.50 log cd/m^2 to -4.59 log cd/m^2 (paired-samples (1-tailed) t-test: p = 0.03). There was no significant difference in any of the other parameters upon inhalation of oxygen (paired-samples (2-tailed) t-test, 0.4 < p < 0.81) (Table 5.9 and Figure 5.4).

Table 5.9 The effect of oxygen inhalation on DA in CF (n = 23)

Parameter	Air (Mean ± SD)	Oxygen (Mean ± SD)	Paired t-test
Cone Constant (minutes)	1.47 ± 0.75	1.41 ± 0.47	0.71
Final Cone Threshold (log cd/m^2)	-2.22 ± 0.56	-2.23 ± 0.15	0.81
Rod- Cone Break Time (minutes)	9.83 ± 2.41	9.45 ± 2.01	0.40
Rod-Rod Break Time (minutes)	16.93 ± 2.73	17.22 ± 1.49	0.59
Final Rod Threshold (log cd/m^2)	-4.50 ±0.27	-4.59 ± 0.21	**0.03***

Key: bold and shaded cells indicate significance; * Indicates 1-tailed t-test when the hypothesis indicates a relationship in a specified direction

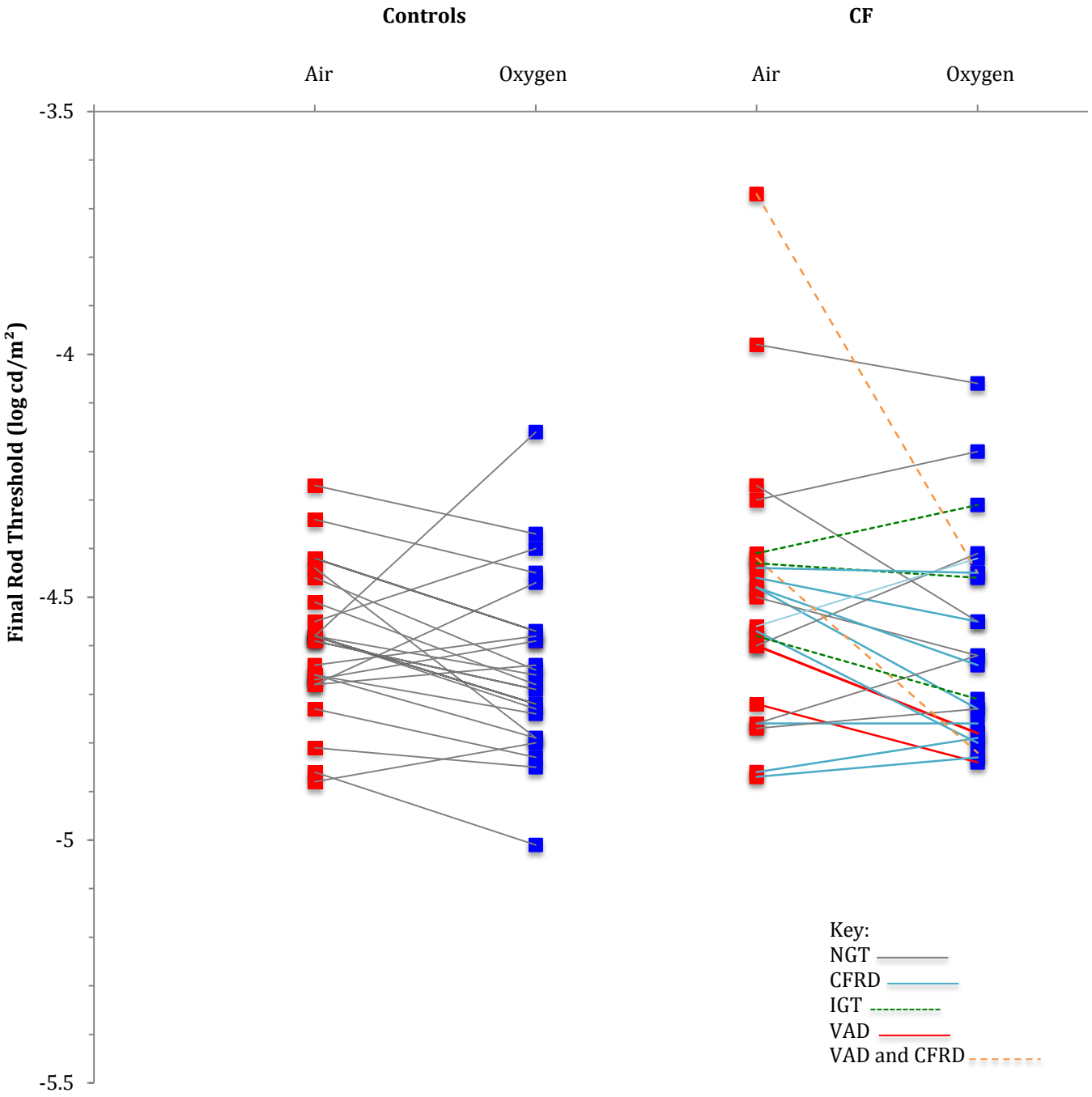

Figure 5.4 Final rod thresholds for controls (n = 23) and CF (n = 23) subjects for oxygen and air inhalation. Diabetic and vitamin A status for CF subjects can be identified according to the key as shown.

5.3.3.3 CFRD subjects

CFRD subjects showed a significant decrease in final rod threshold upon the inhalation of 100% oxygen from -4.48 log cd/m^2 to -4.62 log cd/m^2 (paired-samples (1-tailed) t-test p = 0.04) (Table 5.10 and Figure 5.5). The difference in threshold upon the inhalation of oxygen

is larger for the CFRD group compared to the CF group (0.14 log cd/m^2 and 0.9 log cd/m^2 reductions, respectively) (Figure 5.5). The cone threshold reduced upon inhalation of oxygen, however, the difference did not reach significance (paired-samples (2-tailed) t-test; p = 0.30). There was no significant difference between the cone constant, final cone threshold, rod-cone break or rod-rod break upon inhalation of oxygen in the CFRD group (paired-samples (2-tailed) t-test, p = 0.80, p = 0.30, p = 0.35, p = 0.16, respectively).

Table 5.10 The effect of oxygen inhalation on DA in CFRD subjects (n = 11)

Parameter	Air (Mean ± SD)	Oxygen (Mean ± SD)	Paired t-Test
Cone Constant (minutes)	1.14 ± 0.34	1.19 ± 0.40	0.80
Final Cone Threshold (log cd/m^2)	-2.09 ± 0.22	-2.16 ± 0.12	0.30
Rod- Cone Break Time (minutes)	8.94 ± 2.14	8.68 ± 1.70	0.35
Rod-Rod Break Time (minutes)	15.56 ± 2.55	16.84 ± 1.74	0.16
Final Rod Threshold (log cd/m^2)	-4.45 ± 0.31	-4.60 ± 0.18	**0.04***

Key: bold and shaded cells indicate significance; * Indicates 1-tailed t-test when the hypothesis indicates a relationship in a specified direction

5.3.3.4 NGT CF subjects

There was no significant difference in any of the DA parameters upon inhalation of oxygen in NGT CF subjects (Table 5.11 and Figure 5.5). Whilst significance is not reached, the rod-cone break occurred earlier and the rod-rod break occurred later during the inhalation of oxygen compared to air.

Table 5.11 The effect of oxygen inhalation on DA in NGT CF subjects (n = 9)

Parameter	Air (Mean ± SD)	Oxygen (Mean ± SD)	Paired t-Test
Cone Constant (minutes)	1.44 ± 0.36	1.42 ± 0.36	0.90
Final Cone Threshold (log cd/m^2)	-2.31 ± 0.17	-2.29 ± 0.14	0.80
Rod- Cone Break Time (minutes)	10.86 ± 2.31	10.20 ± 2.31	0.45
Rod-Rod Break Time (minutes)	17.51 ± 1.43	18.48 ± 2.68	0.26
Final Rod Threshold (log cd/m^2)	-4.57 ± 0.28	-4.57 ± 0.28	0.98

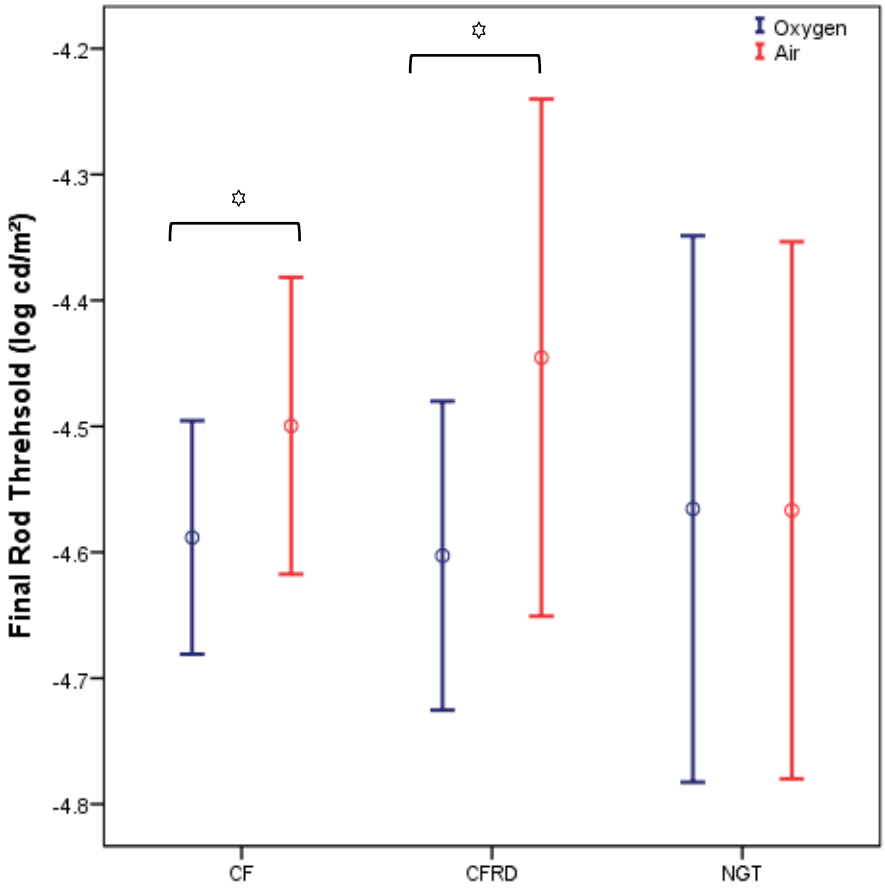

Figure 5.5 The effect of oxygen inhalation on final rod threshold in CF (n = 23), CFRD (n = 11), and NGT (n = 9) subjects (paired-samples (1-tailed) t-test; p = 0.03, p = 0.04 and paired-samples (2-tailed) t-test, p = 0.98 respectively). Star indicates significance.

5.3.3.5 IGT CF subjects

Rod-rod break occurred significantly later during the inhalation of oxygen compared to air (17.67 ± 0.34 minutes and 16.81 ± 0.20 minutes, respectively, paired-samples (2-tailed) t-test, p = 0.04). There was no significant difference in any of the other DA parameters upon inhalation of oxygen (Table 5.12). However, final rod threshold decreased from -4.50 ± 0.08 log cd/m^2 to -4.60 ± 0.13 log cd/m^2 upon inhalation of oxygen, with the difference nearly reaching significance (paired-samples (1-tailed) t-test, p = 0.06). As there were only three IGT subjects, these results must be interpreted with caution. When considered separately, two of the IGT subjects showed no decrease in threshold upon inhalation of oxygen, whilst the other one showed a reasonable decrease in threshold (Figure 5.4 B).

Table 5.12 The effect of oxygen inhalation on DA in IGT CF subjects (n = 3)

Parameter	Air (Mean ± SD)	Oxygen (Mean ± SD)	Paired t-test
Cone Constant (minutes)	2.67 ± 1.49	2.13 ± 0.21	0.63
Final Cone Threshold (log cd/m^2)	-2.43 ± 0.45	-2.32 ± 0.24	0.77
Rod- Cone Break Time (minutes)	9.72 ± 3.24	9.75 ± 1.53	0.99
Rod-Rod Break Time (minutes)	16.81 ± 0.20	17.67 ± 0.34	**0.04**
Final Rod Threshold (log cd/m^2)	-4.50 ± 0.08	-4.60 ± 0.13	0.06*

Key: bold and shaded cells indicate significance; * Indicates 1-tailed t-test when the hypothesis indicates a relationship in a specified direction

5.3.3.6 Correlation of DA parameter with HbA1c

Glycosylated haemoglobin (HbA1c) provides a guide to the average blood glucose reading over a 8-12 week period. There was no significant correlation between HbA1c for any DA parameter measured both during air and oxygen inhalation (Table 5.13). However, a medium, non-significant negative correlation was apparent between HbA1c and the cone constant during inhalation of oxygen (Pearson's r = -0.34; p = 0.12), suggesting that increasing HbA1c is associated with increased speed of cone recovery. This correlation reduced upon inhalation

of air (Pearson's r = -0.13; p = 0.55). Final cone threshold showed moderate positive correlation with HbA1c during the inhalation of oxygen (Pearson's r = 0.33; p = 0.13), suggesting that increasing HbA1c is associated with a higher final cone threshold. This correlation once again reduced upon inhalation of air (Pearson's r = 0.21; p = 0.33). Final rod threshold similarly showed a moderate positive correlation during the inhalation of both oxygen (Pearson's r = 0.27; p = 0.21) and air (Pearson's r = 0.23; p = 0.30), again suggesting that increasing HbA1c is associated with higher final rod threshold.

Table 5.13 Correlation of HbA1c with DA parameters (n = 23)

Parameter		Pearson Correlation	Independent t-test
Cone Constant (minutes)	Oxygen	-0.34	0.12
	Air	-0.13	0.55
Final Cone Threshold (log cd/m^2)	Oxygen	0.33	0.13
	Air	0.21	0.33
Rod- Cone Break Time (minutes)	Oxygen	-0.10	0.67
	Air	-0.03	0.90
Rod-Rod Break Time (minutes)	Oxygen	0.04	0.85
	Air	-0.08	0.71
Final Rod Threshold (log cd/m^2)	Oxygen	0.27	0.21
	Air	0.23	0.30

Key: HbA1c, glycosylated haemoglobin

5.3.4 *The effect of disease status on DA*

5.3.4.1 CF vs Controls

CF had no significant effect on any of the DA parameters during both air and oxygen inhalation except for the rod-cone break, which occurred significantly earlier in CF subjects compared to controls (independent-samples (2-tailed) t-test; p = 0.01 and p = 0.04, respectively). The difference in final rod threshold during inhalation of air approaches significance (independent-samples (1-tailed) t-test; p = 0.07), with the control threshold lower than that of the CF subjects (-4.60 and -4.50 log cd/m^2, respectively). This difference becomes much less significant upon oxygen inhalation. There is a clear trend towards less variability (as shown by smaller SD) of data during inhalation of oxygen compared to air in

CF subjects for all DA parameters examined. It is likely that the larger variability of the CF data during the inhalation of air causes several DA parameters to not reach significance. Similarly, the difference between DA parameters is much less significant during the inhalation of oxygen compared to air for the CF group. (Table 5.14 and Figures 5.6-5.7).

Table 5.14 The effect of CF on dark adaptation during inhalation of air and oxygen (n=23 CF and n = 23 controls)

Parameter		**Controls (Mean ± SD)**	**CF (Mean ± SD)**	**Independent t-test**
Cone Constant (minutes)	Oxygen	1.68 ± 0.50	1.41 ± 0.47	0.07
	Air	1.85 ± 0.45	1.48 ± 0.74	0.05
Final Cone Threshold (log cd/m^2)	Oxygen	-2.12 ± 0.90	-2.23 ± 0.15	0.29
	Air	-2.34 ± 0.16	-2.22 ± 0.26	0.06
Rod-Cone Break Time (minutes)	Oxygen	10.53 ± 1.21	9.45 ± 2.01	**0.04**
	Air	11.17 ± 1.12	9.71 ± 2.42	**0.01**
Rod-Rod Break Time (minutes)	Oxygen	17.44 ± 1.24	17.22 ± 1.49	0.60
	Air	17.28 ± 1.41	16.69 ± 2.90	0.39
Final Rod Threshold (log cd/m^2)	Oxygen	-4.64 ± 0.19	-4.59 ± 0.21	0.37
	Air	-4.60 ± 0.15	-4.50 ± 0.27	0.07*

Key: bold and shaded cells indicate significance; * Indicates 1-tailed t-test when the hypothesis indicates a relationship in a specified direction

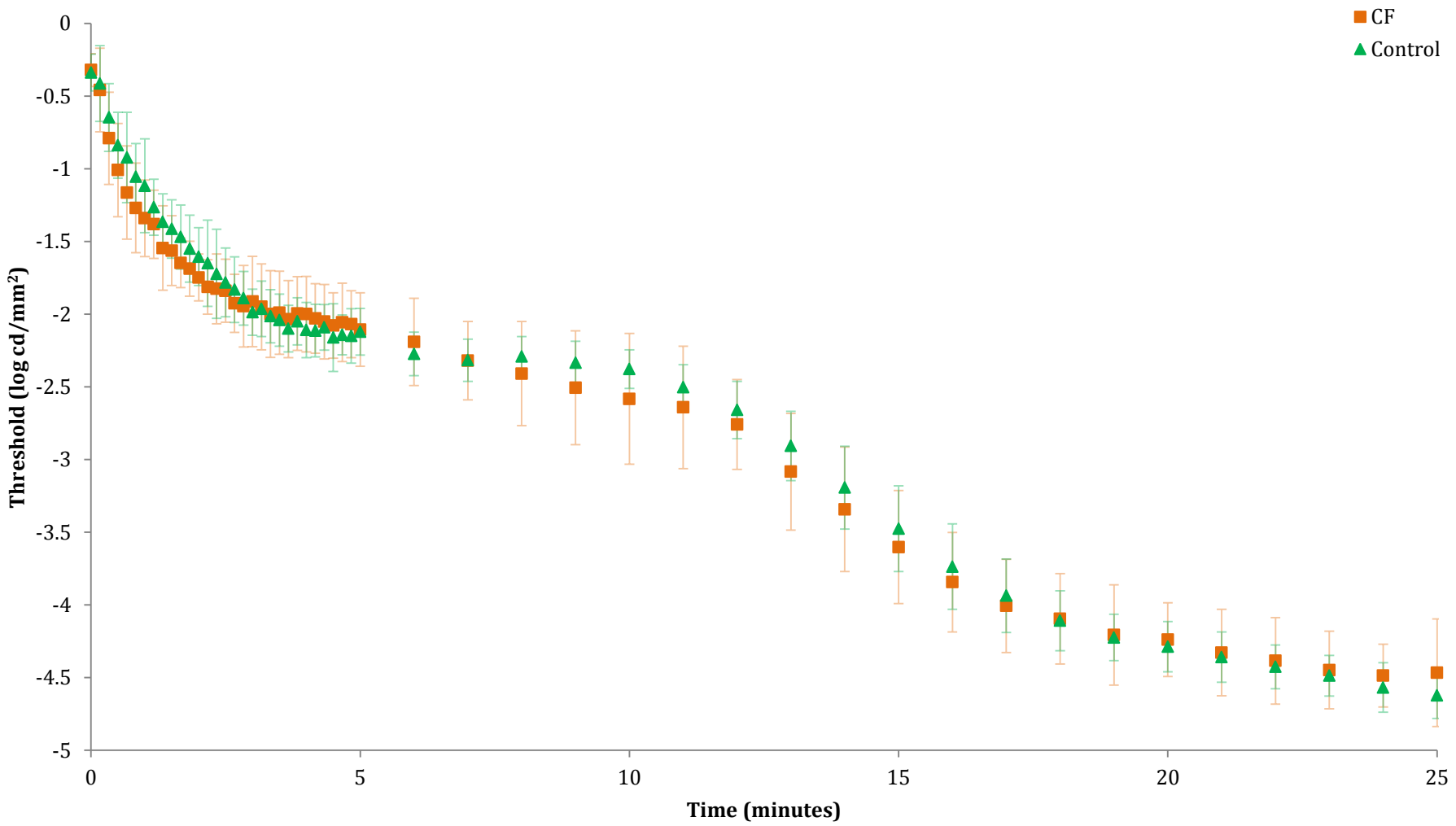

Figure 5.6 A graph showing the mean thresholds for CF and control subjects during the inhalation of air with error bars showing the standard deviation (n = 23 CF; n = 23 controls).

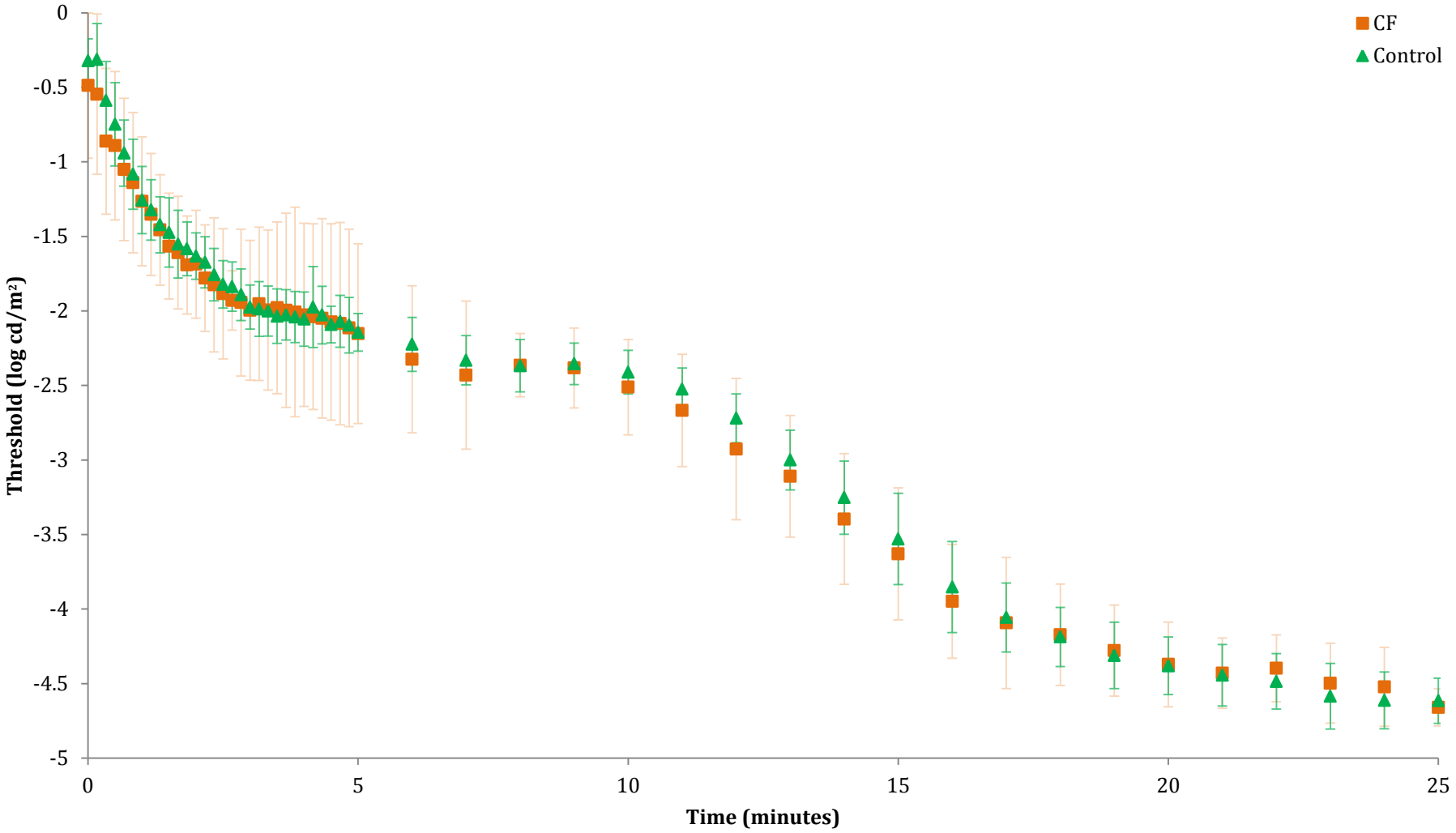

Figure 5.7 A graph showing the mean thresholds for CF and control subjects during the inhalation of oxygen with error bars showing the standard deviation (n = 23 CF; n = 23 controls).

5.3.4.2 CFRD vs controls

The cone constant was significantly lower in CFRD subjects compared to controls during both oxygen (1.19 ± 0.40 minutes and 1.69 ± 0.51 minutes, respectively; independent-samples (2-tailed) t-test, p = 0.02) and air inhalation (1.19 ± 0.36 minutes and 1.89 ± 0.47 minutes, respectively; independent-samples (2-tailed) t-test, p = 0.00), indicating a quicker cone recovery in CFRD subjects. Final cone threshold was significantly higher in CFRD subjects compared to controls during inhalation of both oxygen (-2.16 ± 0.11 log cd/m^2 and -2.30 ± 0.17 log cd/m^2, respectively; independent-samples (2-tailed) t-test, p = 0.04) and air (-2.09 ± 0.22 log cd/m^2 and -2.39 ± 0.12 log cd/m^2, respectively; independent-samples (2-tailed) t-test, p < 0.005). The rod-cone break occurred significantly earlier in CFRD subjects compared to controls during inhalation of both oxygen (8.68 ± 1.70 minutes and 10.33 ±1.35 minutes, respectively; independent-samples (2-tailed) t-test, p = 0.02) and air (8.77 ± 2.10 minutes and 11.34 ± 0.96 minutes, respectively; independent-samples (2-tailed) t-test, p < 0.005). Considering the rod-rod break, this occurred later in the controls compared to the CFRD subjects. Whilst the difference approached significance during inhalation of air it did not achieve statistical significance during either condition (Independent-samples (2-tailed) t-test, p = 0.26 and p = 0.06 for oxygen and air, respectively). Final rod threshold during the inhalation of air was significantly elevated in CFRD subjects compared to controls (4.45± 0.31 and -4.64 ± 0.16, respectively; independent-samples (1-tailed) t-test, p = 0.04), with this difference ameliorated upon the inhalation of 100% oxygen (-4.60 ± 0.18 log cd/m^2 and -4.65 ± 0.22 log cd/m^2, respectively; independent-samples (2-tailed) t-test, p = 0.61). This is summarised in Table 5.15 and Figures 5.8 – 5.14.

Table 5.15 The effect of diabetic status on DA in CF; CFRD vs Controls (n = 11 CFRD; n = 11 controls)

Parameter		Controls (Mean ± SD)	CFRD (Mean ± SD)	Independent t-test
Cone Constant (minutes)	Oxygen	1.69 ± 0.51	1.19 ± 0.40	**0.02**
	Air	1.89 ± 0.47	1.14 ± 0.34	**0.00**
Final Cone Threshold (log cd/m^2)	Oxygen	-2.30 ± 0.17	-2.16 ± 0.12	**0.04**
	Air	-2.39 ± 0.12	-2.09 ± 0.22	**0.00**
Rod- Cone Break Time (minutes)	Oxygen	10.33 ± 1.35	8.68 ± 1.70	**0.02**
	Air	11.34 ± 0.96	8.94 ± 2.14	**0.00**
Rod-Rod Break Time (minutes)	Oxygen	17.68 ± 1.57	16.84 ± 1.74	0.26
	Air	17.13 ± 1.76	15.56 ± 2.55	0.06
Final Rod Threshold (log cd/m^2)	Oxygen	-4.65 ± 0.22	-4.60 ± 0.18	0.61
	Air	-4.64 ± 0.16	-4.45 ± 0.31	**0.04***

Key: bold and shaded cells indicate significance; * Indicates 1-tailed t-test when the hypothesis indicates a relationship in a specified direction

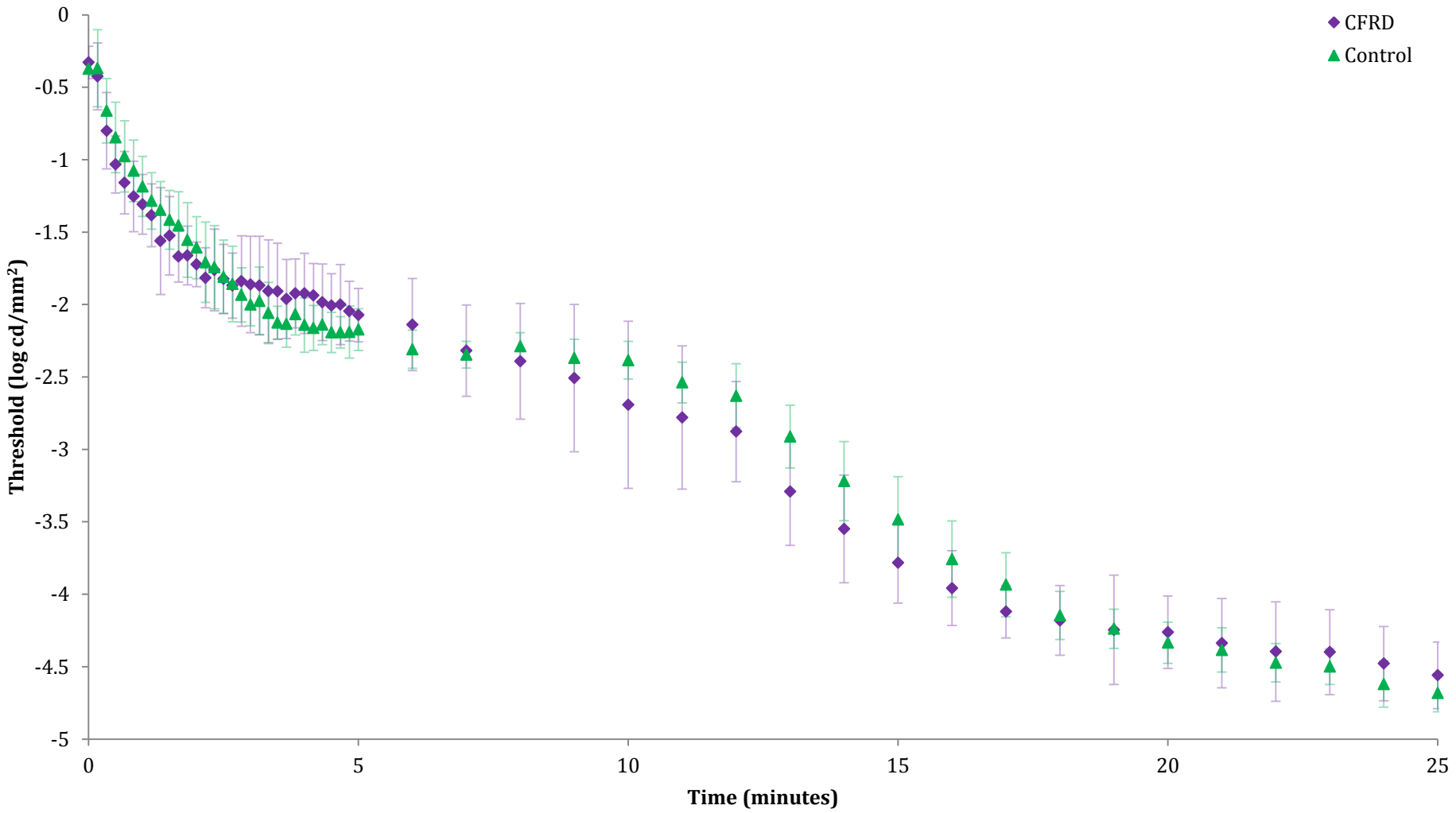

Figure 5.8 A graph showing the mean thresholds for CFRD and control subjects during the inhalation of air with error bars showing the standard deviation (n = 11 CFRD; n = 11 controls).

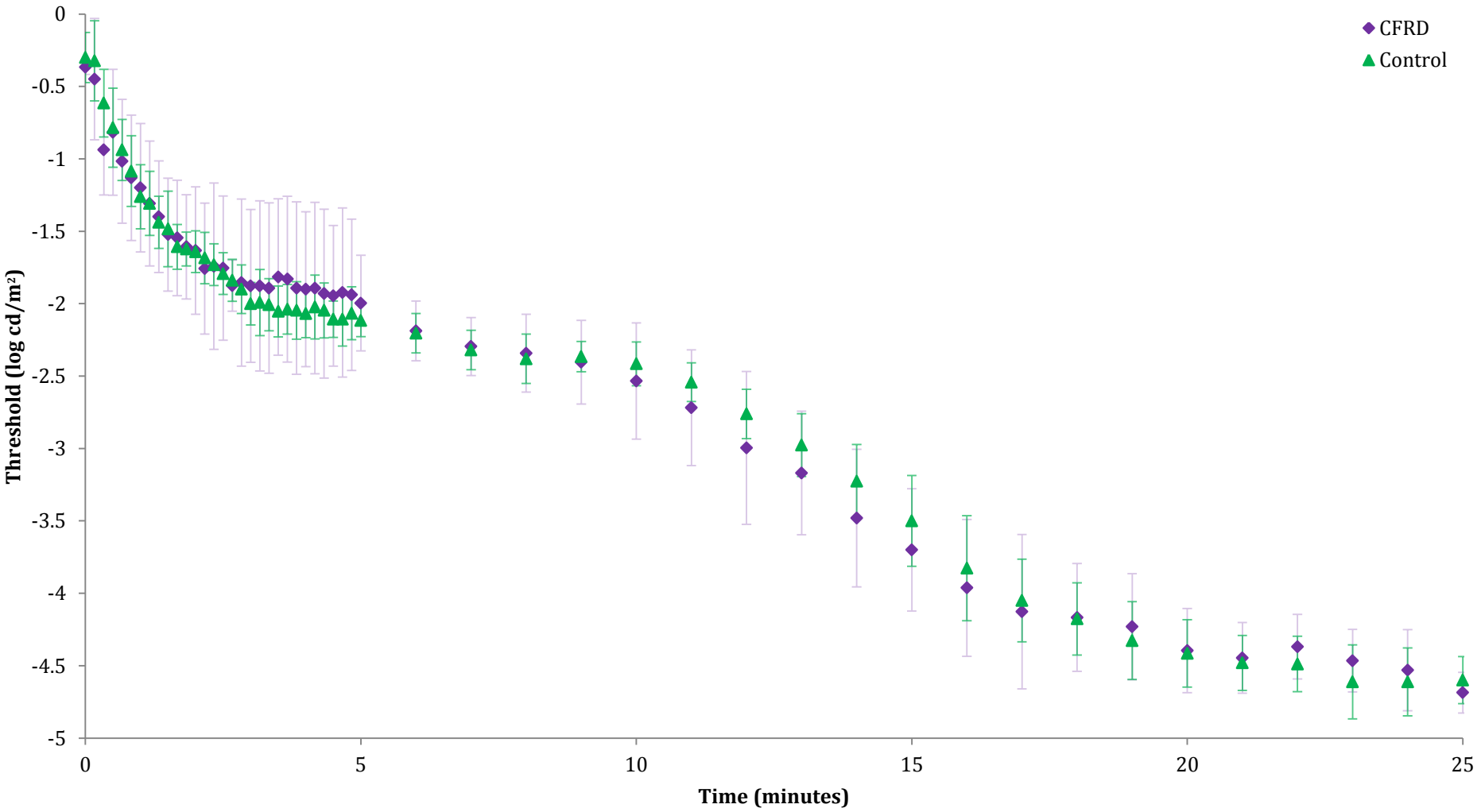

Figure 5.9 A graph showing the mean thresholds for CFRD and control subjects during the inhalation of oxygen with error bars showing the standard deviation (n = 11 CFRD; n = 11 controls).

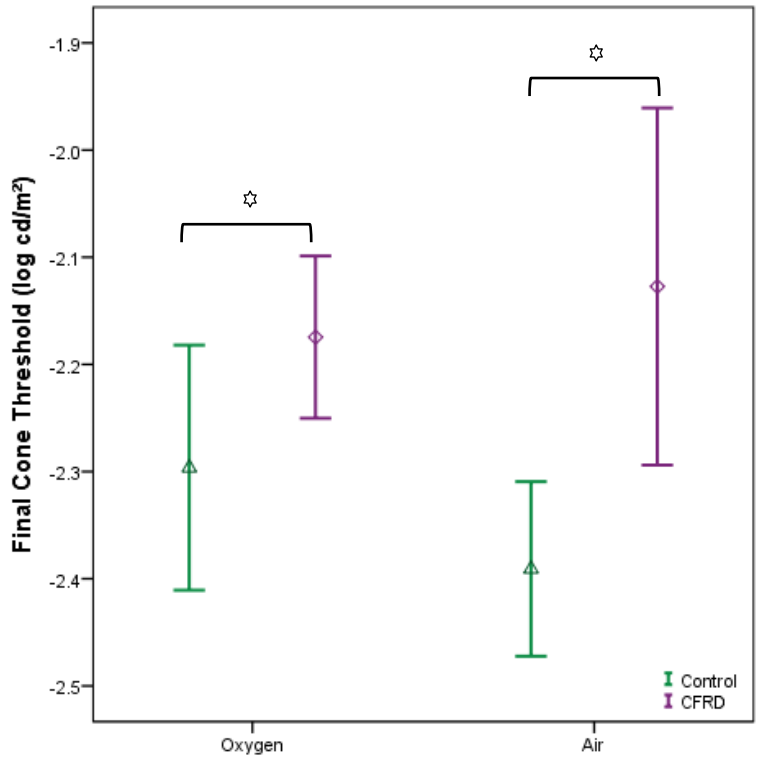

Figure 5.10 The effect of diabetic status on final cone threshold during inhalation of oxygen ($p = 0.02$) and air ($p < 0.005$) ($n = 11$ CFRD; $n = 11$ controls). Error bars indicate the 95% confidence interval. Star indicates significance.

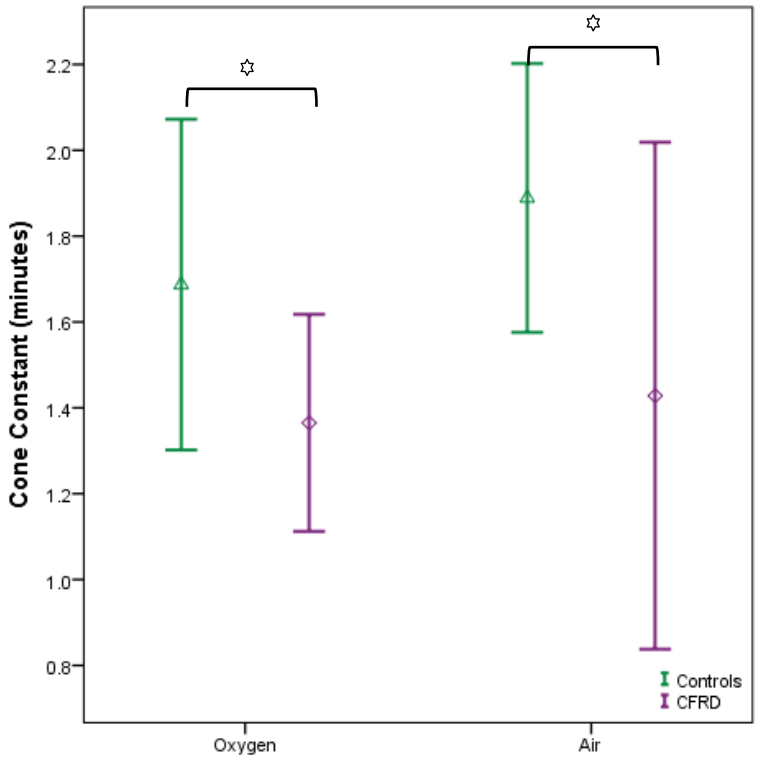

Figure 5.11 The effect of diabetic status on cone constant during inhalation of oxygen ($p = 0.04$) and air ($p < 0.005$) ($n = 11$ CFRD; $n = 11$ controls). Star indicates significance.

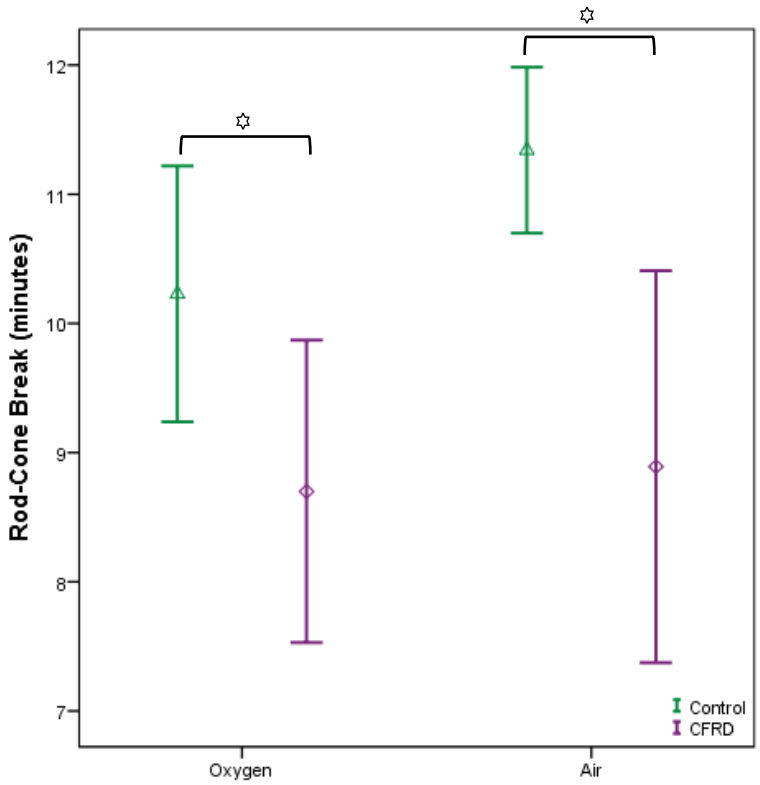

Figure 5.12 The effect of diabetic status on rod-cone break during inhalation of oxygen (p = 0.02) and air (p = 0.00) (n = 11 CFRD; n = 11 controls). Star indicates significance.

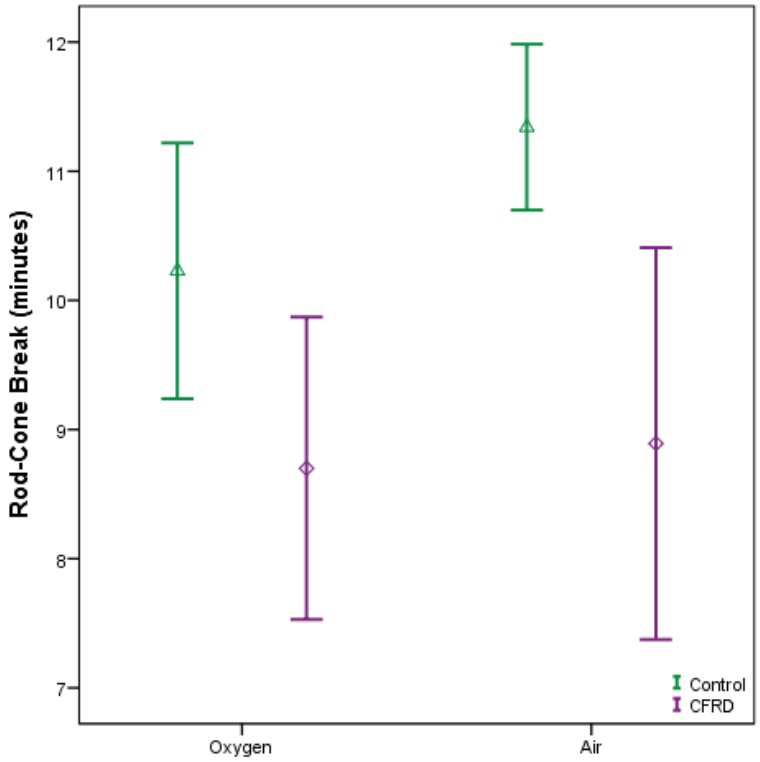

.

Figure 5.13 The effect of diabetic status on rod-rod break during inhalation of oxygen (p = 0.26) and air (p = 0.06) (n = 11 CFRD; n = 11 controls).

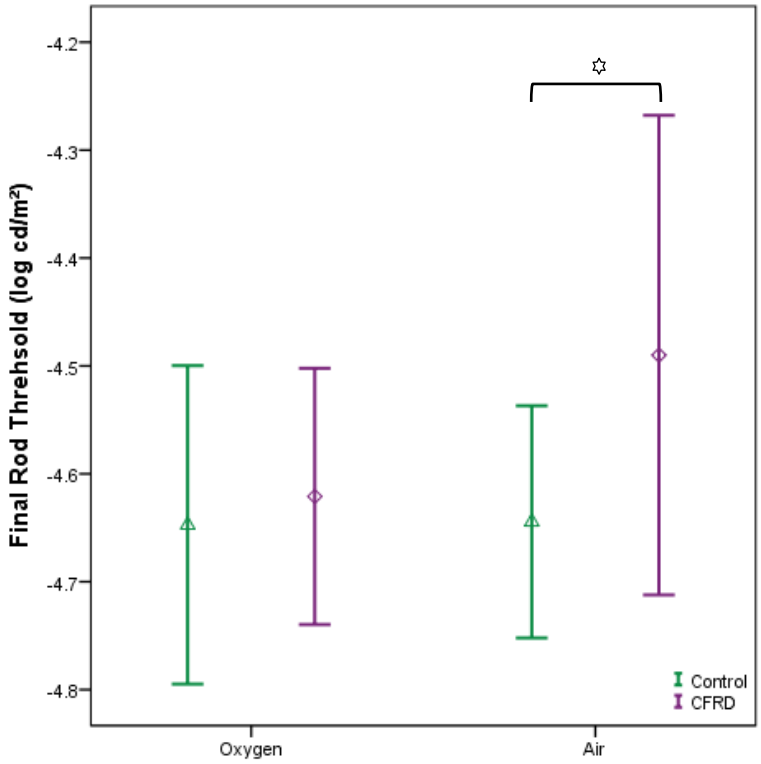

Figure 5.14 The effect of diabetic status on final rod threshold during inhalation of oxygen (p = 0.61) and air (p = 0.04) (n = 11 CFRD; n = 11 controls). Star indicates significance.

5.3.4.2.1 CFRD with diabetic retinopathy

One CFRD subject showed signs of diabetic retinopathy on fundus photography. This subject also showed the greatest reduction in final rod threshold upon inhalation of 100% oxygen, with a decrease in threshold of 0.78 log cd/m^2 from -3.67 log cd/m^2 to -4.45 log cd/m^2 (Figure 5.15) This difference is much larger than 0.15 log cd/m^2, which is the mean change for the CFRD subjects as a whole. Interestingly, whilst this subject was the only one to display signs of diabetic retinopathy, the recorded HbA1c (54 mmol/mol) was just outside the normal range (26-48 mmol/mol) and was certainly not the highest value recorded across all subjects (range 28 – 111 mmol/mol).

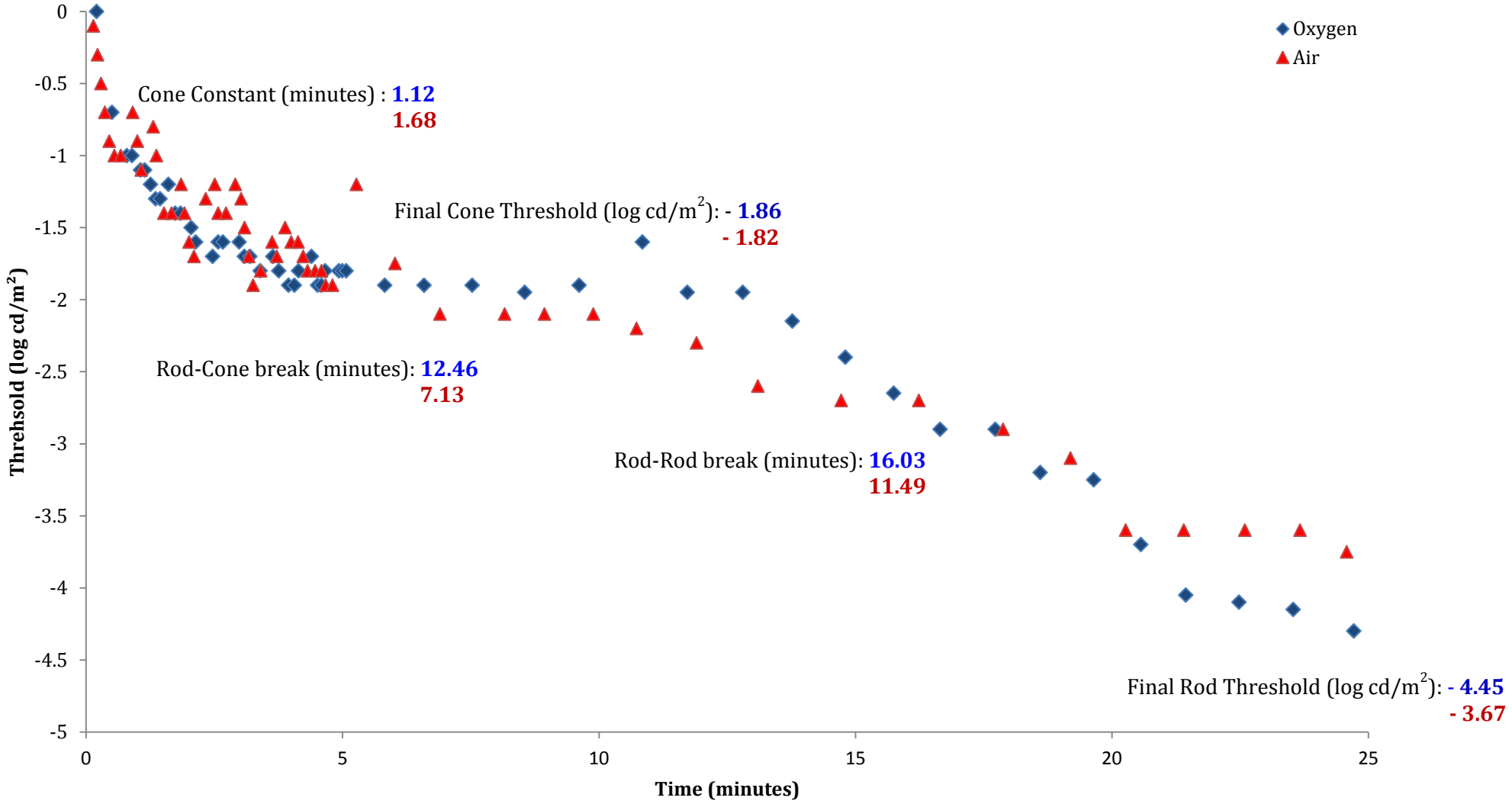

Figure 5.15 A graph showing the dark adaptation curves during inhalation of oxygen and air for a CFRD subject with diabetic retinopathy. DA parameters are shown for both oxygen (blue) and air (red).

5.3.4.3 NGT vs controls

There was no significant difference in any of the parameters between NGT subjects and controls both during inhalation of air and oxygen (Table 5.16).

Table 5.16 The effect of diabetic status on DA; NGT vs Controls (n = 9 NGT; n = 9 controls)

Parameter		Controls (Mean ± SD)	NGT (Mean ± SD)	Independent t-test
Cone Constant (minutes)	Oxygen	1.62 ± 0.54	1.42 ± 0.36	0.37
	Air	1.79 ± 0.49	1.44 ± 0.36	0.10
Final Cone Threshold (log cd/m^2)	Oxygen	-2.28 ± 0.16	-2.29 ± 0.14	0.94
	Air	-2.32 ± 0.15	-2.31 ± 0.17	0.87
Rod- Cone Break Time (minutes)	Oxygen	10.74 ± 1.23	10.20 ± 2.31	0.55
	Air	11.08 ± 1.43	10.86 ± 2.31	0.82
Rod-Rod Break Time (minutes)	Oxygen	17.04 ± 0.73	17.51 ± 1.43	0.39
	Air	17.57 ± 0.86	18.48 ± 2.68	0.36
Final Rod Threshold (log cd/m^2)	Oxygen	-4.62 ± 0.18	-4.57 ± 0.28	0.61
	Air	-4.56 ± 0.15	-4.57 ± 0.28	0.93

Key: NGT, normal glucose tolerance

5.3.4.4 IGT vs controls

There was no significant difference in any of the parameters between IGT subjects and controls both during inhalation of air and oxygen, although the difference in final rod threshold between IGT subjects and controls was larger during the inhalation of air compared to oxygen, with the significance values reflecting this difference (0.08 log cd/m^2 difference vs 0.03 log cd/m^2, respectively) (Table 5.17). However, as there were only three IGT subjects, these results must be viewed with caution.

Table 5.17 The effect of diabetic status on DA; IGT vs Controls (n = 3 NGT; n = 3 controls)

Parameter		Controls (Mean ± SD)	IGT (Mean ± SD)	Independent t-test
Cone Constant (minutes)	Oxygen	1.88 ± 0.41	2.13 ± 0.21	0.40
	Air	1.82 ± 0.33	2.67 ± 1.49	0.39
Final Cone Threshold (log cd/m^2)	Oxygen	-2.20 ± 0.28	-2.32 ± 0.24	0.62
	Air	-2.23 ± 0.28	-2.43 ± 0.45	0.56
Rod- Cone Break Time (minutes)	Oxygen	10.76 ± 0.62	9.75 ± 1.53	0.35
	Air	11.49 ± 1.14	9.72 ± 3.24	0.42
Rod-Rod Break Time (minutes)	Oxygen	17.80 ± 1.25	17.67 ± 0.34	0.87
	Air	16.95 ± 1.67	16.81 ± 0.20	0.88
Final Rod Threshold (log cd/m^2)	Oxygen	-4.63 ± 0.09	-4.60 ± 0.13	0.76
	Air	-4.58 ± 0.14	-4.50 ± 0.08	0.20*

Key: IGT, impaired glucose tolerance; * Indicates 1-tailed t-test when the hypothesis indicates a relationship in a specified direction

5.3.4.5 NGT vs CFRD

The final cone threshold was significantly lower in NGT compared to CFRD subjects during oxygen inhalation (-2.29 ± 0.14 and -2.16 ± 0.11 log cd/m^2, respectively; independent-samples (2-tailed) t-test, p = 0.04) and air inhalation (-2.31 ± 0.17 and -2.09 ± 0.22 respectively, independent-samples (2-tailed) t-test, p = 0.3). Rod-cone break occurred significantly later in NGT compared to CFRD subjects during inhalation of air (10.86 ± 2.31 and 8.77 ± 2.10 minutes, respectively; independent-samples (2-tailed) t-test, p = 0.05)). Rod-rod break occurred significantly later in NGT compared to CFRD subjects during the inhalation of air (18.48 ± 2.68 and 15.19 ± 2.71 minutes, respectively; independent-samples (2-tailed) t-test, p = 0.1). No other significant differences were found between NGT and CFRD subjects for the other parameters (Table 5.18).

Table 5.18 The effect of diabetic status on DA; NGT vs CFRD (n = 9 NGT; n = 11 CFRD)

Parameter		CFRD (Mean ± SD)	NGT (Mean ± SD)	Independent t-test
Cone Constant (minutes)	Oxygen	1.19 ± 0.40	1.42 ± 0.36	0.22
	Air	1.19 ± 0.36	1.44 ± 0.36	0.14
Final Cone Threshold (log cd/m^2)	Oxygen	-2.16 ± 0.11	-2.29 ± 0.14	**0.04**
	Air	-2.09 ± 0.22	-2.31 ± 0.17	**0.03**
Rod- Cone Break Time (minutes)	Oxygen	8.68 ± 1.70	10.20 ± 2.31	0.12
	Air	8.77 ± 2.10	10.86 ± 2.31	**0.05**
Rod-Rod Break Time (minutes)	Oxygen	16.84 ± 1.74	17.51 ± 1.43	0.38
	Air	15.19 ± 2.71	18.48 ± 2.68	**0.01**
Final Rod Threshold (log cd/m^2)	Oxygen	-4.60 ± 0.18	-4.57 ± 0.28	0.12
	Air	-4.45 ± 0.31	-4.57 ± 0.28	0.19*

Key: CFRD, cystic fibrosis related diabetes; NGT, normal glucose tolerance; bold and shaded cells indicate significance; * Indicates 1-tailed t-test when the hypothesis indicates a relationship in a specified direction

5.3.5 *The effect of vitamin A status on DA*

Vitamin A status had no significant effect on any of the DA parameters when compared to controls (ANOVA > 0.05) (Table 5.19). However, VAD subjects showed a trend towards an elevated final rod threshold upon inhalation of air compared to both controls and vitamin A sufficient subjects (-4.35± 0.47, -4.60 ± 0.15 and -4.53 ± 0.22 log cd/m^2 respectively, ANOVA p = 0.47) (Figure 5.16). It is likely that this difference did not reach significance due to small numbers of VAD subjects (n = 4). However, it is unlikely that the final rod threshold is impaired in the VAD subjects due to low vitamin A serum levels as recovery to normal levels is shown upon oxygen inhalation, indicating that hypoxia was the causative factor. Table 5.6 and Figure 5.4B show that two of the VAD subjects also had CFRD, and demonstrated two of the largest improvements in threshold upon oxygen inhalation of all subjects studied, therefore skewing the VAD data significantly.

Table 5.19 The effect of vitamin A status on DA (n = 23 controls; n = 19 vitamin A sufficient; n = 4 vitamin A deficient).

Parameter		Controls (Mean ± SD)	CF		ANOVA
			Vitamin A Sufficient	Vitamin A deficient	
Cone Constant (minutes)	Oxygen	1.68 ± 0.50	1.47 ± 0.39	1.04 ± 0.81	0.07
	Air	1.85 ± 0.45	1.51 ± 0.80	1.34 ± 0.34	0.13
Final Cone Threshold (log cd/m^2)	Oxygen	-2.12 ± 0.90	-2.26 ± 0.14	-2.11±0.19	0.77
	Air	-2.34 ± 0.16	-2.25 ± 2.36	-2.10 ± 0.19	0.08
Rod- Cone Break Time (minutes)	Oxygen	10.53 ± 1.21	9.66 ± 1.80	8.12 ± 3.16	0.32
	Air	11.17 ± 1.12	9.93 ± 2.36	8.37 ± 2.82	0.14
Rod-Rod Break Time (minutes)	Oxygen	17.44 ± 1.24	17.48 ±1.27	14.44 ± 1.25	0.07
	Air	17.28 ± 1.41	17.00 ±2.65	15.23 ± 3.99	0.25
Final Rod Threshold (log cd/m^2)	Oxygen	-4.64 ± 0.19	-4.56 ±0.21	-4.72 ±0.18	0.23
	Air	-4.60 ± 0.15	-4.53 ±0.22	-4.35 ± 0.47	0.47

Key: ANOVA, analysis of variance

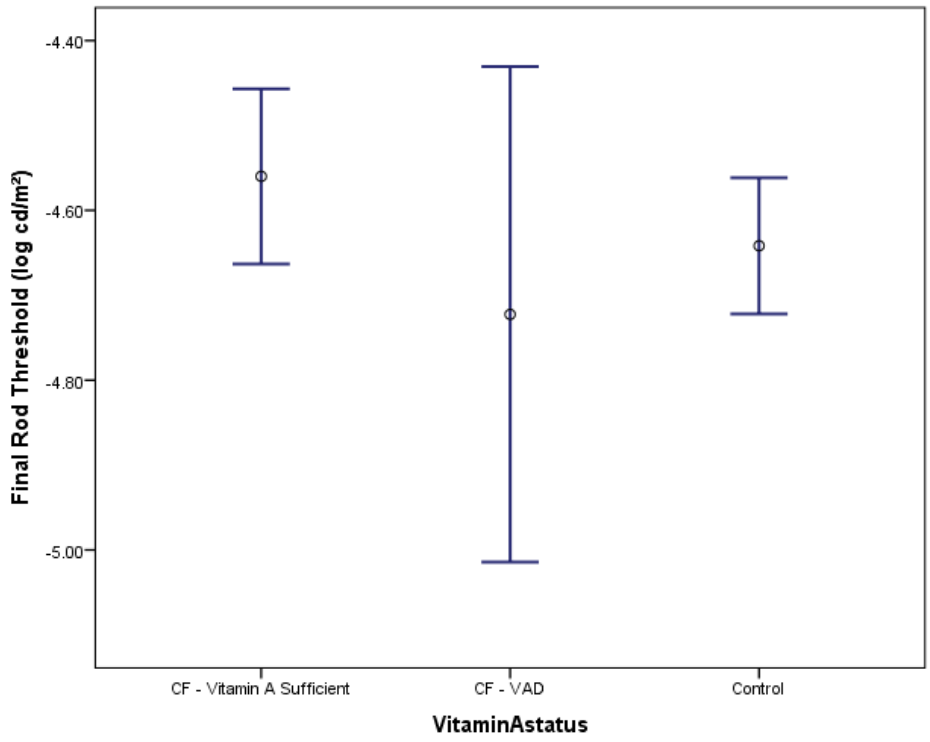

Figure 5.16 The effect of vitamin A status on final rod threshold (n = 23 controls; n = 19 vitamin A sufficient; n = 4 vitamin A deficient).

5.3.6 *The effect of genotype on DA*

CF genotype had no significant effect on any of the DA parameters when compared to controls (ANOVA > 0.05) (Table 5.20).

Table 5.20 The effect of CF genotype on DA (n = 23 controls; n = 7 heterozygous; n = 14 homozygous)

Parameter		Controls (Mean ± SD)	CF		ANOVA
			ΔF508 Heterozygous (Mean ± SD)	ΔF508 Homozygous (Mean ± SD)	
Cone Constant (minutes)	Oxygen	1.68 ± 0.50	1.39 ± 0.37	1.50 ± 0.51	0.30
	Air	1.85 ± 0.45	1.34 ± 0.55	1.56 ± 0.87	0.14
Final Cone Threshold (log cd/m^2)	Oxygen	-2.12 ± 0.90	-2.29 ± 0.07	-2.24 ± 0.16	0.78
	Air	-2.34 ± 0.16	-2.24 ± 0.32	-2.22 ± 0.25	0.24
Rod- Cone Break Time (minutes)	Oxygen	10.53 ± 1.21	10.04 ± 2.59	9.48 ± 1.50	0.17
	Air	11.17 ± 1.12	10.46 ± 2.63	9.31 ± 2.47	0.06*
Rod-Rod Break Time (minutes)	Oxygen	17.44 ± 1.24	17.32 ± 1.30	17.42 ± 1.59	0.98
	Air	17.28 ± 1.41	16.41 ± 3.81	16.61 ± 2.47	0.56
Final Rod Threshold (log cd/m^2)	Oxygen	-4.64 ± 0.19	-4.52 ± 0.25	-4.61 ± 0.20	0.37
	Air	-4.60 ± 0.15	-4.50 ± 0.28	-4.49 ± 0.29	0.30

Key: ANOVA, analysis of variance; * **indicates** Brown-Forsythe test (assumption of homogeneity of variance for ANOVA was violated)

5.3.7 *Correlation with CF lung disease*

Lung function, as expressed by FEV_1 (Forced Expiratory Volume in 1 second) and Northern Score (a score used to describe lung disease on a scale of 0-20, with 0 being no disease) were used to investigate the effect of lung disease severity on DA. FEV_1 had a small, non-significant negative correlation with final rod threshold during the inhalation of air (Figure 5.17; Pearson's r = -0.18; p = 0.42), and a moderate correlation during the inhalation of oxygen, with the relationship tending towards significance (Figure 5.18; Pearson's r = -0.38; p = 0.08). A similar trend was seen with the Northern score, with a small positive correlation seen with the final rod threshold on inhalation of air (Figure 5.19; Pearson's r = 0.19; p = 0.38), and a moderate correlation on inhalation of oxygen (Figure 5.20; Pearson's r = 0.32; p = 0.14).

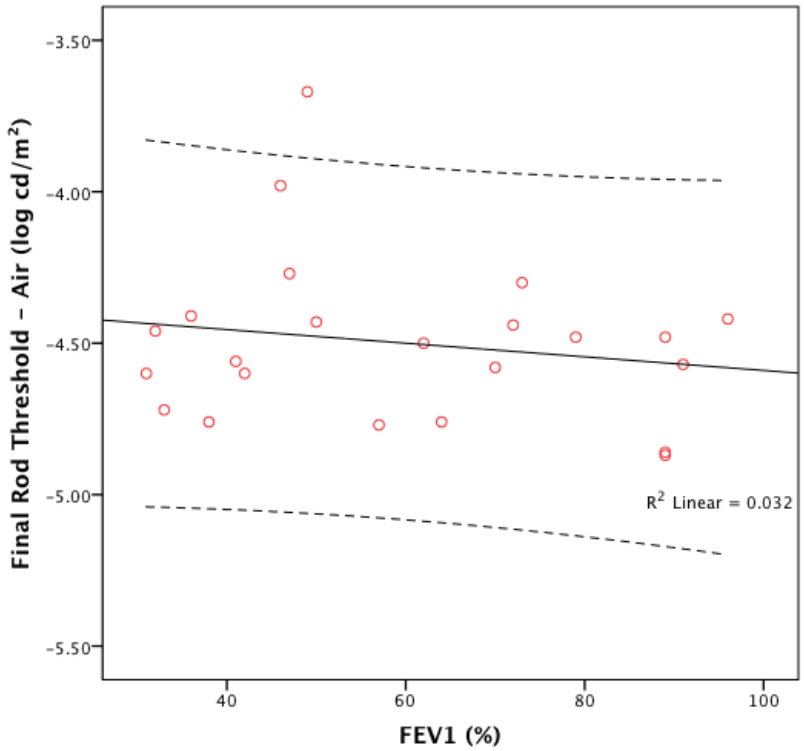

Figure 5.17 The correlation of lung function as expressed by FEV_1 with final rod threshold during inhalation of air (Pearson's r = -0.18; p = 0.42). Dashed lines show 95% confidence intervals.

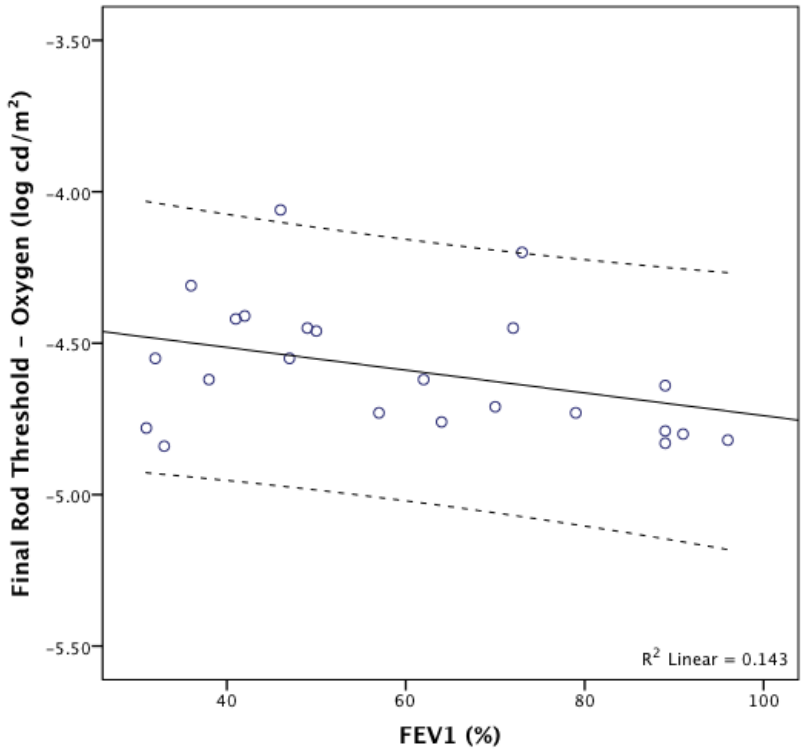

Figure 5.18 The correlation of lung function as expressed by FEV_1 with final rod threshold during inhalation of oxygen (Pearson's r = -0.38; p = 0.08). Dashed lines show 95% confidence intervals.

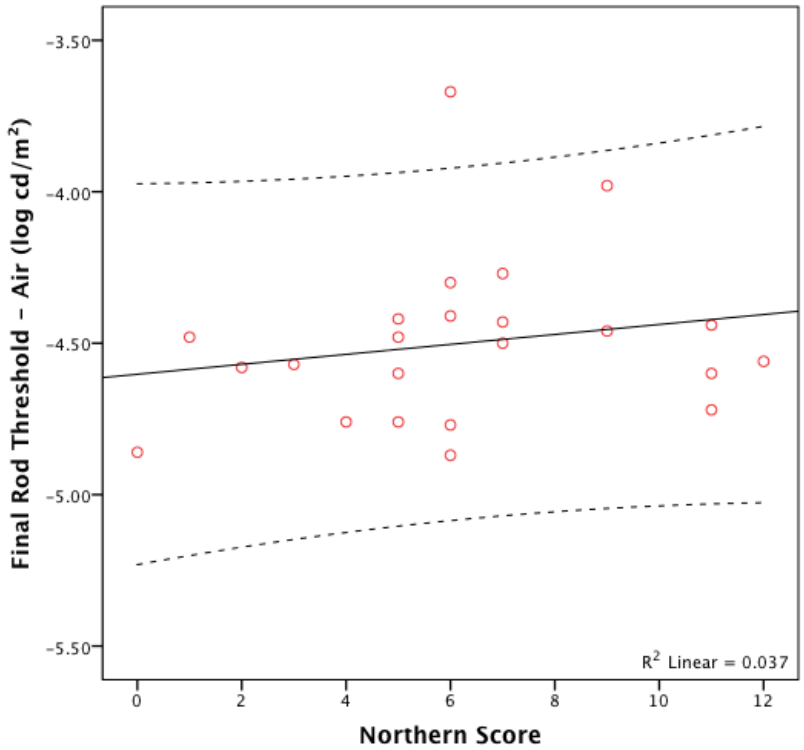

Figure 5.19 The correlation of Northern Score with final rod threshold during inhalation of air (Pearson's r = 0.19; p = 0.38). Dashed lines indicate 95% confidence intervals.

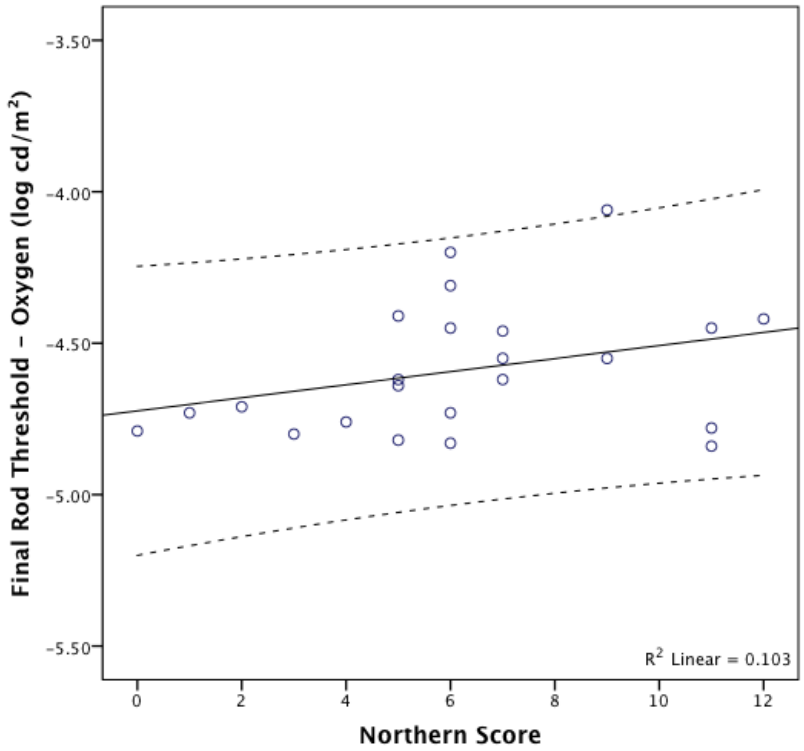

Figure 5.20 The correlation of Northern Score with final rod threshold during inhalation of oxygen (Pearson's r = 0.32; p = 0.14). Dashed lines indicate 95% confidence intervals.

5.3.8 *Summary of findings*

- CF subjects had significantly lower SaO_2 duration inhalation of air compared to healthy controls. Inhalation of oxygen caused a significant increase in SaO_2 in CF and control patients within two minutes of commencing inhalation, resulting in no significant difference in SaO_2 between groups.

- Control subjects showed no improvement in final rod threshold upon the inhalation of oxygen

- Final rod threshold was elevated in CFRD subjects compared to controls during the inhalation of air, but recovered to normal levels upon the inhalation of oxygen. These results suggest abnormal DA in CFRD can be reversed upon oxygen inhalation.

- Final rod threshold during inhalation of both air and oxygen in NGT CF subjects was not significantly different to controls. No significant improvement in threshold was seen upon the inhalation of oxygen in these subjects.

- Final rod threshold was elevated in IGT subjects compared to controls during inhalation of air, though this difference failed to reach significance, likely due to the small number of subjects included in this group. Similar to CFRD subjects, IGT subjects showed an improvement in threshold upon inhalation of oxygen, though this again just failed to reach significance.

- Final rod threshold showed a small negative correlation with FEV1 and a moderate positive correlation with Northern score during the inhalation of oxygen, suggesting elevation of final rod threshold is associated with decreasing lung function.

5.4 Discussion

Air

CF is characterised by chronic airway inflammation and progressive airflow obstruction secondary to chronic hypersecretion of mucous (Bradley et al., 1999; van der Giessen et al., 2012). CF subjects have previously demonstrated reduced SaO_2 levels, with hypoxemia increasing as lung disease progresses (Tepper, Skatrud and Dempsey, 1983; Frangolias and Wilcox, 2001). Similarly, in this study SaO_2 was significantly lower in CF subjects compared to heathly controls during the inhalation of air, indicating low levels of hypoxia exist under normal conditions.

When comparing DA parameters during the inhalation of air between all CF subjects and controls, whilst rod-cone break time was seen to occur significantly earlier in CF, no other parameters, including final rod threshold, showed any significant difference, despite lower SaO_2 in CF. However, when grouped according to their diabetic status, differences between CFRD subjects and controls emerged. CFRD subjects showed significantly elevated final rod thresholds compared to controls during the inhalation of air. This finding is in line with previous studies on type 1 and 2 diabetic subjects (Henson and North, 1979; Arden et al., 1998; Kurtenbach et al., 2006). Similar elevations in threshold can also be seen during oxygen deprivation studies in healthy subjects (McFarland and Evans, 1939; McFarland and Forbes, 1940).

In addition to a significantly elevated final rod threshold, CFRD subjects also showed significantly faster cone recovery and significantly elevated final cone threshold compared to controls. These findings are in contrast to type 1 diabetic subjects in a study by Kurtenbach et al. (2006), who showed no significant differences in cone parameters compared to controls. Cone DA kinetics have shown a deceleration with increasing age within a healthy population, as demonstrated by a larger cone constant (Coile and Baker, 1992; Gaffney, Binns and Margrain, 2012). RPE and photoreceptor cell loss (Gao and Hollyfield, 1992; Curcio et al., 1993) and accumulation of lipofuscin in the RPE (Roth, Bindewald and Holz, 2004) have been reported to occur with increasing age. It is likely that these changes are responsible for impaired pigment regeneration with age, and therefore contribute to a slower cone dark adaptation recovery (Gaffney, 2012). Due to accelerated aging in CF, secondary to chronic respiratory infection and the subsequent increased levels of oxidative stress, CF subjects as a

whole were expected to show slower cone recovery times compared to age and gender matched controls. However, whilst significance was not reached, there was a clear trend towards quicker cone recovery in CF patients compared to controls during the inhalation of air, with this relationship becoming significant when considering CFRD subjects alone. It is therefore not clear why CF subjects tended to recover cone sensitivity quicker than controls. The maxwellian-view optical system was employed to deliver equilibrium bleaches to reduce the risk of subjects receiving different levels of bleach, which would directly affect recovery parameters. As control subjects were recruited from the School of Optometry and Vision Sciences and were often experienced observers, they may have fixated more steadily during bleaching, resulting in them receiving a greater percentage photopigment bleach. This may account for slower cone recovery in controls.

Similar to CFRD subjects, final rod threshold was elevated in IGT subjects compared to controls during inhalation of air, though this difference failed to reach significance, possibly due to the small number of subjects included in this group. Conversely, NGT subjects showed no significant differences in any parameters compared to controls during the inhalation of air. This leads to the suggestion that impaired DA in CF is secondary to CFRD and not a primary manifestation of CF caused by malfunction of CFTR at the RPE or caused by reduced SaO_2 under normal conditions. Subjects with chronic pulmonary insufficiency (and no diabetes) have similarly shown no impairment in their dark adapted threshold secondary to reduced SaO_2 (Thylefors, Piitulainen and Havelius, 2009). Further evidence that impaired DA is not a primary manifestation of CF is that genotype was seen to have no significant effect on any DA parameters, an outcome which is contrary to that of previous research (Evans, 2009). Considering this difference, previous analysis may have included confounding factors, such as vitamin A and diabetic status, which were markedly worse within the homozygous group. Lack of impairment of DA parameters in the NGT subjects suggest that slightly reduced SaO_2 in CF subjects does not negatively impact DA.

Oxygen

Inhalation of 100% oxygen caused a significant increase in SaO_2 in CF and controls within two minutes, bringing SaO_2 between the two groups to comparable levels. This increase in SaO_2 is a finding which is consistent with previous research in Type 1 diabetic subjects and controls (Anderson, 1968; Kurtenbach et al., 2006). It has previously been shown that maximal retinal oxygenation is reached within two minutes of oxygen inhalation (Anderson, 1968), despite

autoregulation promoting a vasoconstrictive response. Supplementary oxygen has been shown to increase oxygenation in all retinal layers in rats, as measured in-vivo with microelectrodes (Yu et al., 1999). It is reasonable to predict that inhalation of 100% oxygen will have caused a similar increase in retinal oxygenation in this experiment, though the study of Yu et al. (1999) could be repeated in CF knockout mice to prove they are truly behaving in the same way.

An increase in SaO_2 upon oxygen breathing had no significant effect on any parameters of DA in controls. Conversely, CFRD subjects showed a decrease in final rod threshold, bringing threshold to a level comparable to controls. Recovery of final rod threshold with inhalation of oxygen, observed for the first time in CFRD subjects, implies that retinal hypoxia is present in CFRD subjects, as previously seen in Type 1 diabetic subjects (Kurtenbach et al., 2006). Whilst CFRD is classed as distinctly separate from Type 1 and 2 diabetes, this finding demonstrates that similarities exist on a microvascular level.

Retinal oxygen tension during dark adaptation is known to approach zero in healthy subjects (Lange and Bainbridge, 2012) due to the high consumption of oxygen by the sodium channels of photoreceprots to maintain the dark current (Kurtenbach et al., 2006). With impaired oxygen delivery in diabetes, secondary to retinal vascular changes (Little, 1976) and decreased oxygen release from haemoglobin (Ditzel, 1972), this tension is believed to drop below zero, resulting in retinal hypoxia (Arden et al., 1998). It is this rod-driven retinal hypoxia which is believed to be the driving force for development of proliferative diabetic retinopathy (Arden, 2001; Yu and Cringle, 2001).

Whilst over half of the CFRD subjects showed a decrease in rod threshold upon inhalation of 100% oxygen, one subject showed no change and, paradoxically, three showed a small increase. It is possible that some of this variability is due to differences in duration of diabetes (Henson and North, 1979), but it may also be attributed to varying regions of ischaemic retina in each subject, a problem which is associated with only testing one area of the retina (Henson and North, 1979). Results may also be affected by varying glucose levels across subjects at the time of testing (Henson and North, 1979). Hyperglycaemia has previously been shown to decrease cone threshold (Kurtenbach et al., 2006), whilst rod threshold is known to increase during periods of hypoglycaemia (Mc, Halperin and Niven, 1946). It may therefore be of benefit to check blood glucose levels at the time of examination, so this effect can be accounted for. As expected, the increase in threshold with inhalation of oxygen was largest in

the subject who displayed diabetic retinopathy, suggesting retinal hypoxia is most severe in patients with more advanced disease (Kurtenbach et al., 2006).

In a previous study, cone threshold decreased in control subjects upon the inhalation of oxygen (Kurtenbach et al., 2006). Whilst a significant reduction was not evident in this study, the cone constant did demonstrate a non-significant reduction upon oxygen breathing in controls, indicating an increase in the speed of cone recovery. Conversely, rod threshold showed no change upon inhalation of 100% oxygen in healthy subjects, which is also in agreement with previous research (Anderson, 1968; Kurtenbach et al., 2006). It was suggested by Kurtenbach et al. (2006) that the different responses by the rod and cone systems upon inhalation of oxygen indicate that each system has a distinct metabolic process. Cones have been shown to have approximately 10x the volume of mitochondria compared to rods (Hoang et al., 2002). It may therefore be suggested that under normal conditions, maximal metabolic rates may have been reached in rods (Wangsa-Wirawan and Linsenmeier, 2003), but not in cones, thus allowing them to further improve their speed of adaptation with the addition of supplemental oxygen. The Mùller cell pathway in cones, allowing an additional and faster mechanism for opsin regeneration (Mata et al., 2002), may also account for the increased speed of recovery seen in cones, but not in rods. Whilst Type 1 diabetics have also previously demonstrated similar improvement in cone threshold upon the inhalation of oxygen (Kurtenbach et al., 2006), CFRD subjects showed neither an increase in the cone constant or final cone threshold, indicating that CFRD subjects may not behave in exactly the same way to Type 1 diabetics.

In contrast to CFRD subjects, NGT subjects showed no change in any DA parameters upon the inhalation of oxygen, despite an increase in SaO_2. Absence of a change in NGT subjects lends further support to the conclusion that DA impairment in CF is secondary to CFRD and not a primary manifestation of CFTR dysfunction at the RPE, or due to hypoxia under normal conditions. It has long been known that healthy persons with altitude induced hypoxia have impaired dark adaption (McFarland and Evans, 1939; McFarland and Forbes, 1940). The effect of oxygen inhalation on DA in subjects with chronic respiratory insufficiency, and hence reduced SaO_2 under normal conditions, similarly showed no improvement in DA upon oxygen inhalation in a different study (Thylefors et al., 2009). It is hypothesised that subjects with chronic respiratory insufficiency do not show impaired DA despite reduced SaO_2 due to the combined effect of hypoxia and hypercapnia inducing vasodilation in both the retinal and choroidal circulation, resulting in a blood flow that would be sufficient to compensate for

reduced arterial oxygen saturation (Harris et al., 1996; Thylefors et al., 2009). In contrast, high altitudes create a state of hypoxia and hypocapnia, which results in reduced oxygenation, but no compensatory increased blood flow due to the vasoconstrictive effects of hypocapnia (Fallon et al., 1985; Kergoat and Faucher, 1999; Poulin et al., 2002; Thylefors et al., 2009).

Established CFRD is often difficult to diagnose as glucose tolerance fluctuates with periods of disease exacerbation (Mackie et al., 2003), and HbA1c is not always reliable in CF, with readings appearing falsely low (Lanng et al., 1995; Solomon et al., 2003). The decision to commence treatment for CFRD is hence rather challenging. Therefore, one of the aims of this study was to assess the effect of oxygen breathing on DA in IGT subjects, in the hope of determining whether hypoxia existed in these patients. If hypoxia was indeed found to exist in IGT subjects, this would demonstrate a level of impairment similar to CFRD subjects, which would lead to the suggestion for prompt diabetic treatment. Whilst significance was not reached, possible due to small subject numbers, IGT subjects tended towards having a higher final rod threshold during the inhalation of air compared to controls, with the difference reduced upon the inhalation of oxygen. When considered separately, two of the IGT subjects showed no decrease in threshold upon inhalation of oxygen, whilst the other showed a reasonable decrease in threshold. The latter subject is likely to have done so due to retinal hypoxia, secondary to diabetic changes, therefore it is possible that this subject would benefit from the commencement of diabetic treatment. This finding indicates that there is reasonable promise for the use of DA in identifying IGT subjects who may benefit from diabetic treatment, when measures like HbA1c would not help with this distinction (Lanng et al., 1995; Solomon et al., 2003).

Only four of the 23 subjects who participated in this study had VAD, representing 17.4% of the cohort. This represents a dramatic reduction in prevalence over the last 5 years, as a study which was carried out in 2008 found 42.9% of their cohort had VAD (Evans, 2009). This reduction demonstrates improved management of pancreatic insufficiency and subsequent vitamin deficiencies. As only four subjects had VAD in this study, statistical analysis between controls, vitamin A sufficient (VAS) and VAD groups must be interpreted with caution. VAD subjects had elevated final rod threshold during the inhalation of air compared to controls and VAS (though significance was not reached). Vitamin A is known to play a key role in the regeneration of photopigment in the retinoid cycle of vision (Lamb and Pugh, 2004), therefore, it is unsurprising that VAD has previously been shown to produce an increase in final rod

threshold which is reversible upon vitamin A supplementation (Kemp et al., 1988). However, it is unlikely that the threshold was elevated due to low serum A levels in this study as recovery to normal levels was shown upon oxygen inhalation, indicating that hypoxia was the causative factor.

In summary, NGT subjects showed no impairment in DA compared to controls, along with no improvement in any DA parameters upon oxygen inhalation, whilst CFRD subjects demonstrated impaired rod threshold, a defect which was ameliorated upon oxygen inhalation. Together, these findings suggest that DA is impaired in CF secondary to retinal hypoxia in CFRD, not by the primary dysfunction of CFTR at the RPE. This is the first study to demonstrate the presence of retinal hypoxia in CFRD subjects. Whilst no firm conclusions can be drawn from the results obtained on the IGT subjects due to small participant numbers, the results show considerable promise that DA may be used to identify IGT patients who show signs of retinal impairment and who therefore may benefit from earlier treatment.

Chapter 6 Investigating Retinal Integrity in Cystic Fibrosis

6.1 Introduction

CFTR has previously been localised to the basal membrane of the RPE (Wills et al., 2000; Wills et al., 2001; Weng et al., 2002; Blaug et al., 2003), and has been indicated to have a functional role in chloride ion (Cl^-) transport from the sub-retinal space (SRS) to the choroid (Miller and Farber, 1984; Blaug et al., 2003). Studies on the RPE indicate that Cl^- transport across the RPE is important in several RPE functions, including fluid absorption (Miller and Edelman, 1990), volume regulation (Ueda and Steinberg, 1994) and ligand-regulated ion and fluid transport (Peterson et al., 1997). The retina produces a large amount of water as a consequence of its high metabolic turnover in photoreceptors and neurons (Strauss, 2005). This creates a need for continual removal of water from the retina to the choroid via the RPE (Marmor, 1990). Epithelial transport of Cl^- and potassium ions provides the driving force for epithelial water transport via trans-cellular pathways, including AQP-1 (Hamann et al., 1998; Stamer et al., 2003; Strauss, 2005).

Disturbance of normal CFTR activity in CF, unless compensated by other Cl^- channels, could cause complications such as oedema and serous retinopathy. Active trans-epithelial chloride transport is known to generate an osmotic gradient, driving fluid secretion. It is hypothesised that reduced secretion of Cl^- from the SRS to the choroid via the RPE would result in accumulation of fluid within the RPE and photoreceptor complex, recognised as increased retinal thickness as measured by OCT. The retina in CF may also be compromised due to increased levels of oxidative stress caused by chronic recurrent respiratory infection (van der Vliet et al., 1997; Lezo et al., 2012), decreased levels of protective antioxidants including lutein and zeaxanthin (Feranchak et al., 1999; Schupp et al., 2004; Grey et al., 2008; Laguna et al., 2008; Maqbool and Stallings, 2008) and impaired transport of glutathione (Qin et al., 2011). Furthermore, the observation of premature drusen in CF subjects could indicate an increased risk of premature age related macular degeneration (AMD) (Evans, 2009).

This chapter explores the retinal structure and the pathogenesis of AMD and investigates the effect of defective CFTR functioning in CF on the retinal structure through quantitative and qualitative evaluation of retinal optical coherence tomography (OCT) scans. All methods were carried out as outlined in Chapter 4.

6.2 Experimental Aims

To quantitatively and qualitatively investigate the retina and RPE in CF through OCT examination, in order to determine the primary and secondary structural effects of CF at the retinal level.

6.2.1 *Experimental Hypothesis*

1. Reduced secretion of chloride ions from the SRS to the choroid by dysfunctional CFTR in CF will result in accumulation of fluid within the RPE and photoreceptor complex. Therefore, CF subjects are hypothesised to show significantly increased retinal thickness, as measured by OCT, compared to controls.
2. OCT examination will reveal sub-clinical signs of premature aging within the CF population compared to controls, secondary to increased levels of oxidative stress and reduced availability of antioxidants due to pancreatic insufficiency and impaired glutathione transport via CFTR.

6.3 Results

56 eyes from 28 CF subjects, and 56 eyes from 28 control subjects were examined. An overview of the disease profile of CF subjects is given in Table 6.1 All retinal thickness measurements for each location were assessed for a relationship with axial length; where a statistically significant correlation was found, the individual values were corrected by linear regression analysis. Individual thickness values for each participant are shown in Appendix C.

Table 6.1 Disease characteristics of CF subjects

Variable	Description
Genotype	n = 14 ΔF508 homozygous
	n = 11 ΔF508 heterozygous
	n = 1 non-ΔF508
	n = 2 unidentified
Pancreatic Function	n = 27 pancreatic insufficient
	n = 1 pancreatic sufficient
Transplant History	n = 1 Lung Transplant
	n = 1 Liver Transplant
Serum Vitamin A concentration	Range: 0.78 – 1.97 μmol/L (Normal range: 1.10 – 2.60 μmol/L)
	Mean ± SD: 1.38 ± 0.35 μmol/L
Vitamin A Status	n = 23 vitamin A sufficient
	n = 5 vitamin A deficient
Serum Vitamin D concentration	Range: 5 – 57.90 μg/L (Normal range: 30 – 100 μg/L)
	Mean ± SD: 23.52 ± 11.71 μg/L
Vitamin D Status	n = 15 vitamin D sufficient
	n = 13 vitamin D deficient
Serum Vitamin E concentration	Range: 12.70 – 53.60 μmol/L (Normal range: 11 – 47 μmol/L)
	Mean ± SD: 25.27 ± 10.00 μmol/L
Vitamin E status	n = 27 vitamin E sufficient
	n = 1 vitamin E deficient
CFRD status	n = 13 NGT; n = 4 IGT; n = 11 CFRD
HbA1c	Range: 28 – 111 mmol/mol (Normal range 26-48 mmol/mol)
	Mean ± SD: 46.97 ± 17.19 mmol/mol
CF Liver disease	n = 12
FEV_1	Range: 0.79 – 4.11 L
	Mean ± SD: 2.25 ± 0.98 L
% Predicted FEV_1	Range: 28 – 96%
	Mean ± SD: 58.03 ± 21.46 %
Northern Score	Range: 0 – 12
	Mean ± SD: 5.71 ± 3.54

Key: * Normal range obtained from laboratory results; CFRD, cystic fibrosis related diabetes; NGT, normal glucose tolerance; IGT, impaired glucose tolerance; HbA1c, glycosylated haemoglobin; FEV_1, forced expiratory volume in 1 second

6.3.1 *Automated retinal thickness measures – Controls vs CF*

Mean automated retinal thickness measures for CF and control subjects are summarised in Table 6.2. There was no significant difference in retinal thickness between right and left eyes

for control subjects for all ETDRS areas (paired-samples (2-tailed) t-test, $p > 0.05$). There was no significant difference in retinal thicknesses between right and left eyes for CF subjects for all ETDRS areas apart from the NI (paired-samples (2-tailed) t-test, $p = 0.01$) and NO (paired-samples (2-tailed) t-test, $p = 0.00$) areas. As previous studies have shown no significant differences in retinal thicknesses between right and left eyes (Massin et al., 2002; Kelty et al., 2008; Wolf-Schnurrbusch et al., 2009; Duan et al., 2010), data from the right eyes only will be used for further analysis.

Mean retinal thickness for CF and control groups is shown as a function of eccentricity in Figure 6.1. All areas analysed were thinner in CF subjects compared to controls, reaching significance in the all outer retinal zones of the ETDRS plot (Table 6.3). For these areas, CF retinas were between 7.01μm (temporal outer) to 10.42μm (nasal outer) thinner.

Table 6.2 Automated retinal thickness measures (Control, n = 28; CF, n = 28)

Retinal Area	Control Mean ± SD		CF Mean ± SD	
	Right	**Left**	**Right**	**Left**
Axial length	24.07 ± 1.32	25.86 ± 1.16	23.80 ± 0.89	23.75 ± 0.90
CS (µm)	254.81 ± 20.89	254.05 ± 12.94	243.51 ± 24.72	244.64 ± 26.53
NI (µm)	313.52 ± 11.72	310.69 ± 19.14	**304.61 ± 26.31**	**310.10 ± 16.00**
TI (µm)	295.44 ± 10.48	293.33 ± 14.10	289.83 ± 14.02	289.19 ± 13.88
SI (µm)	308.58 ± 11.76	309.86 ± 12.16	303.98 ± 14.78	304.51 ± 13.57
II (µm)	304.05 ± 10.30	303.38 ± 13.01	301.65 ± 15.85	302.32 ± 14.56
NO (µm)	283.76 ± 12.70	284.33 ± 13.35	**273.34 ± 15.77**	**276.74 ± 15.92**
TO (µm)	245.83 ± 11.54	239.94 ± 22.92	238.82 ± 10.62	232.64 ± 24.09
SO (µm)	262.02 ± 12.03	262.29 ± 12.23	254.26 ± 11.30	255.71 ± 14.66
IO (µm)	254.04 ± 11.78	253.96 ± 14.34	247.02 ± 12.91	248.50 ± 13.00

Key: CS, central; NI, nasal inner; TI, temporal inner; SI, superior inner; II, inferior inner; NO, nasal outer; TO, temporal outer; SO, superior outer; IO, inferior outer; bold and shaded cells indicate significance

Table 6.3 Retinal thickness in Controls vs CF (Controls, n = 28; CF, n = 28)

Retinal Area	Control (Mean ± SD)	CF (Mean ± SD)	Independent-samples t-test
CS (µm)	254.81 ± 20.89	243.51 ± 24.72	0.07
NI (µm)	313.52 ± 11.72	304.61 ± 26.31	0.15
TI (µm)	295.44 ± 10.48	289.83 ± 14.02	0.10
SI (µm)	308.58 ± 11.76	303.98 ± 14.78	0.20
II (µm)	304.05 ± 10.30	301.65 ± 15.85	0.51
NO (µm)	283.76 ± 12.70	273.34 ± 15.77	**0.01**
TO (µm)	245.83 ± 11.54	238.82 ± 10.62	**0.02**
SO (µm)	262.02 ± 12.03	254.26 ± 11.30	**0.02**
IO (µm)	254.04 ± 11.78	247.02 ± 12.91	**0.04**

Key: CS, central; NI, nasal inner; TI, temporal inner; SI, superior inner; II, inferior inner; NO, nasal outer; TO, temporal outer; SO, superior outer; IO, inferior outer; bold and shaded cells indicate significance

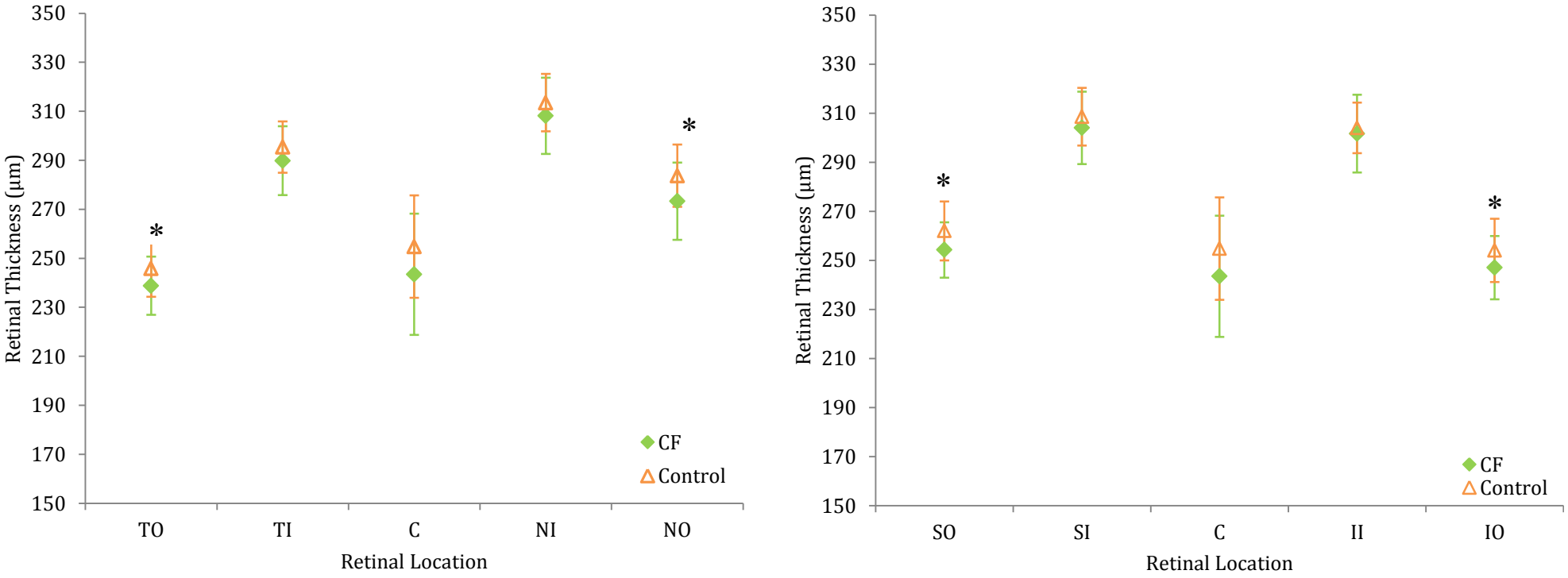

Figure 6.1 Retinal thickness for controls and CF subjects. Error bars show the standard deviation. Areas where the difference between groups was statistically significant ($p < 0.05$) are shown by a star (*).

6.3.2 *RPE/photoreceptor layer thickness*

Mean RPE/photoreceptor layer thickness for the CF and control groups is shown as a function of eccentricity in Figure 6.2. Mean RPE and photoreceptor layer thickness was significantly thinner in CF subjects at all locations analysed, with the greatest difference seen centrally (3.68µm) (Table 6.4).

Table 6.4 RPE/photoreceptor layer thickness in Controls vs CF (Controls, n = 28; CF, n = 28)

Retinal Area	Control (Mean ± SD)	CF (Mean ± SD)	Independent-samples t-test
Central, µm	108.50 ± 4.21	104.82 ± 3.89	**0.00**
Nasal, µm	84.86 ± 4.04	82.79 ± 2.87	**0.03**
Temporal, µm	84.25 ± 2.98	81.86 ± 2.82	**0.00**

Key: bold and shaded cells indicate significance

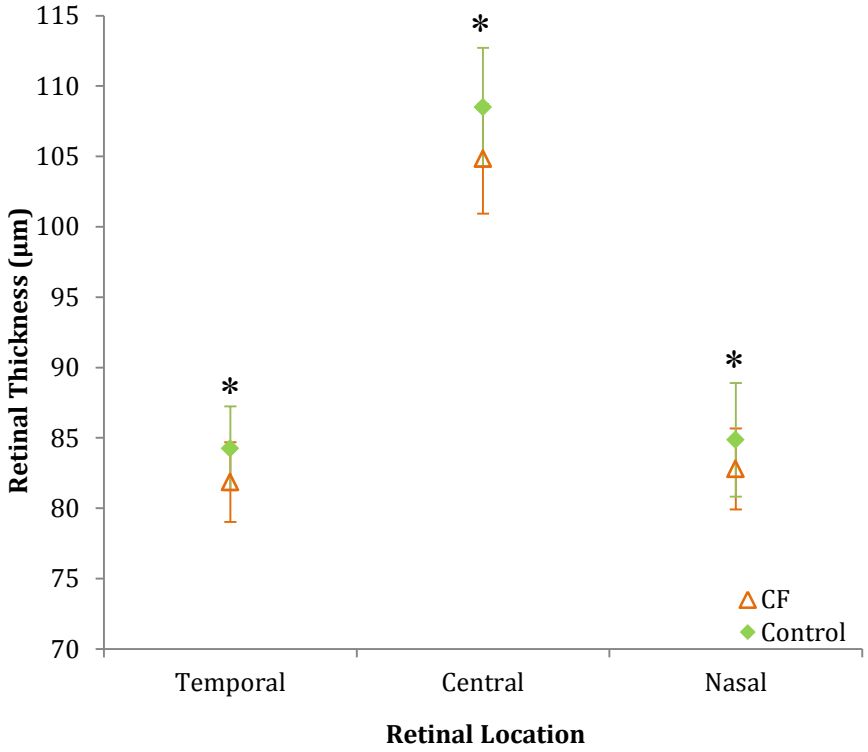

Figure 6.2 RPE/photoreceptor layer thickness for control and CF subjects. Error bars show the standard deviation. Areas where the difference between groups was statistically significant ($p < 0.05$) are shown by a star (*).

6.3.3 *The effect of diabetic status on retinal thickness*

When grouped according to their diabetic status, in general the CFRD group shows a smaller reduction in total retinal thickness compared to the NGT and IGT groups (Table 6.5).

Table 6.5 Retinal thickness grouped according to diabetic status (Control, n = 28; NGT, n = 13; IGT, n = 4; CFRD, n = 11)

Retinal Area	Control (Mean ± SD)	Diabetic Status		
		NGT	IGT	CFRD
CS (µm)	254.81 ± 20.89	241.33 ± 26.32	242.42 ± 22.67	246.48 ± 24.47
NI (µm)	313.52 ± 11.72	307.64 ± 9.69	302.08 ± 9.38	311.03 ± 22.16
TI (µm)	295.44 ± 10.48	290.67 ± 8.91	282.41 ± 14.75	291.54 ± 18.55
SI (µm)	308.58 ± 11.76	303.03 ± 10.00	302.25 ± 18.35	305.73 ± 19.06
II (µm)	304.05 ± 10.30	298.92 ± 11.77	295.58 ± 10.51	307.09 ± 20.55
NO (µm)	283.76 ± 12.70	270.43 ± 9.66	265.58 ± 14.32	279.60 ± 20.49
TO (µm)	245.83 ± 11.54	239.69 ± 5.82	232.75 ± 18.22	240.64 ± 14.84
SO (µm)	262.02 ± 12.03	254.23 ± 9.32	250.08 ± 10.57	255.82 ± 14.06
IO (µm)	254.04 ± 11.78	244.61 ± 11.54	242.58 ± 7.31	251.48 ± 15.38
RPE/Photoreceptor Central (µm)	108.50 ± 4.21	104.92 ± 4.34	106.25 ± 4.50	104.18 ± 3.28
RPE/Photoreceptor Nasal (µm)	84.86 ± 4.04	82.92 ± 3.38	84.00 ± 2.83	82.18 ± 2.27
RPE/Photoreceptor Temporal (µm)	84.25 ± 2.98	82.00 ± 3.14	83.00 ± 2.45	81.27 ± 2.65

Key: CS, central; NI, nasal inner; TI, temporal inner; SI, superior inner; II, inferior inner; NO, nasal outer; TO, temporal outer; SO, superior outer; IO, inferior outer

6.3.3.1 CFRD vs Controls

When CFRD subjects are compared to controls, there are no significant differences between the two groups for any areas of full retinal thickness, with no trend towards a thinner retina in CFRD (independent-samples (2-tailed) t-test, $p > 0.05$). However, there is a clear trend towards thinner RPE/Photoreceptor layer in CFRD subjects, with this difference reaching significance centrally and temporally (independent-samples (2-tailed) t-test, $p < 0.005$; $p < 0.05$, respectively) (Table 6.6).

Table 6.6 Retinal thickness in Controls vs CFRD (Controls, n = 11; CFRD, n = 11)

Retinal Area	Control (Mean ± SD)	CFRD (Mean ± SD)	Independent-samples t-test
CS (µm)	250.79 ± 26.76	246.48 ± 24.47	0.70
NI (µm)	309.54 ± 11.04	311.03 ± 22.16	0.85
TI (µm)	294.70 ± 8.21	291.54 ± 18.55	0.62
SI (µm)	305.18 ± 11.39	305.73 ± 19.06	0.94
II (µm)	300.45 ± 8.57	307.09 ± 20.55	0.34
NO (µm)	282.52 ± 15.11	279.60 ± 20.49	0.71
TO (µm)	243.67 ± 9.39	240.64 ± 14.84	0.57
SO (µm)	261 ± 14.73	255.82 ± 14.06	0.33
IO (µm)	250.58 ± 14.14	251.48 ± 15.38	0.89
RPE/Photoreceptor Central, (µm)	109.72 ± 3.85	104.18 ± 3.28	**0.00**
RPE/Photoreceptor Nasal, (µm)	84.64 ± 3.35	82.18 ± 2.27	0.06
RPE/Photoreceptor Temporal, (µm)	83.91 ± 2.84	81.27 ± 2.65	**0.04**

Key: CS, central; NI, nasal inner; TI, temporal inner; SI, superior inner; II, inferior inner; NO, nasal outer; TO, temporal outer; SO, superior outer; IO, inferior outer; bold and shaded cells indicate significance

6.3.3.2 NGT vs Controls

When NGT subjects are compared to controls, the trend towards a thinner retina in CF is apparent with all ETDRS areas thinner in NGT compared to controls. This difference reaches significance in the NO, TO and IO ETDRS areas (independent-samples (2-tailed) t-test, p <

0.005; $p < 0.05$; $p = < 0.05$, respectively). Whilst significance is not reached in any of the other ETDRS areas, all values tend towards significance. Whilst the RPE/photoreceptor layer also shows a trend towards being thinner in NGT, significance is not reached in any of the areas (independent-samples (2-tailed) t-test, $p > 0.05$) (Table 6.7).

Table 6.7 Retinal thickness in Controls vs NGT (Controls, n = 13; CFRD, n = 13)

Retinal Area	Control (Mean ± SD)	NGT (Mean ± SD)	Independent-samples t-test
CS (µm)	254.56 ± 13.82	241.33 ± 26.32	0.13
NI (µm)	315.08 ± 9.22	307.64 ± 9.69	0.06
TI (µm)	296.59 ± 9.91	290.67 ± 8.91	0.12
SI (µm)	310.18 ± 10.54	303.03 ± 10.00	0.09
II (µm)	306.56 ± 8.99	298.92 ± 11.77	0.08
NO (µm)	284.62 ± 9.93	270.43 ± 9.66	**0.00**
TO (µm)	248.69 ± 11.28	239.69 ± 5.82	**0.01**
SO (µm)	261.59 ± 9.86	254.23 ± 9.32	0.06
IO (µm)	256.82 ± 11.73	244.61 ± 11.54	**0.01**
RPE/Photoreceptor Central, (µm)	107.15 ± 4.36	104.92 ± 4.34	0.20
RPE/Photoreceptor Nasal, (µm)	84.00 ± 4.40	82.92 ± 3.38	0.49
RPE/Photoreceptor Temporal, (µm)	83.69 ± 3.15	82.00 ± 3.14	0.18

Key: CS, central; NI, nasal inner; TI, temporal inner; SI, superior inner; II, inferior inner; NO, nasal outer; TO, temporal outer; SO, superior outer; IO, inferior outer; bold and shaded cells indicate significance

6.3.3.3 IGT vs Controls

When IGT subjects are compared to controls, there is a trend towards a thinner retina in IGT subjects, however, possibly due to the small numbers (n = 4), significance is not reached for any of the full thickness ETDRS areas (independent-samples (2-tailed) t-test, $p > 0.05$). There is a similar trend towards a thinner RPE/Photoreceptor layer in IGT, with a significant difference seen for the temporal area only (independent-samples (2-tailed) t-test, $p < 0.05$) (Table 6.8).

Table 6.8 Retinal thickness in Controls vs IGT (Controls, n = 4; IGT, n = 4)

Retinal Area	Control (Mean ± SD)	IGT (Mean ± SD)	Independent-samples t-test
CS (µm)	266.67 ± 22.98	242.42 ± 22.67	0.18
NI (µm)	319.42 ± 19.37	302.08 ± 9.38	0.18
TI (µm)	293.75 ± 18.99	282.41 ± 14.75	0.38
SI (µm)	312.75 ± 17.05	302.25 ± 18.35	0.43
II (µm)	305.75 ± 17.58	295.58 ± 10.51	0.37
NO (µm)	284.42 ± 16.94	265.58 ± 14.32	0.14
TO (µm)	242.50 ± 18.13	232.75 ± 18.22	0.48
SO (µm)	263.75 ± 13.63	250.08 ± 10.57	0.16
IO (µm)	254.58 ± 14.54	242.58 ± 7.31	0.19
RPE/Photoreceptor Central, (µm)	109.50 ± 4.43	106.25 ± 4.50	0.34
RPE/Photoreceptor Nasal, (µm)	88.25 ± 3.69	84.00 ± 2.83	0.12
RPE/Photoreceptor Temporal, (µm)	87.00 ± 1.15	83.00 ± 2.45	**0.03**

Key: CS, central; NI, nasal inner; TI, temporal inner; SI, superior inner; II, inferior inner; NO, nasal outer; TO, temporal outer; SO, superior outer; IO, inferior outer; bold and shaded cells indicate significance

6.3.3.4 Correlation with HbA1c

There was no correlation between HbA1c and any of the ETDRS full retinal thickness areas, or the RPE/Photoreceptor layer areas (Pearson's, $p > 0.05$).

6.3.4 *Correlation with lung disease severity*

Lung function, as expressed by FEV_1 (Forced Expiratory Volume in 1 second) and the Northern Score (a score used to describe lung disease on a scale of 0-20, with 0 being no disease) were used to investigate the effect of disease severity on DA. FEV_1 had no significant correlation with any ETDRS full retinal thickness areas or any area of the RPE/Photoreceptor layer (Pearson's, -0.13< r <0.18, 0.37< p <0.95). Similarly, Northern Score had no significant correlation with any measures of retinal thickness or RPE/Photoreceptor layer (Pearson's, -0.35< r <0.09, 0.07< p <0.99). The only area that tended towards significance was the nasal RPE/Photoreceptor layer (Figure 6.13), where the retinal thickness decreases with an increase in Northern Score (Pearson's r = -0.35, p = 0.07).

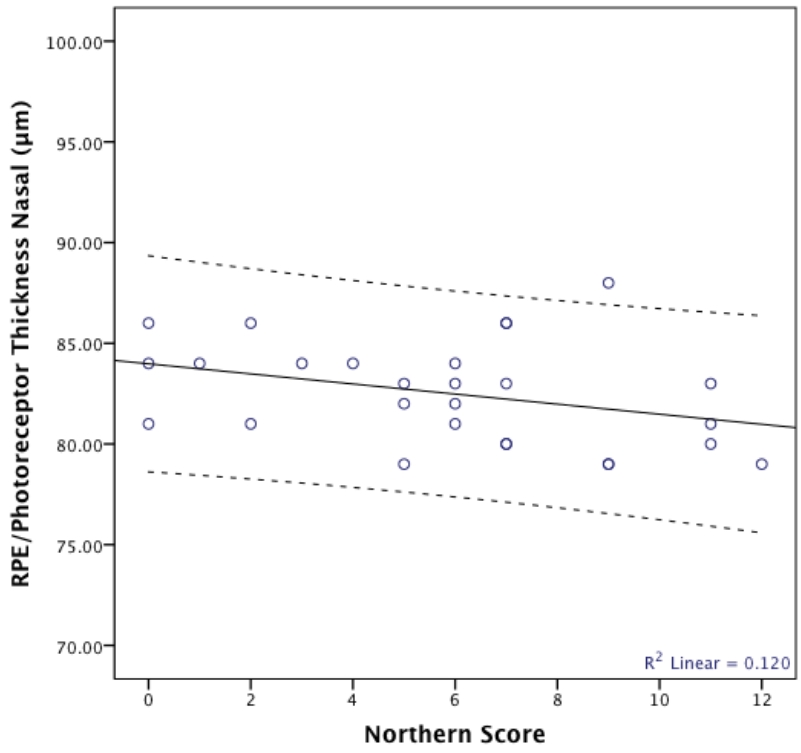

Figure 6.3 The correlation of Northern Score with the nasal RPE/Photoreceptor layer. (Pearson's r = -0.35, p = 0.07). Dotted lines indicate the 95% confidence intervals.

6.3.5 *The effect of vitamin status on retinal thickness*

Vitamin A, D and E levels did not significantly correlate with any measure of retinal thickness (Pearson's, -0.33< r <0.32, 0.1< p <0.98; 0.33< r <0.32, 0.1< p <0.98; 0.33< r <0.32, 0.1< p <0.98, respectively).

When grouped according to vitamin A status, full retinal thickness was significantly different in the NO area only (ANOVA; $p < 0.05$). Post hoc comparisons indicated that there was a significant difference between controls and the vitamin A sufficient group (Bonferroni; $p = 0.01$), with the vitamin A sufficient group having a thinner retina. The TO, SO, IO areas also tended towards significance (ANOVA; $p = 0.06$, $p = 0.07$, $p = 0.09$, respectively). In each area, post hoc comparisons indicated that retinal thickness was tending towards significantly thinner in the vitamin A sufficient group compared to controls (Bonferroni; TO, $p = 0.06$; SO, $p = 0.09$; IO, $p = 0.09$). RPE/photoreceptor layer thickness was significantly different centrally, nasally and temporally (ANOVA; $p < 0.005$, $p = 0.01$, $p = 0.01$, respectively). In the central and temporal areas, post hoc comparisons indicate a significant difference between controls and the vitamin A sufficient group, with the vitamin A sufficient group having a thinner RPE/photoreceptor layer (Bonferroni; Central, $p = 0.00$; Temporal, $p = 0.01$). However, post hoc comparison of the nasal area indicates a significant difference between controls and the vitamin A deficient group, with the vitamin A deficient group having a thinner RPE/photoreceptor layer (Games-Howell, $p = 0.00$). As the VAD group only has 5 subjects, these results must be viewed with caution (Table 6.9).

Table 6.9 The effect of vitamin A status on retinal thickness (Controls, n = 28; Vitamin A sufficient, n = 22; Vitamin A deficient, n = 5)

Retinal Area	Control (Mean ± SD)	Vitamin A Status		ANOVA
		VAS	VAD	
CS (µm)	254.81 ± 20.89	241.11 ±24.71	248.94 ± 26.17	0.12
NI (µm)	313.52 ± 11.72	306.12 ± 15.73	318.40 ± 13.20	0.08
TI (µm)	295.44 ± 10.48	288.85 ±14.60	295.00 ± 12.86	0.17
SI (µm)	308.58 ± 11.76	302.77 ± 14.87	310.20 ± 15.87	0.26
II (µm)	304.05 ± 10.30	300.29 ± 15.14	309.20 ± 19.91	0.35
NO (µm)	283.76 ± 12.70	271.06 ± 14.16	284.20 ± 21.11	**0.01**
TO (µm)	245.83 ± 11.54	238.17 ± 10.85	240.06 ± 11.05	0.06
SO (µm)	262.02 ± 12.03	254.62 ± 10.84	253.80 ± 15.38	0.07
IO (µm)	254.04 ± 11.78	246.18 ± 12.21	252.07 ± 17.17	0.09
RPE/Photoreceptor Central, (µm)	108.50 ± 4.21	104.32 ± 3.78	107.40 ± 4.04	**0.00**
RPE/Photoreceptor Nasal, (µm)	84.86 ± 4.04	82.91 ± 3.10	81.60 ± 0.89	**0.01**
RPE/Photoreceptor Temporal, (µm)	84.25 ± 2.98	81.82 ± 2.68	81.00 ± 2.92	**0.01**

Key: CS, central; NI, nasal inner; TI, temporal inner; SI, superior inner; II, inferior inner; NO, nasal outer; TO, temporal outer; SO, superior outer; IO, inferior outer; bold and shaded cells indicate significance

6.3.6 *The effect of liver disease on retinal thickness*

When grouped according to presence or absence of CF-liver disease (CFLD), full retinal thickness was significantly different in the NO area only, and RPE/photorecptor thickness was significantly different at each location (ANOVA; $p < 0.05$) (Table 6.10). Considering the ON area, post-hoc comparisons indicated that the retina was significantly thinner in Non-CFLD subjects compared to controls (Bonferroni; $p = 0.04$). Post-hoc comparisons of the central RPE/photoreceptor layer indicated that thickness was reduced in both CFLD and non-CFLD compared to controls (Bonferroni; $p = 0.02$ and $p = 0.04$, respectively). For the nasal and temporal RPE/Photoreceptor layer, thickness was reduced in the CFLD group compared to controls (Bonferroni; $p = 0.04$ and $p = 0.02$, respectively). There were no significant differences in thickness between CFLD and non-CFLD subjects.

Table 6.10 The effect of CFLD on retinal thickness (Controls, n = 28; CFLD, n = 12; Non-CFLD, n = 16)

Retinal Area	Control (Mean ± SD)	CF		ANOVA
		CFLD	Non-CFLD	
CS (µm)	254.81 ± 20.89	248.61 ± 24.85	239.69 ± 24.72	0.12
NI (µm)	313.52 ± 11.72	306.53 ± 15.99	309.42 ± 15.65	0.31
TI (µm)	295.44 ± 10.48	289.81± 12.34	289.85 ± 15.56	0.25
SI (µm)	308.58 ± 11.76	302.53 ± 14.71	305.06 ± 15.22	0.40
II (µm)	304.05 ± 10.30	301.39 ± 15.81	301.85 ± 16.40	0.80
NO (µm)	283.76 ± 12.70	273.11 ± 19.35	273.52 ± 13.15	**0.03**
TO (µm)	245.83 ± 11.54	238.78 ± 11.87	238.85 ± 12.22	0.09
SO (µm)	262.02 ± 12.03	253.42 ± 12.39	254.90 ± 10.79	0.05
IO (µm)	254.04 ± 11.78	247.31 ± 15.31	246.81 ± 11.30	0.14
RPE/Photoreceptor Central, (µm)	108.50 ± 4.21	104.42 ± 3.55	105.13 ± 4.21	**0.01**
RPE/Photoreceptor Nasal, (µm)	84.86 ± 4.04	81.83 ± 2.37	83.50 ± 3.08	**0.01**
RPE/Photoreceptor Temporal, (µm)	84.25 ± 2.98	81.42 ± 3.45	82.19 ± 2.31	**0.04**

Key: CS, central; NI, nasal inner; TI, temporal inner; SI, superior inner; II, inferior inner; NO, nasal outer; TO, temporal outer; SO, superior outer; IO, inferior outer; bold and shaded cells indicate significance

6.3.7 *The effect of genotype on retinal thickness*

When grouped according to CF genotype, there was no significant effect on full retinal thickness when compared to controls (ANOVA; $p > 0.05$) (Table 6.11). However, central and temporal RPE/photoreceptor layer thickness was significantly different (ANOVA; $p = 0.01$, $p = 0.02$, respectively). For the central RPE/photoreceptor layer, post hoc comparisons indicated that the RPE/photoreceptor layer was significantly thinner in ΔF508 heterozygotes compared to controls (Bonferroni; $p = 0.02$). Conversely, post hoc comparisons of the temporal RPE/photoreceptor layer indicated that this layer was thinner in ΔF508 homozygotes compared to controls (Bonferroni; $p = 0.04$). No significant differences in thickness were seen between the ΔF508 hetereozygous and homozygous subjects.

Table 6.11 The effect of genotype on retinal thickness (Controls, n = 28; Hetereozygous, n = 11; Homozygous, n = 14)

Retinal Area	Control (Mean ± SD)	CF		ANOVA
		ΔF508 Heterozygous (Mean ± SD)	ΔF508 Homozygous (Mean ± SD)	
CS (μm)	254.81 ± 20.89	241.11 ±24.71	248.94 ± 26.17	0.12
NI (μm)	313.52 ± 11.72	310.82 ± 15.60	308.55 ± 15.14	0.52
TI (μm)	295.44 ± 10.48	292.09 ± 16.18	290.64 ± 11.69	0.45
SI (μm)	308.58 ± 11.76	306.64 ± 13.85	304.55 ± 15.21	0.64
II (μm)	304.05 ± 10.30	304.48 ± 16.13	302.86 ± 15.27	0.95
NO (μm)	283.76 ± 12.70	276.30 ± 10.31	273.16 ± 19.26	0.67
TO (μm)	245.83 ± 11.54	239.91 ± 10.60	239.48 ± 12.66	0.17
SO (μm)	262.02 ± 12.03	256.85 ± 10.51	253.19 ± 11.47	0.07
IO (μm)	254.04 ± 11.78	249.91 ± 13.21	246.40 ± 13.16	0.20
RPE/Photoreceptor Central, (μm)	108.50 ± 4.21	104.36 ± 4.22	105.57 ± 4.01	**0.01**
RPE/Photoreceptor Nasal, (μm)	84.86 ± 4.04	82.91 ± 3.11	82.43 ± 2.10	0.07
RPE/Photoreceptor Temporal, (μm)	84.25 ± 2.98	81.86 ± 2.66	81.91 ± 2.84	**0.02**

Key: CS, central; NI, nasal inner; TI, temporal inner; SI, superior inner; II, inferior inner; NO, nasal outer; TO, temporal outer; SO, superior outer; IO, inferior outer; bold and shaded cells indicate significance

6.3.8 *Qualitative Analysis*

6.3.8.1 Drusen

Drusen were noted in only one CF subject within this study (Figure 6.4). The subject was a 69 year old male of unknown genotype with NGT, HbA1c of 49mmol/mol, FEV_1 18% predicted, and vitamin A sufficiency. Distance VA was slightly reduced at R 0.18 logMAR (6/9.5), L 0.3 logMAR (6/12), but near VA remained acceptable at R 0.4 logMAR (N4), L 0.4 logMAR (N4).

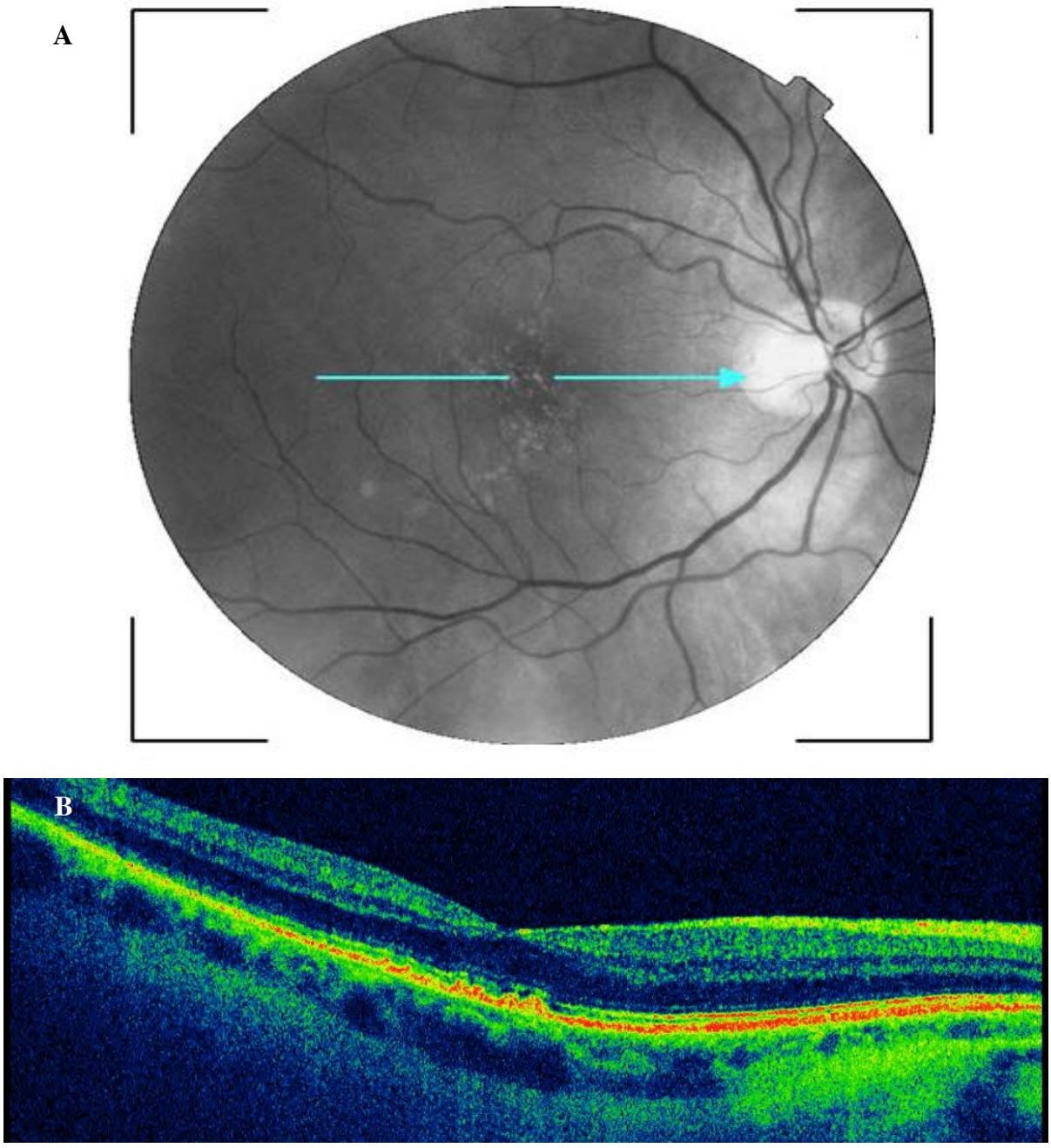

Figure 6.4 Black and white fundus photography (A) and pseudo-colour OCT scan (B) showing scattered macular drusen.

6.3.8.2 Epiretinal membrane

An epiretinal membrane (Figure 6.5) was noted in the left eye of an asymptomatic 31 year old female ΔF508 homozygous CF patient, with NGT, HbA1c of 40mmol/mol, FEV_1 92% predicted and vitamin A sufficiency. Distance and near VA was unaffected at L 0.02 LogMAR (6/6) and 0.0 (N2), respectively.

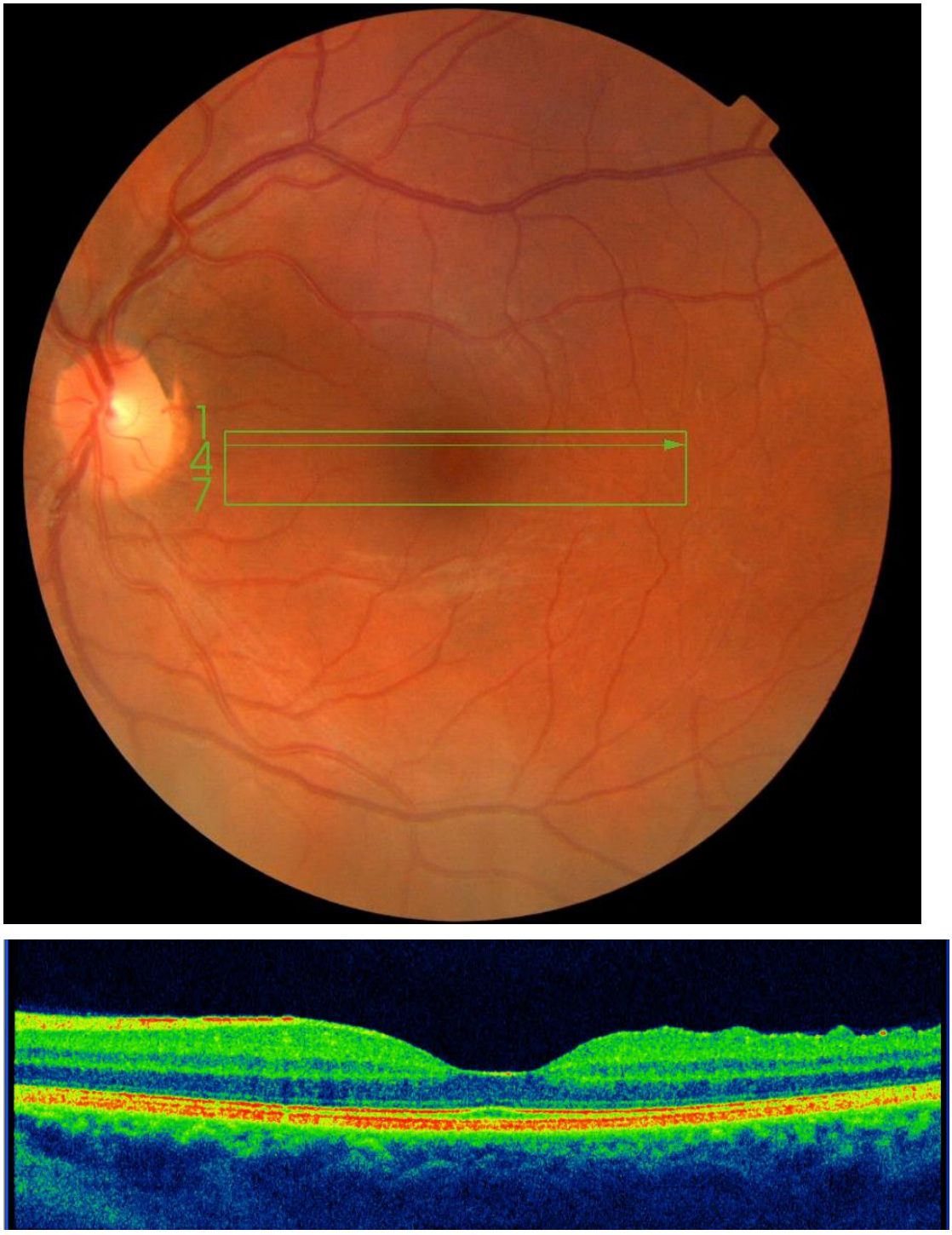

Figure 6.5 Fundus photograph (A) and pseudo-colour OCT scan (B) showing a temporal epiretinal membrane.

6.3.8.3 Branch retinal vein occlusion

A superior-temporal branch retinal vein occlusion (BRVO) (Figure 6.6) was noted in the left eye of an asymptomatic 35 year old male ΔF508 homozygos CF patient, with NGT, HbA1c of 28mmol/mol, FEV_1 31% predicted and VAD. The subject had had a liver transplant at 20 years old. Medications at the time of examination included: pancreatic enzyme replacement therapy, the fat soluble vitamins A,D,E & K, calcium supplements and a bisphosphonate for osteoporosis, inhaled steroid and bronchodilators, nebulised mucolytics DNAse and hypertonic saline; and prophylactic antibiotics including nebulised ceftazidime and oral Azithromycin and flucloxacillin. All medications have no known associated risk with BRVO. Distance VA was normal, measured at -0.06 LogMAR right and left. Further exploratory blood tests results are given in Table 6.12. [2]

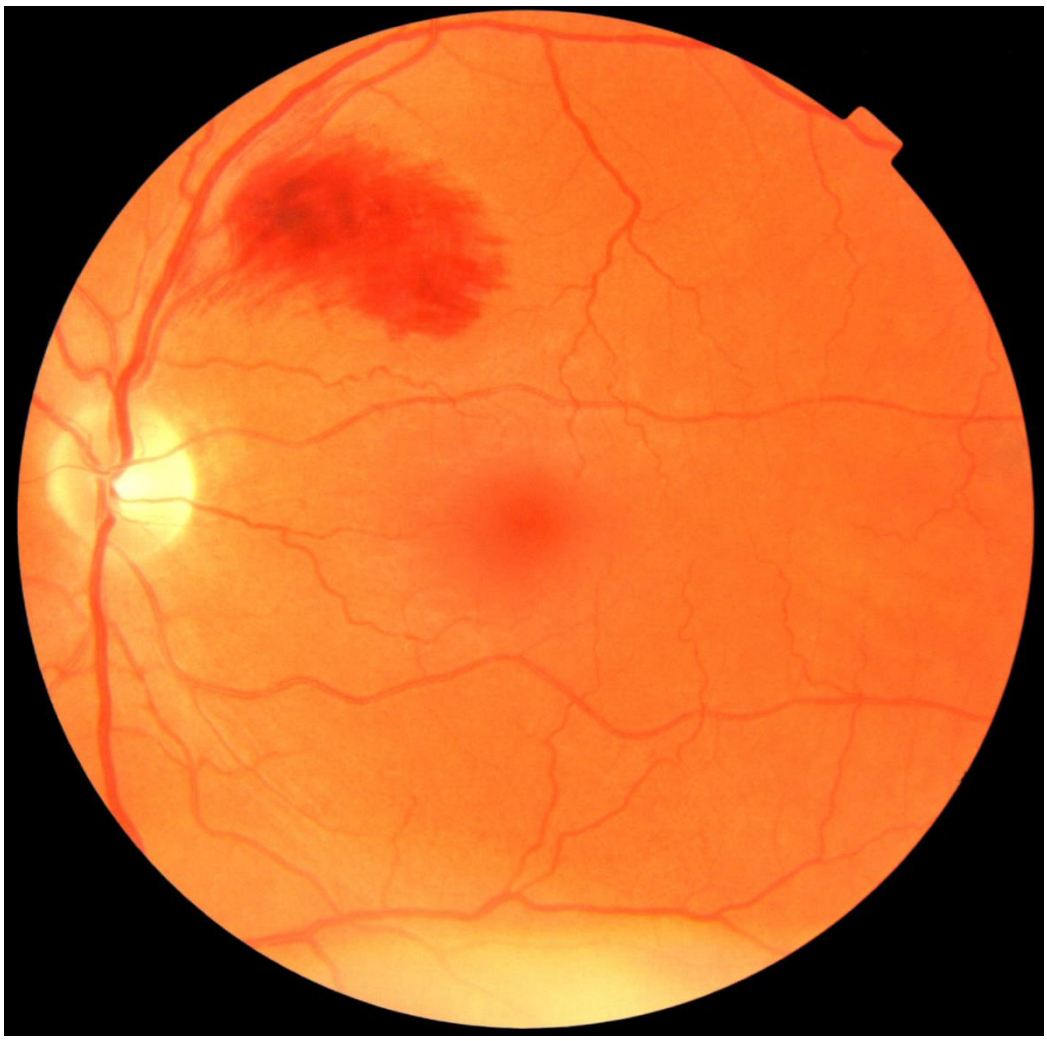

Figure 6.6 Left superior branch retinal vein occlusion with a retinal haemorrhage spanning two disc-diameters and no macular involvement.

Table 6.12 Exploratory blood test results

	Measured level	**Normal value**
Vitamin E	27.12 umol/l	11-47 umol/l
Fibrinogen	5.6 g/l	2-4 g/l
Cholesterol	2.3 mmol/l	2.5-5.2 mmol/l
Platelet Count	276 x 10 g/l	150-400 x 10 g/l
C Reactive protein	69 mg/l	< 6 mg/l
Liver function tests		
Total protein	82 g/l	60-80 g/l
Albumin	33 g/l	35-50 g/l
Total Bilirubin	9 umol/l	1-22 umol/l
Alkaline Phosphatase	81 IU/l	30-130 IU/l
Alanine Transferase	8 u/l	< 59 u/l
Globulin	49 g/l	22-42 g/l

6.3.9 *Summary of Findings*

- All retinal areas analysed were thinner in CF subjects compared to controls, reaching significance in all outer retinal zones of the ETDRS plot. RPE/photoreceptor layer was significantly thinner in CF subjects at all locations analysed compared to controls.

- CFRD subjects alone showed no trend towards a thinner retina compared to controls. However, there is a clear trend towards thinner RPE/photoreceptor layer thickness in CFRD subjects, with the difference reaching significance centrally and temporally.

- NGT subjects show a clear trend towards a thinner retina compared to controls, with differences reaching significance in the NO, TO and IO ETDRS areas. The RPE/photoreceptor layer also shows a trend towards being thinner in NGT compared to controls, but significance was not reached.

- IGT subjects show a trend towards a thinner retina compared to controls, however, significance is not reached for any of the ETDRS areas. The RPE/photoreceptor layer also shows a trend towards being thinner in IGT subjects compared to controls, with a significant difference seen for the TO area only.

- HbA1c, FEV_1 and Northern Score showed no significant correlation with any of the ETDRS areas, or the RPE/photoreceptor layer areas. However, correlation between nasal RPE/photoreceptor layer thickness and Northern Score approaches significance, with retinal thickness decreasing with an increase in Northern Score.

- Vitamin A, D and E levels did not significantly correlate with any measure of retinal thickness. When grouped according to vitamin A status, retinal thickness and RPE/photoreceptor layer tended to be thinner in VAS subjects compared to controls, with this difference reaching significance in the NO area, centrally and temporally. Nasal RPE/photoreceptor layer was significantly thinner in VAD subjects compared to controls.

- Retinal thickness was not significantly affected by disease severity, with homozygotes and heterozygotes showing no differences in retinal thickness.

6.4 Discussion

Quantitative Analysis

The retinal thickness values obtained for controls in this study are comparable to those obtained in other studies which used the Topcon 3D OCT -100 (Leung et al., 2008; Bruce et al., 2009). Also, in line with other studies, retinal thickness was found to be thinnest in the central region of the ETDRS plot (Wood et al., 2011).

Studies on RPE epithelial cells indicate Cl^- transport across the RPE is important in several RPE functions, including fluid absorption (Miller and Edelman, 1990), volume regulation (Ueda and Steinberg, 1994), and ligand-regulated ion and fluid transport (Peterson et al., 1997). Disruption to the ion flux and accompanied movement of water into and out of the RPE cells can result in the accumulation of fluid in the SRS and result in conditions such as serous retinopathy and retinal detachment (RD) (Bird, 1994). With the localisation of CFTR to the RPE and the importance of chloride ion transport in several RPE functions, malfunction of CFTR in CF would be expected to cause problems such as serous retinopathy. The results of this study demonstrate that contrary to the proposed hypothesis, retinal thickness and RPE/photoreceptor layer thickness tends towards being thinner in CF subjects compared to controls, with significance reached for all outer ETDRS areas, and for all areas of the RPE/photoreceptor layer analysed. It therefore appears that other Cl^- channels may be responsible for the majority of Cl^- transport across the basal membrane of the RPE. Results from electrophysiological experiments on canines suggest that CFTR may indeed be less important than other Cl^- channels as a mediator of basal RPE Cl^- transport (Loewen et al., 2003).

Retinal thickness is known to decrease with increasing age, due to the age-related loss of retinal cells (Curcio et al., 1993). CF patients are known to demonstrate accelerated aging, secondary to increased levels of oxidative stress (Ballatori et al., 2009) which may account for the general trend towards a thinner retina in CF. Age-related losses in retinal cells are reported to begin inferiorly and then spread to cause greatest loss in an annular ring between 0.5 to 3mm in eccentricity (Curcio et al., 1993). However, in this study, retinal thickness was found to be most reduced in the outer ETDRS areas, which relates to an eccentricity greater than 3mm.

Retinal thinning has been reported in early AMD (Kaluzny et al., 2009; Malamos et al., 2009; Schuman et al., 2009; Wood et al., 2011), with thinning localised to outer retinal areas directly

overlying drusen (Schuman et al., 2009). This thinning to believed to be secondary to photoreceptor degeneration in AMD (Kaluzny et al., 2009; Malamos et al., 2009; Schuman et al., 2009), a hypothesis which is supported by histological findings (Curcio, Medeiros and Millican, 1996). Whilst an increased prevalence of AMD was hypothesised to be seen in CF subjects, signs of age-related changes were only noted in one CF patient. Therefore, whilst the retinal thinning in CF subjects in this study appeared to be localised to the RPE and photoreceptor layers, it cannot be attributed to clinically-significant early onset AMD. Longitudinal studies which monitor CF patients over time may be useful to monitor the occurrence of AMD in CF.

Interestingly, when results from CFRD subjects were examined as a group, they showed no trend towards a thinner retina compared to controls, whilst NGT and IGT subjects with CF did. Previous studies on retinal thickness in type 1 and 2 diabetics with no diabetic retinopathy are varied, with some studies suggesting there is no change in retinal thickness (Bressler et al., 2008; Kashani et al., 2010; Demir et al., 2013), whilst others suggest there is a decrease (Browning, Fraser and Clark, 2008; Esmaeelpour et al., 2011) or an increase (Sánchez-Tocino et al., 2002; Sugimoto et al., 2005; Sng et al., 2012) in retinal thickness compared to controls. Some of the discrepancy in previous findings may be accounted for by lack of control of confounding factors including age, gender, ethnicity and refractive error (Sng et al., 2012), and varying recruitment criteria. There is more common consensus upon increased retinal thickness in diabetic subjects with more severe diabetic retinopathy, where retinal thickness is seen to be increased compared to controls (Schaudig et al., 2000; Sánchez-Tocino et al., 2002; Sng et al., 2012). Such increases in retinal thickness with increasing retinopathy may be explained by the break-down of the blood-retinal barrier and increased vascular permeability of perifoveal and macular capillaries (Sng et al., 2012). Whilst only one CFRD subject had signs of background diabetic retinopathy, the observed increased retinal thickness secondary to diabetes, as seen in previous studies on type 1 and 2 diabetics,is likely to account for the increased retinal thickness in CFRD subjects compared to NGT and IGT subjects. Whilst CFRD is classed as a distinct disease compared to type 1 and 2 diabetes, these results in CFRD subjects suggest that there may be microvascular similarties at the retinal level.

All but one subject who participated in this study were pancreatic insufficient, a common feature of CF which results in reduced levels of pancreatic enzymes reaching the small intestine and causes fat maldigestion (Karlet, 2000). Despite pancreatic enzyme replacement

therapy, CF patients have still been found to have an alteration in their plasma fatty acid profile, with decreased concentrations of linoleic acid and docosahexaenoic acid (DHA) (Aldamiz-Echevarria et al., 2009). DHA is the most abundant fatty acid found in rod outer-segments (Anderson, 1970; Anderson and Maude, 1972), and is known to be derived from dietary DHA (Li, Chen and Anderson, 2001a). DHA is not only an important structural component of retinal membranes (SanGiovanni and Chew, 2005), but may also play a role in the regeneration of rhodopsin as it transports 11-cis-retinal from the RPE (Chen et al., 1996). Reduced availability of DHA for the generation of rod photoreceptor outer-segments in CF may account for the finding of a thinner retina, and RPE/Photoreceptor layer compared to controls. Rod photoreceptor density is known to be maximal approximately 5.5mm from the central fovea (Curcio et al., 1990), which may explain the trend towards a greater difference in thickness between controls and CF subjects in the outer retinal zones. As the liver plays an essential role in synthesising DHA from its precursor linoleic acid (Scott and Bazan, 1989), the effect of CF-liver disease (CFLD) was examined, with the expectation that CFLD subjects would have thinner retinas, however, this was not apparent in this study. This may be due to small group numbers, or confounding factors including CFRD which may mask underlying trends.

One potential limitation of this study was that transverse magnification was not taken into account when taking measurements of the RPE/Photoreceptor layer. Whilst the axial component of an OCT image is laser dependent, and is therefore unaffected by magnification effects of varying axial length, transverse parameters are affected by optical magnification. Therefore, correction should be applied when measuring along the transverse direction of an OCT image (as discussed in Section 1.3.1.3.3), as per the following equation (Littmann, 1982; Bennett et al. 1994; Leung et al. 2007):

$$t = 3.3822(0.01306(x - 1.82))s \qquad \textit{Equation 1}$$

Where: t = true size of retinal feature, μm

x = axial length, mm

s = measured size of retinal feature, μm

Based upon *Equation 1*, the magnification factor for the shortest (21.71 mm) and longest (27.22 mm) axial lengths included in this study would be 0.88x and 1.12x, respectively. This

transverse magnification was not taken into account when taking manual measurements of retinal thickness as the retina appears to be a constant thickness at the eccentricity chosen.

Qualitative Analysis

AMD

CF subjects were hypothesised to display signs of premature aging, secondary to increased levels of oxidative stress (van der Vliet et al., 1997; Lezo et al., 2012), reduced availability of antioxidants (Feranchak et al., 1999; Grey et al., 2008; Laguna et al., 2008; Maqbool and Stallings, 2008) and impaired transport of glutathione (Qin et al., 2011). However, drusen were only noted in one 69 year old male CF subject, which given the advancing age was not unusual. In a study conducted in 2008, drusen were noted in two young CF patients (aged 20-25 years old) (Evans, 2009). It is possible that the absence of signs of premature aging in this study reflect the improvement in nutritional supplementation and management of inflammation and infection.

Epiretinal Membrane

Epiretinal membranes (ERM) develop at the vitreoretinal interface and consist of glial cells which have gained access to the retinal surface through breaks in the internal limiting membrane (Meyer et al., 2004). ERM may be idiopathic, occurring in otherwise healthy individuals, or secondary to retinal breaks, ocular surgery or ocular inflammation (Trese, Chandler and Machemer, 1983; Fraser-Bell et al., 2003). Idiopathic ERM most commonly develop following posterior vitreous detachment and are generally observed in patients over 50 years of age (Appiah, Hirose and Kado, 1988), with a prevalence of 7-11% (Klein et al., 1994b; Mitchell et al., 1997). As ERM occurs bilaterally in 31% of cases, a systemic cause is suggested (Mitchell et al., 1997), with diabetes identified as a risk factor (Mitchell et al., 1997). Whilst an ERM was noted in an asymptomatic, 31 years old, NGT, female patient, there is no reason to believe that the occurrence is related to CF.

BRVO

Despite BRVO being relatively uncommon in patients under 65 years of age (Weger et al., 2005), a superior-temporal BRVO was spotted identified in an asymptomatic 35 year old male CF patient during this study. Retinal vascular abnormalities have previously been reported in CF patients, with retinal vein tortuosity and engorgement and retinal haemorrhages noted only in those patients with moderate to severe pulmonary disease, and often showing resolution with

improvement of respiratory function (Bruce, Denning and Spalter, 1960). Similar retinal vascular findings have been reported in patients with chronic pulmonary insufficiency and carbon dioxide retention from other causes (Spalter and Bruce, 1964). CF patients may be at increased risk of RVO for numerous reasons, including:

- Approximately 50% of CF patients over 30 years of age suffer from diabetes, a known risk factor for RVO (Rehak and Wiedemann, 2010).
- Increased incidence of vascular thrombosis has been described in CF patients fitted with totally implantable venous access devices (TIVADs) (Munck et al., 2004), with the insertion site significantly influencing the incidence of thrombosis.
- Oxidative stress, which is exacerbated in CF during times of pulmonary infection, has also been implicated in the development of thrombosis. Oxidative stress may be a constant local feature at epithelial surfaces in CF, because CFTR is not only a chloride channel but also a channel for the antioxidant glutathione (Leoncini et al., 2009).
- CF patients show an increase in circulating activated platelets, and platelet-leukocyte complexes (O'Sullivan et al., 2005). Previous data have shown platelet activation and hypercoaguability inducing thrombus formation may be an important factor in the development of RVO (Leoncini et al., 2009).

Whilst the exact pathogenesis of RVO remains unclear, the primary mechanism is considered to be a multifactorial process involving a combination of haemodynamic changes, degenerative changes of the vessel wall and blood hypercoagulability (Rehak and Rehak, 2008). Identified risk factors include: systemic atherosclerotic vascular disease, hypertension, diabetes mellitus, dyslipidaemia, high body mass index and smoking (Rehak and Wiedemann, 2010). The pathogenesis in younger persons is poorly understood; the association with cardiovascular disease is less common and it is suggested that thrombophilic disorders may play a greater role (Rehak et al., 2008). An acquired prothrombotic condition is often present in CF secondary to protein C and S deficiency due to poor vitamin K absorption (protein S is a vitamin K-dependent co-factor which forms a complex with activated protein C) and some degree of liver failure (Takemoto, 2012). In this case, the likely cause of BRVO is elevated fibrinogen levels resulting in an increased risk of thrombosis (Koster et al., 1994). Fibrinogen is an acute phase reactant; its concentration rises in inflammatory conditions (Lind, 2003), explaining why

fibrinogen levels may be raised in CF and why retinal changes may be noted at times of pulmonary exacerbation.

In summary, investigation of the retinal structure in CF through OCT has provided evidence to suggest that primary dysfunction of CFTR at the RPE does not cause an increase in retinal thickness. In contrast to the proposed hypothesis, retinal and RPE/photoreceptor layer thickness was significantly reduced in CF subjects compared to controls, with accelerated aging, early onset AMD and fatty acid deficiency all proposed as possible causes for this reduction in thickness. No overall retinal thickness differences were seen in CFRD subjects alone, possibly due to retinal thickening secondary to break down of the blood retinal barrier. It is clear that further work is necessary to determine the cause of reduced retinal thickness in CF, and if this reduced thickness has any functional consequences. Secondary manifestations of CF, including an elevated inflammatory state secondary to chronic lung infection, may be associated with increased risk of retinal occlusive events and AMD, both of which were observed in asymptomatic CF subjects in this study.

Chapter 7 Conclusions and Future work

7.1 Conclusions

The primary objective of this thesis was to investigate the retina in Cystic Fibrosis (CF) through dark adaptation (DA) and optical coherence tomography (OCT) examination, in order to determine whether malfunction of CFTR at the RPE has direct, primary effects on both retinal structure and function. Oxygen inhalation studies on DA aimed to increase understanding of the aetiology behind impaired DA in CF, with the hope of also gaining additional insight into CF-related diabetes (CFRD).

The experimental hypotheses were:

OCT

1. Primary dysfunctional of CFTR in CF will result in accumulation of fluid within the RPE and photoreceptor complex; therefore CF subjects were hypothesised to show significantly increased retinal thickness compared to controls.
2. OCT examination will reveal sub-clinical signs of premature aging within the CF population compared to controls, secondary to increased levels of oxidative stress and reduced availability of antioxidants due to pancreatic insufficiency and impaired glutathione transport via CFTR.

Dark Adaptation

3. Impaired DA in CF is secondary manifestation of CF caused by CFRD, therefore CFRD subjects will show improvements in DA thresholds upon inhalation of 100% oxygen breathing.

Chapter 1 introduced the pathogenesis of CF and discussed the current literature available on the ocular manifestations of CF in relation to the localisation of CFTR to ocular epithelia. Chapters 2 and 3 were developmental chapters towards the protocols. Chapter 2 discussed the principles of OCT and described the development of a suitable imaging protocol for reliably assessing retinal thickness and RPE/photoreceptor layer thickness with the Topcon 3D OCT-1000. The protocol developed in Chapter 2 was later used during the CF study, as described in Chapter 6. In Chapter 3 the development of a specialised computerised dark adaptometer (CDA) using a cathode ray tube screen and Matlab programming software was described. The CDA was verified against the current gold-standard for dark adaptation assessment, the

Goldmann-Weekers adaptometer, with results showing that parameters of dark adaptation were comparable between the two. Repeatability of the CDA was also assessed, with results indicating the CDA had high levels of repeatability. This led to the use of the CDA to investigate DA in CF subjects, as described in Chapter 5. Chapter 4 brought together the findings of the preliminary experiments as described in Chapters 2 and 3 and set out the experimental protocol which was used for the study of DA and retinal structure in CF.

Chapter 5 investigated the effect of oxygen inhalation on DA in CF subjects and healthy controls. DA was shown to be impaired in the CF group as a whole compared to controls during the inhalation of air, as shown by elevated final rod threshold. When CF subjects were grouped according to their diabetic status, only CFRD subjects showed a significant elevation in final rod threshold compared to controls. This finding suggests for the first time that impaired dark adaptation in CF is secondary to CFRD, and not a primary manifestation of CFTR malfunction at the RPE. Upon inhalation of oxygen, whilst controls and normal glucose tolerance (NGT) CF subjects showed no significant improvement in final rod threshold, CFRD subjects showed a significant decrease in threshold, bringing threshold to a level comparable to controls. This response is in line with previous findings in type 1 and type 2 diabetic subjects (Kurtenbach et al., 2006), and leads to the suggestion that CFRD subjects have retinal hypoxia. These findings suggest that DA is impaired in CF secondary to retinal hypoxia in CFRD, not by the primary dysfunction of CFTR at the RPE. Whilst one of the aims of this study was to investigate how CF subjects with impaired glucose tolerance (IGT) responded to inhalation of oxygen, no firm conclusions could be drawn from the results due to small participant numbers. However, with a trend towards improvement in final rod threshold upon inhalation of oxygen, results show considerable promise that DA may be used to identify IGT patients who are showing signs of retinal hypoxia and who therefore may benefit from earlier treatment. This is the first time this has been noted in CF.

Chapter 6 described the investigation of retinal and RPE/photoreceptor layer thickness in CF subjects compared to controls using the Topcon 3D OCT-1000. Results demonstrated for the first time, and contrary to the proposed hypothesis, that retinal thickness and RPE/ photoreceptor layer thickness is thinner in CF subjects compared to controls. It therefore appears that other Cl^- channels may be responsible for the majority of Cl^- transport across the basal membrane of the RPE. It was suggested that a thinner retina may be secondary to accelerated aging in CF , as retinal thickness is known to decrease with increasing age due to

age-related loss of retinal cells (Curcio et al., 1993). Other theories put forward as to why the retina may be thinner in CF include thinning associated with early onset AMD (Kaluzny et al., 2009; Malamos et al., 2009; Schuman et al., 2009; Wood et al., 2011), and impaired formation of photoreceptor outer segments due to fatty acid deficiency in CF (Anderson, 1970; Anderson and Maude, 1972; Aldamiz-Echevarria et al., 2009). Interestingly, CFRD subjects showed no decrease in retinal thickness compared to controls. It was postulated that any CF related thinning was negated in CFRD subjects due to retinal thickening secondary to break down of the blood retinal barrier as seen in type 1 and 2 diabetic subjects (Sánchez-Tocino et al., 2002; Sugimoto et al., 2005; Sng et al., 2012). Whilst qualitative analysis of OCT scans was hypothesised to show early onset aging changes in CF subjects compared to controls, secondary to reduced availability of antioxidants and increased levels of oxidative stress, only one 69 years old CF subject displayed signs of drusen. In a study conducted in 2008, drusen were noted in two young CF patients (aged 20-25 years old) (Evans, 2009). It is possible that the absence of signs of premature aging in this study reflect the improvement in nutritional supplementation and management of inflammation and infection.

In conclusion, primary dysfunction of CFTR at the RPE does not appear to have a direct impact on retinal structure or function in CF. This is a particularly important finding as it suggests that other ion channels compensate for CFTR dysfunction. Impairment of DA in CF appears to be secondary to retinal hypoxia in CFRD, therefore hope remains that DA and oxygen inhalation may be used to identify IGT subjects who would benefit from earlier diabetic treatment. A reduction in retinal thickness in CF, specifically at the RPE/photoreceptor layer, may be secondary to premature aging, early onset AMD or impaired formation of photoreceptor outer segments due to fatty acid deficiency. Whilst premature signs of aging were not seen in younger CF subjects in this study, a branch retinal vein occlusion (BRVO) was observed in one subject. CF subjects may be at increased risk of retinal occlusive events secondary to an elevated inflammatory state. Given the findings of this thesis, it is important that CF subjects are educated about the importance of regular eye examinations, and that eye care professionals are aware of the potential systemic implications of ocular findings in CF.

7.2 Future work

Following on from the DA research, it would be of considerable benefit to examine larger numbers of IGT subjects, to strengthen the findings in this group and determine whether DA

could be used as a diagnostic tool to identify those subjects who require diabetic treatment. However, recruitment of CF subjects will always be difficult, due to the relatively small number of sufferers, and the severity of the condition, which can result in many subjects being too ill to participate. Conducting the study at the hospital may improve participation in the study, as in-patient subjects would not have to travel and data collection could be split into two smaller, more manageable sessions.

Given the chance findings of AMD, BRVO and epiretinal membrane in CF subjects in this study, it would be of considerable interest to use OCT to image a larger group of CF patients to determine whether the occurrence of these abnormalities is more common place in CF. It would also be of interest to conduct a longitudinal study which images the same subjects on multiple occasions, both during pulmonary exacerbations and during times of relative health, in order to build up a picture of how acute periods of increased oxidative stress affect retinal integrity. Performing assessments at the hospital, during both inpatient and outpatient clinics would again improve subject participation and improve the strength of any results obtained.

Whilst only one subject with AMD was noted in this study through structural examination with OCT, previous research has shown that CF subjects have lower levels of macular pigment compared to controls (Schupp et al., 2004), suggesting they are more susceptible to developing AMD. Increased levels of oxidative stress (Lezo et al., 2012), and reduced availability of antioxidants in CF (Feranchak et al., 1999; Grey et al., 2008; Laguna et al., 2008; Maqbool and Stallings, 2008) further increases the risk. It would be of considerable interest to determine whether CF subjects display functional signs of early onset aging changes. One way this could be achieved is through the electroretinogram (ERG) photostress test, a dynamic test of outer retinal function which has the capacity to differentiate between healthy controls and subjects with early age-related maculopathy (Binns and Margrain, 2007).

Recently, a histological examination of the lacrimal gland of a CF subject showed increased in vacuole density (Alghadyan et al., 2013), despite CFTR not being localised to the lacrimal gland epithelia. Given the presence of CFTR at the RPE, and the findings in this study of decreased retinal thickness in CF, as opposed to the increase expected, it would be of considerable interest to histologically examine the retina and RPE in CF. Staining of the photoreceptor layer with Oil Red O (Rudolf and Curcio, 2009), a stain which identifies fatty

acids, and comparing the relative amount of staining in a CF sample to a control sample may help to determine if reduced retinal thickness in CF is secondary to diminished levels of fatty acids. The RPE/photoreceptor layer could also be imaged with electron microscopy, enabling a more detailed view of the structure than can be obtained with OCT.

Type 1 and 2 diabetic subjects have previously demonstrated reduced corneal nerve sensitivity compared to controls, secondary to peripheral neuropathy (Schwartz, 1974; Daubs, 1975; Nielsen, 1978; Rogell, 1980). It would be of substantial interest to investigate corneal sensitivity in CFRD, IGT and NGT subjects to see if diabetic CF subjects display similar reductions in corneal sensitivity. If corneal sensitivity is indeed reduced in CFRD, corneal aesthesiometry may prove to be a simple, non-invasive, cost effective technique to determine IGT subjects who are displaying signs of diabetic nerve damage, and hence may require more aggressive diabetic therapy. Assessment of corneal nerves by *in-vivo* corneal confocal microscopy may aid in the examination of corneal nerves CFRD subjects (Tavakoli, Petropoulos and Malik, 2012), giving a structural map of nerve architecture which could be used in conjunction with sensory function.

References

Abbott-Johnson W J, Kerlin P, Abiad G, Clague A E, and Cuneo R C (2011) Dark adaptation in vitamin A-deficient adults awaiting liver transplantation: improvement with intramuscular vitamin A treatment. *Br J Ophthalmol* 95: 544-548.

Age-Related Eye Disease Study Reasearch Group (2000) Risk factors associated with age-related macular degeneration. A case-control study in the age-related eye disease study: Age-Related Eye Disease Study Report Number 3. *Ophthalmology* 107: 2224-2232.

Ahmed F, Ellis J, Murphy J, Wooton S, and Jackson A A (1990) Excessive faecal losses of vitamin A (retinol) in cystic fibrosis. *Arch Dis Child* 65: 589-593.

Aiello L P, Northrup J M, Keyt B A, Takagi H, and Iwamoto M A (1995) Hypoxic regulation of vascular endothelial growth factor in retinal cells. *Arch Ophthalmol* 113: 1538-1544.

Al-Nakkash L, and Reinach P S (2001) Activation of a CFTR-mediated chloride current in a rabbit corneal epithelial cell line. *Invest Ophthalmol Vis Sci* 42: 2364-2370.

Aldamiz-Echevarria L, Prieto J A, Andrade F, Elorz J, Sojo A, Lage S, Sanjurjo P et al. (2009) Persistence of essential fatty acid deficiency in cystic fibrosis despite nutritional therapy. *Pediatr Res* 66: 585-589.

Alder V A, and Cringle S J (1985) The effect of the retinal circulation on vitreal oxygen tension. *Curr Eye Res* 4: 121-129.

Alghadyan A, Aljindan M, Alhumeidan A, Kazi G, and McMhon R (2013) Lacrimal glands in cystic fibrosis. *Saudi Journal of Ophthalmology* 27: 113-116.

Algvere P V, and Seregard S (2003) Drusen maculopathy: a risk factor for AMD. Can we prevent visual loss? *Acta Ophthalmol Scand* 81: 427-429.

Allikmets R, Shroyer N F, Singh N, Seddon J M, Lewis R A, Bernstein P S, Peiffer A et al. (1997) Mutation of the Stargardt disease gene (ABCR) in age-related macular degeneration. *Science* 277: 1805-1807.

Alm A, and Bill A (1972) The oxygen supply to the retina. II. Effects of high intraocular pressure and of increased arterial carbon dioxide tension on uveal and retinal blood flow in cats. A study with radioactively labelled microspheres including flow determinations in brain and some other tissues. *Acta Physiol Scand* 84: 306-319.

Alton E W, Boyd A C, Cheng S H, Cunningham S, Davies J C, Gill D R, Griesenbach U et al. (2013) A randomised, double-blind, placebo-controlled phase IIB clinical trial of repeated application of gene therapy in patients with cystic fibrosis. *Thorax*: Epub ahead of print.

Ambati J, Ambati B K, Yoo S H, Ianchulev S, and Adamis A P (2003) Age-related macular degeneration: etiology, pathogenesis, and therapeutic strategies. *Surv Ophthalmol* 48: 257-293.

Amemiya T (1977) Dark adaptation in diabetics. *Ophthalmologica* 174: 322-326.

Ames A, 3rd (1992) Energy requirements of CNS cells as related to their function and to their vulnerability to ischemia: a commentary based on studies on retina. *Can J Physiol Pharmacol* 70 Suppl: S158-164.

Anand-Apte B, and Hollyfield J G (2009) Developmental anatomy of the retinal and choroidal vasculature. In: Besharse J, and Bok D [eds.] *Encyclopedia of the Eye*. London: Academic Press, Elsvier Books.

Andersen H U, Lanng S, Pressler T, Laugesen C S, and Mathiesen E R (2006) Cystic fibrosis-related diabetes: the presence of microvascular diabetes complications. *Diabetes Care* 29: 2660-2663.

Anderson B, Jr. (1968) Ocular effects of changes in oxygen and carbon dioxide tension. *Trans Am Ophthalmol Soc* 66: 423-474.

Anderson D H, Mullins R F, Hageman G S, and Johnson L V (2002) A role for local inflammation in the formation of drusen in the aging eye. *Am J Ophthalmol* 134: 411-431.

Anderson M P, Gregory R J, Thompson S, Souza D W, Paul S, Mulligan R C, Smith A E et al. (1991) Deomonstration that CFTR is a chloride channel by alteration of its anion selectivity. *Science* 253: 202-205.

Anderson O H (1939) Cystic fibrosis of the pancreas, vitamin A deficiency, and bronchiectasis. *J Pediatr* 15: 763-767.

Anderson R E (1970) Lipids of ocular tissues. IV. A comparison of the phospholipids from the retina of six mammalian species. *Exp Eye Res* 10: 339-344.

Anderson R E, and Maude M B (1972) Lipids of ocular tissues. 8. The effects of essential fatty acid deficiency on the phospholipids of the photoreceptor membranes of rat retina. *Arch Biochem Biophys* 151: 270-276.

Anger E M, Unterhuber A, Hermann B, Sattmann H, Schubert C, Morgan J E, Cowey A et al. (2004) Ultrahigh resolution optical coherence tomography of the monkey fovea. Identification of retinal sublayers by correlation with semithin histology sections. *Exp Eye Res* 78: 1117-1125.

Ansari E A, Sahni K, Etherington C, Morton A, Conway S P, Moya E, and Littlewood J M (1999) Ocular signs and symptoms and vitamin A status in patients with cystic fibrosis treated with daily vitamin A supplements. *Br J Ophthalmol* 83: 688-691.

Ansari N H, Zhang W, Fulep E, and Mansour A (1998) Prevention of pericyte loss by trolox in diabetic rat retina. *J Toxicol Environ Health A* 54: 467-475.

Appiah A P, Hirose T, and Kado M (1988) A review of 324 cases of idiopathic premacular gliosis. *Am J Ophthalmol* 106: 533-535.

Arden G B (2001) The absence of diabetic retinopathy in patients with retinitis pigmentosa: implications for pathophysiology and possible treatment. *Br J Ophthalmol* 85: 366-370.

Arden G B (2006) Origin and significance of the electro-oculogram. In: Heckenlively J R, and Arden G B [eds.] *Principles and Practice of Clinical Electrophysiology of Vision*. (2nd edn.) Cambridge, Massachusetts: MIT Press, pp. 123-138.

Arden G B, Gunduz M K, Kurtenbach A, Volker M, Zrenner E, Gunduz S B, Kamis U et al. (2010) A preliminary trial to determine whether prevention of dark adaptation affects the course of early diabetic retinopathy. *Eye (Lond)* 24: 1149-1155.

Arden G B, Jyothi S, Hogg C H, Lee Y F, and Sivaprasad S (2011) Regression of early diabetic macular oedema is associated with prevention of dark adaptation. *Eye (Lond)* 25: 1546-1554.

Arden G B, Sidman R L, Arap W, and Schlingemann R O (2005) Spare the rod and spoil the eye. *Br J Ophthalmol* 89: 764-769.

Arden G B, Wolf J E, and Tsang Y (1998) Does dark adaptation exacerbate diabetic retinopathy? Evidence and a linking hypothesis. *Vision Res* 38: 1723-1729.

AREDS (2001) A randomized, placebo-controlled, clinical trial of high-dose supplementation with vitamins C and E, beta carotene, and zinc for age-related macular degeneration and vision loss: AREDS report no. 8. *Arch Ophthalmol* 119: 1417-1436.

Arend O, Wolf S, Jung F, Bertram B, Postgens H, Toonen H, and Reim M (1991) Retinal microcirculation in patients with diabetes mellitus: dynamic and morphological analysis of perifoveal capillary network. *Br J Ophthalmol* 75: 514-518.

Aris R M, Merkel P A, Bachrach L K, Borowitz D S, Boyle M P, Elkin S L, Guise T A et al. (2005) Guide to bone health and disease in cystic fibrosis. *J Clin Endocrinol Metab* 90: 1888-1896.

Asefzadeh B, Cavallerano A A, and Fisch B M (2007) Racial differences in macular thickness in healthy eyes. *Optom Vis Sci* 84: 941-945.

Ashcroft F M (2000) Cystic Fibrosis Transmembrane Conductance Regulator.*Ion channels and disease*. San Diego: Academic Press, pp. 211-230.

Augood C A, Vingerling J R, de Jong P T, Chakravarthy U, Seland J, Soubrane G, Tomazzoli L et al. (2006) Prevalence of age-related maculopathy in older Europeans: the European Eye Study (EUREYE). *Arch Ophthalmol* 124: 529-535.

Back E I, Frindt C, Nohr D, Frank J, Ziebach R, Stern M, Ranke M et al. (2004) Antioxidant deficiency in cystic fibrosis: when is the right time to take action? *Am J Clin Nutr* 80: 374-384.

Ballatori N, Krance S M, Notenboom S, Shi S, Tieu K, and Hammond C L (2009) Glutathione dysregulation and the etiology and progression of human diseases. *Biol Chem* 390: 191-214.

Baudouin C (2001) The pathology of dry eye. *Surv Ophthalmol* 45: 211-220.

Bauer P J (2002) The complex of cGMP-gated channel and Na+/Ca2+, K+ exchanger in rod photoreceptors. *Adv Exp Med Biol* 514: 253-274.

Baylor D A, Lamb T D, and Yau K W (1979) The membrane current of single rod outer segments. *J Physiol* 288: 589-611.

Bazan N G (1989) The metabolism of omega-3 polyunsaturated fatty acids in the eye: the possible role of docosahexaenoic acid and docosanoids in retinal physiology and ocular pathology. *Prog Clin Biol Res* 312: 95-112.

Bear C E, Li C H, Bridges N K R J, Jensen T J, Ramjeesingh M, and Riordan J R (1992) Purifaction and functional reconstruction of the cystic fibrosis transmembrane conductance regulator (CFTR). *Cell* 68: 809-818.

Beatty S, Koh H, Phil M, Henson D B, and Boulton M (2000) The role of oxidative stress in the pathogenesis of age-related macular degeneration. *Surv Ophthalmol* 45: 115-134.

Beer R D, MacLeod D I A, and Miller T P (2005) The extended maxwellian view (BIGMAX): a high-intensity, high-saturation color display for clinical diagnosis and vision research. *Behav Res Methods Instrum Comp* 37: 513-521.

Beneyto P, Ibanez M, Leal M A, Garcia A, Carezas M, and Morente P (2007) Measurement of lens density with a Scheimpflug camera in diabetic patients. *Arch Soc Esp Oftalmol* 82: 141-145.

Bennett A G, and Rabbetts R B (1998) *Bennett and Rabbetts' Clinical Visual Optics*. Third Edition ed. Avon, Great Britain: Butterworth-Heinemann Ltd.

Bennett A G, Rudnicka A R, and Edgar D F (1994) Improvements on Littmann's method of determining the size of retinal features by fundus photography. *Graefes Arch Clin Exp Ophthalmol* 232: 361-367.

Bentur L, Kalnins D, Levison H, and al. e (1996) Dietry intakes of adolescent males and females - is there a difference? *J Pediatr Gastroenterol Nutr* 22: 254-258.

Berendschot T T, Willemse-Assink J J, Bastiaanse M, de Jong P T, and van Norren D (2002) Macular pigment and melanin in age-related maculopathy in a general population. *Invest Ophthalmol Vis Sci* 43: 1928-1932.

Bernstein P S, Zhao D Y, Wintch S W, Ermakov I V, McClane R W, and Gellermann W (2002) Resonance Raman measurement of macular carotenoids in normal subjects and in age-related macular degeneration patients. *Ophthalmology* 109: 1780-1787.

Biemans-Oldehinkel E, Doeven M K, and Poolman B (2006) ABC transporter architecture and regulatory roles of accessory domains. *FEBS Letters* 580 (4): 1023-1035.

Binns A M, and Margrain T H (2007) Evaluating retinal function in age-related maculopathy with the ERG photostress test. *Invest Ophthalmol Vis Sci* 48: 2806-2813.

Birch J (1998) *Diagnosis of Defective Colour Vision*. Oxford: Butterworth-Heinemann.

Bird A (1994) Pathogeneisis of serous detachment of the retina and pigment epihtelium. *Retina* 2: 1019-1026.

Birol G, Wang S, Budzynski E, Wangsa-Wirawan N D, and Linsenmeier R A (2007) Oxygen distribution and consumption in the macaque retina. *Am J Physiol Heart Circ Physiol* 293: H1696-1704.

Bismuth E, Laborde K, Taupin P, Velho G, Ribault V, Jennane F, Grasset E et al. (2008) Glucose tolerance and insulin secretion, morbidity and death in patients with CF. *J Pediatr* 152: 540-545.

Blackman S M, Hsu S, Vanscoy L L, Collaco J M, Ritter S E, Naughton K, and Cutting G R (2009) Genetic modifiers play a substantial role in diabetes complicating cystic fibrosis. *J Clin Endocrinol Metab* 94: 1302-1309.

Blakemore C, and Rushton W A (1965) The rod increment threshold during dark adaptation in normal and rod monochromat. *J Physiol* 181: 629-640.

Bland J M, and Altman D G (1986) Statistical methods for assessing agreement between two methods of clinical measurement. *Lancet* 1: 307-310.

Bland J M, and Altman D G (1995) Multiple significance tests: the Bonferroni method. *BMJ* 310: 170.

Bland J M, and Altman D G (2009) Analysis of continuous data from small samples. *BMJ* 338: a3166.

Blaug S, Quinn R, OQuong J, Jalickee S, and Miller S S (2003) Retinal pigment epithelial function: a role for CFTR. *Doc Ophthalmol* 106: 43-50.

Bobadilla J L, Macek Jr M, Fine J P, and Farrell P M (2002) Cystic fibrosis: A worldwide analysis of CFTR mutations - Correlation with incidence data and application to screening. *Human Mutation* 19 (6): 575-606.

Bok D, Ong D E, and Chytil F (1984) Immunocytochemical localization of cellular retinol binding protein in the rat retina. *Invest Ophthalmol Vis Sci* 25: 877-883.

Bonanno J A, Yi G, Kang X J, and Srinivas S P (1998) Reevaluation of Cl-/HCO3- exchange in cultured bovine corneal endothelial cells. *Invest Ophthalmol Vis Sci* 39: 2713-2722.

Borish E T, Pryor W A, Venugopal S, and Deutsch W A (1987) DNA synthesis is blocked by cigarette tar-induced DNA single-strand breaks. *Carcinogenesis* 8: 1517-1520.

Borowitz D, Baker R D, and Stallings V (2002) Consensus report on nutrition for pediatric patients with CF. *J Pediatr Gastroenterol Nutr* 35: 246-259.

Borowitz D, Robinson K A, Rosenfeld M, Davis S D, Sabadosa K A, and al. e (2009) Cystic Fibrosis Foundation evidence based guidelines for management of infants with cystic fibrosis. *J Pediatr* 155: S73-93.

Bosl M R, Stein V, Hubner C, Zdebik A A, Jordt S E, Mukhopadhyay A K, Davidoff M S et al. (2001) Male germ cells and photoreceptors, both dependent on close cell-cell interactions, degenerate upon ClC-2 Cl(-) channel disruption. *EMBO J* 20: 1289-1299.

Botelho S Y, Goldstein A M, and Rosenlund M L (1973) Tear sodium, potassium, chloride, and calcium at various flow rates: Children with cystic fibrosis and unaffected siblings with and without corneal staining. *The Journal of Pediatrics* 83: 601-606.

Boucher R C (2007) Airway surface dehydration in cystic fibrosis: pathogenesis and therapy. *Annu Rev Med* 58: 157-170.

Bradley S, Solin P, Wilson J, Johns D, Walters E H, and Naughton M T (1999) Hypoxemia and hypercapnia during exercise and sleep in patients with cystic fibrosis. *Chest* 116: 647-654.

Brainard D H (1989) Calibration of a computer controlled color monitor. *Color Research and Application* 14: 23-34.

Brainard D H (1997) The Psychophysics Toolbox. *Spatial Vision* 10: 433-436.

Brainard D H, Pelli D G, and Robson T (2002) Display characterization. In: Hornak J [ed.] *The encyclopedia of imaging science and technology*. New York: Wiley, pp. 172-188.

Brennan A L, Geddes D M, Gyi K M, and Baker E H (2004) Clinical importance of cystic fibrosis-related diabetes. *Journal of Cystic Fibrosis* 3: 209-222.

Bressler N M, Edwards A R, Antoszyk A N, Beck R W, Browning D J, Ciardella A P, Danis R P et al. (2008) Retinal thickness on Stratus optical coherence tomography in people with diabetes and minimal or no diabetic retinopathy. *Am J Ophthalmol* 145: 894-901.

Bressler S B, Maguire M G, Bressler N M, and Fine S L (1990) Relationship of drusen and abnormalities of the retinal pigment epithelium to the prognosis of neovascular macular degeneration. The Macular Photocoagulation Study Group. *Arch Ophthalmol* 108: 1442-1447.

Bron A J, Tiffany J M, Gouveia S M, Yokoi N, and Voon L W (2004) Functional aspects of the tear film lipid layer. *Exp Eye Res* 78: 347-360.

Brooks L, H., Driebe W T, and Schemmer G G (1990) Xerophthalmia and Cystic Fibrosis. *Arch Ophthalmol* 108: 354-357.

Brown D M, Kaiser P K, Michels M, Soubrane G, Heier J S, Kim R Y, Sy J P et al. (2006) Ranibizumab versus verteporfin for neovascular age-related macular degeneration. *N Engl J Med* 355: 1432-1444.

Brown R K, and Kelly F J (1994) Evidence for increased oxidative damage in patients with cystic fibrosis. *Pediatr Res* 36: 487-493.

Browning D J, Fraser C M, and Clark S (2008) The Relationship of Macular Thickness to Clinically Graded Diabetic Retinopathy Severity in Eyes without Clinically Detected Diabetic Macular Edema. *Ophthalmology* 115: 533-539.e532.

Brownlee M (2005) The pathobiology of diabetic complications: a unifying mechanism. *Diabetes* 54: 1615-1625.

Bruce A, Pacey I E, Dharni P, Scally A J, and Barrett B T (2009) Repeatability and reproducibility of macular thickness measurements using fourier domain optical coherence tomography. *Open Ophthalmol J* 3: 10-14.

Bruce G M, Denning C R, and Spalter H F (1960) Ocular findings in Cystic Fibrosis of the Pancreas. A preliminary report. *Archives of Ophthalmology* 63: 391-401.

Buntain H M, Greer R M, Schluter P J, Wong J C, Batch J A, Potter J M, Lewindon P J et al. (2004) Bone mineral density in Australian children, adolescents and adults with cystic fibrosis: a controlled cross sectional study. *Thorax* 59: 149-155.

Burney T J, and Davies J C (2012) Gene therapy for the treatment of cystic fibrosis. *Appl Clin Genet* 5: 29-36.

Bursell S E, Clermont A C, Kinsley B T, Simonson D C, Aiello L M, and Wolpert H A (1996) Retinal blood flow changes in patients with insulin-dependent diabetes mellitus and no diabetic retinopathy. *Invest Ophthalmol Vis Sci* 37: 886-897.

Campbell D C, Tole D M, Doran R M L, and Conway S P (1998) Vitamin A deficiency in cystic fibrosis resulting in xerophthalmia. *Journal of Human Nutrition and Dietetics* 11: 529-532.

Campbell F W, and Rushton W A (1955) Measurement of the scotopic pigment in the living human eye. *J Physiol* 130: 131-147.

Candia O A (2004) Electrolyte and fluid transport across corneal, conjunctival and lens epithelia. *Exp Eye Res* 78: 527-535.

Cantin A M, White T B, Cross C E, Forman H J, Sokol R J, and Borowitz D (2007) Antioxidants in cystic fibrosis. Conclusions from the CF antioxidant workshop, Bethesda, Maryland, November 11-12, 2003. *Free Radic Biol Med* 42: 15-31.

Cao L, Zhang X D, Liu X, Chen T Y, and Zhao M (2010) Chloride channels and transporters in human corneal epithelium. *Exp Eye Res* 90: 771-779.

Caprara C, and Grimm C (2012) From oxygen to erythropoietin: relevance of hypoxia for retinal development, health and disease. *Prog Retin Eye Res* 31: 89-119.

Carlson A, and Bok D (1992) Promotion of the release of 11-cis-retinal from cultured retinal pigment epithelium by interphotoreceptor retinoid-binding protein. *Biochemistry* 31: 9056-9062.

Castagna I, Roszkowska A M, Fama F, Sinicropi S, and Ferreri G (2001) The eye in cystic fibrosis. *Eur J Ophthalmol* 11: 9-14.

Cawood T J, McKenna M J, Gallagher C G, Smith D, Chung W Y, Gibney J, and O'Shea D (2006) Cystic fibrosis-related diabetes in adults. *Ir Med J* 99: 83-86.

Chan A, Duker J S, Ko T H, Fujimoto J G, and Schuman J S (2006) Normal macular thickness measurements in healthy eyes using Stratus optical coherence tomography. *Arch Ophthalmol* 124: 193-198.

Chen Y, Houghton L A, Brenna J T, and Noy N (1996) Docosahexaenoic acid modulates the interactions of the interphotoreceptor retinoid-binding protein with 11-cis-retinal. *J Biol Chem* 271: 20507-20515.

Cheng S H, Rich D P, Marshall J, Gregory R J, Welsh M J, and Smith A E (1991) Phosphorylation of the R domain by cAMP-dependent protein kinase regulates the CFTR chloride channel. *Cell* 66 (5): 1027-1036.

Chiu C J, and Taylor A (2007) Nutritional antioxidants and age-related cataract and maculopathy. *Exp Eye Res* 84: 229-245.

Cho E, Hung S, Willett W C, Spiegelman D, Rimm E B, Seddon J M, Colditz G A et al. (2001) Prospective study of dietary fat and the risk of age-related macular degeneration. *Am J Clin Nutr* 73: 209-218.

Christen W G, Glynn R J, Manson J E, Ajani U A, and Buring J E (1996) A prospective study of cigarette smoking and risk of age-related macular degeneration in men. *JAMA* 276: 1147-1151.

Christoforidis J, and Zhang X (2011) Learning effect of dark adaptation among normal subjects. *Graefes Arch Clin Exp Ophthalmol* 249: 1345-1352.

Cideciyan A V, Pugh Jr. E N, Lamb T D, Huang Y, and Jacobson S G (1997) Rod plateaux during dark adaptation in Sorby's fundus dystrophy and vitamin A deficiency. *Invest Ophthalmol Vis Sci* 38: 1786-1794.

Ciulla T A, Harris A, Chung H S, Danis R P, Kagemann L, McNulty L, Pratt L M et al. (1999) Color Doppler imaging discloses reduced ocular blood flow velocities in nonexudative age-related macular degeneration. *Am J Ophthalmol* 128: 75-80.

Ciulla T A, Harris A, Latkany P, Piper H C, Arend O, Garzozi H, and Martin B (2002) Ocular perfusion abnormalities in diabetes. *Acta Ophthalmol Scand* 80: 468-477.

Ciulla T A, Harris A, and Martin B J (2001) Ocular perfusion and age-related macular degeneration. *Acta Ophthalmol Scand* 79: 108-115.

Clermont A C, and Bursell S E (2007) Retinal blood flow in diabetes. *Microcirculation* 14: 49-61.

Cogan D G, and Kuwabara T (1963) CAPILLARY SHUNTS IN THE PATHOGENESIS OF DIABETIC RETINOPATHY. *Diabetes* 12: 293-300.

Coile D C, and Baker H D (1992) Foveal dark adaptation, photopigment regeneration, and aging. *Vis Neurosci* 8: 27-39.

Colombo C, Battezzati P M, Crosignani A, Morabito A, Costantini D, Padoan R, and Giunta A (2002) Liver disease in cystic fibrosis: a prospective study on incidence, risk factors and outcome. *Hepatology* 36: 1374-1382.

Comeau A M, Parad R B, Dorkin H L, Dovey M, Gerstle R, Haver K, Lapey A et al. (2004) Population-based newborn screening for genetic disorders when multiple mutation DNA testing is incorporated: a cystic fibrosis newborn screening model demonstrating increased sensitivity but more carrier detections. *Pediatrics* 113: 1573-1581.

Constable P A, Lawrenson J G, and Arden G B (2006) Light and alcohol evoked electro-oculograms in cystic fibrosis. *Doc Ophthalmol* 113: 133-143.

Costa R A, Skaf M, Melo L A, Jr., Calucci D, Cardillo J A, Castro J C, Huang D et al. (2006) Retinal assessment using optical coherence tomography. *Prog Retin Eye Res* 25: 325-353.

Couce M, O'Brien T D, Moran A, Roche P C, and Butler P C (1996) Diabetes mellitus in cystic fibrosis is characterized by islet amyloidosis. *J Clin Endocrinol Metab* 81: 1267-1272.

Crabb J W, Miyagi M, Gu X, Shadrach K, West K A, Sakaguchi H, Kamei M et al. (2002) Drusen proteome analysis: an approach to the etiology of age-related macular degeneration. *Proc Natl Acad Sci U S A* 99: 14682-14687.

Cringle S J, Yu D Y, Yu P K, and Su E N (2002) Intraretinal oxygen consumption in the rat in vivo. *Invest Ophthalmol Vis Sci* 43: 1922-1927.

Crossley J R, Smith P A, Edgar B W, Gluckman P D, and Elliott R B (1981) Neonatal screening for cystic fibrosis, using immunoreactive trypsin assay in dried blood spots. *Clin Chim Acta* 113: 111-121.

Cruickshanks K J, Klein R, and Klein B E (1993) Sunlight and age-related macular degeneration. The Beaver Dam Eye Study. *Arch Ophthalmol* 111: 514-518.

Curcio C A, Medeiros N E, and Millican C L (1996) Photoreceptor loss in age-related macular degeneration. *Invest Ophthalmol Vis Sci* 37: 1236-1249.

Curcio C A, Millican C L, Allen K A, and Kalina R E (1993) Aging of the human photoreceptor mosaic: evidence for selective vulnerability of rods in central retina. *Invest Ophthalmol Vis Sci* 34: 3278-3296.

Curcio C A, Sloan K R, Jr., Packer O, Hendrickson A E, and Kalina R E (1987) Distribution of cones in human and monkey retina: individual variability and radial asymmetry. *Science* 236: 579-582.

Curcio C A, Sloan K R, Kalina R E, and Hendrickson A E (1990) Human photoreceptor topography. *J Comp Neurol* 292: 497-523.

Curtis T M, Gardiner T A, and Stitt A W (2009) Microvascular lesions of diabetic retinopathy: clues towards understanding pathogenesis? *Eye (Lond)* 23: 1496-1508.

Cystic Fibrosis Foundation (2009) *National Patient Registry Annual Data Report*. Bethesda, Maryland: Cystic Fibrosis Foundation.

Cystic Fibrosis Foundation (2011) *Patient Registry: Annual Data Report 2008*. Bethesda, Maryland: Cystic Fibrosis Foundation.

Cystic Fibrosis Trust (2013) *Cystic Fibrosis Trust Annual Data Report 2011*. Chair Bilton D. Kent: Cystic Fibrosis Trust.

Danis R P, Glassman A R, Aiello L P, Antoszyk A N, Beck R W, Browning D J, Ciardella A P et al. (2006) Diurnal variation in retinal thickening measurement by optical coherence tomography in center-involved diabetic macular edema. *Arch Ophthalmol* 124: 1701-1707.

Dankert-Roelse J E, and Merelle M E (2005) Review of outcomes of neonatal screening for cystic fibrosis versus non-screening in Europe. *J Pediatr* 147: S15-20.

Dartnall H J (1972) Visual pigment of the coelacanth. *Nature* 239: 341-342.

Dartt D A (2002) Regulation of mucin and fluid secretion by conjunctival epithelial cells. *Progress in Retinal and Eye Research* 21: 555-576.

Darzins P, Mitchell P, and Heller R F (1997) Sun exposure and age-related macular degeneration. An Australian case-control study. *Ophthalmology* 104: 770-776.

Daubs J G (1975) Diabetes screening with corneal aesthesiometer. *Am J Optom Physiol Opt* 52: 31-35.

Davidson D J, and Dorin J R (2001) A model of the proposed structure of the cystic fibrosis transmembrane conductance regulator (CFTR). *Expert Reviews in Molecular Medicine*.

Davies N, Akhtar S, Turner H C, Candia O A, To C H, and Guggenheim J A (2004) Chloride channel gene expression in the rabbit cornea. *Mol Vis* 10: 1028-1037.

Davis P B (2006) Cystic fibrosis since 1938. *American Journal of Respiratory and Critical Care Medicine* 173: 475-482.

de Grip W J, Daemen F J, and Bonting S L (1972) Enrichment of rhodopsin in rod outer segment membrane preparations. Biochemical aspects of the visual process. 18. *Vision Res* 12: 1697-1707.

Dean F M, Arden G B, and Dornhorst A (1997) Partial reversal of protan and tritan colour defects with inhaled oxygen in insulin dependent diabetic subjects. *Br J Ophthalmol* 81: 27-30.

Delaey C, and Van De Voorde J (2000) Regulatory mechanisms in the retinal and choroidal circulation. *Ophthalmic Res* 32: 249-256.

Delmelle M (1978) Retinal sensitized photodynamic damage to liposomes. *Photochem Photobiol* 28: 357-360.

Delori F C, Dorey C K, Staurenghi G, Arend O, Goger D G, and Weiter J J (1995) In vivo fluorescence of the ocular fundus exhibits retinal pigment epithelium lipofuscin characteristics. *Invest Ophthalmol Vis Sci* 36: 718-729.

Demir M, Dirim B, Acar Z, x, lmaz M, and Sendul Y (2013) Cental Macular Thickness in Patients with Type 2 Diabetes Mellitus without Clinical Retinopathy. *Journal of Ophthalmology* 2013: 4.

Di Leo M A, Caputo S, Falsini B, Porciatti V, Minnella A, Greco A V, and Ghirlanda G (1992) Nonselective loss of contrast sensitivity in visual system testing in early type I diabetes. *Diabetes Care* 15: 620-625.

di Sant'Agnese P A (1968) Guest editorial-Fertility and the young adult with cystic fibrosis. *New England Journal of Medicine* 279: 103-105.

Dimitrov P N, Guymer R H, Zele A J, Anderson A J, and Vingrys A J (2008) Measuring rod and cone dynamics in age-related maculopathy. *Invest Ophthalmol Vis Sci* 49: 55-65.

Ditzel J (1972) Impaired oxygen release caused by alterations of the metabolism in the erythrocytes in diabetes. *Lancet* 1: 721-723.

Dodge J A, and Turck D (2006) Cystic fibrosis: nutritional consequences and management. *Best Pract Res Clin Gastroenterol* 20: 531-546.

Dolan Jr T F (1986) Microangiopathy in a young adult with cystic fibrosis-related diabetes. *Diabet Med* 20: 425-436.

Donaldson S H, Bennett W D, Zeman K L, Knowles M R, Tarran R, and Boucher R C (2006) Mucus Clearance and Lung Function in Cystic Fibrosis with Hypertonic Saline. *New England Journal of Medicine* 354: 241-250.

Donoso L A, Kim D, Frost A, Callahan A, and Hageman G (2006) The role of inflammation in the pathogenesis of age-related macular degeneration. *Surv Ophthalmol* 51: 137-152.

Dorey C K, Wu G, Ebenstein D, Garsd A, and Weiter J J (1989) Cell loss in the aging retina. Relationship to lipofuscin accumulation and macular degeneration. *Invest Ophthalmol Vis Sci* 30: 1691-1699.

Dowling J E (1960) Chemistry of visual adaptation in the rat. *Nature* 188: 114-118.

Drasdo N, Chiti Z, Owens D R, and North R V (2002) Effect of darkness on inner retinal hypoxia in diabetes. *Lancet* 359: 2251-2253.

Drasdo N, and Fowler C W (1974) Non-linear projection of the retinal image in a wide-angle schematic eye. *Br J Ophthalmol* 58: 709-714.

Drexler W (2004) Ultrahigh-resolution optical coherence tomography. *J Biomed Opt* 9: 47-74.

Drexler W, and Fujimoto J G (2008) State-of-the-art retinal optical coherence tomography. *Prog Ret Res* 27: 45-88.

Duan X R, Liang Y B, Friedman D S, Sun L P, Wong T Y, Tao Q S, Bao L et al. (2010) Normal macular thickness measurements using optical coherence tomography in healthy eyes of adult Chinese persons: the Handan Eye Study. *Ophthalmology* 117: 1585-1594.

Durie P R (2000) Pancreatic aspects of cystic fibrosis and other inherited causes of pancreatic dysfunction. *Medical Clinics of North America* 84: 609-620.

EDCCS (1993) Antioxidant status and neovascular age-related macular degeneration. Eye Disease Case-Control Study Group. *Arch Ophthalmol* 111: 104-109.

Edwards R B, and Adler A J (2000) IRBP enhances removal of 11- cis -retinaldehyde from isolated RPE membranes. *Exp Eye Res* 70: 235-245.

Eigen H, Rosenstein B J, FitzSimmons S C, and Schidlow D V (1995) Cystic fibrosis Foundation Prednisone Trial Group. A multicentre study of alternate-day prednisone therapy in patients with cystic fibrosis. *J Pediatr* 126: 515-523.

Eisenfeld A J, Bint-Milam A H, and Saari J C (1985) Localization of retinoid-binding proteins in developing rat retina. *Exp Eye Res* 41: 299-304.

Ejaz S, Chekarova I, Ejaz A, Sohail A, and Lim C W (2008) Importance of pericytes and mechanisms of pericyte loss during diabetes retinopathy. *Diabetes Obes Metab* 10: 53-63.

El-Dairi M A, Asrani S G, Enyedi L B, and Freedman S F (2009) Optical coherence tomography in the eyes of normal children. *Arch Ophthalmol* 127: 50-58.

Eriksson U, and Alm A (2009) Macular thickness decreases with age in normal eyes: a study on the macular thickness map protocol in the Stratus OCT. *Br J Ophthalmol* 93: 1448-1452.

Esmaeelpour M, Považay B, Hermann B, Hofer B, Kajic V, Hale S L, North R V et al. (2011) Mapping Choroidal and Retinal Thickness Variation in Type 2 Diabetes using Three-Dimensional 1060-nm Optical Coherence Tomography. *Invest Ophthalmol Vis Sci* 52: 5311-5316.

Evans J R (2001) Risk factors for age-related macular degeneration. *Prog Retin Eye Res* 20: 227-253.

Evans J R, Schwartz S D, McHugh J D, Thamby-Rajah Y, Hodgson S A, Wormald R P, and Gregor Z J (1998) Systemic risk factors for idiopathic macular holes: a case-control study. *Eye (Lond)* 12 (Pt 2): 256-259.

Evans K S E (2009) *Cystic Fibrosis and the Eye*. Cardiff University.

Fallon T J, Maxwell D, and Kohner E M (1985) Retinal vascular autoregulation in conditions of hyperoxia and hypoxia using the blue field entoptic phenomenon. *Ophthalmology* 92: 701-705.

Fallon T J, Sleightholm M A, Merrick C, Chahal P, and Kohner E M (1987) The effect of acute hyperglycemia on flow velocity in the macular capillaries. *Invest Ophthalmol Vis Sci* 28: 1027-1030.

Fama F, Castagna I, Palamara F, Roszkowska A M, and Ferreri P (1998) Cystic Fibrosis and Lens Opacity. *Ophthalmologica* 212: 178-179.

Fama F, Castagna I, and Salmeri G (1993) Influence of pseudoexfoliation in human lens transparency. *Ann Ophthalmol* 25: 12-14.

Feeney-Burns L, Hilderbrand E S, and Eldridge S (1984) Aging human RPE: morphometric analysis of macular, equatorial, and peripheral cells. *Invest Ophthalmol Vis Sci* 25: 195-200.

Feigl B (2009) Age-related maculopathy - linking aetiology and pathophysiological changes to the ischaemia hypothesis. *Prog Retin Eye Res* 28: 63-86.

Feke G T, Buzney S M, Ogasawara H, Fujio N, Goger D G, Spack N P, and Gabbay K H (1994) Retinal circulatory abnormalities in type 1 diabetes. *Invest Ophthalmol Vis Sci* 35: 2968-2975.

Feke G T, Zuckerman R, Green G J, and Weiter J J (1983) Response of human retinal blood flow to light and dark. *Invest Ophthalmol Vis Sci* 24: 136-141.

Feranchak A P, Sontag M K, Wagener J S, Hammond K B, Accurso F J, and Sokol R J (1999) Prospective, long-term study of fat-soluble vitamin status in children with cystic fibrosis identified by newborn screen. *J Pediatr* 135: 601-610.

Fesenko E E, Kolesnikov S S, and Lyubarsky A L (1985) Induction by cyclic GMP of cationic conductance in plasma membrane of retinal rod outer segment. *Nature* 313: 310-313.

Fine S L, Berger J W, Maguire M G, and Ho A C (2000) Age-related macular degeneration. *N Engl J Med* 342: 483-492.

Finkelstein S M, Wielinski C L, Elliott G R, Warwick W J, Barbosa J, Wu S C, and Klein D J (1988) Diabetes mellitus associated with cystic fibrosis. *J Pediatr* 112: 373-377.

Fischbarg J, and Montoreano R (1982) Osmotic permeabilities across corneal endothelium and antidiuretic hormone-stimulated toad urinary bladder structures. *Biochem*. *Biophys*. *Acta* 690: 207-214.

Fishman G A, and Sokol S (1990) *Electrophysiologic testing in disorders of the retina, optic nerve and visual pathway*. San Francisco: American Academy of Ophthalmology.

Flammer J, and Mozaffarieh M (2008) Autoregulation, a balancing act between supply and demand. *Can J Ophthalmol* 43: 317-321.

Fong D S, Aiello L, Gardner T W, King G L, Blankenship G, Cavallerano J D, Ferris F L et al. (2004) Diabetic retinopathy. *Diabetes Care* 27: 2540-2553.

Frangolias D D, and Wilcox P G (2001) Predictability of oxygen desaturation during sleep in patients with cystic fibrosis : clinical, spirometric, and exercise parameters. *Chest* 119: 434-441.

Fraser-Bell S, Guzowski M, Rochtchina E, Wang J J, and Mitchell P (2003) Five-year cumulative incidence and progression of epiretinal membranes: the Blue Mountains Eye Study. *Ophthalmology* 110: 34-40.

Friedman D S, and He M (2008) Anterior chamber angle assessment techniques. *Surv Ophthalmol* 53: 250-273.

Friedman D S, Katz J, Bressler N M, Rahmani B, and Tielsch J M (1999) Racial differences in the prevalence of age-related macular degeneration: the Baltimore Eye Survey. *Ophthalmology* 106: 1049-1055.

Friedman D S, O'Colmain B J, Munoz B, Tomany S C, McCarty C, de Jong P T, Nemesure B et al. (2004) Prevalence of age-related macular degeneration in the United States. *Arch Ophthalmol* 122: 564-572.

Friedman E, Krupsky S, Lane A M, Oak S S, Friedman E S, Egan K, and Gragoudas E S (1995) Ocular blood flow velocity in age-related macular degeneration. *Ophthalmology* 102: 640-646.

Fuchs H J, Borowitz D S, Christiansen D H, Morris E M, Nash M L, Ramsey B W, Rosenstein B J et al. (1994) Effect of aerosolized recombinant human DNase on exacerbations of respiratory symptoms and on pulmonary function in patients with cystic fibrosis. The Pulmozyme Study Group. *N Engl J Med* 331: 637-642.

Fuchsjager-Mayrl G, Malec M, Amoako-Mensah T, Kolodjaschna J, and Schmetterer L (2003) Changes in choroidal blood flow during light/dark transitions are not altered by atropine or propranolol in healthy subjects. *Vision Res* 43: 2185-2190.

Fuchsjager-Mayrl G, Polska E, Malec M, and Schmetterer L (2001) Unilateral light-dark transitions affect choroidal blood flow in both eyes. *Vision Res* 41: 2919-2924.

Fulton A B, Hansen R M, Underwood B A, Shwachman H, and Barg D C (1982) Scotopic thresholds and plasma retinol in cystic fibrosis. *Invest Ophthalmol Vis Sci* 23: 364-370.

Gadsby D C (2009) Ion channels versus ion pumps: the principle difference, in principle. *Nature Reviews Molecular Cell Biology* 10: 344-352.

Gaffney A J (2012) *Characterising adaptational dysfunction in age-related macular degeneration* Cardiff University

Gaffney A J, Binns A M, and Margrain T H (2011) The repeatability of the Goldmann-Weekers adaptometer for measuring cone adaptation. *Doc Ophthalmol* 122: 71-75.

Gaffney A J, Binns A M, and Margrain T H (2012) Aging and cone dark adaptation. *Optom Vis Sci* 89: 1219-1224.

Gaillard E R, Atherton S J, Eldred G, and Dillon J (1995) Photophysical studies on human retinal lipofuscin. *Photochem Photobiol* 61: 448-453.

Gallemore R P, and Steinberg R H (1993) Light-evoked modulation of basolateral membrane Cl^- conductance in chick retinal pigment epithelium: the light peak and fast oscillation. *J Neurophysiol* 70: 1669-1680.

Galli F, Battistoni A, Gambari R, Pompella A, Bragonzi A, Pilolli F, Iuliano L et al. (2012) Oxidative stress and antioxidant therapy in cystic fibrosis. *Biochim Biophys Acta* 1822: 690-713.

Gamble R C (1940) Keratomalacia and cystic fibrosis of the pancreas. *Am J Ophthalmol* 23: 539-544.

Gao H, and Hollyfield J G (1992) Aging of the human retina: differential loss of neurons and retinal pigment epithelial cells. *Invest Ophthalmol Vis Sci* 33: 1-17.

Gao L, Kim K J, Yankaskas J R, and Forman H J (1999) Abnormal glutathione transport in cystic fibrosis airway epithelia. *Am J Physiol* 277: L113-118.

Gass J D (2003) Drusen and disciform macular detachment and degeneration. 1972. *Retina* 23: 409-436.

Geiser M H, Riva C E, Dorner G T, Diermann U, Luksch A, and Schmetterer L (2000) Response of choroidal blood flow in the foveal region to hyperoxia and hyperoxia-hypercapnia. *Curr Eye Res* 21: 669-676.

Giani A, Cigada M, Choudhry N, Deiro A P, Oldani M, Pellegrini M, Invernizzi A et al. (2010) Reproducibility of retinal thickness measurements on normal and pathologic eyes by different optical coherence tomography instruments. *Am J Ophthalmol* 150: 815-824.

Gibson L E, and Cooke R E (1959) A test for concentration of electrolytes in sweat in cystic fibrosis of the pancreas utilizing pilocarpine by iontophoresis. *Pediatrics* 23: 545-549.

Gilmore E D, Hudson C, Nrusimhadevara R K, Harvey P T, Mandelcorn M, Lam W C, and Devenyi R G (2007a) Retinal arteriolar diameter, blood velocity, and blood flow response to an isocapnic hyperoxic provocation in early sight-threatening diabetic retinopathy. *Invest Ophthalmol Vis Sci* 48: 1744-1750.

Gilmore E D, Hudson C, Nrusimhadevara R K, Ridout R, Harvey P T, Mandelcorn M, Lam W C et al. (2007b) Retinal arteriolar hemodynamic response to an acute hyperglycemic provocation in early and sight-threatening diabetic retinopathy. *Microvasc Res* 73: 191-197.

Gilmore E D, Hudson C, Nrusimhadevara R K, Ridout R, Harvey P T, Mandelcorn M, Lam W C et al. (2008) Retinal arteriolar hemodynamic response to a combined isocapnic hyperoxia and glucose provocation in early sight-threatening diabetic retinopathy. *Invest Ophthalmol Vis Sci* 49: 699-705.

Gobel W, Hartmann F, and Haigis W (2001) [Determination of retinal thickness in relation to the age and axial length using optical coherence tomography]. *Ophthalmologe* 98: 157-162.

Goldberg J, Flowerdew G, Smith E, Brody J A, and Tso M O (1988) Factors associated with age-related macular degeneration. An analysis of data from the first National Health and Nutrition Examination Survey. *Am J Epidemiol* 128: 700-710.

Golden T R, and Melov S (2001) Mitochondrial DNA mutations, oxidative stress, and aging. *Mech Ageing Dev* 122: 1577-1589.

Golestaneh N, Nicolas C, Picaud S, Ferrari P, and Mirshahi M (2000) The epithelial sodium channel (ENaC) in rodent retina, ontogeny and molecular identity. *Curr Eye Res* 21: 703-709.

Gollapalli D R, Maiti P, and Rando R R (2003) RPE65 operates in the vertebrate visual cycle by stereospecifically binding all-trans-retinyl esters. *Biochemistry* 42: 11824-11830.

Gollapalli D R, and Rando R R (2003) Specific inactivation of isomerohydrolase activity by 11-cis-retinoids. *Biochim Biophys Acta* 1651: 93-101.

Gottfredsdottir M S, Sverrisson T, Musch D C, and Stefansson E (1999) Age related macular degeneration in monozygotic twins and their spouses in Iceland. *Acta Ophthalmol Scand* 77: 422-425.

Gottsch J D, Bynoe L A, Harlan J B, Rencs E V, and Green W R (1993) Light-induced deposits in Bruch's membrane of protoporphyric mice. *Arch Ophthalmol* 111: 126-129.

Grahn B H, Paterson P G, Gottschall-Pass K T, and Zhang Z (2001) Zinc and the eye. *J Am Coll Nutr* 20: 106-118.

Green W R, and Key S N, 3rd (1977) Senile macular degeneration: a histopathologic study. *Trans Am Ophthalmol Soc* 75: 180-254.

Greenstein V C, Thomas S R, Blaustein H, Koenig K, and Carr R E (1993) Effects of early diabetic retinopathy on rod system sensitivity. *Optom Vis Sci* 70: 18-23.

Grey V, Atkinson S, Drury D, Casey L, Ferland G, Gundberg C, and Lands L C (2008) Prevalence of low bone mass and deficiencies of vitamins D and K in pediatric patients with cystic fibrosis from 3 Canadian centers. *Pediatrics* 122: 1014-1020.

Griesenbach U, and Alton E W (2009) Gene transfer to the lung: lessons learned from more than 2 decades of CF gene therapy. *Adv Drug Deliv Rev* 61: 128-139.

Griesenbach U, and Alton E W (2013) Moving forward: cystic fibrosis gene therapy. *Hum Mol Genet*.

Grizzard S W, Arnett D, and Haag S L (2003) Twin study of age-related macular degeneration. *Ophthalmic Epidemiol* 10: 315-322.

Grossniklaus H E, Cingle K A, Yoon Y D, Ketkar N, L'Hernault N, and Brown S (2000) Correlation of histologic 2-dimensional reconstruction and confocal scanning laser microscopic imaging of choroidal neovascularization in eyes with age-related maculopathy. *Arch Ophthalmol* 118: 625-629.

Grossniklaus H E, Ling J X, Wallace T M, Dithmar S, Lawson D H, Cohen C, Elner V M et al. (2002) Macrophage and retinal pigment epithelium expression of angiogenic cytokines in choroidal neovascularization. *Mol Vis* 8: 119-126.

Groth S, Stafanger G, Dirksen H, Andersen J B, Falk M, and Kelstrup M (1985) Positive expiratory pressure (PEP-mask) physiotherapy improves ventilation and reduces volume of trapped gas in cystic fibrosis. *Bull Eur Physiopathol Respir* 21: 339-343.

Grunwald J E, Brucker A J, Grunwald S E, and Riva C E (1993) Retinal hemodynamics in proliferative diabetic retinopathy. A laser Doppler velocimetry study. *Invest Ophthalmol Vis Sci* 34: 66-71.

Grunwald J E, Hariprasad S M, DuPont J, Maguire M G, Fine S L, Brucker A J, Maguire A M et al. (1998) Foveolar choroidal blood flow in age-related macular degeneration. *Invest Ophthalmol Vis Sci* 39: 385-390.

Grunwald J E, Metelitsina T I, Dupont J C, Ying G S, and Maguire M G (2005) Reduced foveolar choroidal blood flow in eyes with increasing AMD severity. *Invest Ophthalmol Vis Sci* 46: 1033-1038.

Grunwald J E, Riva C E, Brucker A J, Sinclair S H, and Petrig B L (1984a) Altered retinal vascular response to 100% oxygen breathing in diabetes mellitus. *Ophthalmology* 91: 1447-1452.

Grunwald J E, Riva C E, Martin D B, Quint A R, and Epstein P A (1987) Effect of an insulin-induced decrease in blood glucose on the human diabetic retinal circulation. *Ophthalmology* 94: 1614-1620.

Grunwald J E, Riva C E, Petrig B L, Sinclair S H, and Brucker A J (1984b) Effect of pure O2-breathing on retinal blood flow in normals and in patients with background diabetic retinopathy. *Curr Eye Res* 3: 239-241.

Gupta B, Grewal J, Adewoyin T, Pelosini L, and Williamson T H (2009) Diurnal variation of macular oedema in CRVO: prospective study. *Graefes Arch Clin Exp Ophthalmol* 247: 593-596.

Guymer R, Luthert P, and Bird A (1999) Changes in Bruch's membrane and related structures with age. *Prog Retin Eye Res* 18: 59-90.

Hageman G S, Luthert P J, Victor Chong N H, Johnson L V, Anderson D H, and Mullins R F (2001) An integrated hypothesis that considers drusen as biomarkers of immune-mediated processes at the RPE-Bruch's membrane interface in aging and age-related macular degeneration. *Prog Retin Eye Res* 20: 705-732.

Hageman G S, and Mullins R F (1999) Molecular composition of drusen as related to substructural phenotype. *Mol Vis* 5: 28.

Hageman G S, Mullins R F, Russell S R, Johnson L V, and Anderson D H (1999) Vitronectin is a constituent of ocular drusen and the vitronectin gene is expressed in human retinal pigmented epithelial cells. *FASEB J* 13: 477-484.

Hahn T J, Squires A E, Halstead L R, and Strominger D B (1979) Reduced serum 25-hydroxyvitamin D concentration and disordered mineral metabolism in patients with cystic fibrosis. *J Pediatr* 94: 38-42.

Haimovici R, Owens S L, Fitzke F W, and Bird A C (2002) Dark adaptation in age-related macular degeneration: relationship to the fellow eye. *Graefes Arch Clin Exp Ophthalmol* 240: 90-95.

Hall N F, Gale C R, Syddall H, Phillips D I, and Martyn C N (2001) Risk of macular degeneration in users of statins: cross sectional study. *BMJ* 323: 375-376.

Hamann S, Zeuthen T, La Cour M, Nagelhus E A, Ottersen O P, Agre P, and Nielsen S (1998) Aquaporins in complex tissues: distribution of aquaporins 1-5 in human and rat eye. *Am J Physiol* 274: C1332-1345.

Hangai M, Murata T, and Miyawaki N (2001) Angiopoietin-1 upregulation by vascular endothelial growth factor in human retinal pigment epithelial cells. *Invest Ophthalmol Vis Sci* 42: 1617.

Hansen L G, and Warwick W J (1990) High-freuency chest compression system to aid in clearance of mucous from the lung. *Biomed Instrum Technol* 24: 289-294.

Hardarson S H, Basit S, Jonsdottir T E, Eysteinsson T, Halldorsson G H, Karlsson R A, Beach J M et al. (2009) Oxygen saturation in human retinal vessels is higher in dark than in light. *Invest Ophthalmol Vis Sci* 50: 2308-2311.

Harosi F I (1975) Absorption spectra and linear dichroism of some amphibian photoreceptors. *J Gen Physiol* 66: 357-382.

Harris A, Arend O, Danis R P, Evans D, Wolf S, and Martin B J (1996) Hyperoxia improves contrast sensitivity in early diabetic retinopathy. *Br J Ophthalmol* 80: 209-213.

Haugh-Scheidt L M, Linsenmeier R A, and Griff E R (1995) Oxygen consumption in the isolated toad retina. *Exp Eye Res* 61: 63-72.

Havelius U, Hansen F, Hindfelt B, and Krakau T (1999) Human ocular vasodynamic changes in light and darkness. *Invest Ophthalmol Vis Sci* 40: 1850-1855.

Hayreh S S (1975) Segmental nature of the choroidal vasculature. *Br J Ophthalmol* 59: 631-648.

Hecht S (1937) Rods, cones. and the chemical basis of vision. *Physiological Reviews* 17: 239-290.

Hecht S, Haig C, and Chase A M (1937) The influence of light adaptation on subsequent dark adaptation of the eye. *J Gen Physiol* 20: 831-850.

Hecht S, Haig C, and Wald G (1935) The dark adaptation of retinal fields of different size and location. *J Gen Physiol* 19: 321-337.

Heck M, Schadel S A, Maretzki D, and Hofmann K P (2003) Secondary binding sites of retinoids in opsin: characterization and role in regeneration. *Vision Res* 43: 3003-3010.

Heeschen C, Jang J J, Weis M, Pathak A, Kaji S, Hu R S, Tsao P S et al. (2001) Nicotine stimulates angiogenesis and promotes tumor growth and atherosclerosis. *Nat Med* 7: 833-839.

Henson D B, and North R V (1979) Dark adaptation in diabetes mellitus. *Br J Ophthalmol* 63: 539-541.

Heriot W J, Henkind P, Bellhorn R W, and Burns M S (1984) Choroidal neovascularization can digest Bruch's membrane. A prior break is not essential. *Ophthalmology* 91: 1603-1608.

Hermann B, Fernandez E J, Unterhuber A, Sattmann H, Fercher A F, Drexler W, Prieto P M et al. (2004) Adaptive-optics ultrahigh-resolution optical coherence tomography. *Opt Lett* 29: 2142-2144.

Herse P (1995) A new method for quantification of the dynamics of dark adaptation. *Optom Vis Sci* 72: 907-910.

Heuberger R A, Mares-Perlman J A, Klein R, Klein B E, Millen A E, and Palta M (2001) Relationship of dietary fat to age-related maculopathy in the Third National Health and Nutrition Examination Survey. *Arch Ophthalmol* 119: 1833-1838.

Hickam J B, Frayser R, and Ross J C (1963) A study of retinal venous blood oxygen saturation in human subjects by photographic means. *Circulation* 27: 375-385.

Hickam J B, and Sieker H O (1960) Retinal vascular reactivity in patients with diabetes mellitus and with atherosclerosis. *Circulation* 22: 243-246.

Hickam J B, Sieker H O, and Frayser R (1959) Studies of retinal circulation and A-V oxygen difference in man. *Trans Am Clin Climatol Assoc* 71: 34-44.

Hipper A, Mall M, Greger R, and Kunzelmann K (1995) Mutatrion in the putative pore-forming domain of CFTR do not change anion selectivity of the cAMP-activated Cl^- conductance. *FEBS Letters* 374: 312-316.

Ho J, Sull A C, Vuong L N, Chen Y, Liu J, Fujimoto J G, Schuman J S et al. (2009) Assessment of artifacts and reproducibility across spectral- and time-domain optical coherence tomography devices. *Ophthalmology* 116: 1960-1970.

Hoang Q V, Linsenmeier R A, Chung C K, and Curcio C A (2002) Photoreceptor inner segments in monkey and human retina: mitochondrial density, optics, and regional variation. *Vis Neurosci* 19: 395-407.

Hodson S (1974) The regulation of corneal hydration by a salt pump requiring the presence of sodium bicarbonate ions. *J Physiol* 236: 271-302.

Holfort S K, Jackson G R, and Larsen M (2010) Dark adaptation during transient hyperglycemia in type 2 diabetes. *Exp Eye Res* 91: 710-714.

Hollins M, and Alpern M (1973) Dark adaptation and visual pigment regeneration in human cones. *J Gen Physiol* 62: 430-447.

Hollister J R, and Bowyer S L (1987) Adverse side effects of corticosteroids. *Semin Respir Med* 8: 400-405.

Holz F G, Bellman C, Staudt S, Schutt F, and Volcker H E (2001) Fundus autofluorescence and development of geographic atrophy in age-related macular degeneration. *Invest Ophthalmol Vis Sci* 42: 1051-1056.

Huang D, Swanson E A, Lin C P, Schuman J S, Stinson W G, Chang W, Hee M R et al. (1991) Optical coherence tomography. *Science* 254: 1178-1181.

Huang D, Tan O, and Fujimoto J G (2005) Optical Coherence Tomography. In: Huang D, Kaiser P K, Lowder C Y, and Traboulsi E [eds.] *Retinal Imaging*. Elsevier.

Huang J, Liu X, Wu Z, Guo X, Xu H, Dustin L, and Sadda S (2011a) Macular and Retinal Nerve Fiber Layer Thickness Measurements in Normal Eyes With the Stratus OCT, the Cirrus HD-OCT, and the Topcon 3D OCT-1000. *J Glaucoma* 20: 118-125.

Huang J, Liu X, Wu Z, and Sadda S (2011b) Image quality affects macular and retinal nerve fibre layer thickness measurements on fourier-domain optical coherence tomography. *Ophthalmic Surg Lasers Imaging* 31: 1-6.

Huang J, Liu X, Wu Z, Xiao H, Dustin L, and Sadda S (2009) Macular thickness measurements in normal eyes with time-domain and Fourier-domain optical coherence tomography. *Retina* 29: 980-987.

Huet F, Semama D, Maingueneau C, Charavel A, and Nivelon J L (1997) Vitamin A deficiency and nocturnal vision in teenagers with cystic fibrosis. *Eur J Pediatr* 156: 949-951.

Hughes B A, Adorante J S, Miller S S, and Lin H (1989) Apical electrogenic $Na^+HCO_3^-$ cotransport. A mechanism for HCO_3^- absorption across the retinal pigment epithelium. *J Gen Physiol* 94: 125-150.

Hurt K, and Bilton D (2012) Cystic fibrosis. *Medicine* 40: 273-276.

Hyman L, Schachat A P, He Q, and Leske M C (2000) Hypertension, cardiovascular disease, and age-related macular degeneration. Age-Related Macular Degeneration Risk Factors Study Group. *Arch Ophthalmol* 118: 351-358.

Hyman L G, Lilienfeld A M, Ferris F L, 3rd, and Fine S L (1983) Senile macular degeneration: a case-control study. *Am J Epidemiol* 118: 213-227.

Itoh R, Kawamoto S, Miyamoto Y, Kinoshita S, and Okubo K (2000) Isolation and characterization of a Ca2+ activated chloride channel from human corneal epithelium. *Curr Eye Res* 21: 918-925.

Jackson G R, Owsley C, and McGiwin G (1999) Aging and dark adaptation. *Vision Research* 39: 3975-3982.

Jean-Louis S, Lovasik J V, and Kergoat H (2005) Systemic hyperoxia and retinal vasomotor responses. *Invest Ophthalmol Vis Sci* 46: 1714-1720.

Jelamskii S, Sun X C, Herse P, and Bonanno J A (2000) Basolateral Na^+-K^+-$2Cl^-$ cotransport in cultured and fresh bovine corneal endothelium. *Invest Ophthalmol Vis Sci* 41: 488-495.

Jentsch T, Keller S, Koch M, and Wiederholt M (1984) Evidence for coupled transport of bicarbonate and sodium in cultured bovine corneal endothelial cells. *J Membr Biol* 81: 189-204.

Jin M, Li S, Nusinowitz S, Lloyd M, Hu J, Radu R A, Bok D et al. (2009) The role of interphotoreceptor retinoid-binding protein on the translocation of visual retinoids and function of cone photoreceptors. *J Neurosci* 29: 1486-1495.

Jo Y J, Heo D W, Shin Y I, and Kim J Y (2011) Diurnal Variation of Retina Thickness measured with Time Domain and Spectral Domain Optical Coherence Tomography in Normal Subjects. *Invest Ophthalmol Vis Sci*.

Johnson C, Butler S M, Konstan M W, Morgan W J, and Wohl M E (2003) Factors influencing outcomes in cystic fibrosis: a centre-based analysis. *Chest* 123: 20-27.

Johnson L V, Leitner W P, Staples M K, and Anderson D H (2001) Complement activation and inflammatory processes in Drusen formation and age related macular degeneration. *Exp Eye Res* 73: 887-896.

Johnson L V, Ozaki S, Staples M K, Erickson P A, and Anderson D H (2000) A potential role for immune complex pathogenesis in drusen formation. *Exp Eye Res* 70: 441-449.

Justesen B L, Mistry P, Chaturvedi N, Thom S A, Witt N, Kohler D, Hughes A D et al. (2010) Retinal arterioles have impaired reactivity to hyperoxia in type 1 diabetes. *Acta Ophthalmol* 88: 453-457.

Kaercher T, and Bron A J (2008) Classification and diagnosis of dry eye. *Dev Ophthalmol* 41: 36-53.

Kalayci D, Kiper N, Ozcelik U, Gocmen A, and Hasiripi H (1996) Clinical status, ocular surface changes and tear ferning in patients with cystic fibrosis. *Acta Ophthalmol Scand* 74: 563-565.

Kaluzny J J, Wojtkowski M, Sikorski B L, Szkulmowski M, Szkulmowska A, Bajraszewski T, Fujimoto J G et al. (2009) Analysis of the outer retina reconstructed by high-resolution, three-dimensional spectral domain optical coherence tomography. *Ophthalmic Surg Lasers Imaging* 40: 102-108.

Kaplan E, Shwachman H, Perlmutter A D, Rule A, Khaw K-T, and Holsclaw D S (1968) Reproductive failure in males with cystic fibrosis. *New England Journal of Medicine* 279: 65-69.

Kaplan P W, Rawal K, Erwin C W, D'Souzza B J, and Spock A (1988) Visual and somatosensory evoked potentials in vitamin E deficiency with cystic fibrosis. *Electroencephalogr Clin Neurophysiol* 71: 266-272.

Karlet M C (2000) An update on cystic fibrosis and implications for anesthesia. *AANA J* 68: 141-148.

Kashani A H, Zimmer-Galler I E, Shah S M, Dustin L, Do D V, Eliott D, Haller J A et al. (2010) Retinal thickness analysis by race, gender, and age using Stratus OCT. *Am J Ophthalmol* 149: 496-502 e491.

Kawarai M, and Koss M C (1998) Sympathetic vasoconstriction in the rat anterior choroid is mediated by alpha1-adrenoceptors. *Eur J Pharmacol* 363: 35-40.

Kawasaki R, Wang J J, Aung T, Tan D T, Mitchell P, Sandar M, Saw S M et al. (2008) Prevalence of age-related macular degeneration in a Malay population: the Singapore Malay Eye Study. *Ophthalmology* 115: 1735-1741.

Kelty P J, Payne J F, Trivedi R H, Kelty J, Bowie E M, and Burger B M (2008) Macular thickness assessment in healthy eyes based on ethnicity using Stratus OCT optical coherence tomography. *Invest Ophthalmol Vis Sci* 49: 2668-2672.

Kemp C M, Faulkner D J, and Jacobson S G (1988) The distribution and kinetics of visual pigments in the cat retina. *Invest Ophthalmol Vis Sci* 29: 1056-1065.

Kennedy C J, Rakoczy P E, and Constable I J (1995) Lipofuscin of the retinal pigment epithelium: a review. *Eye (Lond)* 9 (Pt 6): 763-771.

Kerem E, Corey M, Kerem B S, Rommens J M, Markiewicz D, Levison H, Tsui L C et al. (1990) The relation between genotype and phenotype in cystic fibrosis analysis the common mutation (F508) *New England Journal of Medicine* 323: 1517-1522.

Kerem E, and Kerem B (1996) Genotype-phenotype correlations in cystic fibrosis. *Pediatric Pulmonology* 22: 387-395.

Kergoat H, and Faucher C (1999) Effects of oxygen and carbogen breathing on choroidal hemodynamics in humans. *Invest Ophthalmol Vis Sci* 40: 2906-2911.

Khandhadia S, Cherry J, and Lotery A J (2012a) Age-related macular degeneration. *Adv Exp Med Biol* 724: 15-36.

Khandhadia S, Cipriani V, Yates J R, and Lotery A J (2012b) Age-related macular degeneration and the complement system. *Immunobiology* 217: 127-146.

Kiel J W (1999) Modulation of choroidal autoregulation in the rabbit. *Exp Eye Res* 69: 413-429.

Kimble E A, Svoboda R A, and Ostroy S E (1980) Oxygen consumption and ATP changes of the vertebrate photoreceptor. *Exp Eye Res* 31: 271-288.

Kinnman N, Lindblad A, Housset C, Buentke E, Scheynius A, Strandvik B, and Hultcrantz R (2000) Expression of cystic fibrosis transmembrane conductance regulator in liver tissue from patients with cystic fibrosis. *Hepatology* 32: 334-340.

Kiss B, Polska E, Dorner G, Polak K, Findl O, Mayrl G F, Eichler H G et al. (2002) Retinal blood flow during hyperoxia in humans revisited: concerted results using different measurement techniques. *Microvasc Res* 64: 75-85.

Klaver C C, Wolfs R C, Assink J J, van Duijn C M, Hofman A, and de Jong P T (1998) Genetic risk of age-related maculopathy. Population-based familial aggregation study. *Arch Ophthalmol* 116: 1646-1651.

Klein B E, and Klein R (1982) Cataracts and macular degeneration in older Americans. *Arch Ophthalmol* 100: 571-573.

Klein B E K, Klein R, and Lee K E (1998) Diabetics, cardiovascular disease, selected cardivascular disease risk factors, and the 5-year incidence of age-related cataract and progression of lens opacities. The Beaver Dam Eye Study. *Am J Ophthalmol* 126: 782-790.

Klein M L, Mauldin W M, and Stoumbos V D (1994a) Heredity and age-related macular degeneration. Observations in monozygotic twins. *Arch Ophthalmol* 112: 932-937.

Klein R, J. C K, D. N S, E.M. K, Javier N F, Huang G H, Pankow J S et al. (2010) The prevalence of age-related macular degeneration and associated risk factors. *Arch Ophthalmol* 128: 750-758.

Klein R, Klein B E, Jensen S C, Cruickshanks K J, Lee K E, Danforth L G, and Tomany S C (2001) Medication use and the 5-year incidence of early age-related maculopathy: the Beaver Dam Eye Study. *Arch Ophthalmol* 119: 1354-1359.

Klein R, Klein B E, Jensen S C, and Meuer S M (1997) The five-year incidence and progression of age-related maculopathy: the Beaver Dam Eye Study. *Ophthalmology* 104: 7-21.

Klein R, Klein B E, and Linton K L (1992) Prevalence of age-related maculopathy. The Beaver Dam Eye Study. *Ophthalmology* 99: 933-943.

Klein R, Klein B E, Marino E K, Kuller L H, Furberg C, Burke G L, and Hubbard L D (2003a) Early age-related maculopathy in the cardiovascular health study. *Ophthalmology* 110: 25-33.

Klein R, Klein B E, and Moss S E (1998) Relation of smoking to the incidence of age-related maculopathy. The Beaver Dam Eye Study. *Am J Epidemiol* 147: 103-110.

Klein R, Klein B E, Tomany S C, and Cruickshanks K J (2003b) Association of emphysema, gout, and inflammatory markers with long-term incidence of age-related maculopathy. *Arch Ophthalmol* 121: 674-678.

Klein R, Klein B E, Wang Q, and Moss S E (1994b) The epidemiology of epiretinal membranes. *Trans Am Ophthalmol Soc* 92: 403-425; discussion 425-430.

Klein R, Meuer S M, Knudtson M D, Iyengar S K, and Klein B E (2008) The epidemiology of retinal reticular drusen. *Am J Ophthalmol* 145: 317-326.

Klein R, Peto T, Bird A, and Vannewkirk M R (2004) Perspective: the epidemiology of age-related macular degeneration. *Am J Ophthalmol* 137: 486-495.

Klein R, Wang Q, Klein B E, Moss S E, and Meuer S M (1995) The relationship of age-related maculopathy, cataract, and glaucoma to visual acuity. *Invest Ophthalmol Vis Sci* 36: 182-191.

Klyce S D, and Crosson C E (1985) Transport processes across the rabbit corneal epithelium: a review. *Curr Eye Res* 4: 323-331.

Knowles M, Gatzy J, and Boucher R (1983) Relative ion permeability of normal and cystic fibrosis nasal epithelium. *Journal of Clinical Investigation* 71: 1410-1417.

Koch D, Rainisio M, Madessani U, Harms H K, Hodson M E, Mastella G, McKenzie S G et al. (2001) Presence of cystic fibrosis-related diabetes mellitus is tightly linked to poor lung function in patients with cystic fibrosis: data from the European Epidemiologic Registry of Cystic Fibrosis. *Pediatric Pulmonology* 32: 343-350.

Kolb H (1995) Simple Anatomy of the Retina. In: Kolb H, Fernandez E, and Nelson R [eds.] *Webvision: The Organization of the Retina and Visual System*. Salt Lake City UT.

Kolb H (2013) Photoreceptors. http://webvision.med.utah.edu/: Accessed 11/10/2013.

Konno S, Feke G T, Yoshida A, Fujio N, Goger D G, and Buzney S M (1996) Retinal blood flow changes in type I diabetes. A long-term follow-up study. *Invest Ophthalmol Vis Sci* 37: 1140-1148.

Konstan M W, Byard P J, Hoppel C L, and Davis P B (1999) Effect of high-dose ibuprofen in patients with cystic fibrosis: trends and physician attitudes. *Chest* 124: 689-693.

Kopelman H, Durie P, Gaskin K, Weizman Z, and Forstner G (1985) Pancreatic fluid secretion and protein hyperconcentration in cystic fibrosis. *New England Journal of Medicine* 312: 329-334.

Kopito L E, Kosasky H J, Sturgis S H, Lieberman B L, and Shwachman H (1973) Water and electrolytes in human cervical mucous. *Fertil Steril* 24: 499-506.

Kornak U, Kasper D, Bosl M R, Kaiser E, Schweizer M, Schulz A, Friedrich W et al. (2001) Loss of the ClC-7 chloride channel leads to osteopetrosis in mice and man. *Cell* 104: 205-215.

Koster T, Rosendaal F R, Reitsma P H, van der Velden P A, Briet E, and Vandenbroucke J P (1994) Factor VII and fibrinogen levels as risk factors for venous thrombosis. A case-control study of plasma levels and DNA polymorphisms--the Leiden Thrombophilia Study (LETS). *Thromb Haemost* 71: 719-722.

Kraemer R, RÜDeberg A, Hadorn B, and Rossi E (1978) Relative underweight in cystic fibrosis and its prognostic value. *Acta Pædiatrica* 67: 33-37.

Krastel H, and Moreland D (1991) Colour vision deficiences in ophthalmic diseases. In: Foster D H [ed.] *Inherited and aquired colour vision deficiencies* Boston: CRC Press, Inc, pp. 115-172.

Krinsky N I, and Yeum K J (2003) Carotenoid-radical interactions. *Biochem Biophys Res Commun* 305: 754-760.

Kukreja R C, and Hess M L (1992) The oxygen free radical system: from equations through membrane-protein interactions to cardiovascular injury and protection. *Cardiovasc Res* 26: 641-655.

Kunzelmann K, Schreiber R, Nitschke R, and Mall M (2000) Control of epithelial Na^+ conductance by the cystic fibrosis transmembrane conductance regulator. *Pflugers Archive* 440: 193-201.

Kur J, Newman E A, and Chan-Ling T (2012) Cellular and physiological mechanisms underlying blood flow regulation in the retina and choroid in health and disease. *Prog Retin Eye Res* 31: 377-406.

Kuroki M, Voest E E, Amano S, Beerepoot L V, Takashima S, Tolentino M, Kim R Y et al. (1996) Reactive oxygen intermediates increase vascular endothelial growth factor expression in vitro and in vivo. *J Clin Invest* 98: 1667-1675.

Kurtenbach A, Mayser H M, Jagle H, Fritsche A, and Zrenner E (2006) Hyperoxia, hyperglycemia, and photoreceptor sensitivity in normal and diabetic subjects. *Visual Neuroscience* 23: 651-661.

Laguna T, Sontag M K, Osberg I, Wagener J S, Accurso F J, and Sokol R (2008) Decreased total serum coenzyme-Q10 concentrations: a lungitudinal study in children with cystic fibrosis. *J Pediatr* 153: 402-407.

Lam D S, Leung K S, Mohamed S, Chan W M, Palanivelu M S, Cheung C Y, Li E Y et al. (2007) Regional variations in the relationship between macular thickness measurements and myopia. *Invest Ophthalmol Vis Sci* 48: 376-382.

Lamb T D (1981) The involvement of rod photoreceptors in dark adaptation. *Vision Res* 21: 1773-1782.

Lamb T D, and Pugh E N, Jr. (2004) Dark adaptation and the retinoid cycle of vision. *Prog Retin Eye Res* 23: 307-380.

Lamb T D, and Pugh E N, Jr. (2006) Phototransduction, dark adaptation, and rhodopsin regeneration the proctor lecture. *Invest Ophthalmol Vis Sci* 47: 5137-5152.

Lange C A, and Bainbridge J W (2012) Oxygen sensing in retinal health and disease. *Ophthalmologica* 227: 115-131.

Lange C A, Stavrakas P, Luhmann U F, de Silva D J, Ali R R, Gregor Z J, and Bainbridge J W (2011) Intraocular oxygen distribution in advanced proliferative diabetic retinopathy. *Am J Ophthalmol* 152: 406-412 e403.

Langhans M, Michelson G, and Groh M J (1997) Effect of breathing 100% oxygen on retinal and optic nerve head capillary blood flow in smokers and non-smokers. *Br J Ophthalmol* 81: 365-369.

Lanng S, Hansen A, Thorsteinsson B, Nerup J, and Koch C (1995) Glucose tolerance in patients with cystic fibrosis: five year prospective study. *BMJ* 311: 655-659.

Lanng S, Thorsteinsson B, Nerup J, and Koch C (1992) Influence of the development of diabetes mellitus on clinical status in patients with cystic fibrosis. *Eur J Pediatr* 151: 684-687.

Lanng S, Thorsteinsson B, Nerup J, and Koch C (1994) Diabetes mellitus in cystic fibrosis: effect of insulin therapy on lung function and infections. *Acta Paediatr* 83: 849-853.

Larsen M, Wang M, and Sander B (2005) Overnight thickness variation in diabetic macular edema. *Invest Ophthalmol Vis Sci* 46: 2313-2316.

Lass J H, Spurney R V, Dutt R M, Andersson H, Kochar H, Rodman H M, Stern R C et al. (1985) A morphologic and fluorophotometric analysis of the corneal endothelium in type I diabetes mellitus and cystic fibrosis. *Am J Ophthalmol* 100: 783-788.

Leguire L E, Pappa K S, Kachmer M L, Rogers G L, and Bremer D L (1991) Loss of contrast sensitivity in cystic fibrosis. *Am J Ophthalmol* 111: 427-429.

Leguire L E, Pappa K S, McGregor M L, Rogers G L, and Bremer D L (1992) Electro-oculogram in vitamin A deficiency associated with cystic fibrosis. Short communication. *Ophthalmic Paediatr Genet* 13: 187-189.

Leibowitz H (1954) The use and calibration of the Maxwellian view in visual instrumentation. *Am J Psychol* 67: 530-532.

Leibowitz H M, Krueger D E, Maunder L R, Milton R C, Kini M M, Kahn H A, Nickerson R J et al. (1980) The Framingham Eye Study monograph: An ophthalmological and epidemiological study of cataract, glaucoma, diabetic retinopathy, macular degeneration, and visual acuity in a general population of 2631 adults, 1973-1975. *Surv Ophthalmol* 24: 335-610.

Leibrock C S, Reuter T, and Lamb T D (1998) Molecular basis of dark adaptation in rod photoreceptors. *Eye (Lond)* 12 (Pt 3b): 511-520.

Leitgeb R, Hitzenberger C K, and Fercher A F (2003) Performance of Fourier domain vs. time domain optical coherence tomography. *Opt Express* 11: 889-894.

Leoncini G, Signorello M G, Segantin A, Giacobbe E, Armani U, Piana A, and Camicione P (2009) In retinal vein occlusion platelet response to thrombin is increased. *Thrombosis Research* 124: 48-55.

Leske M C, Chylack L T, and Wu S (1991) The lens opacities case-control study. Risk factors for cataract. *Arch Ophthalmol* 109: 244-251.

Leske M C, Wu S Y, Hyman L, Hennis A, Nemesure B, and Schachat A P (2004) Four-year incidence of macular changes in the Barbados Eye Studies. *Ophthalmology* 111: 706-711.

Leung C K, Cheng A C, Chong K K, Leung K S, Mohamed S, Lau C S, Cheung C Y et al. (2007) Optic disc measurements in myopia with optical coherence tomography and confocal scanning laser ophthalmoscopy. *Invest Ophthalmol Vis Sci* 48: 3178-3183

Leung C K, Cheung C Y, Weinreb R N, Lee G, Lin D, Pang C P, and Lam D S (2008) Comparison of macular thickness measurements between time domain and spectral domain optical coherence tomography. *Invest Ophthalmol Vis Sci* 49: 4893-4897.

Levin M H, and Verkman A S (2004) Aquaporin-dependent water permeation at the mouse ocular surface: in vivo microfluorimetric measurements in cornea and conjunctiva. *Invest Ophthalmol Vis Sci* 46: 1428-1434.

Levin M H, and Verkman A S (2005) CFTR-regulated chloride transport at the ocular surface in living mice measured by potential differences. *Invest Ophthalmol Vis Sci* 46: 1428-1434.

Levin M H, and Verkman A S (2006) Aquaporins and CFTR in ocular epithelial fluid transport. *J Membr Biol* 210: 105-115.

Lewis M J, Lewis E H, 3rd, Amos J A, and Tsongalis G J (2003) Cystic fibrosis. *Am J Clin Pathol* 120 Suppl: S3-13.

Lezo A, Biasi F, Massarenti P, Calabrese R, Poli G, Santini B, and Bignamini E (2012) Oxidative stress in stable cystic fibrosis patients: Do we need higher antioxidant plasma levels? *J Cyst Fibros*.

Li C H, Cai Z, Chen J H, Xu Z, and Sheppard D N (2007) The cystic fibrosis transmembrane conductance regulator Cl^- channel: a versatile engine for transepithelial ion transport. *Sheng Li Xue Bao* 59: 416-430.

Li F, Chen H, and Anderson R E (2001a) Biosynthesis of docosahexaenoate-containing glycerolipid molecular species in the retina. *J Mol Neurosci* 16: 205-214; discussion 215-221.

Li Y, Kuang K, Yerxa B, Wen Q, Rosskothen H, and Fischbarg J (2001b) Rabbit conjunctival epithelium transports fluid, and P2Y2(2) receptor agonists stimulate Cl^- and fluid secretion. *Am J Physiol Cell Physiol* 281: C595-C602.

Liang F Q, and Godley B F (2003) Oxidative stress-induced mitochondrial DNA damage in human retinal pigment epithelial cells: a possible mechanism for RPE aging and age-related macular degeneration. *Exp Eye Res* 76: 397-403.

Lim L S, Mitchell P, Seddon J M, Holz F G, and Wong T Y (2012) Age-related macular degeneration. *Lancet* 379: 1728-1738.

Lim M C, Hoh S T, Foster P J, Lim T H, Chew S J, Seah S K, and Aung T (2005) Use of optical coherence tomography to assess variations in macular retinal thickness in myopia. *Invest Ophthalmol Vis Sci* 46: 974-978.

Lind L (2003) Circulating markers of inflammation and atherosclerosis. *Atherosclerosis* 169: 203-214.

Lindblad A, Diczfalusy U, Hultcrantz R, Thorell A, and Strandvik B (1997) Vitamin A concentration in the liver decreases with age in patients with cystic fibrosis. *J Pediatr Gastroenterol Nutr* 24: 264-270.

Linsdell P, and Hanrahan J W (1998) Glutathione permeability of CFTR. *Am J Physiol* 275: C323-326.

Linsenmeier R A (1986) Effects of light and darkness on oxygen distribution and consumption in the cat retina. *J Gen Physiol* 88: 521-542.

Linsenmeier R A, and Braun R D (1992) Oxygen distribution and consumption in the cat retina during normoxia and hypoxemia. *J Gen Physiol* 99: 177-197.

Linsenmeier R A, Braun R D, McRipley M A, Padnick L B, Ahmed J, Hatchell D L, McLeod D S et al. (1998) Retinal hypoxia in long-term diabetic cats. *Invest Ophthalmol Vis Sci* 39: 1647-1657.

Liou G I, Geng L, and Baehr W (1991) Interphotoreceptor retinoid-binding protein: biochemistry and molecular biology. *Prog Clin Biol Res* 362: 115-137.

Little H L (1976) The role of abnormal hemorrheodynamics in the pathogenesis of diabetic retinopathy. *Trans Am Ophthalmol Soc* 74: 573-636.

Littmann H (1982) [Determination of the real size of an object on the fundus of the living eye]. *Klin Monbl Augenheilkd* 180: 286-289.

Loewen M E, Smith N K, Hamilton D L, Grahn B H, and Forsyth G W (2003) CLCA protein and chloride transport in canine retinal pigment epithelium. *Am J Physiol Cell Physiol* 285: C1314-1321.

Longo A, Geiser M, and Riva C E (2000) Subfoveal choroidal blood flow in response to light-dark exposure. *Invest Ophthalmol Vis Sci* 41: 2678-2683.

Lopez P F, Sippy B D, Lambert H M, Thach A B, and Hinton D R (1996) Transdifferentiated retinal pigment epithelial cells are immunoreactive for vascular endothelial growth factor in surgically excised age-related macular degeneration-related choroidal neovascular membranes. *Invest Ophthalmol Vis Sci* 37: 855-868.

Lyon A, and Bilton D (2002) Fertility issues in cystic fibrosis. *Paediatric Respiratory Reviews* 3: 236-240.

Lyons T J, Jenkins A J, Zheng D, Lackland D T, McGee D, Garvey W T, and Klein R L (2004) Diabetic retinopathy and serum lipoprotein subclasses in the DCCT/EDIC cohort. *Invest Ophthalmol Vis Sci* 45: 910-918.

Machlin L J, and Bendich A (1987) Free radical tissue damage: protective role of antioxidant nutrients. *FASEB J* 1: 441-445.

Mackie A D, Thornton S J, and Edenborough F P (2003) Cystic fibrosis-related diabetes. *Diabet Med* 20: 425-436.

Macular Photocoagulation Study Group (1986) Recurrent choroidal neovascularization after argon laser photocoagulation for neovascular maculopathy. *Arch Ophthalmol* 104: 503-512.

Maguire P, and Vine A K (1986) Geographic atrophy of the retinal pigment epithelium. *Am J Ophthalmol* 102: 621-625.

Majure M, Mroueh S, and Spock A (1989) Risk factors for the developmene of posterior subcapsular cataracts in patients with cystic fibrosis and allergic bronchopulmonary aspergillosis treated with corticosteroids. *Pediatric Pulmonology* 6: 260-262.

Malamos P, Sacu S, Georgopoulos M, Kiss C, Pruente C, and Schmidt-Erfurth U (2009) Correlation of high-definition optical coherence tomography and fluorescein angiography imaging in neovascular macular degeneration. *Invest Ophthalmol Vis Sci* 50: 4926-4933.

Maleki N, Alsop D C, Dai W, Hudson C, Han J S, Fisher J, and Mikulis D (2011) The effect of hypercarbia and hyperoxia on the total blood flow to the retina as assessed by magnetic resonance imaging. *Invest Ophthalmol Vis Sci* 52: 6867-6874.

Manassakorn A, Chaidaroon W, Ausayakhun S, Aupapong S, and Wattananikorn S (2008) Normative database of retinal nerve fiber layer and macular retinal thickness in a Thai population. *Jpn J Ophthalmol* 52: 450-456.

Maqbool A, and Stallings V A (2008) Update on fat-soluble viatmins in cystic fibrosis. *Curr Opin Pulm Med* 14: 574-581.

Mares-Perlman J A, Brady W E, Klein R, VandenLangenberg G M, Klein B E, and Palta M (1995) Dietary fat and age-related maculopathy. *Arch Ophthalmol* 113: 743-748.

Margrain T H, and Thomson D (2002) Sources of variability in the clinical photostress test. *Ophthalmic and Physiological Optics* 22: 61-67.

Marmor M F (1990) Control of subretinal fluid: experimental and clinical studies. *Eye (Lond)* 4 (Pt 2): 340-344.

Marmor M F, and Wolfensberger T J (1998) *The retinal pigment epithelium; function and disease*. Oxford University Press.

Marse-Perlman J A, Fisher A I, Klein R, Palta M, Block G, Millen A E, and Wright J D (2001) Lutein and Zeaxanthin in the Diet and Serum and Their Relation to Age-related Maculopathy in the Third National Health and Nutrition Examination Survey. *American Journal of Epidemiology* 153: 424-432.

Marshall B C, Butler S M, Stoddard M, Moran A M, Liou T G, and Morgan W J (2005) Epidemiology of cystic fibrosis-related diabetes. *J Pediatr* 146: 681-687.

Massin P, Erginay A, Haouchine B, Mehidi A B, Paques M, and Gaudric A (2002) Retinal thickness in healthy and diabetic subjects measured using optical coherence tomography mapping software. *Eur J Ophthalmol* 12: 102-108.

Mata N L, Moghrabi W N, Lee J S, Bui T V, Radu R A, Horwitz J, and Travis G H (2004) Rpe65 is a retinyl ester binding protein that presents insoluble substrate to the isomerase in retinal pigment epithelial cells. *J Biol Chem* 279: 635-643.

Mata N L, Radu R A, Clemmons R C, and Travis G H (2002) Isomerization and oxidation of vitamin a in cone-dominanyt retinas: a novel pathway for visual pigment regeneration in daylight. *Neuron* 36: 69-80.

Matsui H, Grubb B R, Tarran R, and al. e (1998) Evidence for periciliary liquid layer depleion, not abnormal ion compostion, in the pathogenesis of cystic fibrosis airways disease. . *Cell* 95: 1005-1015.

Matthews L W, Doershuk C F, Wise M, Eddy G, Nudelman H, and Spector S (1964) A therapeutic regimen for patients with cystic fibrosis. *J Pediatr* 65: 558-575.

Mc F R, Halperin M H, and Niven J I (1946) Visual thresholds as an index of physiological imbalance during insulin hypoglycemia. *Am J Physiol* 145: 299-313.

McAlinden C, Khadka J, and Pesudovs K (2011) Statistical methods for conducting agreement (comparison of clinical tests) and precision (repeatability or reproducibility) studies in optometry and ophthalmology. *Ophthalmic and Physiological Optics* 31: 330-338.

McBee J K, Palczewski K, Baehr W, and Pepperberg D R (2001) Confronting complexity: the interlink of phototransduction and retinoid metabolism in the vertebrate retina. *Prog Retin Eye Res* 20: 469-529.

McCarty C A, Mukesh B N, Fu C L, Mitchell P, Wang J J, and Taylor H R (2001) Risk factors for age-related maculopathy: the Visual Impairment Project. *Arch Ophthalmol* 119: 1455-1462.

McConnell V, and Silvestri G (2005) Age-related macular degeneration. *Ulster Med J* 74: 82-92.

McCormick J, Conway S P, and Mehta A (2007) Paediatric Northern Score centile charts for the chest radiograph in cystic fibrosis. *Clin Radiol* 62: 78-81.

McFarland R A, and Evans J N (1939) Alterations in dark adaptation under reduced oxygen tension *Am J Physiol* 127: 37-50.

McFarland R A, and Forbes W H (1940) The effects of variations in the concentration of oxygen and of glucose on dark adaptation. *J Gen Physiol* 24: 69-98.

McGwin G, Jr., Jackson G R, and Owsley C (1999) Using nonlinear regression to estimate parameters of dark adaptation. *Behav Res Methods Instrum Comput* 31: 712-717.

McKone E F, Emerson S S, Edwards K L, and Aitken M L (2003) Effect of genotype on phenotype and mortality in cystic fibrosis: a retrospective cohort study. *Lancet* 361: 1671-1676.

McLeod D S, Grebe R, Bhutto I, Merges C, Baba T, and Lutty G A (2009) Relationship between RPE and choriocapillaris in age-related macular degeneration. *Invest Ophthalmol Vis Sci* 50: 4982-4991.

McLeod D S, Taomoto M, Otsuji T, Green W R, Sunness J S, and Lutty G A (2002) Quantifying changes in RPE and choroidal vasculature in eyes with age-related macular degeneration. *Invest Ophthalmol Vis Sci* 43: 1986-1993.

Meachery G, De Soyza A, Nicholson A, Parry G, Hasan A, Tocewicz K, Pillay T et al. (2008) Outcomes of lung transplantation for cystic fibrosis in a large UK cohort. *Thorax* 63: 725-731.

Menke M N, Dabov S, Knecht P, and Sturm V (2009) Reproducibility of retinal thickness measurements in patients with age-related macular degeneration using 3D Fourier-domain optical coherence tomography (OCT) (Topcon 3D-OCT 1000). *Acta Ophthalmol*.

Messenheimer J A, Greenwood R S, Tennison M B, Brickley J J, and Ball C J (1984) Reversible visual evoked potential abnormalities in vitamin E deficiency. *Ann Neurol* 15: 499-501.

Metha A, Vingrys A J, and Badcock D (1993) Calibration of a colour monior for visual psychophyics. *Behav Res Methods Instrum Comp* 25: 371-383.

Meyer C H, Rodrigues E B, Mennel S, Schmidt J C, and Kroll P (2004) Spontaneous separation of epiretinal membrane in young subjects: personal observations and review of the literature. *Graefes Arch Clin Exp Ophthalmol* 242: 977-985.

Meyers S M, Greene T, and Gutman F A (1995) A twin study of age-related macular degeneration. *Am J Ophthalmol* 120: 757-766.

Milla C E, Billings J, and Moran A (2005) Diabetes is associated with dramatiaclly decreased survival in female but not male subjects with cystic fibrosis. *Diabetes Care* 28: 2141-2144.

Miller S, and Farber D (1984) Cyclic AMP modulation of ion transport across frog retinal pigment epithelium. Measurements in the short-circuit state. *J Gen Physiol* 83: 853-874.

Miller S S, and Edelman J L (1990) Active ion transport pathways in the bovine retinal pigment epithelium. *J Physiol* 424: 283-300.

Miller S S, Rabin J, Strong T V, Ianuzzi M, Adams A J, Collins F, Reenstra W et al. (1992) Cystic fibrosis gene product is expressed in retina and retinal pigment epithelium. *Invest Ophthalmol Vis Sci* 33: 1009.

Mischler E H, Chesney P J, Chesney R W, and Mazess R B (1979) Demineralization in cystic fibrosis detected by direct photon absorptiometry. *American Journal of Diseases of Children* 133: 632-635.

Mishima S, and Maurice D M (1961) Oily layer of tear film and evaporation from corneal surface *Exp Eye Res* 1: 39-45.

Mitchell P, Smith W, Chey T, Wang J J, and Chang A (1997) Prevalence and associations of epiretinal membranes. The Blue Mountains Eye Study, Australia. *Ophthalmology* 104: 1033-1040.

Mitchell P, Wang J J, Foran S, and Smith W (2002a) Five-year incidence of age-related maculopathy lesions: the Blue Mountains Eye Study. *Ophthalmology* 109: 1092-1097.

Mitchell P, Wang J J, Smith W, and Leeder S R (2002b) Smoking and the 5-year incidence of age-related maculopathy: the Blue Mountains Eye Study. *Arch Ophthalmol* 120: 1357-1363.

Mitchell P, Wang J J, Smith W, and Leeder S R (2002c) Smoking and the 5-Year Incidence of Age-Related Maculopathy: The Blue Mountains Eye Study. *Arch Ophthalmol* 120: 1357-1363.

Miyazono S, Shimauchi-Matsukawa Y, Tachibanaki S, and Kawamura S (2008) Highly efficient retinal metabolism in cones. *Proc Natl Acad Sci U S A* 105: 16051-16056.

Mohan K, Miller H, Dyce P, Grainger R, Hughes R, Vora J, Ledson M et al. (2009) Mechanisms of glucose intolerance in cystic fibrosis. *Diabet Med* 26: 582-588.

Moran A, Dunitz J, Nathan B, and et al (2009) Cystic fibrosis-related diabetes: current trends in prevalence, incidence, and mortality. *Diabetes Care* 32: 1626-1631.

Moran A, Hardin D S, Rodman D, Allen H, Beall R J, Borowitz D, and al. e (1999) Diagnosis, screening and management of cystic fibrosis-related diabetes mellitus: a consensus conference report. *Diabetes Res Clin Pract* 45: 61-73.

Mordant P, Bonnette P, Puyo P, Sage E, Grenet D, Stern M, Fischler M et al. (2010) Advances in lung transplantation for cystic fibrosis that may improve outcome. *Eur J Cardiothorac Surg* 38: 637-643.

Mori F (2001) The role of choroidal haemodynamic abnormalities in the pathogenesis of age related macular degeneration. *Br J Ophthalmol* 85: 1399-1400.

Mori F, Konno S, Hikichi T, Yamaguchi Y, Ishiko S, and Yoshida A (2001) Pulsatile ocular blood flow study: decreases in exudative age related macular degeneration. *Br J Ophthalmol* 85: 531-533.

Morkeberg J C, Edmund C, Prause J U, Lanng S, Koch C, and Michaelsen K F (1995) Ocular findings in cystic fibrosis patients receiving vitamin A supplementation. *Graefes Arch Clin Exp Ophthalmol* 233: 709-713.

Morton A M (2009) The nutritional challenges of the young adult with cystic fibrosis: transition. *Proceedings of the Nutrition Society* 68: 430-440.

Mrugacz M, Bakunowicz-łazarczyk A, Minarowska A, and Zywalewska N (2005a) Evaluation of the tears secretion in young patients with cystic fibrosis. *Klin Oczna* 107: 90-92.

Mrugacz M, Tobolczyk J, and Minarowska A (2005b) Retinol binding protein status in relation to ocular surface changes in patients with cystic fibrosis treated with daily vitamin A supplements. *Eur J Pediatr* 164: 202-206.

Mrugacz M, Zak J, Bakunowicz-Lazarczyk A, Wysocka J, and Kaczmarski M (2007a) ICAM-1 expression on conjunctival epithelial cells in patients with cystic fibrosis. *Cytometry B Clin Cytom* 72: 204-208.

Mrugacz M, Zak J, Bakunowicz-Lazarczyk A, Wysocka J, and Minarowska A (2007b) Flow cytometric analysis of HLA-DR antigen in conjunctival epithelial cells of patients with cystic fibrosis. *Eye (Lond)* 21: 1062-1066.

Mullins R F, Russell S R, Anderson D H, and Hageman G S (2000) Drusen associated with aging and age-related macular degeneration contain proteins common to extracellular deposits associated with atherosclerosis, elastosis, amyloidosis, and dense deposit disease. *FASEB J* 14: 835-846.

Munck A, Malbezin S, Bloch J, Gerardin M, Lebourgeois M, Derelle J, Bremont F et al. (2004) Follow-up of 452 totally implantable vascular devices in cystic fibrosis patients. *Eur Respir J* 23: 430-434.

Nash K L, Allison M E, McKeon D, Lomas D J, Haworth C S, Bilton D, and Alexander G J (2008) A single centre experience of liver disease in adults with cystic fibrosis 1995-2006. *Journal of Cystic Fibrosis* 173: 475-482.

Nathan B M, Laguna T, and Moran A (2010) Recent trends in cystic fibrosis related diabetes. *Current Opinion in Endocrinology, Diabetes and Obesity* 17: 335-341.

Neugebauer M A, Vernon S A, Brimlow G, Tyrrell J C, Hiller E J, and Marenah C (1989) Nyctalopia and conjunctival xerosis indicating vitamin A deficiency in cystic fibrosis. *Eye* 3: 360-364.

Nguyen Q D, Shah S M, Van Anden E, Sung J U, Vitale S, and Campochiaro P A (2004) Supplemental oxygen improves diabetic macular edema: a pilot study. *Invest Ophthalmol Vis Sci* 45: 617-624.

Nielsen N V (1978) Corneal sensitivity and vibratory perception in diabetes mellitus. *Acta Ophthalmol (Copenh)* 56: 406-411.

Nishimura T, Goodnight R, Prendergast R A, and Ryan S J (1990) Activated macrophages in experimental subretinal neovascularization. *Ophthalmologica* 200: 39-44.

North R V, Farrell U, Banford D, Jones C, Gregory J W, Butler G, and Owens D R (1997) Visual function in young IDDM patients over 8 years of age. A 4-year longitudinal study. *Diabetes Care* 20: 1724-1730.

Nowak J Z (2006) Age-related macular degeneration (AMD): pathogenesis and therapy. *Pharmacol Rep* 58: 353-363.

Nozaki M, Raisler B J, Sakurai E, Sarma J V, Barnum S R, Lambris J D, Chen Y et al. (2006) Drusen complement components C3a and C5a promote choroidal neovascularization. *Proc Natl Acad Sci U S A* 103: 2328-2333.

O'Riordan S M, Robinson P D, Donaghue K C, and Moran A (2009) Management of cystic fibrosis-related diabetes in children and adolescents. *Pediatr Diabetes* 10: 43-50.

O'Sullivan B P, Linden M D, Frelinger A L, 3rd, Barnard M R, Spencer-Manzon M, Morris J E, Salem R O et al. (2005) Platelet activation in cystic fibrosis. *Blood* 105: 4635-4641.

Oh H, Takagi H, Takagi C, Suzuma K, Otani A, Ishida K, Matsumura M et al. (1999) The potential angiogenic role of macrophages in the formation of choroidal neovascular membranes. *Invest Ophthalmol Vis Sci* 40: 1891-1898.

Ohno-Matsui K, Morita I, Tombran-Tink J, Mrazek D, Onodera M, Uetama T, Hayano M et al. (2001) Novel mechanism for age-related macular degeneration: an equilibrium shift between the angiogenesis factors VEGF and PEDF. *J Cell Physiol* 189: 323-333.

Okada D, Nakai T, and Ikai A (1989) Transducin activation by molecular species of rhodopsin other than metarhodopsin II. *Photochem Photobiol* 49: 197-203.

Olson J A, and Tanumihardjo S A (1998) Evaluation of vitamin A status. *Am J Clin Nutr* 67: 148-152.

Omar R, and Herse P (2004) Quantification of dark adaptation dynamics in retinitis pigmentosa using non-linear regression analysis. *Clin Exp Optom* 87: 386-389.

Oppenheimer E A, Case A L, Esterly J R, and Rothberg R M (1970) Cervical mucous in cystic fibrosis: a possible cause of infertility. *Am J Obstetrics Gynecol* 108: 673-674.

Ostedgaard L S, Baldursson O, and Welsh M J (2001) Regulation of the cystic fibrosis transmembrane conductance regulator Cl- channel by its R domain. *Journal of Biological Chemistry*. 276: 7689-7692.

Osterberg G (1935) Topography of the layer of rods and cones in the human retina. *Acta Ophthalmol Suppl* 6: 1-103.

Padman R, McColley S A, Miller D P, Konstan M W, Morgan W J, Schechter M S, Ren C L et al. (2007) Infant Care Patterns at Epidemiologic Study of Cystic Fibrosis Sites That Achieve Superior Childhood Lung Function. *Pediatrics* 119: e531-537.

Panda-Jonas S, Jonas J B, and Jackobczyk-Zmija M (1995) Retinal photoreceptor density decreases with age. *Ophthalmology* 102: 1853-1859.

Paques M, Massin P, Sahel J A, Gaudric A, Bergmann J F, Azancot S, Levy B I et al. (2005) Circadian fluctuations of macular edema in patients with morning vision blurring: correlation with arterial pressure and effect of light deprivation. *Invest Ophthalmol Vis Sci* 46: 4707-4711.

Parker R O, Fan K, Nickerson J M, Liou G I, and Crouch R K (2009) Normal cone function requires the interphotoreceptor binding protein *J Neurosci* 29: 4616-4621.

Pauleikhoff D, Spital G, Radermacher M, Brumm G A, Lommatzsch A, and Bird A C (1999) A fluorescein and indocyanine green angiographic study of choriocapillaris in age-related macular disease. *Arch Ophthalmol* 117: 1353-1358.

Paunescu L A, and Schuman J S P, L.L. et al. (2004) Reproducibility of nerve fibre layer thickness, macular thickness, and optic nerve head measurements using stratus OCT. *Invest Ophthalmol Vis Sci* 45: 1716-1724.

Peterson W M, Meggyesy C, Yu K, and Miller S S (1997) Extracellular ATP activates calcium signaling, ion, and fluid transport in retinal pigment epithelium. *J Neurosci* 17: 2324-2337.

Pflugflder S C (2004) Antiinflammatory therapy for dry eye. *Ophthalmol* 137: 337-342.

Phillipsborn H F J, Lawrence G, and Lewis K C (1944) The diagnosis of fibrocystic disease of the pancreas. *J Pediatr* 25: 284-298.

Phipps J A, Yee P, Fletcher E L, and Vingrys A J (2006) Rod photoreceptor dysfunction in diabetes: activation, deactivation, and dark adaptation. *Invest Ophthalmol Vis Sci* 47: 3187-3194.

Pieramici D J, Bressler N M, Bressler S B, and Schachat A P (1994) Choroidal neovascularization in black patients. *Arch Ophthalmol* 112: 1043-1046.

Pierro L, Gitsidis S M, Mantovani E, and Gagliardi M (2010) Macular thickness interoperator and intraoperator reproducibility in healthy eyes using 7 optical coherence tompgraphy instruments. *Am J Ophthalmol* 150: 199-204.

Polito A, Del Borrello M, Polini G, Furlan F, Isola M, and Bandello F (2006) Diurnal variation in clinically significant diabetic macular edema measured by the Stratus OCT. *Retina* 26: 14-20.

Polito A, Polini G, Chiodini R G, Isola M, Soldano F, and Bandello F (2007) Effect of posture on the diurnal variation in clinically significant diabetic macular edema. *Invest Ophthalmol Vis Sci* 48: 3318-3323.

Potsaid B, Gorczynska I, Srinivasan V J, Chen Y, Jiang J, Cable A, and Fujimoto J G (2008) Ultrahigh speed spectral / Fourier domain OCT ophthalmic imaging at 70,000 to 312,500 axial scans per second. *Opt Express* 16: 15149-15169.

Poulin M J, Fatemian M, Tansley J G, O'Connor D F, and Robbins P A (2002) Changes in cerebral blood flow during and after 48 h of both isocapnic and poikilocapnic hypoxia in humans. *Exp Physiol* 87: 633-642.

Poulsen J H, Fischer H, Illeck B, and Machen T E (1994) Bicarbonate conductance and pH regulatory capability of cystic fibrosis transmembrane conductance regulator. *Proceedings of the National Academy of Sciences*. 91: 5340-5344.

Pournaras C, Tsacopoulos M, and Chapuis P (1978) Studies on the role of prostaglandins in the regulation of retinal blood flow. *Exp Eye Res* 26: 687-697.

Pournaras C J, Riva C E, Tsacopoulos M, and Strommer K (1989) Diffusion of O2 in the retina of anesthetized miniature pigs in normoxia and hyperoxia. *Exp Eye Res* 49: 347-360.

Pournaras C J, Rungger-Brandle E, Riva C E, Hardarson S H, and Stefansson E (2008) Regulation of retinal blood flow in health and disease. *Prog Retin Eye Res* 27: 284-330.

Proesman M, Vermeulen F, and De Boeck K (2008) What's new in cystic fibrosis? From treating symptoms to correction of the basic defect. *European Journal of Pediatrics* 167: 839-849.

Pryor J A, Webber B A, Hodson M E, and Batten J C (1979) Evaluation of the forced expiration technique as an adjunct to postural drainage in treatment of cystic fibrosis. *Br Med J* 2: 417-418.

Pugh E N (1975) Rushton's paradox: rod adaptation after flash photolysis. *J Physiol* 248: 413-431.

Qin L, Bartlett H, Griffiths H R, Eperjesi F, Armstrong R A, and Gherghel D (2011) Macular pigment optical density is related to blood glutathione levels in healthy individuals. *Invest Ophthalmol Vis Sci* 52: 5029-5033.

Qtaishat N M, Wiggert B, and Pepperberg D R (1999) Effect of interphotoreceptor retinoid-binding protein (IRBP) on the release and protection of all-trans retinol. *Invest Ophthalmol Vis Sci* 40: S212 (abstract).

Quattrucci S, Cimino G, Bertasi S, Benedetti Valentini S, Bossi A, D'Alu V, Locorriere L et al. (2008) Lung transplantation for cystic fibrosis in Italy. *Transplant Proc* 40: 2003-2005.

Ramsey B W, Pepe M S, Quan J M, Otto K L, Montgomery A B, Williams-Warren J, Vasiljev K M et al. (1999) Intermittent administration of inhaled tobramycin in patients with cystic fibrosis. Cystic Fibrosis Inhaled Tobramycin Study Group. *N Engl J Med* 340: 23-30.

Ratjen F, and Doring G (2003) Cystic Fibrosis. *Lancet* 361: 681-689.

Rayner R J, Tyrrell J C, Hiller E J, Marenah C, Neugebauer M A, Vernon S A, and Brimlow G (1989) Night blindness and conjunctival xerosis caused by vitamin A deficiency in patients with cystic fibrosis. *Arch Dis Child* 64: 1151-1156.

Redmond T M, Yu S, Lee E, Bok D, Hamasaki D, Chen N, Goletz P et al. (1998) Rpe65 is necessary for production of 11-cis-vitamin A in the retinal visual cycle. *Nat Genet* 20: 344-351.

Rehak J, and Rehak M (2008) Branch retinal vein occlusion: pathogenesis, visual prognosis, and treatment modalities. *Curr Eye Res* 33: 111-131.

Rehak M, Rehak J, Muller M, Faude S, Faude F, Siegemund A, Krcova V et al. (2008) The prevalence of activated protein C (APC) resistance and factor V Leiden is significantly higher in patients with retinal vein occlusion without general risk factors. *Journal of Thrombosis and Haemostasis* 99: 925-929.

Rehak M, and Wiedemann P (2010) Retinal vein thrombosis: pathogenesis and management. *Journal of Thrombosis and Haemostasis* 8: 1886-1894.

Reigada D, and Mitchell C H (2005) Release of ATP from retinal pigment epithelial cells involves both CFTR and vesicular transport. *Am J Physiol* 288: C132-C140.

Resnikoff S, Pascolini D, Etya'ale D, Kocur I, Pararajasegaram R, Pokharel G P, and Mariotti S P (2004) Global data on visual impairment in the year 2002. *Bull World Health Organ* 82: 844-851.

Riley M, Winkler B, Starnes C, and Peters M (1997) Fluid and ion transport in corneal endothelium: insensitivity to modulators of Na-K-2Cl cotransport. *Am J Physiol Cell Physiol* 273: C1480-C1486.

Rimmer T, Fallon T J, and Kohner E M (1989) Long-term follow-up of retinal blood flow in diabetes using the blue light entoptic phenomenon. *Br J Ophthalmol* 73: 1-5.

Riordan J R, Rommens J M, Kerem B, Alon N, Rozmahel R, Grzelczak Z, Zielenski J et al. (1989) Identification of the cystic fibrosis gene: cloning and characterization of complementary DNA. *Science* 245: 1066-1073.

Riva C E, Grunwald J E, and Petrig B L (1983a) Reactivity of the human retinal circulation to darkness: a laser Doppler velocimetry study. *Invest Ophthalmol Vis Sci* 24: 737-740.

Riva C E, Grunwald J E, and Sinclair S H (1983b) Laser Doppler Velocimetry study of the effect of pure oxygen breathing on retinal blood flow. *Invest Ophthalmol Vis Sci* 24: 47-51.

Riva C E, Petrig B L, and Grunwald J E (1987) Near infraref retinal laser Doppler velocimetry. *Lasers Ophthalmol* 1: 211-215.

Robinson M, and Bye P T (2002) Mucociliary clearance in cystic fibrosis. *Pediatr Pulmonol* 33: 293-306.

Rodman H M, Doershuk C F, and Roland J M (1986) The interaction of 2 diseases: diabetes mellitus and cystic fibrosis. *Medicine (Baltimore)* 65: 389-397.

Rogell G D (1980) Corneal hypesthesia and retinopathy in diabetes mellitus. *Ophthalmology* 87: 229-233.

Rolando M, Baldi F, and Calabria G (1988) Tear mucous crystallization in children with cystic fibrosis. *Ophthalmologica* 197: 202-206.

Rolando M, and Zierhut M (2001) The ocular surface and tear film and their dysfunction in dry eye disease. *Surv Ophthalmol* 45 Suppl 2: S203-210.

Rosenfeld M (2005) Overview of published evidence on outcomes with early diagnosisfrom large US observational studies. *J Pediatr* 147: S11-14.

Rosenfeld P J, Brown D M, Heier J S, Boyer D S, Kaiser P K, Chung C Y, and Kim R Y (2006) Ranibizumab for neovascular age-related macular degeneration. *N Engl J Med* 355: 1419-1431.

Rosenstein B J, and Cutting G R (1998) The diagnosis of cystic fibrosis: a consensus statement. Cystic Fibrosis Foundation Consensus Panel. *J Pediatr* 132: 589-595.

Roth F, Bindewald A, and Holz F G (2004) Key pathophysiologic pathways in age-related macular disease. *Graefes Arch Clin Exp Ophthalmol* 242: 710-716.

Roum J H, Buhl R, McElvaney N G, Borok Z, and Crystal R G (1993) Systemic deficiency of glutathione in cystic fibrosis. *J Appl Physiol* 75: 2419-2424.

Rowe S M, Miller S, and Sorsscher E J (2005) Mechansims of disease: Cystic Fibrosis. *New England Journal of Medicine* 352: 1992-2001.

Rowntree R K, and Harris A (2003) The phenotypic consequences of CFTR mutations. *Annals of Human Genetics*. 67: 471-485.

Roy C C, Darling P, and Weber A M (1984) A rational approach to meeting macro and micronutrient needs in cystic fibrosis. *J Pediatr Gastroenterol Nutr* 3: S154-S162.

Rubio M A, Davalos A R, and Campisi J (2004) Telomere length mediates the effects of telomerase on the cellular response to genotoxic stress. *Exp Cell Res* 298: 17-27.

Rudolf M, and Curcio C A (2009) Esterified cholesterol is highly localized to Bruch's membrane, as revealed by lipid histochemistry in wholemounts of human choroid. *J Histochem Cytochem* 57: 731-739.

Rungger-Brandle E, Dosso A A, and Leuenberger P M (2000) Glial reactivity, an early feature of diabetic retinopathy. *Invest Ophthalmol Vis Sci* 41: 1971-1980.

Rushton W A, and Powell D S (1972) The rhodopsin content and the visual threshold of human rods. *Vision Res* 12: 1073-1081.

Rushton W A H (1961) Dark-adaptation and the regeneration of rhodopsin. *J Physiol* 156: 166-178.

Ruskell G L (1997) Peripapillary venous drainage from the choroid: a variable feature in human eyes. *Br J Ophthalmol* 81: 76-79.

Rust P, Eichler I, Renner S, and Elmadfa I (2000) Long-term oral beta-carotene supplementation in patients with cystic fibrosis - effects on antioxidative status and pulmonary function. *Ann Nutr Metab* 44: 30-37.

Sadda S R, Joeres S, Wu Z, Updike P, Romano P, Collins A T, and Walsh A C (2007) Error correction and quantitaive subanalysis of optical coherence tomography data using computer-assisted grading. *Invest Ophthalmol Vis Sci* 48: 839-848.

Samarawickrama C, Wang J J, Huynh S C, Wang X Y, Burlutsky G, Stapleton F, and Mitchell P (2009) Macular thickness, retinal thickness, and optic disc parameters in dominant compared with nondominant eyes. *Journal of AAPOS* 13: 142-147.

Sánchez-Tocino H, Alvarez-Vidal A, Maldonado M J, Moreno-Montañés J, and García-Layana A (2002) Retinal Thickness Study with Optical Coherence Tomography in Patients with Diabetes. *Investigative Ophthalmology & Visual Science* 43: 1588-1594.

Sanders T A, Haines A P, Wormald R, Wright L A, and Obeid O (1993) Essential fatty acids, plasma cholesterol, and fat-soluble vitamins in subjects with age-related maculopathy and matched control subjects. *Am J Clin Nutr* 57: 428-433.

SanGiovanni J P, and Chew E Y (2005) The role of omega-3 long-chain polyunsaturated fatty acids in health and disease of the retina. *Prog Retin Eye Res* 24: 87-138.

Sarks J P, Sarks S H, and Killingsworth M C (1988) Evolution of geographic atrophy of the retinal pigment epithelium. *Eye (Lond)* 2 (Pt 5): 552-577.

Sarks J P, Sarks S H, and Killingsworth M C (1994) Evolution of soft drusen in age-related macular degeneration. *Eye* 8: 269-283.

Sarks S H (1976) Ageing and degeneration in the macular region: a clinico-pathological study. *Br J Ophthalmol* 60: 324-341.

Sayanagi K, Sharma S, and Kaiser P K (2009) Comparison of retinal thickness measurements between three-dimensional and radial scans on spectral-domain optical coherence tomography. *Am J Ophthalmol* 148: 431-438.

Schadel S A, Heck M, Maretzki D, Filipek S, Teller D C, Palczewski K, and Hofmann K P (2003) Ligand channeling within a G-protein-coupled receptor. The entry and exit of retinals in native opsin. *J Biol Chem* 278: 24896-24903.

Schaudig U H, Glaefke C, Scholz F, and Richard G (2000) Optical coherence tomography for retinal thickness measurement in diabetic patients without clinically significant macular edema. *Ophthalmic Surg Lasers* 31: 182-186.

Scheele G A, Fukuoka S I, Kern H F, and Hreedman S D (1996) Pancreatic dysfunction in cystic fibrosis occurs as a result of impairments in luminal pH, apical trafficking of zymogen granule membranes, and solubilization of secretory enzymes. *Pancreas* 12: 1-9.

Schertler G F, Villa C, and Henderson R (1993) Projection sucture of rhodopsin. *Nature* 362: 770-772.

Schick J H, Iyengar S K, Klein B E, Klein R, Reading K, Liptak R, Millard C et al. (2003) A whole-genome screen of a quantitative trait of age-related maculopathy in sibships from the Beaver Dam Eye Study. *Am J Hum Genet* 72: 1412-1424.

Schmetterer L, Wolzt M, Lexer F, Alschinger C, Gouya G, Zanaschka G, Fassolt A et al. (1995) The effect of hyperoxia and hypercapnia on fundus pulsations in the macular and optic disc region in healthy young men. *Exp Eye Res* 61: 685-690.

Schmidt S, Klaver C, Saunders A, Postel E, De La Paz M, Agarwal A, Small K et al. (2002) A pooled case-control study of the apolipoprotein E (APOE) gene in age-related maculopathy. *Ophthalmic Genet* 23: 209-223.

Schoni M H (1989) Autogenic drainage: a modern approach to physiotherapy in cystic fibrosis. *J R Soc Med* 82: 32-37.

Schuman S G, Koreishi A F, Farsiu S, Jung S H, Izatt J A, and Toth C A (2009) Photoreceptor layer thinning over drusen in eyes with age-related macular degeneration imaged in vivo with spectral-domain optical coherence tomography. *Ophthalmology* 116: 488-496 e482.

Schupp C, Olano-Martin E, Gerth C, Morrissey B M, Cross C E, and Werner J S (2004) Lutein, zeaxanthin, macular pigment, and visual function in adult cystic fibrosis patients. *Am J Clin Nutr* 79: 1045-1052.

Schwartz D E (1974) Corneal sensitivity in diabetics. *Arch Ophthalmol* 91: 174-178.

Schwarzenberg S J, Thomas W, Olsen T W, Grover T, Walk D, Milla C, and Moran A (2007) Microvascular complications in cystic fibrosis-related diabetes. *Diabetes Care* 30: 1056-1061.

Scott B L, and Bazan N G (1989) Membrane docosahexaenoate is supplied to the developing brain and retina by the liver. *Proc Natl Acad Sci U S A* 86: 2903-2907.

Seddon J M, Afshari M A, Sharma S, Bernstein P S, Chong S, Hutchinson A, Petrukhin K et al. (2001a) Assessment of mutations in the Best macular dystrophy (VMD2) gene in patients with adult-onset foveomacular vitelliform dystrophy, age-related maculopathy, and bull's-eye maculopathy. *Ophthalmology* 108: 2060-2067.

Seddon J M, Ajani U A, and Mitchell B D (1997) Familial aggregation of age-related maculopathy. *Am J Ophthalmol* 123: 199-206.

Seddon J M, Ajani U A, Sperduto R D, Hiller R, Blair N, Burton T C, Farber M D et al. (1994) Dietary carotenoids, vitamins A, C, and E, and advanced age-related macular degeneration. Eye Disease Case-Control Study Group. *JAMA* 272: 1413-1420.

Seddon J M, and Chen C A (2004) The epidemiology of age-related macular degeneration. *Int Ophthalmol Clin* 44: 17-39.

Seddon J M, Cote J, and Rosner B (2003) Progression of age-related macular degeneration: association with dietary fat, transunsaturated fat, nuts, and fish intake. *Arch Ophthalmol* 121: 1728-1737.

Seddon J M, Rosner B, Sperduto R D, Yannuzzi L, Haller J A, Blair N P, and Willett W (2001b) Dietary fat and risk for advanced age-related macular degeneration. *Arch Ophthalmol* 119: 1191-1199.

Shepard A R, and Rae J L (1998) Ion transporters and receptors in cDNA libraries from lens and corneal epithelia. *Curr Eye Res* 7: 708-714.

Sheppard J D, Orenstein D M, Chao C C, Butala S, and Kowalski R P (1989) The ocular surface in cystic fibrosis. *Ophthalmology* 96: 1624-1630.

Shepro D, and Morel N M (1993) Pericyte physiology. *FASEB J* 7: 1031-1038.

Sheth S S, Rush R B, and Natarajan S (2012) Inner and outer retinal volumetric and morphologic analysis of the macula with spectral domain optical coherence tomography in retinitis pigmentosa. *Middle East Afr J Ophthalmol* 19: 227-230.

Shichida Y, Imai H, Imatmoto Y, Fukada Y, and Yoshizawa T (1994) Is chicken green-sensitive cone visual pigment a rhodopsin-like pigment? A comparative study of the molecular properties between chicken green and rhodopsin. *Biochemistry* 33: 9040-9044.

Shiue M H, Gukasyan H J, Kim K, Loo D D, and Lee V H L (2002) Characterization of cyclic AMP-regulated chloride conductance in the pigmented rabbit conjunctival epithelial cells. *Can. J. Physiol. Pharmacol*. 80: 533-540.

Shiue M H, Kulkarni A A, Gukasyan H J, Swisher J B, Kim K J, and Lee V H (2000) Pharmacological modulation of fluid secretion in the pigmented rabbit conjunctiva. *Life Sci* 66: PL105-111.

Short D B, Trotter K W, Reczek D, Kreda S M, Bretscher A, Boucher R, Stutts M J et al. (1998) An apical PDZ protein anchors the cystic fibrosis transmembrane conductance regulator to the cytoskeleton. *Journal of Biological Chemistry*. 273: 19797-19801.

Shwachman H, Leubner H, and Catzel P (1955) Mucoviscidosis. *Adv Pediatr* 7: 249-252.

Sloane P A, and Rowe S M (2010) Cystic fibrosis transmembrane conductance regulator protein repair as a therapeutic strategy in cystic fibrosis. *Current Opinion in Pulmonary Medicine* 16: 591-597.

Smith W, Assink J, Klein R, Mitchell P, Klaver C C, Klein B E, Hofman A et al. (2001) Risk factors for age-related macular degeneration: Pooled findings from three continents. *Ophthalmology* 108: 697-704.

Smith W, Mitchell P, and Leeder S R (2000) Dietary fat and fish intake and age-related maculopathy. *Arch Ophthalmol* 118: 401-404.

Smith W, Mitchell P, Webb K, and Leeder S R (1999) Dietary antioxidants and age-related maculopathy: The blue mountains eye study. *Ophthalmology* 106: 761-767.

Smith W C (2006) Phototransduction and Photoreceptor Physiology. In: Heckenlively J R, and Arden G B [eds.] *Principles and practice of clinical electrophysiology of vision*. London: MIT Press, pp. 65-78.

Sng C C, Cheung C Y, Man R E, Wong W, Lavanya R, Mitchell P, Aung T et al. (2012) Influence of diabetes on macular thickness measured using optical coherence tomography: the Singapore Indian Eye Study. *Eye (Lond)* 26: 690-698.

Snodderly D M (1995) Evidence for protection against age-related macular degeneration by carotenoids and antioxidant vitamins. *Am J Clin Nutr* 62: 1448S-1461S.

Solomon M P, Wilson D C, Corey M, Kalnins D, Zielenski J, Tsui L C, Pencharz P et al. (2003) Glucose intolerance in children with cystic fibrosis. *J Pediatr* 142: 128-132.

Sommer A (1983) Effects of vitamin A deficiency on the ocular surface. *Ophthalmology* 90: 592-600.

Sommer A (1989) Vitamin A deficiency today: conjunctival xerosis in cystic fibrosis. *J R Soc Med* 82: 1-2.

Sommer A (1998) Xerophthalmia and viatmin A status. *Prog Retin Eye Res* 17: 9-31.

Sommer A, Tielsch J M, Katz J, Quigley H A, Gottsch J D, Javitt J C, Martone J F et al. (1991) Racial differences in the cause-specific prevalence of blindness in east Baltimore. *N Engl J Med* 325: 1412-1417.

Song W K, Lee S C, Lee E S, Kim C Y, and Kim S S (2010) Macular thickness variations with sex, age, and axial length in healthy subjects: a spectral domain-optical coherence tomography study. *Invest Ophthalmol Vis Sci* 51: 3913-3918.

Spaide R F, Diamond G, D'Amico R A, Gaerlan P F, and Bisberg D S (1987) Ocular findings in cystic fibrosis. *Am J Ophthalmol* 103: 204-210.

Spalter H F, and Bruce G M (1964) Ocular Changes In Pulmonary Insufficiency. *Trans Am Acad Ophthalmol Otolaryngol* 68: 661-676.

Sperling G (1971) The description and luminous calibration of cathode ray oscilloscope visual displays. *Behav Res Methods Instrum Comp* 3: 148-151.

Sponsel W E, DePaul K L, and Zetlan S R (1992) Retinal hemodynamic effects of carbon dioxide, hyperoxia, and mild hypoxia. *Invest Ophthalmol Vis Sci* 33: 1864-1869.

Sproul A, and Huang N (1964) Growth patterns in children with cystic fibrosis. *J Pediatr* 65: 664-676.

Srinivasan V J, Adler D C, Chen Y, Gorczynska I, Huber R, Duker J S, Schuman J S et al. (2008) Ultrahigh-speed optical coherence tomography for three-dimensional and en face imaging of the retina and optic nerve head. *Invest Ophthalmol Vis Sci* 49: 5103-5110.

Stamer W, Bok D, Hu J, Jaffe G J, and McKay B S (2003) Aquaporin-1 channels in human retinal pigment epithelium: role in transepithelial water movement. *Invest Ophthalmol Vis Sci* 44: 2803-2808.

Stamer W D, Peppel K, O'Donnell M E, Roberts B C, Wu F, and Epstein D L (2001) Expression of aquaporin-1 in human trabecular meshwork cells: role in resting cell volume. *Invest Ophthalmol Vis Sci* 42: 1803-1811.

Stecenko A A, and Moran A (2010) Update on cystic fibrosis-related diabetes. *Curr Opin Pulm Med* 16: 611-615.

Stefansson E, Geirsdottir A, and Sigurdsson H (2011) Metabolic physiology in age related macular degeneration. *Prog Retin Eye Res* 30: 72-80.

Steinberg R H, Linsenmeier R A, and Griff E R (1985) Retinal pigment epithelial cell contributions to the electroretinogram and electro-oculogram. *Prog Ret Res* 4: 33-66.

Sternberg P, Jr., Davidson P C, Jones D P, Hagen T M, Reed R L, and Drews-Botsch C (1993) Protection of retinal pigment epithelium from oxidative injury by glutathione and precursors. *Invest Ophthalmol Vis Sci* 34: 3661-3668.

Stobrawa S M, Breiderhoff T, Takamori S, Engel D, Schweizer M, Zdebik A A, Bosl M R et al. (2001) Disruption of ClC-3, a chloride channel expressed on synaptic vesicles, leads to a loss of the hippocampus. *Neuron* 29: 185-196.

Strauss O (1995) The Retinal Pigment Epithelium. In: Kolb H, Fernandez E, and Nelson R [eds.] *Webvision: The Organization of the Retina and Visual System*. Salt Lake City UT.

Strauss O (2005) The retinal pigment epithelium in visual function. *Physiological Reviews* 85: 845-881.

Stutts M J, Canessa C M, Olsen J C, Hamrick M, Cohn J A, and Rossier B C (1995) CFTR as a cAMP-dependent regulator of sodium channels. *Science* 269334: 847-850.

Suan E, Bedrossian E H, Eagle R C, and Laibson P R (1990) Corneal perforation in patients with vitamin A deficiency in United States. *Arch Ophthalmol* 108: 350-353.

Sugimoto M, Sasoh M, Ido M, Wakitani Y, Takahashi C, and Uji Y (2005) Detection of early diabetic change with optical coherence tomography in type 2 diabetes mellitus patients without retinopathy. *Ophthalmologica* 219: 379-385.

Sull A C, Vuong L N, Price L L, Srinivasan V J, Gorczynska I, Fujimoto J G, Schuman J S et al. (2010) Comparison of spectral/Fourier domain optical coherence tomography instruments for assessment of normal macular thickness. *Retina* 30: 235-245.

Sullivan M M, and Denning C R (1989) Diabetic microangiopathy in patients with cystic fibrosis. *Pediatrics* 84: 642-647.

Sun X C, and Bonanno J A (2002) Expression, localization, and functional evaluation of CFTR in bovine corneal endothelial cells. *Am J Physiol Cell Physiol* 282: C673-683.

Sun X C, McCutheon C, Bertram P, Xie Q, and Bonanno J A (2001) Studies on the expression of mRNA for anion transport related proteins in corneal endothelial cells. *Curr Eye Res* 22: 1-7.

Sun X C, Zhai C B, Cui M, Chen Y, Levin L R, Buck J, and Bonanno J A (2003) HCO_3^- -dependent soluble adenylyl cyclase activates cystic fibrosis transmembrane conductance regulator in corneal endothelium. *Am J Physiol Cell Physiol* 284: C1114-1122.

Suttle C M, and Harding G F (1998) The VEP and ERG in a young infant with cystic fibrosis. A case report. *Doc Ophthalmol* 95: 63-71.

Swanson W H, and Cohen J M (2003) Color vision. *Ophthalmol Clin North Am* 16: 179-203.

Takemoto C M (2012) Venous thromboembolism in cystic fibrosis. *Pediatr Pulmonol* 47: 105-112.

Tate D J, Jr., Miceli M V, and Newsome D A (1995) Phagocytosis and H2O2 induce catalase and metallothionein gene expression in human retinal pigment epithelial cells. *Invest Ophthalmol Vis Sci* 36: 1271-1279.

Tavakoli M, Petropoulos I N, and Malik R A (2012) Assessing corneal nerve structure and function in diabetic neuropathy. *Clin Exp Optom* 95: 338-347.

Taylor H R, Munoz B, West S, Bressler N M, Bressler S B, and Rosenthal F S (1990) Visible light and risk of age-related macular degeneration. *Trans Am Ophthalmol Soc* 88: 163-173; discussion 173-168.

Taylor H R, West S, Munoz B, Rosenthal F S, Bressler S B, and Bressler N M (1992) The long-term effects of visible light on the eye. *Arch Ophthalmol* 110: 99-104.

Tepper R S, Skatrud J B, and Dempsey J A (1983) Ventilation and oxygenation changes during sleep in cystic fibrosis. *Chest* 84: 388-393.

The Cystic Fibrosis Genetic Analysis Consortium (2011) *Cystic Fibrosis Mutation Database* [Online]. Available at: http://www.genet.sickkids.on.ca/cftr/app [Accessed: 3rd October].

The Eye Disease Case-Control Study Group (1992) Risk factors for neovascular age-related macular degeneration. The Eye Disease Case-Control Study Group. *Arch Ophthalmol* 110: 1701-1708.

Thiagarajah J R, and Verkman A S (2002) Aquaporin deletion in mice reduces corneal water permeability and delays restoration of transparency after swelling. *J Biol Chem* 277: 19139-19144.

Thomas M M, and Lamb T D (1999) Light adaptation and dark adaptation of human rod photoreceptors measured from the a-wave of the electroretinogram. *J Physiol* 518 (Pt 2): 479-496.

Thor H, Smith M T, Hartzell P, Bellomo G, Jewell S A, and Orrenius S (1982) The metabolism of menadione (2-methyl-1,4-naphthoquinone) by isolated hepatocytes. A study of the implications of oxidative stress in intact cells. *J Biol Chem* 257: 12419-12425.

Thylefors J, Piitulainen E, and Havelius U (2009) Dark adaptation during systemic hypoxia induced by chronic respiratory insufficiency. *Invest Ophthalmol Vis Sci* 50: 1307-1312.

Tiedeman J S, Kirk S E, Srinivas S, and Beach J M (1998) Retinal oxygen consumption during hyperglycemia in patients with diabetes without retinopathy. *Ophthalmology* 105: 31-36.

Tiffany J M (2008) The normal tear film. *Dev Ophthalmol* 41: 1-20.

Tinley C G, Withers N J, Sheldon C D, Quinn A G, and Jackson A A (2008) Zinc therapy for night blindness in cystic fibrosis. *J Cyst Fibros* 7: 333-335.

Tirouvanziam R, Conrad C K, Bottiglieri T, Herzenberg L A, Moss R B, and Herzenberg L A (2006) High-dose oral N-acetylcysteine, a glutathione prodrug, modulates inflammation in cystic fibrosis. *Proc Natl Acad Sci U S A* 103: 4628-4633.

Travis D (1991) Effective color displays. Theory and practice. In: Gaines B R, and Monk A [eds.] *Computers and People Series*. London: Academic Press, pp. 152-190.

Trehan A, Canada F J, and Rando R R (1990) Inhibitors of retinyl ester formation also prevent biosynthesis of 11-cis-retinol. *Biochemistry* 29: 309-312.

Trese M, Chandler D B, and Machemer R (1983) Macular pucker. II. Ultrastructure. *Graefes Arch Clin Exp Ophthalmol* 221: 16-26.

Trezise A E, and Buchwald M (1991) In vivo cell-specific expression of the cystic fibrosis transmembrane conductance regulator. *Nature* 353: 434-437.

Trick G L, and Berkowitz B A (2005) Retinal oxygenation response and retinopathy. *Prog Retin Eye Res* 24: 259-274.

Trick G L, Edwards P, Desai U, and Berkowitz B A (2006) Early supernormal retinal oxygenation response in patients with diabetes. *Invest Ophthalmol Vis Sci* 47: 1612-1619.

Tsinopoulos I, Nousia-Arvanitakis S, Galli-Tsinopoulou A, Roubies N, Tentzidou K, Xefteri M, and Stangos N (2000) Role of electroretinography in the assessment of retinal function as an indicator of vitamin A status. *Doc Ophthalmol* 101: 211-221.

Tsui L C (1992) The spectrum of cystic fibrosis mutations *Trends in Genetics*. 8: 392-398.

Turner H C, Alvarez L J, Bildin V N, and Candia O A (2000) Immunolocalization of Na-K-ATPase, Na-K-Cl and Na-glucose cotransporters in the conjunctival epithelium. *Curr Eye Res* 21: 843-850.

Turner H C, Bernstein A, and Canada O A (2002) Presence of CFTR in conjunctival epithelium. *Curr Eye Res* 24: 182-187.

Turner H C, and Candia O A (2001) Localization of CFTR in the conjunctival epithelium. *Investigative Ophthalmology & Visual Science* 42: 2697.

Ueda Y, and Steinberg R H (1994) Chloride currents in freshly isolated rat retinal pigment epithelial cells. *Exp Eye Res* 58: 331-342.

UK CF Registry (2013) *Annual Data Report 2011*. Cystic Fibrosis Trust

Underwood B A, and Denning C R (1972) Blood and liver concentrations of vitamin A and E in children with cystic fibrosis of the pancreas. *Pediatr Res* 6: 26-31.

van den Berg J M, Morton A M, Kok S W, Pijl H, Conway S P, and Heijerman H G (2008) Microvascular complications in patients with cystic fibrosis-related diabetes (CFRD). *J Cyst Fibros* 7: 515-519.

van der Giessen L, Bakker M, Joosten K, Hop W, and Tiddens H (2012) Nocturnal oxygen saturation in children with stable cystic fibrosis. *Pediatr Pulmonol* 47: 1123-1130.

van der Schaft T L, Mooy C M, de Bruijn W C, and de Jong P T (1993) Early stages of age-related macular degeneration: an immunofluorescence and electron microscopy study. *Br J Ophthalmol* 77: 657-661.

van der Vliet A, Eiserich J P, Marelich G P, Halliwell B, and Cross C E (1997) Oxidative stress in cystic fibrosis: does it occur and does it matter? *Adv Pharmacol* 38: 491-513.

Varma R, Fraser-Bell S, Tan S, Klein R, and Azen S P (2004) Prevalence of age-related macular degeneration in Latinos: the Los Angeles Latino eye study. *Ophthalmology* 111: 1288-1297.

Varma S D, Chand D, Sharma Y R, Kuck J F, and Richards R D (1984) Oxidative stress on the lens and cataract formation: Role of light and oxygen. *Curr Eye Res* 3: 35-37.

Velsor L W, van Heeckeren A, and Day B J (2001) Antioxidant imbalance in the lungs of cystic fibrosis transmembrane conductance regulator protein mutant mice. *Am J Physiol Lung Cell Mol Physiol* 281: L31-38.

Venkataraman S T, Hudson C, Fisher J A, and Flanagan J G (2006) Novel methodology to comprehensively assess retinal arteriolar vascular reactivity to hypercapnia. *Microvasc Res* 72: 101-107.

Verhoeff F H, and Grossman H P (1937) The Pathogenesis of Disciform Degeneration of the Macula. *Trans Am Ophthalmol Soc* 35: 262-294.

Vernon S A, Neugebauer M A, Brimlow G, Tyrrell J C, and Hiller E J (1989) Conjunctival xerosis in cystic fibrosis. *Journal of the Roual Society of Medicine* 82: 46-47.

Wagner-Schuman M, Dubis A M, Nordgren R N, Lei Y, Odell D, Chaiao H, Weh E et al. (2010) Racial and gender differences in retinal thickness and foveal pit morphology. *Invest Ophthalmol Vis Sci* Abstract ahead of print.

Wakitani Y, Sasoh M, Sugimoto M, Ito Y, Ido M, and Uji Y (2003) Macular thickness measurements in healthy subjects with different axial lengths using optical coherence tomography. *Retina* 23: 177-182.

Wald G, Jeghers H, and Arminio J (1938) An experiment in human dietary night-blindness. *Am J Physiol* 123: 732-746.

Walport M J (2001) Complement. First of two parts. *N Engl J Med* 344: 1058-1066.

Wang J S, and Kefalov V J (2009) An alternative pathway mediates the mouse and human cone visual cycle. *Curr Biol* 19: 1665-1669.

Wang J S, and Kefalov V J (2011) The cone-specific visual cycle. *Prog Retin Eye Res* 30: 115-128.

Wangsa-Wirawan N D, and Linsenmeier R A (2003) Retinal oxygen: fundamental and clinical aspects. *Arch Ophthalmol* 121: 547-557.

Wechsler H L (1979) Vitamin A deficiency following small-bowel bypass surgery for obesity. *Arch. Dermatol* 115: 73.

Weeks D E, Conley Y P, Mah T S, Paul T O, Morse L, Ngo-Chang J, Dailey J P et al. (2000) A full genome scan for age-related maculopathy. *Hum Mol Genet* 9: 1329-1349.

Weeks D E, Conley Y P, Tsai H J, Mah T S, Schmidt S, Postel E A, Agarwal A et al. (2004) Age-related maculopathy: a genomewide scan with continued evidence of susceptibility loci within the 1q31, 10q26, and 17q25 regions. *Am J Hum Genet* 75: 174-189.

Wefers H, and Sies H (1983) Hepatic low-level chemiluminescence during redox cycling of menadione and the menadione-glutathione conjugate: relation to glutathione and NAD(P)H:quinone reductase (DT-diaphorase) activity. *Arch Biochem Biophys* 224: 568-578.

Weger M, Renner W, Steinbrugger I, Cichocki L, Temmel W, Stanger O, El-Shabrawi Y et al. (2005) Role of thrombophilic gene polymorphisms in branch retinal vein occlusion. *Ophthalmology* 112: 1910-1915.

Weisinger H S, Vingrys A J, and Sinclair A (1996) Electrodiagnostic methods in vision. Part 1. Clinical application and measurement. *Clin Exp Optom* 79: 50-61.

Welsh M J, Tsui L C, Boat T F, and Beaudet A L (1995) Cystic fibrosis. In: Scriver C R, Beaudet A L, Sly W S, and Walle D [eds.] *The Metabolic And Molecular Basis of Inherited Diseases*. New York: McGraw-Hill, pp. 3799-3876.

Weng T X, Godley B F, Jin G F, Mangini N J, Kennedy B G, Yu A S, and Wills N K (2002) Oxidant and antioxidant modulation of chloride channels expressed in human retinal pigment epithelium. *Am J Physiol Cell Physiol* 283: C839-849.

Werkmeister R M, Palkovits S, Told R, Groschl M, Leitgeb R A, Garhofer G, and Schmetterer L (2012) Response of retinal blood flow to systemic hyperoxia as measured with dual-beam bidirectional Doppler Fourier-domain optical coherence tomography. *PLoS One* 7: e45876.

Werner J S, Bieber M L, and Schefrin B E (2000) Senescence of foveal and parafoceal cone sensitivities and their relations to macular pigment density. *J Opt Soc Am A* 17: 1918-1932.

West K P J (2003) Vitamin A deficiency disorders in children and women. *Food and Nutrition Bulletin* 24: S78-90.

Westheimer G (1966) The Maxwellian view. *Vision Res* 6: 669-682.

Whatham A, Suttle C, Blumenthal C, Allen J, and Gaskin K (2009) ERGs in children with pancreatic enzyme insufficient and pancreatic enzyme sufficient cystic fibrosis. *Doc Ophthalmol* 119: 43-50.

Williams R A, Brody B L, Thomas R G, Kaplan R M, and Brown S I (1998) The psychosocial impact of macular degeneration. *Arch Ophthalmol* 116: 514-520.

Willison H J, Muller D P, Matthews S, Jones S, Kriss A, Stead R J, Hodson M E et al. (1985) A study of the relationship between neurological function and serum vitamin E concentrations in patients with cystic fibrosis. *J Neurol Neurosurg Psychiatry* 48: 1097-1102.

Wills N K, Weng T, Mo L, Hellmich H L, Yu A, Wang T, Buchheit S et al. (2000) Chloride channel expression in cultured human fetal RPE cells: response to oxidative stress. *Invest Ophthalmol Vis Sci* 41: 4247-4255.

Wills N K, Weng T X, Godley B F, Jin G F, Mangini N J, Yu A S L, and Kennedy B G (2001) Chloride channel expression in human adult retinal pigment epithelial cells. *Invest Ophthalmol Vis Sci* 42: S775.

Wilson H L, Schwartz D M, Bhatt H R, McCulloch C E, and Duncan J L (2004) Statin and aspirin therapy are associated with decreased rates of choroidal neovascularization among patients with age-related macular degeneration. *Am J Ophthalmol* 137: 615-624.

Winkler B, Riley M, Peters M, and Williams F (1992) Chloride is required for fluid transport by the rabbit corneal endothelium. *Am J Physiol Cell Physiol* 262: C1167-C1174.

Winklhofer-Roob B M, Schlegel-Haueter S E, Khoschsorur G, van't Hof M A, Suter S, and Shmerling D H (1996) Neutrophil elastase/alpha 1-proteinase inhibitor complex levels decrease in plasma of cystic fibrosis patients during long-term oral beta-carotene supplementation. *Pediatr Res* 40: 130-134.

Witkin A, J., Ko T H, Fujimoto J G, Chan A, Drexler W, Schuman J S, Reichel E et al. (2006) Ultra-high resolution optical coherence tomography assessment of photoreceptors in retinitis pigmentosa and related diseases. *Am J Ophthalmol* 142: 945-952.

Witmer A N, Vrensen G F J M, Van Noorden C J F, and Schlingemann R O (2003) Vascular endothelial growth factors and angiogenesis in eye disease. *Prog Retin Eye Res* 22: 1-29.

Wojtkowski M, Leitgeb R, and Kowalczyk A (2002) In vivo human retinal imaging by fourier domain optical coherence tomography. *J Biomed Opt* 7: 457-463.

Wolf-Schnurrbusch U E K, Ceklic L, Brinkmann C K, Iliev M E, Frey M, Rothenbuehler S P, Enzmann V et al. (2009) Macular thickness measurements in healthy eyes using six different optical coherence tomography instruments. *Invest Ophthalmol Vis Sci* 50: 3432-3437.

Wolfs R C, Grobbee D E, Hofman A, and de Jong P T (1997) Risk of acute angle-closure glaucoma after diagnostic mydriasis in nonselected subjects: the Rotterdam Study. *Invest Ophthalmol Vis Sci* 38: 2683-2687.

Wong A C, Chan C W, and Hui S P (2005) Relationship of gender, body mass index, and axial length with central retinal thickness using optical coherence tomography. *Eye (Lond)* 19: 292-297.

Wong P Y (1998) CFTR gene and male infertility. *Mol Hum Reprod* 4: 107-110.

Wood A, Binns A, Margrain T, Drexler W, Povazay B, Esmaeelpour M, and Sheen N (2011) Retinal and choroidal thickness in early age-related macular degeneration. *Am J Ophthalmol* 152: 1030-1038 e1032.

Worlitzsch D, Tarran R, and Ulrich M e a (2002) Effects of reducted mucous oxygen concentration in airway Pseudomonas infections of cystic fibrosis patients. *Journal of Clinical Investigation* 109: 317-325.

Wu J, Marmorstein A D, and Peachey N S (2006) Functional abnormalities in the retinal pigment epithelium of CFTR mutant mice. *Exp Eye Res* 83: 424-428.

Yang H, Reinach P S, Koniarek J P, Wang Z, Iserovich P, and Fischbarg J (2000) Fluid transport by cultured corneal epithelial cell layers. *Br J Ophthalmol* 84: 199-204.

Yanoff M, and Fine B S (1982) *Ocular Pathology: A text and Atlas*. Philadelphia: Harper and Row.

Yau K W (1994) Phototransduction mechanism in retinal rods and cones. The Friendenwald lecture. *Invest Ophthalmol Vis Sci* 35: 9-32.

Yau K W, and Hardie R C (2009) Phototransduction motifs and varisations *Cellular and molecular life sciences : CMLS* 139: 246-264.

Ye X D, Laties A M, and Stone R A (1990) Peptidergic innervation of the retinal vasculature and optic nerve head. *Invest Ophthalmol Vis Sci* 31: 1731-1737.

Yu D Y, and Cringle S J (2001) Oxygen distribution and consumption within the retina in vascularised and avascular retinas and in animal models of retinal disease. *Prog Retin Eye Res* 20: 175-208.

Yu D Y, Cringle S J, Alder V, and Su E N (1999) Intraretinal oxygen distribution in the rat with graded systemic hyperoxia and hypercapnia. *Invest Ophthalmol Vis Sci* 40: 2082-2087.

Yung B, Landers A, Mathalone B, Gyi K M, and Hodson M E (1998) Diabetic retinopathy in adult patients with cystic fibrosis-related diabetes. *Respir Med* 92: 871-872.

Zeitlin P L (2007) Emerging drug treatments for cystic fibrosis. *Expert Opin Emerg Drugs* 12: 329-336.

Zele A J, and Vingrys A J (2005) Cathode-ray-tube monitor artefacts in neurophysiology. *J Neurosci Methods* 141: 1-7.

Zielenski J (2000) Genotype and Phenotype in Cytstic Fibrosis. *Respiration* 67: 117-133.

Zuckerman R, and Weiter J J (1980) Oxygen transport in the bullfrog retina. *Exp Eye Res* 30: 117-127.

Appendix A

Monitor Calibration

```
function [ gammaTable1, gammaTable2, displayBaseline, displayRange,
displayGamma ] = CalibrateMonitorPhotometer( numMeasures )

global vals;
global inputV;

if(nargin < 1)
numMeasures = 17;
end

input(sprintf(['When black screen appears, point photometer, \n' ...
          'get reading in cd/m^2, input reading using numpad and press
enter. \n' ...
          'A screen of higher luminance will be shown. Repeat %d times. '
...
          'Press enter to start'], numMeasures));

origclut = repmat([0:255]'/255,1,3);
psychlasterror('reset');

try
SpotSize = 5.4*20.8;
offsetCenteredspotRect = [640-SpotSize 512-SpotSize 640+SpotSize
512+SpotSize]; % size and position of spot on screen
win = Screen('OpenWindow', 0, 0);

BackupCluts;
Screen('LoadNormalizedGammaTable', win, origclut );

vals = [];
inputV = [0:256/(numMeasures - 1):256];
inputV(end) = 255;
for i = inputV
Screen('FillRect',win,0);
Screen('FillOval', win, i, offsetCenteredspotRect)
Screen('Flip',win);

fprintf('Value? ');
resp = GetNumber;
fprintf('\n');
vals = [vals resp];
end

RestoreCluts;
Screen('CloseAll');
catch
RestoreCluts;
Screen('CloseAll');
psychrethrow(psychlasterror);
end

displayRange = (max(vals) - min(vals));
```

```
displayBaseline = min(vals);

%Normalize values
vals = (vals - displayBaseline)/(max(vals) - min(vals));
inputV = inputV/255;
```

Appendix B

Computerised Dark Adaptometer

```
clear all

subjectID = input('Please enter subject ID >','s');

% Input co ordinates and sizes for cross and spot
HorizontalLocation = 0
VerticalLocation = 0
SpotSize = 5.4 * 20.8; % size of spot in pixels (There are 20.8 pixels per
degree horizontally)

KbName('UnifyKeyNames');
% The Try, Catch, End commands will respond to bugs / problems
try
% Set up all the parameters
whichScreen = 0;
window = Screen(whichScreen,'OpenWindow');
white = WhiteIndex(window); % pixel value for white
black = BlackIndex(window); % pixel value for black
gray = (white+black)/2;
inc = white-gray;

% Set the parameters for the spot, 1st and 3rd numbers give the horizontal
position
offsetCenteredspotRect                  =                  [640-SpotSize,512-
SpotSize,640+SpotSize,512+SpotSize];
offsetCenteredspotRect2                 =              [640-SpotSize+17.5,512-
SpotSize+17.5,640+SpotSize-17.5, 512+SpotSize-17.5];

% Set up the sounds
correctSound = sin(2*pi*100*[0:0.00125:2.0]);
incorrectSound = sin(2*pi*40*[0:0.00125:2.0]);
NewFilterSound = sin (2*pi*200*[0:0.00125:10.0]);
thresholdSound = sin (2*pi*300*[0:0.00125:5.0]);

% Intial psychophysical increment step size
incrementStep = 0.4;
SpotLuminance = 1.5;

% Set up various flags
response = 0;
responseCounter = 0;
reversalCounter = 1; % counts reversals (reset after each threshold)
DarkAdptCounter = 0; % counts the number of thresholds recorded.
presentationCounter=1; % counts all presentations
dataCounter=1; % counts all reversals
thresholdCounter = 1; % counts the number of threshold points
AdjustmentFilter1 = 2.0; % optical density of the first ND filter
AdjustmentFilter2 = 0; % optical density of the second ND filter
AdjustmentFilter3 = 0; % optical density of the third ND filter

SecondNDFIlterFlag = 0; % flag to stop the luminance being raised if the
spot       luminance hits it's lowest level a second time
resultTime = 1;
```

```
resultThreshold = 1;
BreakFlag=0;

% Set keys up.
rightKey = KbName('RightArrow');
leftKey = KbName('LeftArrow');
escapeKey = KbName('ESCAPE');

% Screen instructions
Screen(window, 'FillRect', 0);
Screen('DrawText', window, 'DARK ADAPTATION GOLDMANN-WEEKERS', 300, 200,
white);
Screen('DrawText', window, 'Hit any key to start experiment', 300, 400,
white);
Screen(window, 'Flip');
KbWait;% duration of instruction presentation

% Set up the timer.
startTime = now;
durationInSeconds = 1500;
durationEachThreshold = 1;
numberOfSecondsRemaining = durationInSeconds;
SecondsRemaining = durationEachThreshold;

% Screen calibration variables
MinScreenLum = 0.103; % Keep: contrast = 100 & brightness = 63
GammaFunc = 2.22;
MaxScreenLum = 155.2;

% Experiment loop.
fprintf('Experiment started'),
StartExptSecs = GetSecs; % this times the experiment

while GetSecs - StartExptSecs < durationInSeconds% Keep experiment running

% Set up flags to re enter the threshold loop
stopRule = 1; %keeps loop running till stop rules met, then =0

while stopRule > 0 % Keep looking for threshold

GammaCorrectSpotLum = 255*(((10^SpotLuminance) MinScreenLum)/MaxScreenLum)
^(1/GammaFunc);
%This calculates the grey scale required for the desired luminance
%SpotLuminance raised to power of 10 to 'un-log' the number

%Procedure for the first 5 minutes
if GetSecs - StartExptSecs <= 300

% Present stimulus
Screen('DrawText', window, ['GammaCorr: ' num2str(SpotLuminance,4)], 970,
940, [0,0,240]);
LineSpectrum = [256 0 0];
Screen('FillOval', window, GammaCorrectSpotLum, offsetCenteredspotRect); %
draws white spot
Screen(window, 'Flip'); % presents test
WaitSecs (0.2); % presentation time

%Remove stimulus
```

```
Screen('DrawText', window, ['GammaCorr: ' num2str(SpotLuminance,4)], 970,
940, [0,0,240]);
Screen(window, 'Flip');
ResponseSecs = GetSecs;

% Procedure for after 5 minutes
elseif GetSecs - StartExptSecs > 300

Screen('DrawText', window, ['GammaCorr: ' num2str(SpotLuminance,4)], 970,
940, [0,0,240]);
if GetSecs - StartExptSecs == 300
end

LineSpectrum = [256 0 0];
Screen('FillOval', window, GammaCorrectSpotLum, offsetCenteredspotRect); %
draws white spot
Screen(window, 'Flip'); % presents test
WaitSecs (0.2); % presentation time

%Remove stimulus
Screen('DrawText', window, ['GammaCorr: ' num2str(SpotLuminance,4)], 970,
940, [0,0,240]);
Screen(window, 'Flip'); % blanks out test
ResponseSecs = GetSecs;% gets the time the stimulus was flipped out
end

% Threshold procedure for first 5 minutes
if GetSecs - StartExptSecs <= 300
% Wait for a response
while 1
[ keyIsDown, timeSecs, keyCode ] = KbCheck;
if keyIsDown

if keyCode(escapeKey)% Escape loop
BreakFlag=1;
break
end

if (timeSecs - ResponseSecs)<0.6;
response = 1; % this means the response was correct
sound(correctSound)
else
response = -1; %  incorrect response (too slow)
sound (incorrectSound)
break
end

while KbCheck; end % avoids KbCheck reporting multiple events
break
end

% If no button is pressed
SecsNow = GetSecs;
timeSincePresentation = (SecsNow - ResponseSecs);
if timeSincePresentation > 1;
response = -1; % incorrect response (missed)
break
end
end
```

```
if BreakFlag==1  % Escape loop
break
end

% Record each presentation.
presentationTime(presentationCounter)= (GetSecs - StartExptSecs);
presentationThreshold(presentationCounter)=                    SpotLuminance-
AdjustmentFilter1-AdjustmentFilter2-AdjustmentFilter3;
presentationCounter = presentationCounter + 1;

% Adjust next stimulus increment on the basis of the response
if response > 0; % correct

if incrementStep > 0.0; % this is a threshold
resultTime (thresholdCounter) = (GetSecs - StartExptSecs);
resultThreshold   (thresholdCounter)   =   SpotLuminance-AdjustmentFilter1-
AdjustmentFilter2-AdjustmentFilter3;
thresholdCounter = thresholdCounter + 1;
stopRule = -1;
end

incrementStep = -0.3; % next increment = down 0.3 log units
WaitSecs (0.5 + rand(1.5))
end

if response < 0; % incorrect
incrementStep = 0.1;
WaitSecs (rand(1.0))
end

% Adjust stimulus for next presentation
SpotLuminance = SpotLuminance + incrementStep;
if SpotLuminance > 2
SpotLuminance = 2;
end

% Reset the stimulus intensity when the minimum luminance is reached
if SpotLuminance < -0.6;
SecondNDFIlterFlag = SecondNDFIlterFlag + 1;
sound (NewFilterSound) % inset new filter
if SecondNDFIlterFlag == 1
AdjustmentFilter2 = 1.2;
WaitSecs (5.0)
SpotLuminance  =  SpotLuminance  +  AdjustmentFilter2;  %  resets  stimulus
intensity to the maximum brightness
end
if SecondNDFIlterFlag == 2
AdjustmentFilter3= 2.4;
WaitSecs (5.0)
SpotLuminance = SpotLuminance + AdjustmentFilter3; % resets the stimulus
intensity to the maximum brightness
end

end

% this presents the stimulus every minute after 5 minutes
elseif GetSecs - StartExptSecs > 300
while 1[ keyIsDown, timeSecs, keyCode ] = KbCheck;
if keyIsDown
```

```
if keyCode(escapeKey)% Escape loop
BreakFlag=1;
break
end

if (timeSecs - ResponseSecs)<0.8;
response = 1; % correct
responseCounter = responseCounter + 1;
sound(correctSound)
else
response = -1; % incorrect (too slow)
responseCounter = responseCounter - 1;
sound (incorrectSound)
break
end


while KbCheck; end % avoids KbCheck reporting multiple events
break
end

% If no button is pressed
SecsNow = GetSecs;
timeSincePresentation = (SecsNow - ResponseSecs);
if timeSincePresentation > 1;
response = -1; %  incorrect (missed)
break
end
end

if BreakFlag==1 % escape loop
break
end

% Record each presentation.
presentationTime(presentationCounter)= (GetSecs - StartExptSecs);
presentationThreshold(presentationCounter)=                    SpotLuminance-
AdjustmentFilter1-AdjustmentFilter2-AdjustmentFilter3;
presentationCounter = presentationCounter + 1;


% Adjust next stimulus increment on the basis of the response
if response > 0; % correct

if incrementStep > 0.0; % that is, threshold was raised up on the last
step, this must be a threshold
resultTime (thresholdCounter) = (GetSecs - StartExptSecs);
resultThreshold   (thresholdCounter)   =   SpotLuminance-AdjustmentFilter1-
AdjustmentFilter2-AdjustmentFilter3;
thresholdCounter = thresholdCounter + 1;
stopRule = -1;
end

incrementStep = -0.6;
WaitSecs (40);
sound (thresholdSound);
if BreakFlag==1 % escape loop
break
end
end
```

```
if response < 0; % incorrect
incrementStep = 0.05;
WaitSecs (rand(1.0))
end

% Alter stimulus for next presentation
SpotLuminance = SpotLuminance + incrementStep;
if SpotLuminance > 2
SpotLuminance = 2;
end

% Reset stimulus intensity when the minimumluminance is reached
if SpotLuminance < -0.6;
SecondNDFIlterFlag = SecondNDFIlterFlag + 1;
sound (NewFilterSound)
if SecondNDFIlterFlag == 1
AdjustmentFilter2 = 1.2;
WaitSecs (5.0)
SpotLuminance = SpotLuminance + AdjustmentFilter2; % resets stimulus
intensity to maximum brightness
end

if SecondNDFIlterFlag == 2 % This is the 2nd loop i.e. the 2nd time the
subject reaches -0.5 log cd/m2
AdjustmentFilter3= 2.4;
WaitSecs (5.0)
SpotLuminance = SpotLuminance + AdjustmentFilter3; % resets stimulus
intensity to the maximum brightness
end
end
end

end % this ends the search for a threshold
beep

if BreakFlag==1 % escape loop
break
end

end

% Display the results
presentationTime = presentationTime (:);
presentationThreshold = presentationThreshold (:);
plot(presentationTime, presentationThreshold,'b*')% plots every
presentation
xlabel('Time(s)')
ylabel('Log Threshold')
axis ([0 300 -1.5 2.5])
hold on

resultTime = resultTime(:);
resultThreshold = resultThreshold(:);
plot(resultTime, resultThreshold,':ko') % plots the threshold

Screen('CloseAll');

% Output all the data to Excel spreadsheet
```

```
presentationData = [presentationTime, presentationThreshold];
thresholdData = [resultTime, resultThreshold];
xlswrite(strcat('c:\RachelHiscox\Results\DarkAdaptation_',subjectID,'.xls')
, presentationData,'Model','A2');
xlswrite(strcat('c:\RachelHiscox\Results\DarkAdaptation_',subjectID,'.xls')
, thresholdData,'Model','D2');
xlswrite(strcat('d:\RachelHiscox\Results\DarkAdaptation_'
,subjectID,'.xls'), presentationData,'Model','A2');
xlswrite(strcat('d:\RachelHiscox\Results\DarkAdaptation_'
,subjectID,'.xls'), thresholdData,'Model','D2');

catch
Screen('CloseAll');
rethrow(lasterror);
psychrethrow(psychlasterror);
end
```

Appendix C

CF Subject Number	Retinal Location								
	OS	IS	ON	IN	C	IT	OT[1]	II	OI
001	246.00	299.67	267.33	310.33	258.67	290.33	222.13	305.33	237.33
002	251.00	287.67	271.67	299.67	210.67	272.67	241.77	279.67	245.00
003	253.67	279.33	257.33	285.33	246.00	270.67	239.30	287.00	239.33
004	240.67	304.33	264.33	316.67	249.67	299.00	249.78	309.00	235.33
005	236.67	274.33	257.33	274.67	217.00	256.67	245.45	273.33	229.67
006	269.67	326.00	287.33	327.00	242.00	301.33	229.69	323.67	268.00
007	263.00	310.33	274.67	308.00	262.00	299.67	240.74	302.00	249.00
008	233.67	279.33	246.33	277.33	201.67	266.67	242.09	278.00	227.00
009	268.00	307.33	290.00	314.33	259.33	294.33	257.01	302.00	264.00
010	259.33	319.33	295.33	327.67	231.33	303.33	234.75	322.67	257.00
011	250.00	298.67	263.33	295.67	196.67	286.67	239.06	293.00	243.33
012	264.67	307.67	272.00	313.33	275.33	294.00	241.64	299.33	246.00
013	246.33	291.67	257.00	293.67	214.33	281.00	253.29	280.33	223.33
014	259.00	312.00	275.33	310.67	229.33	293.00	241.02	308.00	248.00
015	247.67	298.33	258.33	302.33	251.67	286.00	236.28	299.33	247.33
016	259.67	309.00	275.00	312.33	216.33	297.67	225.95	305.33	249.67
017	253.33	297.33	273.00	302.00	271.67	271.33	235.19	287.00	244.33
018	235.00	279.67	244.33	289.67	240.67	268.33	254.16	286.00	232.33
019	260.00	314.00	285.67	335.67	276.00	314.33	225.00	330.00	265.33
020	268.67	308.67	288.33	319.67	266.00	293.33	240.43	298.33	246.33
021	248.67	299.33	269.33	302.33	269.33	285.67	215.19	294.00	240.33
022	245.00	331.00	302.33	336.00	256.00	304.00	240.19	335.00	274.67
023	252.33	312.67	271.33	316.00	244.67	303.00	246.33	306.67	239.67
024	257.00	295.67	269.00	300.00	203.00	285.00	225.87	291.67	241.33
025	268.67	320.00	288.00	318.00	240.00	303.33	225.00	317.33	263.33
026	280.00	315.33	311.33	323.67	283.67	296.33	246.86	315.67	265.67
027	252.33	323.00	270.00	304.33	241.00	292.33	237.54	304.00	244.00
028	249.33	309.67	268.33	312.67	264.33	305.33	255.18	312.67	250.00

Control Subject Number	Retinal Location								
	OS	IS	ON	IN	C	IT	OT	II	OI[1]
111	265.67	317.67	281.00	334.67	273.67	314.33	256.33	327.00	253.67
112	261.00	314.67	280.67	319.00	259.33	312.33	263.00	316.00	251.33
113	249.33	293.00	271.00	303.00	257.67	280.00	227.67	297.00	249.33
114	254.00	303.00	279.33	309.00	264.33	289.33	240.33	307.33	248.67
115	245.00	298.00	276.67	311.67	240.67	288.00	238.33	303.67	253.00
116	265.33	300.33	275.00	297.00	209.00	279.33	241.33	285.33	242.67
117	251.67	298.67	267.67	303.33	236.67	284.67	231.33	294.67	241.00
118	252.00	303.33	273.67	311.00	278.00	298.67	236.67	304.33	243.00
119	257.33	301.33	281.67	313.33	267.33	290.33	236.67	298.33	255.67
120	254.33	301.33	279.00	306.00	212.33	299.67	248.00	301.33	246.00
121	270.00	328.00	293.33	337.33	292.33	309.00	248.33	322.67	261.00
122	292.00	319.33	312.33	321.33	258.00	299.00	261.00	309.67	272.67
123	265.33	314.00	299.33	313.67	252.00	294.67	244.33	295.33	254.00
124	280.33	313.67	292.33	306.00	227.67	305.33	258.00	307.00	270.33
125	253.33	297.33	273.00	302.00	271.67	271.33	225.00	287.00	244.33
126	269.33	313.67	284.33	313.33	238.33	299.33	246.67	310.00	253.33
127	266.33	319.00	287.67	317.67	243.33	304.00	248.33	308.00	256.67
128	276.00	330.00	299.33	329.00	269.00	302.33	256.33	315.33	279.33
129	243.67	301.67	257.00	305.33	252.33	294.00	233.00	296.33	225.00
130	243.00	283.67	263.67	301.00	290.33	281.67	235.67	292.67	236.67
131	271.67	307.00	284.00	307.00	246.00	292.33	263.00	297.67	271.33
132	268.00	318.67	297.00	332.67	281.33	302.00	234.00	313.67	261.33
133	264.67	316.67	285.00	317.00	237.00	299.33	242.00	305.33	251.33
134	260.33	308.33	284.00	310.00	253.00	298.33	248.67	304.00	251.00
135	271.67	319.67	302.00	321.67	251.67	292.33	263.33	304.67	278.00
136	252.00	292.00	280.67	295.33	270.33	292.67	242.00	291.33	243.67
137	280.00	327.00	303.67	335.00	266.00	310.00	265.33	318.67	272.00
138	253.33	299.33	281.00	305.33	235.33	288.00	248.67	299.00	247.00

[1] Corrected for axial length

Appendix D

Peer reviewed poster presentations

1. **Hiscox** R, North R, Purslow C and Evans K. The repeatability of optical coherence tomography in the investigation of retinal thickness. British Congress of Vision Science, Birmingham, September 2011
2. **Hiscox** R, Purslow C, North R,. Ketchell I, Evans K. Dark Adaptation and the effect of Oxygen Inhalation in Cystic Fibrosis. ARVO, Seattle, May 2013

Published abstracts

1. **Hiscox** R, North R, Purslow C and Evans K (2012) The repeatability of optical coherence tomography in the investigation of retinal thickness. *Ophthalmic and Physiological Optics* 32: 169
2. **Hiscox** R, Purslow C, North R, Ketchell I, and Evans K (2013) Dark Adaptation and the effect of Oxygen Inhalation in Cystic Fibrosis. *ARVO Meeting Abstracts* 54: 3016

Other publications

1. Hiscox R, Purslow C, North R, Evans K (2013) Vision in Cystic Fibrosis. *Optometry Today*, 53 (18): 51-55

2

BAUSCH + LOMB
Academy of Vision Care

Sponsored by
BAUSCH + LOMB
See better. Live better.

The eye in cystic fibrosis

Rachel Hiscox BSc (Hons), MCOptom; Katharine Evans PhD, BSc (Hons), MCOptom, FBCLA, FHEA; Christine Purslow PhD, BSc (Hons), MCOptom, FBCLA, FIACLE; Rachel North PhD, MSc, FCOptom

Cystic fibrosis (CF) is the most common lethal autosomal disorder in Caucasian populations. It is characterised by a variable degree of pulmonary infections, pancreatic enzyme insufficiency and premature death. Ocular complications in CF range from abnormal tear volume to impaired dark adaptation. With improvements in CF life expectancy, ocular complications are of greater relevance to the optometrist. This article provides an overview of the ocular complications associated with CF.

Course code C-33362 | Deadline: October 18, 2013

General Optical Council
Approved CET
For Optometrists

Learning objectives

To obtain relevant history and symptoms for patients presenting with CF (Group 1.1.1)

To recognise the manifestations of ocular disease in CF (Group 6.1.13)

COMMUNICATION

OCULAR DISEASE

General Optical Council
Approved CET
For Dispensing Opticians

Learning objectives

Understand the implications of the manifestations of ocular disease in CF (Group 8.1.5)

OCULAR ABNORMALITIES

About the authors

Rachel Hiscox is currently a postgraduate researcher and optometrist at Cardiff University, investigating the effect of cystic fibrosis on the retina. She has taught in undergraduate clinics over the last three years, with most involvement in the second year contact lens module. She has experience in private practice and hospital optometry.

Dr Katharine Evans completed her thesis 'Cystic fibrosis and the eye' in 2009, presenting her work at numerous international conferences. She was appointed as a lecturer at Cardiff University in September 2009.

Professor Christine Purslow has undertaken a variety of clinical roles in hospital optometry, private practice and teaching before embarking on an academic career in 2002. She was awarded her PhD from Aston University in 2005 and has worked as a senior lecturer and researcher at Cardiff University, as well as being the director of postgraduate taught courses within WOPEC. More recently, she was appointed as Professor and head of optometry at Plymouth University.

Professor Rachel North is the director of clinics at Cardiff University with teaching experience across a wide variety of clinical topics and primary research interests in diabetes mellitus and glaucoma. She is a member of British Universities Committee of Optometry, Optometry Wales and the Vision 2020 Eye Research Group.

1 CET POINT

Cystic fibrosis (CF) is the most common lethal autosomal recessive disorder (see Figure 1) in Caucasian populations,[1] currently affecting over 9,000 people in the UK alone.[2] It results from the defective functioning of an epithelial membrane protein known as Cystic Fibrosis Transmembrane Conductance Regulator (CFTR). CFTR acts as a chloride ion channel and is found in the epithelial cells of many organs, including the pancreas, lung, gastrointestinal tract, kidneys and the eyes.[3,4] Chloride transport is the driving force for maintaining the correct balance of electrolytes and fluids within many different organs. Without proper chloride transport via CFTR, organs such as the lungs and the pancreas can become damaged with thick, viscous secretions. There is a wide spectrum of genetic mutations in CF; some are very mild, causing only a slight decrease in normal chloride transport, while other mutations, which result in complete absence of CFTR from the epithelium, cause a particularly severe form of the disease.

As CFTR is found in multiple organs throughout the body, the effects of CF are far-reaching, leading to multi-organ and system dysfunction. The lungs are most critically affected in CF, with progressive lung disease and secondary pulmonary complications accounting for over 90% of all deaths in CF.[5]

Vitamin deficiencies (A, D, E and K) and CF-related diabetes (CFRD) are common secondary complications of CF. Vitamin deficiency in CF is the result of fat maldigestion due to damaged pancreatic cells which are not releasing the necessary pancreatic enzymes. Along with poor growth and increased mortality,[6] clinical consequences of vitamin A deficiency (VAD) also include impaired dark adaptation,[7] in addition to conjunctival and corneal xerosis.[8-11]

CFRD affects 45-50% of CF patients over the age of 30.[12] While it has features common to both Type 1 and Type 2 diabetes which optometrists are more familiar with, it is classified as a distinctly different disease. Although the pathogenesis of CFRD is not completely understood, increasing evidence suggests that insulin-deficiency, exacerbated by peripheral and liver insulin resistance, is the primary cause.[13-15] Insulin-deficiency results from β-cell apoptosis in the pancreas in conjunction with defective insulin secretion by the remaining β-cells.[16-19] CFRD is often particularly difficult to control as insulin resistance is aggravated by respiratory infection and corticosteroid treatment, and therefore fluctuates over time.[20,21]

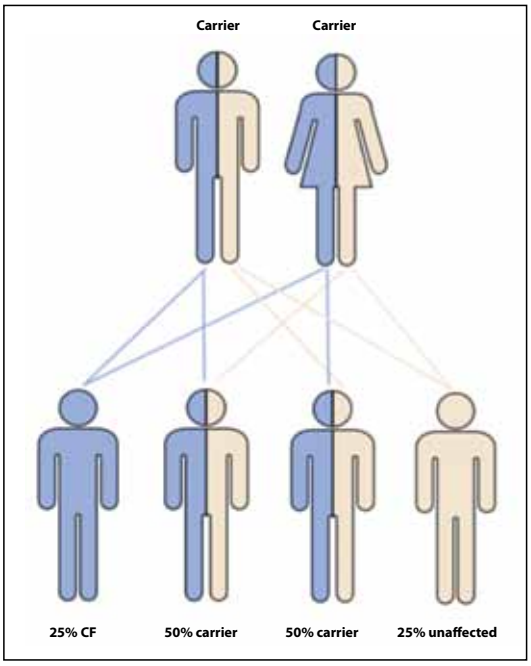

Figure 1 Autosomal recessive inheritance of CF

Due to the wide-reaching health complications associated with CF, many different forms of treatment are required to adequately manage the disease. Treatment regimes include physiotherapy, nutritional supplementation, pancreatic enzyme replacement and pharmaceutical treatment to control chronic respiratory infection and inflammation. Gradual progress is being made in emerging protein repair and gene therapy, both of which aim to develop therapeutic strategies which target specific CFTR mutations, in order to improve or restore CFTR function.[22-27] Although further development is needed before these emerging therapies become a viable option, it is hoped that they may continue to change the outlook for CF patients in the future. Until then, lung transplantation remains the only definitive treatment option for patients with progressive respiratory failure.[28,29]

Following dramatic improvements in patient treatment and management, the median predicted survival age is now 41.5 years, and that is expected to increase in the future with the development of gene therapy.[30] This is a major improvement compared to survival in the 1950s when life expectancy for those diagnosed with CF was just five years of age. However, with the improvement in CF life expectancy, ocular complications associated with the disease are likely to become more of a pressing concern.

CFTR and the eye

To date, CFTR has been found in human corneal and conjunctival epithelium, corneal endothelium and retinal pigment epithelium,[34] where it has been shown to play an active part in chloride ion secretion across cell membranes. Active transport of chloride ions is known to provide the driving force for subsequent osmotically-driven fluid secretion. Within the eye, chloride ion transport is involved in: basal tear production, the preservation of corneal transparency via the endothelial pump, and subretinal space volume regulation.[31-37] The absence

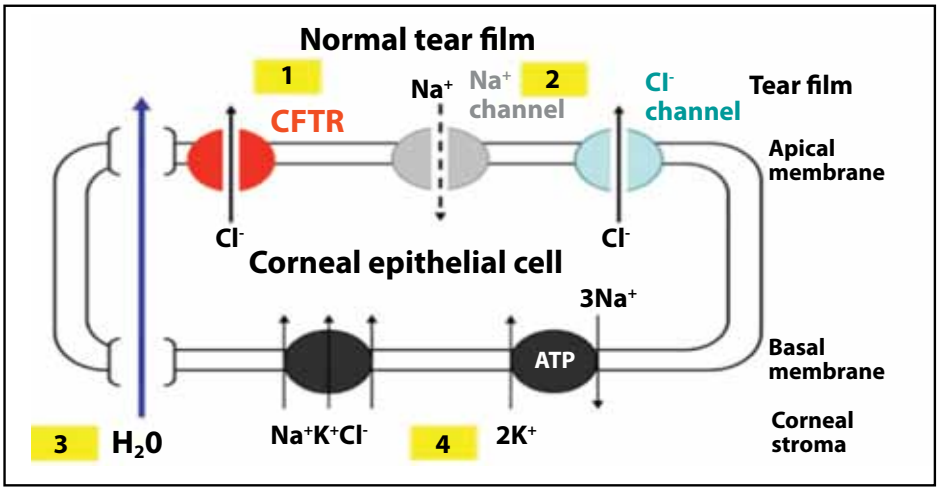

Figure 2 Diagram of a simplified corneal epithelial cell. Movement of chloride ions (Cl^-) out of the cell via CFTR and other Cl^- channels on the apical membrane (1), together with sodium ion (Na^+) movement into the cell (2), causes water (H_2O) to move out of the corneal stroma into the tear film (3). Basal membrane transporters load the epithelial cell with Cl^- to maintain the electrochemical driving force for Cl^- movement at the apical membrane (4)

of normal CFTR activity in CF suggests that ocular structure and function may be compromised. It is, therefore, possible that ocular abnormalities in CF are primary manifestations of the disease. However, with vitamin A deficiency and CFRD being common complications in CF, it is likely that some ocular defects are secondary manifestations.

Ocular complications in CF

The Tear Film

Classically, the tear film is reported to consist of three layers: an outer lipid layer, a middle aqueous layer and an inner mucous layer. The production and turnover of the pre-ocular tear film is essential in providing tissues with nourishment and lubrication, and for maintaining ocular health.[38] The aqueous layer, which is composed of proteins, electrolytes, enzymes, metabolites and water[39] is principally produced by the lacrimal gland and accessory lacrimal glands, although recent evidence suggests a small proportion of electrolytes and water are secreted by the cornea and conjunctiva, via ion channels,[40] including CFTR (see Figure 2).[41]

Several clinical studies have reported an increase in signs of dry eye in CF patients compared to controls. Abnormally low tear secretion, as assessed by Schirmer's test, has been observed in 29-81% of CF patients in a number of separate studies.[42-45] Findings of decreased tear break-up time in CF subjects compared to healthy controls indicates poor tear quality in CF.[46] Additionally, reports of corneal fluorescein staining in 60-82% of CF patients,[42,43] along with increased expression of inflammatory markers adds further evidence to the link between dry eye and CF.[47,48]

With the localisation of CFTR to the corneal and conjunctival epithelium, and its known contribution to basal tear secretion, it is thought that dry eye could be a primary manifestation of CF. However, as increased vitamin A deficiency (VAD) has been correlated with reduced TBUT in CF,[46] it is possible that this secondary complication also adds to the clinical observation of dry eye in CF. In light of these findings, practitioners should be aware of the increased likelihood of CF patients suffering from signs and symptoms of dry eye. It may, therefore, be appropriate to ask CF patients tailored questions relating to dry eye when taking their history and symptoms.

Xerophthalmia

As discussed, vitamin A deficiency (VAD), is a common secondary complication of CF. Xerophthalmia refers to the entire clinical spectrum of ocular manifestations caused by VAD.[49] It is the leading cause of childhood blindness worldwide, but is uncommon in developed countries.[50] The primary manifestation of xerophthalmia is extreme dryness of the conjunctiva and cornea due to a failure of the secretory activity of the mucin-secreting goblet cells of the conjunctiva. Xerophthalmia also encompasses night blindness, conjunctival and corneal xerosis, Bitot spots and corneal ulceration.[10] Early descriptions of CF found a high prevalence of xerophthalmia.[51,52,53] However, with recent improvements in supplementation for CF patients, reports of xerophthalmia have almost been eliminated.[10]

Figure 3 Fundus photograph of a male patient aged 40 with a 13-year duration of CFRD, showing dot and flame haemorrhages indicating background diabetic retinopathy

Although cases of xerophthalmia in patients with CF are rare, it highlights the importance of considering VAD in those patients who present with ocular complications.[11] It also demonstrates the importance of regular eye examinations, with any patients showing signs of xerophthalmia being referred appropriately for further examination by their CF consultant to confirm clinical vitamin A deficiency before treatment is commenced.[9]

Corneal morphology and integrity

CFTR expression has previously been localised to the apical membrane of the corneal endothelium,[31,33,54] where it is known to facilitate fluid efflux in order to maintain corneal transparency.[33] It is, therefore, reasonable to predict that loss of CFTR function in CF could cause an increase in corneal thickness and a decrease in transparency, unless other Cl^- channels provide a certain level of compensation.

Only two studies have investigated corneal thickness in CF, with equivocal outcomes. The most recent study, which used the Oculus

1 CET POINT

Pentacam, found no significant difference in either central or peripheral corneal thickness in CF subjects compared to healthy controls.[55] Conversely, a preceding study found corneal thickness to be increased in CF, as determined using contact video specular microscopy.[56] Reduced endothelial cell area, elevated endothelial cell density and permeability, as well as increased relative endothelial pump rate were also observed. These morphological differences suggest that the corneal endothelium actively compensates for impaired Cl^- transport via CFTR.

Cataracts

Steroid use, a known risk factor for the development of posterior subcapsular cataracts, is commonplace in CF for managing pulmonary inflammation. It is, therefore, unsurprising that posterior subcapsular cataracts have been observed in CF patients receiving steroid treatment.[57]

Antioxidants, including vitamins A, C and E are associated with reduced cataract formation.[58,59] Digestive insufficiency, secondary to pancreatic insufficiency in CF, causes vitamin deficiency and lowers antioxidant availability.[60] Therefore, a higher incidence of cataract may be expected. Crystalline lens transparency can be significantly reduced in CF patients, with the greatest reduction in transparency seen in those with more severe digestive insufficiency.[46,61]

The role of oxidative stress in the aetiology of cataract formation has been clearly established,[59] and persistent pulmonary infection in CF is known to increase levels of oxidative stress.[62] This, combined with decreased levels of antioxidants, which usually protect the crystalline lens,[63] could contribute to the development of decreased lens transparency in CF. While diabetes is also strongly associated with the development of cataracts,[58,64] the effect of CFRD on the lens in CF is yet to be determined.

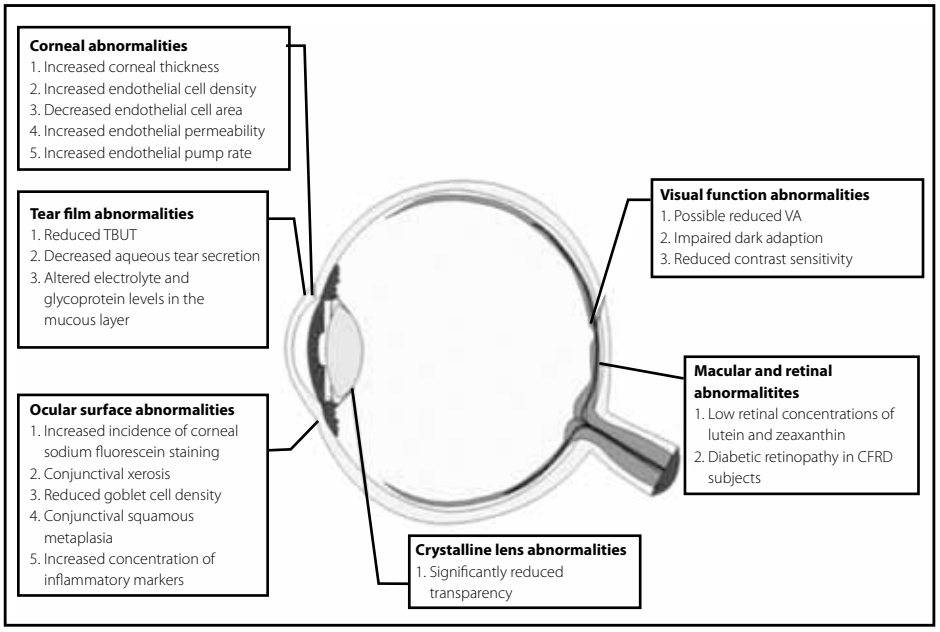

Figure 4 Summary of the ocular complications associated with CF

The retina and diabetic retinopathy

Due to the increased mortality of CF patients with CFRD, life expectancy was previously considered to be too short for the development of diabetic complications, including diabetic retinopathy (DR).[65] However, greater longevity of CF patients has been accompanied by increasing reports of microvascular complications.[66,67] DR is predominantly seen in patients with duration of CFRD of at least 10 years (see Figure 3).[68-70] Interestingly, the prevalence of DR in CFRD has been found to be significantly lower compared to age and disease duration matched Type 1 diabetic subjects.[65]

Several factors may account for the lower prevalence of DR in CFRD compared to other forms of diabetes:

- Maintenance of a variable degree of insulin secretion, which may have a protective effect on cell survival[70]
- Dislipoproteinemia appears to play a role in the pathogenesis of diabetic retinopathy,[71] but cholesterol levels are low in CF due to digestive insufficiency[70]
- Hypertension, a known risk factor in the development of DR,[72,73] is generally mild in CF[70]
- Tendency towards more stringent diabetic control in CF due to regular outpatient appointments.[65]

Retinal vascular abnormalities have previously been reported in CF patients, with retinal haemorrhages, retinal vein tortuosity and engorgement, noted only in those patients with moderate to severe pulmonary disease, and often showing resolution with improvement of respiratory function.[74] Similar retinal vascular findings have been reported in patients with chronic pulmonary insufficiency and carbon dioxide retention from other causes.[75]

The macula

Although supplementation of the major

vitamins is common practice in patients with CF, this does not typically include carotenoids, resulting in low carotenoid concentrations.[76,77] Carotenoids, including lutein and zeaxanthin, are antioxidant micronutrients,[78] and are particularly important in CF patients who, due to persistent pulmonary infection, are susceptible to higher levels of oxidative stress.[62]

Lutein and zeaxanthin accumulate at the macula and are believed to play a major part in protecting the retina from free-radicals, by absorbing the phototoxic effects of short-wavelength light and through their action as free radical scavenging antioxidants.[79,80] Low plasma concentration of lutein and zeaxanthin is associated with an increased incidence of macular degeneration.[81] Lutein and zeaxanthin are responsible for macular pigment and account for the yellow colouration of the macula due to their absorption of short wavelength light.[82] Patients with macular degeneration have been reported to have significantly lower concentrations of macular pigment, compared to those with normal vision.[83]

As CF patients are known to have low concentrations of carotenoids, combined with increased levels of oxidative stress, it could be predicted that their macular carotenoid levels would be reduced, making CF patients more susceptible to premature age-related macular changes. Indeed, the literature demonstrates that CF patients have significantly lower serum concentrations of lutein and zeaxanthin compared to controls, correlated with lower retinal macular pigment density concentrations;[84] these findings may explain the observation of premature drusen in two young CF patients (aged 20 to 25 years) in a recent study,[55] and highlight the importance of a thorough macular examination in all CF patients seen in practice.

Visual function

To date, a large-scale assessment of visual acuity, ametropia and binocular status in CF patients has not been undertaken. However, one small-scale study reported that VA, binocular status and refractive error in CF adults was comparable to matched controls,[55] suggesting normal emmetropisation[85] and orthophorisation occur in CF.[86] However, low birth weight and prematurity are associated with CF,[87] which are both linked with a greater incidence of ametropia, strabismus and amblyopia,[88] highlighting the importance of regular eye examinations in children with CF.

Contrast sensitivity, colour vision and dark adaptation have all been found to be impaired in CF patients.[7,55,89-92] CFTR has been localised to the RPE where it is believed to contribute to Cl^- transport.[93] Unless other Cl^- channels compensate for this fundamental CFTR dysfunction, normal photoreceptor function may be affected by altered inter-photoreceptor matrix composition. With the RPE's involvement in several functions, vital for the maintenance of normal visual function, including transport of nutrients to photoreceptors and retinal regeneration,[94] it seems clear that RPE impairment could result in photoreceptor degradation and reduced visual function.

It is well established that vitamin A is essential for normal photoreceptor function,[95] therefore it is unsurprising that VAD in CF has been identified as a causative factor for impaired measures of visual function including contrast sensitivity[90] and dark adaptation.[7,92,96] The observed relationship between abnormal dark adaptation and decreased serum retinol levels[7,92] in CF subjects suggests that abnormal dark adaptation is not caused by dysfunctional CFTR at the RPE, but is a secondary consequence of maldigestion and malabsorption of nutrients. However, elevated dark adaptation thresholds, despite normal vitamin A serum concentrations[97,98] may suggest another cause for the abnormality.

While there are no published studies on visual function levels in CFRD subjects, there is substantial evidence that dark adaptation,[99-102] colour vision,[103,104] and contrast sensitivity[104] are adversely affected in type 1 and type 2 diabetes, even in the absence of DR. Retinal hypoxia, secondary to abnormal retinal perfusion and ischaemia in diabetes has been identified as the cause of this defect.[104,105] It is reasonable to predict that visual function would be similarly affected by CFRD, and may account for some of the reductions in visual function seen in previous studies.

Conclusion

It is apparent that numerous ocular complications exist in CF (see Figure 4). It is, therefore, important that CF patients are advised to have regular eye examinations, and those with CFRD to attend annual retinal screening. Eye care practitioners must be aware of the breadth of ocular complications associated with CF in order to provide tailored and appropriate care to CF patients. Further improvements in life expectancy in CF are likely to be coupled with increases in the frequency of DR, cataract and potentially, AMD. Given the risk of significant visual loss associated with DR and AMD, CF patients should be educated to take appropriate action, in the event of any visual problems.

MORE INFORMATION

References Visit www.optometry.co.uk/clinical, click on the article title and then on 'references' to download.

Exam questions Under the new enhanced CET rules of the GOC, MCQs for this exam appear online at www.optometry.co.uk/cet/exams. Please complete online by midnight on October 18, 2013. You will be unable to submit exams after this date. Answers will be published on www.optometry.co.uk/cet/exam-archive and CET points will be uploaded to the GOC every two weeks. You will then need to log into your CET portfolio by clicking on "MyGOC" on the GOC website (www.optical.org) to confirm your points.

Reflective learning Having completed this CET exam, consider whether you feel more confident in your clinical skills – how will you change the way you practice? How will you use this information to improve your work for patient benefit?